
THE UNIVERSITY
*of* EDINBURGH

# *Infection biology and life cycle of*

# *Ramularia collo-cygni*

*Maciej Kaczmarek*

Thesis submitted to the University of Edinburgh for the degree of Doctor of Philosophy


March 2015

**Declaration**

I hereby declare that this thesis has been composed by me and that the work is my own, except as acknowledged by means of references. This thesis has not been submitted for any other degree or professional qualification except as specified.

Maciej Kaczmarek

March 2015

## Table of contents

## List of figures

## List of tables

## List of abbreviations

μm- micrometres

AF- aflatoxin

AFLP- amplified fragment length polymorphism

*aflR*- transcription factor gene encoding aflatoxin regulatory protein

*aflT*- ABC transporter protein, necessary for aflatoxin efflux

ANOVA- analysis of variance

AVN- averantin

Bp - base pairs, units to size nucleotide sequences

CFW- calcofluor white dye

CLSM- confocal laser scanning microscope

CR- cercosporin

*crg*1 - Zn(II)Cys6 transcription factor involved in cercosporin biosynthesis reported

a *ctb1, ctb2, ctb3, ctb8*- component genes of cercosporin biosynthesis cluster

*Cyp51*- sterol 14α- demethylase

*cypA/ cypX* – cytochrome P-450 monooxygenase

*Cytb*- cytochrome b gene

$dH_2O$- distilled $H_20$

DHOMST- dihydro-O-methylsterigmatocystin

DIC- differential interference contrast microscopy

DMST- demethylsterigmatocystin

dNTP- deoxynucleotide triphosphates

Dpi- days post inoculation

DS- dothistromin

dsRed- red fluorescent protein

EDTA- ethylenediaminetetraacetic acid

FAA- glacial acetic acid fixative

FAD- flavin adenine dinucleotide

*fas-1*/ *fas-2*- fatty acid synthase genes 1 and 2

GFP- green fluorescent protein

GS- growth stage

$H_20_2$- hydrogen peroxide

HGCA- Home Grown Cereals Authority

ITS- internal transcribed spacer

Kb- kilo base pairs = 1000 base pairs

MAT- mating type locus

*Mat1-1/ mat1-2* – mating type genes

MEA- malt extract agar

Min- minutes

*Mlo*/*mlo*- mildew susceptibility/mildew resistance gene

NCBI- National Center for Biotechnology Information

nm- nanometres

NOR norsolorinic acid

*nor-1/ norA/ norB*- a dehydrogenase encoding genes

ºC- degrees Celsius

OMST- O-methylsterigmatocystin

PCR- polymerase chain reaction

PDA- potato dextrose agar

Pi- post inoculation

*pksA/* AflC - polyketide synthase gene

QoI- quinone outside inhibitors

qPCR- quantitative PCR

RLS- Ramularia leaf spot

Rpm- revolutions per minute

rRNA- ribosomal RNA

SDHI- succinate dehydrogenase inhibitors

SDW- sterile distilled water

SRUC- Scotland's Rural College

SSR- simple sequence repeats/ microsatellites markers

ST- sterigmatocystin

TBE- Tris-borate, EDTA

TE- Tris, EDTA

UK- United Kingdom

UV- ultraviolet

*Ver-1/* AflM- versicolorin reductase 1

*verA/* VERB- versicolorin A/ B ketoreductase gene

## Abstract

In recent years, a new threat to barley crops has emerged and gained substantial attention due to its rising economic importance. Relatively little is known about the infection strategy and development of Ramularia leaf spot (RLS) disease on barley. Therefore the overall aim of this project was to increase the understanding of fundamental biology and life cycle of the causal agent, *R. collo-cygni.*

Chapter 2 describes the horizontal transmission of the fungus on barley. Both field and transgenic *R. collo-cygni* isolates expressing GFP and dsRed fluorescent reporter markers were utilised to visualise the infection progression in living host tissues by various light and confocal microscopy. The existence of a previously unknown structure called stomatopodium (infection peg), involved in the penetration of stomata, was demonstrated. The fungus initially exhibited symptomless epiphytic growth, extending above epidermis and connecting the hyphal aggregates inside substomatal cavities and subsequent initial sporulation. However, during the transition into symptomatic phase, the organised intercellular growth of hyphae into the mesophyll was observed. This hyphal network was involved in the production of asexual spores demonstrating that the raprture of epidermal layer was responsible for local necrosis observed for RLS. In addition to barley, several other speculated *R. collo-cygni* hosts have been used to verify their compatibility to the pathogen.

In chapter 3, a whole plant inoculation assay was developed to investigate the mode of the fungal seed-borne transmission by using GFP expressing strain of the fungus. It is shown here for the first time that the vertical transmission is systemic, involving symptomless colonisation of embryo and closely resembled the mode of

dissemination observed for *Neotyphodium* species, mutualistic fungal endosymbionts on grasses.The impact of fungal infection on seed germination ability was also examined that revealed no significant difference between clean, moderate and high levels of *R. collo-cygni* DNA.

Chapter 4 represents an attempt to discover and analyse the sexual development in *R. collo-cygni.* As a first step to understand the sexual reproduction cycle in this apparently asexual species, the genetic structure of the mating system was characterised by using PCR-based techniques which demonstrated the heterothallic nature of the fungus. The defined population of *R. collo-cygni* field isolates was then screened for the presence of the discovered mating type idiomorphs (*mat*) to determine the frequencies of the mating types in the defined *R. collo-cygni* populations. The segregation ratio of *mat1* and *mat2* close to 1:1 indicated a frequent sexual reproduction. In order to verify the existence of functional sexual stage in *R. collo-cygni*, potential sexual development was induced using the potentially compatible isolates and a comprehensive analysis was undertaken by correlative use of light-, confocal- and low temperature scanning electron microscopy. Two types of multicellular bodies were observed and described. First was the speculated *Asteromella* stage (male donor) that carries spore-like spermatia. The second structure initially resembled sclerotia that in only a few instances developed into perythecium/ pseudothecium that appeared to carry the sexual spores, ascospores enveloped in asci.

Chapter 5 demonstrates the role of rubellin toxin in symptom development by using autofluorescence phenomenon. The structure of putative molecular machinery

involved in rubellin biosynthesis was addressed by using bioinformatics approaches and the complete *R. collo-cygni* genome sequence. A gene cluster encompassing several components of other known secondary metabolite biosynthesis pathways, such as that of dothistromin and aflatoxin, was found and putative protein function of the genes is hypothesised.

## Lay person summary

Barley is one of the most important crops in the world and it is therefore often a subject to attack by a wide range of microbes that cause diseases. *R. collo-cygni* has now been listed amongst the most important pathogens that pose a threat to barley and may cause significant yield loss. The fungus was described in 1893 in Italy, however only in recent years has become a major pathogen of barley, spreading across the globe. The disease it causes, called Ramularia leaf spot (RLS), can be controlled by fungicide treatments however a rapid development of fungicide resistance in this fungus has been observed. It is therefore of great importance to discover and employ more efficient and sustainable strategies of RLS management. To achieve this, a more in-depth knowledge of the biology and life cycle of *R. collo-cygni* is required.

This project utilised modern microscopy techniques combined with molecular and cell biology tools to study the fundamental biology of infection and key components of the fungal life cycle in much greater detail than previously attempted. For instance, live cell imaging using confocal microscopy allowed exploration of the disease development in controlled environment. Barley inoculation experiments showed the mode of seed infection by *R. collo-cygni* which facilitates its survival over winter period. An important aspect of this research was to discover the unknown sexual cycle by using a combination of molecular biology approaches and correlative use of several microscopy techniques. It showed for the first time that sexual reproduction may occur in this fungus. Recently sequenced *R. collo-cygni* genome was used to study the putative molecular machinery involved in biosynthesis of the toxins, called rubellins, produced by this fungus that are involved in symptom

development on barley which ultimately leads to yield loss. The genetic structure of molecular components of rubellin synthesis was elucidated which could have major implications for the future development of more successful strategies of RLS management.

**Acknowledgements**

First of all, I would like to thank my supervisors: Dr Neil Havis, Dr James Fountaine and Professor Nick Read for all their continuous help and support I have received throughout the course of my PhD. This thesis would not have been possible without you.

I would like to acknowledge generous funding provided by BASF. I would also like to thank Professor Adrian Newton at The James Hutton Institute for his invaluable support and making this project possible by providing access to the essential equipment, without which many objectives of this research project would not have been possible to achieve. A big thank you also goes to Dr Graham McGrann at SRUC for his invaluable comments, suggestions and general support during writing up of this thesis. It is greatly appreciated.

I would like to thank my friend and colleague Marta with whom I shared all the discoveries and struggles that we faced due to quite bizarre and difficult subject of our projects, *R. collo-cygni.* I would also like to thank my friend Jaan for all the extracurricular activities and truly great times we have had together for the last four years.

Massive thank you goes to my partner and best friend Dominika for her patience, understanding and unconditional love and support that she has given me throughout my Masters and PhD studies.

Finally, a very big thank you to my parents Krystyna and Henryk and my sister Joanna for believing in me even if some decisions that I have made seemed very strange. I am sure there is more to come…

# Chapter 1

## Introduction: Ramularia leaf spot of barley

## (*Ramularia collo-cygni* Sutton et Waller)

# 1. Introduction: Ramularia leaf spot of barley (*Ramularia collo-cygni* Sutton et Waller)

Plants, including barley, are subject to a wide range of disease and disorders that affect their growth and development. Although the definition of plant disease is controversial, most pathologists agree that it involves a malfunction of plant processes and may occur during plant growth or while the plant is dormant. Diseases in plants are caused by the same type of agents that cause disease in animals. They could be either an infectious pathogen such as fungi and bacteria, or a non-infectious agent, e.g. mineral deficiency. All these agents need to maintain the process of disease development over certain period of time (Mathre, 1997).

Fungi are the most abundant plant pathogens (Mathre, 1997; Scheffer, 1997; Agrios, 2005). They are small chlorophyll lacking microorganisms, whose bodies comprise a network of filamentous threads, called hyphae. They usually reproduce by forming spores, which can be spread by the wind, rain and machinery. To colonise the plants, fungi penetrate directly through the cuticle or via natural openings such as stomata. They can survive as spores or resting bodies, e.g. sclerotia, in soil or plant debris, or as mycelium in living plant tissue (Mathre, 1997).

## 1.1. Barley

As one of the world's oldest crops (Nevo, 1992), barley (*Hordeum vulgare* L.) is currently the fourth most cultivated cereal crop in the world after maize, rice and wheat in terms of both quantity produced and area of cultivation (FAO, 2007). Although the main use of barley is as animal feed, the production of alcoholic drinks accounts for the major consumption in human population (Newton *et al.*, 2011).

Barley is mostly grown in temperate areas both as a spring and winter crop. In 1998, the international trade in barley amounted to 19 million tons (=13% of production) (Oerke & Dehne, 2004).

Barley yield loss worldwide is mainly caused by weeds (23%). This is followed by fungal pathogens that cause combined losses of up to 15%. The main economically important pathogens are: *Pyrenophora teres* f. *teres* and f. *maculata* (net blotch, net form and spot form respectively), *Rhynchosporium commune* (leaf scald), *Puccinia hordei* (brown rust), *Blumeria graminis* f.sp. *hordei* (barley powdery mildew) and *Cochliobolus sativus* (foot rot). Leaf scald caused by *R. commune* is the most damaging barley disease in the UK, causing a national yield loss after treatment worth £4.8 million (at £100/t) (HGCA, 2011). In recent years however, a new major threat to barley crops has emerged and gained substantial attention due to its rising agricultural hence economic importance. The filamentous fungus *Ramularia collo-cygni* causes small necrotic spots on a range of host plants, including barley, wheat, maize and other *Gramineae* (reviewed in Walters *et al.,* 2008). The early leaf senescence induced by Ramularia leaf spot (RLS) can result in the premature loss of green leaf area in crops leading to substantial yield losses. The systemic colonisation of barley appears to be at first asymptomatic (Havis & Oxley, 2006; Havis *et al.,* 2006a; Havis *et al.,* 2006b) until the emergence of the ear, when the development of typical symptoms is observed. Symptom expression is thought to be triggered by the transition of plant from vegetative to reproductive growth (Salamati & Reitan, 2006). It is not known however, if environmental conditions can also play a role in appearance of disease symptoms and fungal sporulation late in the season. Although the role of rubellins as a putative virulence factor has been established (Heiser *et al.,*

2003), the evidence of molecular *Ramularia*-host plant interaction is almost non-existent. In order to develop an effective and durable strategy of RLS management, more complete understanding of the pathogen's fundamental biology is required.

## 1.2. The pathogen

### 1.2.1. Taxonomy of *R. collo-cygni*

More than 850 species have been introduced in *Ramularia* Unger and it is therefore one of the larger and more homogeneous of hyphomycete form-genera. Many of the species assigned to it comprise anamorphs of the ascomycete genus *Mycosphaerella* (reviewed in Braun & Sutton, 1991). The generic name and the corresponding species names have been extensively used in mycological literature for more than 150 years (Braun & Sutton, 1991). Many species of *Ramularia* cause foliar spot diseases which are widespread and occur on many diverse crops such as *R. obovata* on *Rumex* (Ellis and Everhart, 1885), *R. vallisumbrosae* on *Narcissus* (Gregory, 1939), *R. onobrychidis* on sainfoin (Hughes, 1949) and most importantly *R. collo-cygni* on barley (Sutton & Waller, 1988).

The fungus *R. collo-cygni* was first reported in 1893 in Italy by Cavara who classified it as a new genus *Ophiocladium* with *O. hordei* as a single species that had been isolated from barley leaves. The original description: 'Hyphae fertiles fasciculatae, anguineo-tortuosae; conidia acrogena, hyalina, continua' summarised a basic morphology of hyphae and conidiation in this new fungal species. In addition, the author also presented a small drawing of tortuous conidiophores and ellipsoid conidia (Cavara, 1893; Figure 1.1).

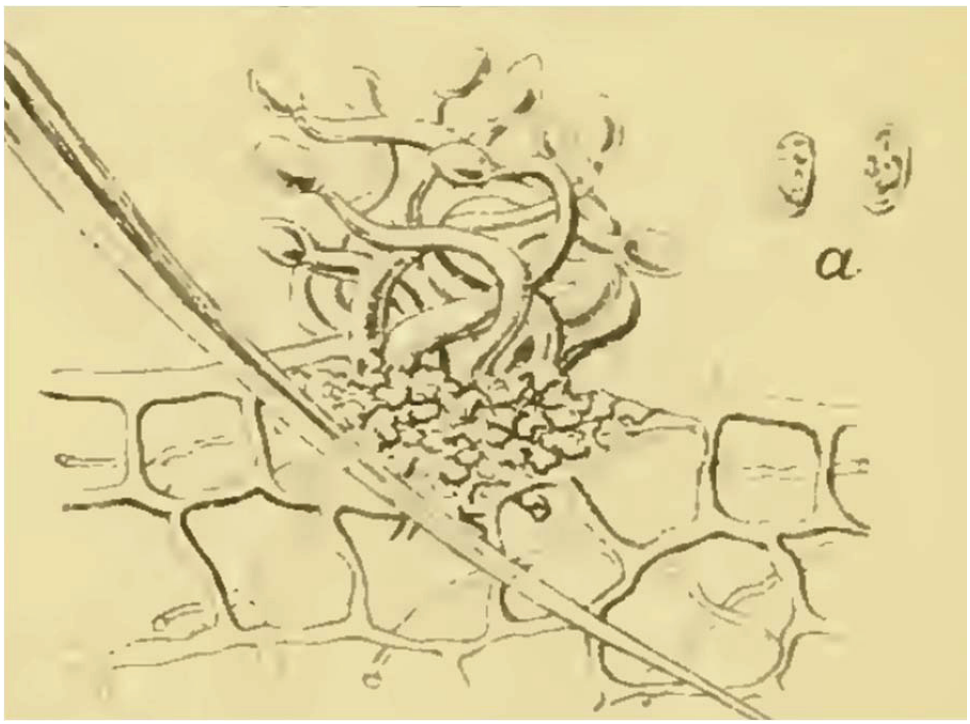


Figure 1.1
The original drawings of tortuous conidiophores and ellipsoid conidia in *O. hordei* (syn. *R. collo-cygni*) by Cavara (1893)

The species was again observed on barley in Italy by Cavara (1894) and Saccardo (1895) who accepted the proposed name *O. hordei*. A second species, *O. anguineum,* was added to the genus *Ophiocladium* by Lindau (1907), based on *Oidium anguineum*, described from *Silybum marianum* (*Compositae*) (cited in Sutton & Waller, 1988). Since then, *O. hordei* started gradually being recorded on barley across the globe. For instance, Joerstad (1930; cited in Sutton & Waller, 1988) reported the fungus in Norway, and Davis (1937) was first to isolate the species from *Phalaris arundinacea* in North America in Wisconsin, USA. Davis (1937) also distinguished *Ophiocladium* from *Ovularia* by the tortuous conidiophores (cited in Sutton & Waller, 1988).

The first discussion of the taxonomy of the genus and species in any detail was attempted by Sprague (1946) who observed the fungus again on *P. arundinacea* and also noted its absence in North America on *Hordeum sativum.* For Sprague the differences between *Ophiocladium* and *Ovularia* were insufficient to warrant separation at the generic level and therefore reclassification of the fungus into *Ovularia* genus was formally proposed (cited in Sutton and Waller, 1988). In 1948, Sprague discussed O. *hordei* in relation to a collection on *Festuca kingii* from Utah, USA and compared it with *Ovularia holci-lanati* Cav., *O. lolii* Volk., and the genus *Ramulaspera* Liro. He suggested that the observed differences in morphology between species such as variation in conidial size and conidiophore length between isolates obtained from different hosts might be the distinctive phases of the same *'Ramularia* - like species' (Sprague, 1948). This was followed by the proposed host range for O. *hordei* that included *Festuca kingii, Glyceria grandis* S.Wats., *Lolium multifiorum* Lam., *L. perenne* L. and *Phalaris arundinacea* from North America. *Ovularia lolii* was 'assigned' to O. *hordei* although the species was kept separated in the text with the comment that it might be a developing phase of *Ramulaspera holci-lanati* (Cav.) Lindau (syn. *Ovularia holci-lanati* Cav.) (Sprague, 1950). Finally, Sprague (1955) suggested keeping the whole group of the *Ovularia* species on *Gramineae* as one species. Thus, the species: *O. pusilla*, *O. lolii*, *O. holci-lanati*, *O. hordei* and *O. baldingerae* effectively became synonymous names.

The name *Ramularia* was first introduced by Unger in 1833 (cited in Sutton and Waller, 1988). The genus comprised two species: *R. pusilla* Unger on *Poa nemoralis* and *R. didyma* Unger on *Ranunculus polyanthemos* L. After many amendments and changes to the species by a variety of different authors (Sutton and Waller, 1988 and

references therein), the genus *Ramularia* was re-described and the new genus *Ovularia* was proposed (Saccardo, 1880; cited in Sutton & Waller, 1988). The species *R. urticae* and *R. cynarae* were the examples of the genus. Also two species were listed: *O. obovata* (syn. *Ramularia obovata*) and *O. sphaeroidea* (syn. *Ramularia sphaeroidea*).

On the basis of morphological studies, the general conclusion was made that the *Ovularia* was a heterogeneous taxon that overlapped with *Ramularia* (Hughes, 1949). In 1958, Hughes (cited in Sutton & Waller, 1988) proposed the names *Ovularia* and *Ramularia* to be synonymous. Subsequently, many authors took two different approaches to the problem of generic concepts in the *'Ramularia - Ovularia'* complex. For instance, Sutton & Pirozynski (1963) and Deighton (1973) maintained the concept of *Ramularia* and *Ovularia* as a synonymy. On the other hand, Carmichael *et al.* (1980) and Ingham (1986) proposed that *Ramularia* and *Ovularia* are distinct genera. Ingham (1986) suggested the artificial distinction between the two genera should be based on catenate conidia compared with solitary conidia. Similarly, Von Arx (1983; cited in Sutton & Waller, 1988) also maintained the opinion that these two genera are close yet distinct and kept them separate on the basis of solitary versus catenate nature of the conidia.

In 1939, the only early experimental evidence was provided by Gregory, who studied *Ramularia vallisumbrosae* Cav. He observed that conidia and conidiophores not only varied greatly in different specimens, but even in different parts of the same leaf. The fungus appeared capable of producing continuous variation of conidiospores from amerospores through phragmospores to scolecospores. Both amerospores and

phragmospores were solitary and sometimes catenate, whilst amerospore production dominated under very humid conditions (Figure 1.2).

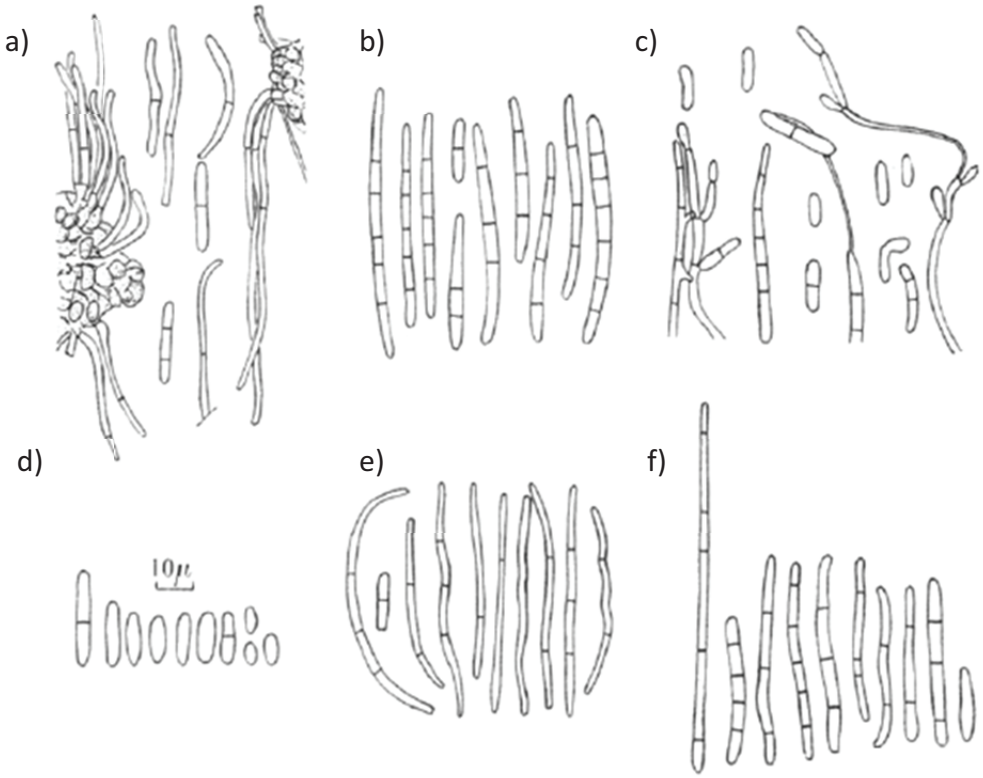


Figure 1.2
Original drawings of spore types observed in *R. vallisumbrosae* on different cultivars of *Narcissus* grown under various environmental conditions: a) phragmospores and scolecospores; b) conidia, collected dry from cv. Victoria; c) conidia after placing in humid conditions; d) conidia collected from *Narcissus* cv. Golden Spur, grown in unusually moist situation; e-f) conidia, collected dry from cv. Golden Spur (Gregory, 1938).

These features somewhat supported the conclusions made by Hughes (1949) that the genera of *Ramularia* and *Ovularia* overlap each other. Although they could be separated by conidial morphology, i.e. they differed in one particular character and

they showed remarkable similarities in all other features, so it seemed reasonable to accept *Ramularia* and *Ovularia* as a synonym. Similarly, since the genus *Ophiocladium* was considered as a synonym of *Ovularia* by Sprague (1946, 1948, 1950, 1955), it was logical to place *Ophiocladium* as a synonym of *Ramularia* as well (Sutton & Waller, 1988). Furthermore, a necrotrophic strategy, pigmentation, conidial development and conidiogenous cell proliferation, scar formation and conidial morphology confirm that *Ophiocladium* is indeed identical with *Ramularia* (Sutton & Waller, 1988). Therefore, it appeared that the genus *Ophiocladium* could only be separated from *Ramularia* by the tortuous (serpentine) nature of the conidiophore apices, a feature that had been suggested previously (Davis, 1937; Sprague, 1950).

More recently, it has been argued that there is no clear purpose in maintaining *Ophiocladium* as distinct taxon on the basis of only one small detail in conidial characteristics (Sutton & Waller, 1988). Placing *Ophiocladium* in synonymy with *Ramularia* in one genus brings together a group of very closely related species on *Gramineae* such as *R. holci-lanati* (Cav.) Deighton and *R. pusilla* Unger. The tortuous conidiophores however, could still be of value in species determination (Sutton & Waller, 1988).

The taxonomic name *Ramularia collo-cygni* was assigned to the fungus by Sutton & Waller (1988). This descriptive nomenclature was based on the characteristic serpentine swan neck-like conidiophores (etymology: *collum* – neck, *cygnus* – swan). Previously, *R. collo-cygni* was not considered as a 'typical' *Ramularia* due to its curled conidiophores and conidial scars (Braun, 1998; Crous, 2000). Although Braun (1998) continued to describe the fungus as *Ophiocladium hordei* (after

Cavara, 1893), in accordance to the existing and accepted taxonomy of genus *Ramularia* as a synonym of previously described genera *Ophiocladium* and *Ovularia* (Sutton & Waller, 1988), the fungi *Ophiocladium hordei* (Cavara, 1893) and *Ovularia hordei* (Sprague, 1946), are now known under the name *R. collo-cygni*.

More recently, using phylogenetic approaches, Crous *et al.* (2000) have classified *R. collo-cygni* together with other *Ramularia* anamorphs based on ITS-1, ITS-2 and 5.8S DNA sequence data from 46 species of *Mycosphaerellaceae.* This study also suggested that the teleomorph of *R. collo-cygni*, if it exists, should be a species of *Mycosphaerella.* This was supported by the report of an *asteromella* stage by Salamati & Reitan (2006).

The summary of taxonomy and nomenclature is listed below:

*Ramularia collo-cygni* Sutton & Waller (1988)

= *Ophiocladium hordei* Cavara, 1893.

= *Ovularia hordei* (Cavara) Sprague, 1946.

= *Ramularia hordeicola* Braun, 1988.

### 1.2.2. Disease symptoms

The appearance of RLS symptoms is typically observed on plants late in the season, usually during the ear emergence (Walters *et al.,* 2008). The lesions are usually linear to rectangular, 1-3 mm long × 0.3 mm wide, in most cases lacking a definite margin (Sutton & Waller, 1988) and are often sharply delineated by leaf veins (Huss & Sachs, 1998). Once the necrotic lesions appear, the remainder of the leaf becomes chlorotic and then necrotic, usually starting from the tip and leaf margins (Huss, 2004). These small pale to medium brown speckles are usually surrounded by a

yellow halo (Salamati & Reitan, 2006). The numerous local infections of the leaf tissue that usually occur during mass sporulation can often coalesce to form larger necrotic areas. A great deal of uncertainties exists with regards to correct diagnosis of RLS. This is due to the fact that the symptoms are very similar to those of abiotic physiological spotting on leaves (Walters *et al.,* 2008; Oxley *et al.,* 2010; Figure 1.3). In some instances they could also be potentially confused with the necrotic lesions on the plants infected with *Pyrenophora teres*, the pathogen responsible for net blotch of barley (Sachs *et al.,* 1998; Walters *et al.,* 2008). In fact, Frei *et al.* (2007) observed that *R. collo-cygni* was never the single cause of necrotic leaf spotting in experiments carried out under field conditions in Switzerland. In their study, the majority of necrotic leaf spotting was caused by the abiotic physiological leaf spotting complex.

Figure 1.3
Typical ramularia leaf spot symptoms on barley (left) versus physiological leaf spotting complex (right). Figure adopted from Oxley *et al.* (2010).

### 1.2.3. Pathogen biology

#### 1.2.3.1. Infection

*R. collo-cygni* gains its entry exclusively through opened stomata within 24 hours after germination of spore on the leaf surface (Sutton & Waller, 1988; Walters *et al.,* 2008) which is common with other closely related stealth plant pathogens such as *Mycosphaerella graminicola* (Thirugnanasambandam *et al.,* 2011). The apparently directional growth of young hyphae towards stomata has been observed *in planta* however the way that the pathogen detects the presence of stomatal pore in the near vicinity is not yet understood (Stabentheiner *et al.*, 2009). It has been hypothesised that *R. collo-cygni* could have been an endophyte tolerated by its host plant (Salamati & Reitan, 2006) that evolved to be a pathogen.

#### 1.2.3.2. Pathogen morphology, germination of conidia and sporulation characteristics

Typical *R. collo-cygni* stromata are substomatal, up to 30 µm diameter, composed of hyaline to very pale brown, thin-walled densely packed pseudoparenchymal cells that appear angular in cross section (=*textura angularis;* Sutton & Waller, 1988). Caespituli are hypogenous, very rarely epigenous, linearly arranged between leaf veins, whitish pink, dry, discrete and rarely confluent. Conidiophores are 30-56 µm long (including the recurved region), arising in caespituli of up to 15 through the stomatal openings or as lateral or upright branches from conidiophore production. Each apical region of the conidiophore produces up to five conidia (Walters *et al.,* 2008). Within 5 hours conidia produce one or occasionally two up to 12 µm long germ tubes per spore (Stabentheiner *et al*., 2009). The conidia are typically obovoid

to ellipsoid, with a verrucose surface, having an eccentrically located basal hilum and are 7-11 μm long and 3-6 μm wide (Stabentheiner *et al.*, 2009). They are ornamented with spikes, with the spikes flattened and enlarged around the eccentric area.

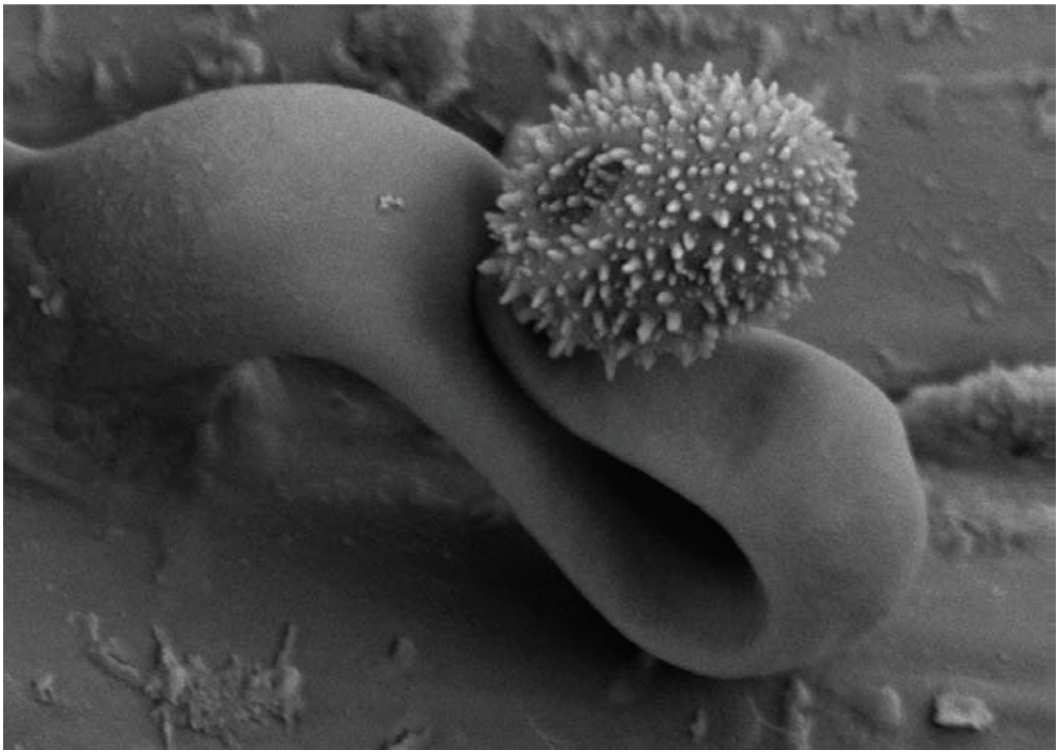

Figure 1.4
Scanning electron micrograph of serpentine swan-neck conidiophore bearing *R. collo-cygni* spore with characteristic surface ornamentation and a scar (Oxley *et al.,* 2010)

### 1.2.3.3. Rubellins

Several fungal pathogens of plants produce toxins that are responsible for the formation of reactive oxygen species (ROS) inside plant cells (Heiser *et al.*, 1998). It has been observed *in vitro* that the colour of ***R. collo-cygni*** colonies on agar medium

varies depending on the type of media. It produces dark pinkish to dark purple coloured colonies on Oxoid Czapek Dox V8 Juice agar (CZV8CM), red coloured colonies on V8 juice agar, and yellow coloured colonies on potato dextrose agar (Salamati & Reitan, 2006; Sutton & Waller, 1988). This colony appearance had started speculations that ***R.*** *collo-cygni* could produce anthraquinone-derived photoactive toxins similar to cercosporin in closely related *Cercospora* species. The compound was subsequently identified as rubellin D (Heiser *et al.*, 2003a; Figure 1.5). This was followed by the discovery that apart from producing rubellin D, ***R.*** *collo-cygni* also produces rubellin A, B, C and E (Heiser *et al.*, 2003a; Miethbauer *et al.*, 2003; Miethbauer *et al.*, 2006). These studies showed that when rubellin D was isolated and introduced into leaves it triggered a necrotic reaction.

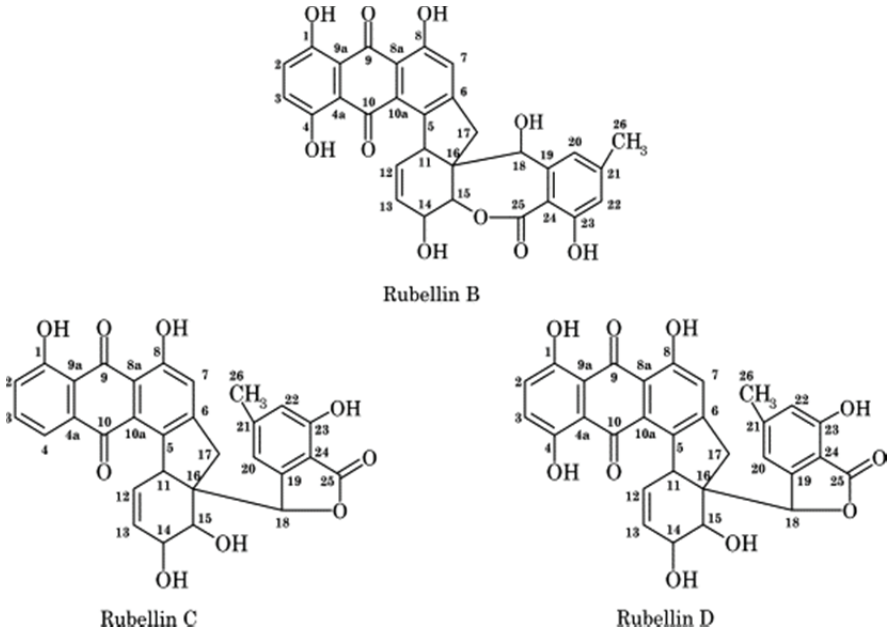


Figure 1.5
Biochemical structure of rubellin B, C and D (Heiser *et al.,* 2003)

### 1.2.4. Epidemiology

#### 1.2.4.1. Distribution of RLS

In recent years, there have been an increasing number of reports of the disease across the globe. For instance, the fungus has been isolated from crops across Europe, Mexico, South America and New Zealand (Stabentheiner *et al.,* 2009). Specifically, in Europe, RLS has been reported in Denmark (Pinnschmidt & Hovmöller, 2004), Germany (Sachs, 2000), Austria (Huss *et al.,* 1987), Scotland (Oxley *et al.,* 2002), the Czech Republic (Minařiková *et al.,* 2004) and Poland (Professor Malgorzata Jedryczka, Institute of Plant Genetics, Polish Academy of Science; personal communication) (Figure 1.6). In New Zealand the fungus has been identified by Sheridan (2000) and Harvey (2002). Most recently, there has been a report of the detection of the pathogen in barley seed in Argentina (Havis *et al*., 2013)

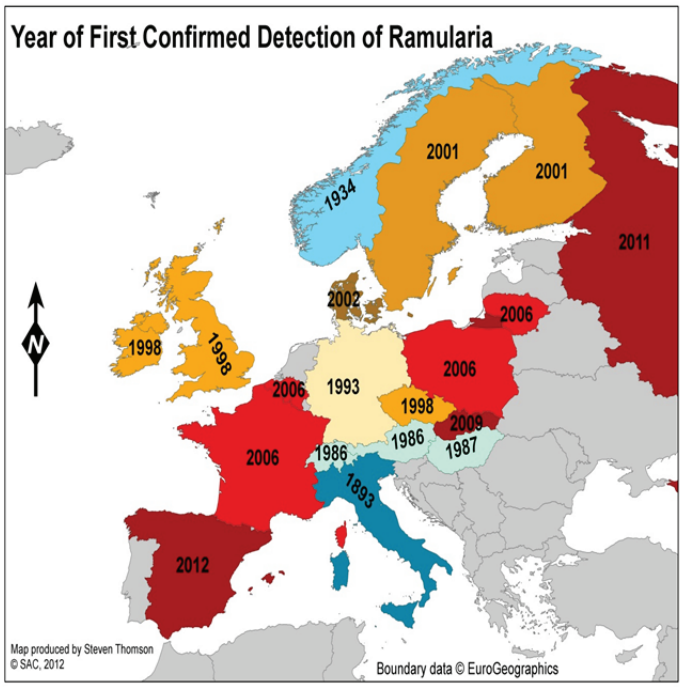


Figure 1.6
Map of *R. collo-cygni* distribution in Europe with year of first report (Steven Thomson, SRUC, 2012).

#### 1.2.4.2. Dispersal of the disease

##### 1.2.4.2.1. Spore dispersal

Characteristic conidial morphology and rapid spread clearly suggests that *R. collo-cygni* spores are airborne (Huss, 2004). The spores are equipped with warts which could facilitate their attachment to any air particle (Salamati & Reitan, 2006). The fungus sporulates abundantly *in planta.* Minihofer (2003) calculated a number of approximately $3 \times 10^{12}$ spores/hectar from a severely attacked barley field. It has also been estimated that up to 50 000 conidia can be produced and discharged from a single heavily infected leaf (Huss, 2004).

##### 1.2.4.2.2. Seed-borne stage

Evidence exists that the fungus may overwinter as a seed-borne stage (Havis *et al.,* 2006a, b; Matusinsky *et al.,* 2011*;* Havis *et al.*, 2013). A recently developed PCR-based diagnostic method for the rapid detection of *R. collo-cygni* confirmed the transmission of the pathogen via seed (Havis *et al.,* 2006a, b). During field experiments in 1999 and 2004 in Scotland, the pathogen was indeed detected in harvested barley grain. Microscopic examination of seedlings cultivated from these seed samples revealed the presence of *R. collo-cygni* within leaves, although it was not present on the leaf surface (Havis *et al.,* 2006a; Havis *et al.,* 2013). Therefore the existence of *R. collo-cygni* seed-borne stage could have serious implications for barley cultivation as the fungus may be present in the majority of crops prior to symptom expression (Havis *et al.,* 2006a).

### 1.2.4.2.3. *Asteromella*

The *Asteromella*-type spermogonial stage has been potentially identified in *R. collo-cygni.* First reports that *Asteromella*-like structures had been observed on barley in close association with *R. collo-cygni*, came from Argentina (R. Delhey; cited by Braun, 2004). Although Braun (2004) suggested that these structures could be the microsporidial state of the fungus, it was not proven experimentally that the spermogonia indeed belong to this pathogen. Since then, there has been an attempt to induce *asteromella* in culture (Salamati & Reitan, 2006; Figure 1.7). The authors were able to observe spermogonium-like structures that formed on barley straw introduced to old *R. collo-cygni* cultures *in vitro*, however no evidence of the presence of spermatia was demonstrated. Therefore it remains unknown whether these structures could play a role in sexual reproduction leading to the production of important disease dispersal structures called ascospores. Alternatively, they could still simply be amorphous sclerotia, a type of asexual resting structures that could also be an important primary inoculum source.

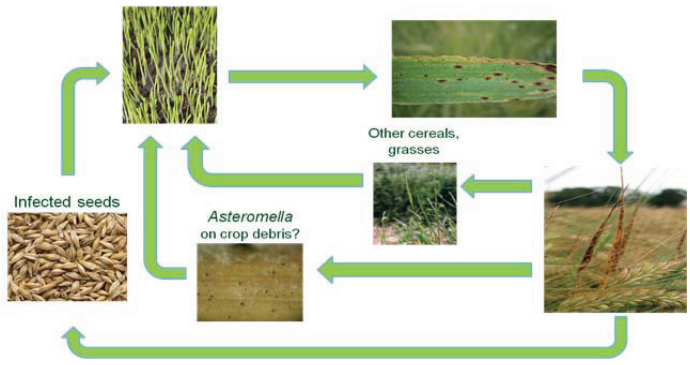


Figure 1.7
Current understanding of the *R. collo-cygni* life cycle that includes asexual cycle comprising horizontal (conidiospores) and vertical transmission (seed), alternate hosts and a suggested secondary structure of unknown function (*Asteromella*). Figure prepared by the author. Individual images source: www.google.com.

#### 1.2.4.2.4. Host range

The pathogen's host range is considered as wide with reports of the disease on winter and spring barley, wheat, oat, maize and perennial grasses (Salamati & Reitan, 2006).

Important insights into the potential *R. collo-cygni* host range have been provided by Huss (2004). Soon after the snow has melted away, they observed the disease on leaves of winter barley. This was followed by spring barley, rye, wheat and oat. Spring barley was massively infected, together with oat in some years. RLS symptoms appeared regularly on rye, however on wheat they developed only under favourable conditions. Maize was colonised in autumn. Although the infection of maize is mainly asymptomatic, certain cultivars may develop characteristic disease symptoms.

Common couch grass (*Elymus repens*) is an important host for the fungus. The annual wild barley *Hordeum murinum* can also become heavily infected. The annual grass *Echinochloa crus-galli,* a common weed in many fields, is not infected in a significant manner. Huss (2004) concluded that the establishment of *R. collo-cygni* as a regularly occurring parasite of barley has led to a considerable infection pressure on other cereals and grasses. This observation was supported by the incidence of the disease in false oat (*Arrhenatherum elatius*). This grass species only showed RLS symptoms if barley was heavily infected. Another common grass species determined to be a compatible host is silky bent-grass, *Apera spica-venti* (Frei, 2004).

In New Zealand, apart from the typical cereal hosts, *R. collo-cygni* has also been recorded on several grass species such as *Agrostis* spp., *Bromus cartharticus* and

*Glyceria fluitans* (Cromey *et al.*, 2004). Most recently, Peraldi *et al.* (2014) have demonstrated that the fungus is also capable of infecting a model grass species, *Brachypodium distachyon.* The most intriguing example of a potential host is certainly the report of RLS on *Cannabis sativa* (Scheuer, 1999).

#### 1.2.4.3. The effect of environmental conditions on disease development

In many cases, spores of fungal pathogens require moisture on leaf surface that could be delivered by fog, dew or rain for germination and successful infection (Schrödter, 1987). Huss (2004) demonstrated that morning dew was a sufficient source of moisture to trigger a massive RLS infection. This study also determined that direct sunlight does not influence the development of necrosis on the leaf, contrary to the observations of Obst and Baumer (1998) and Habermeier *et al.* (2002). Formayer *et al.* (2004) supported the observation that radiation intensity has no effect on RLS development in Austria. They also found that the key factor in disease development is the leaf wetness. It was noted that the Ramularia leaf spots develop preferably on the exposed, pendent parts of the barley leaf blades, where the highest concentration of dew droplets can be observed.

### 1.2.5. Disease control

#### 1.2.5.1. Chemical control

In order to effectively control RLS, the application of mixtures of at least two fungicides active against the fungus is currently recommended to broaden disease protection. A maximum of two applications are applied each growing season. This will provide good protection against the disease and lowers the risk of the

development of fungicide resistance (Oxley *et al.*, 2010). The mixtures of fungicides recommended for control of RLS of barley in the UK are presented in Table 1.1.

Table 1.1
Mixtures of fungicides recommended by HGCA to control RLS in barley (adapted from HGCA, 2013)

| Partner 1 | Partner 2 |
|---|---|
| prothioconazole (Proline 275)* | chlorothalonil (Bravo)* |
| fluoxastrobin + prothioconazole (Fandago)* | chlorothalonil (Bravo)* |
| boscalid + epoxiconazole (Tracker)* | chlorothalonil (Bravo)* |
| isopyrazam + epoxiconazole (Seguris)* | chlorothalonil (Bravo)* |
| isopyrazam + cyprodinil (Bontima)* | chlorothalonil (Bravo)* |
| prothioconazole + bixafen (Siltra Xpro)* | chlorothalonil (Bravo)* |
| prothioconazole (Proline 275)* | azoxystrobin + chlorothalonil (Amistar Opti)* |
| epoxiconazole (Ignite)* | azoxystrobin + chlorothalonil (Amistar Opti)* |

*commercial names of fungicides

To achieve the best control of RLS, it is necessary to apply fungicides before the symptoms emergence, i.e. before flowering. Currently, the recommended time to apply the mixtures of fungicides is at growth stage (GS) 45-49 (Oxley *et al.,* 2010). Earlier treatments, such as at tillering (GS 20-29) or stem extension (GS 30-39), will not provide the total control of RLS. Importantly, after appearance of symptoms, no fungicide will provide an effective protection (Oxley *et al*., 2010), but it is also not permitted to apply fungicides to barley at this late stage. The last date allowed is the start of flowering, GS 61.

### 1.2.5.2. Plant genetic resistance

There are no known varieties of barley that are fully resistant to *R. collo-cygni.* Some cultivars express better resistance than others. Current HGCA ratings for resistance to RLS and other major barley pathogens are presented in Table 1.2

Table 1.2
Spring barley variety resistance ratings presented in 1-9 scale, where higher number represents better disease resistance, e.g. 9 = best resistance. *Ramularia* scores are based on SRUC assessments of Recommended List trials in Scotland (HGCA, 2013)

| Variety | Rhynchosporium | Mildew | Yellow rust | Brown rust | Ramularia |
|---|---|---|---|---|---|
| NFC Tipple | 5 | 9 | 3 | 9 | 6 |
| Oxbridge | 7 | 8 | 4 | 7 | 6 |
| Cocktail | 7 | 8 | 4 | 8 | 5 |
| Westminster | 8 | 9 | 5 | 5 | 6 |
| Troon | 4 | 9 | 8 | 6 | 4 |
| Carafe | 4 | 9 | 3 | 9 | 6 |
| Cellar | 4 | 9 | 4 | 8 | 6 |
| Prestige | 4 | 9 | 4 | 9 | 4 |
| Chalice | 5 | 9 | 7 | 4 | 6 |
| Optic | 4 | 5 | 8 | 6 | 6 |
| Decanter | 5 | 9 | 8 | 6 | 8 |
| Waggon | 4 | 9 | 5 | 9 | 6 |
| Tocada | 4 | 6 | 3 | 4 | 7 |
| Wicket | 6 | 7 | 6 | 8 | 6 |
| Power | 6 | 9 | 6 | 6 | 7 |
| Doyen | 8 | 8 | 3 | 7 | 6 |
| Spire | 4 | 6 | 5 | 5 | 5 |
| Rebecca | 7 | 7 | 3 | 5 | 7 |
| Kirsty | 5 | 7 | 4 | 9 | 6 |
| Static | 5 | 9 | 6 | 8 | 6 |
| Riviera | 5 | 8 | 5 | 6 | 6 |

McGrann *et al.* (2014) have recently investigated the trade-off between the highly effective resistance to powdery mildew conferred by *mlo* mutant alleles and increased susceptibility to RLS. The presence of *mlo* alleles increased severity of RLS in both field trials and seedling tests. One QTL was identified in a doubled-haploid population for susceptibility to RLS, co-localising with the *mlo-11* allele for mildew resistance. The results suggested that the widespread use of *mlo* mildew

resistance alleles may be one of the factors that contributed to the emergence of RLS as a major disease of barley.

## 1.3. Molecular diagnostics and cell biology tools

Significant progress has been made in the understanding of the *R. collo-cygni* life cycle by the development of PCR-based methods for detection of fungus in barley tissue (Havis *et al.,* 2006a; Frei *et al.,* 2007; Taylor *et al.,* 2009) and also the application of scanning electron microscopy techniques (Stabentheiner *et al.,* 2009). A recent report of the first successful stable genetic transformation of the fungus (Thirugnanasambandam *et al.,* 2011) has now provided an excellent tool for studying the infection and fundamental biology of this economically important ascomycete.

### 1.3.1. Studies of biology and life cycle in fungal plant pathogens using PCR

In order to gain a better understanding and accuracy of the incidence and distribution of plant pathogens as well as their early detection, a reliable and rapid molecular diagnostic assay is required. The internal transcribed spacer (ITS) regions of ribosomal RNA (rRNA) have been shown to be a suitable basis for the development of a molecular detection assay in fungi (Goodwin *et al.,* 1995; Langrell, 2002). The nested PCR approach has been successfully utilised in the identification and detection of other plant pathogens (Hamelin *et al.,* 2000; Langrell, 2005). Furthermore, the ready accessibility of these regions using universal primers (White *et al.,* 1990) makes them particularly attractive for sequence characterisation and the eventual design of species-specific primers.

Consequently, Havis *et al.* (2006a) and Frei *et al.* (2007) have developed a species-specific and sensitive nested PCR-based method for the rapid detection of *R. collo-cygni* direct from barley. Such tools were useful in elucidating the basic epidemiology of this important pathogen. The nested PCR methods were followed by a quantitative real-time PCR assay (Taylor *et al.,* 2009) which allows not only recognition of the pathogen, but also quantification of its DNA concentration within host tissue. This assay proved successful in determining the close correlation of *R. collo-cygni* DNA levels and symptom expression.

### 1.3.2. Live-cell imaging with fluorescent protein labelling

A visual reporter molecule is a truly powerful tool for many different biological applications, including the observation of the disease progression in plants. Several reporter genes have been applied in investigations of the disease development and molecular pathogen – host plant interactions. These include Green Fluorescent Protein (GFP) and monomeric Red Fluorescent Protein (mRFP) or DsRed fluorescent protein.

Utilisation of the genetically transformed isolates expressing fluorescent protein genes in combination with confocal laser scanning microscopy (CLSM) offers tremendous potential for in-depth analysis of the infection process in living host tissue as demonstrated in many studies of fungal and oomycete pathogens (Spellig *et al.,* 1996; Maor *et al.,* 1998; van West *et al.,* 1999; Balint-Kurti *et al.,* 2001; Sexton and Howlett, 2001; Skadsen and Hohn, 2004; Linsell *et al.,* 2010). Most recently, live-tissue imaging of the colonisation and asymptomatic phase of *R. collo-cygni* on barley leaves has been reported (Thirugnanasambandam *et al.,* 2011).

#### 1.3.2.1. Using green fluorescent protein (GFP) as a reporter molecule

The GFP gene was first cloned from the jellyfish *Aequorea victoria* by Prasher (1992). Shortly after, it was successfully expressed and conferred fluorescence to bacteria, followed by yeast, mammals, *Drosophila*, plants and filamentous fungi (reviewed in Lorang *et al.,* 2001). The success of GFP as a reporter is attributed to its qualities. Unlike other reporter molecules such as β-glucuronidase (GUS) or β-galacturonidase (GUSB), it requires only UV or blue light between 395 and 475 nm for excitation and emits light at a maximum of 508 nm. Furthermore, GFP is extremely stable *in vivo* and can be fused to the C or N terminus of many proteins without loss of activity. This property permits tagging of proteins for gene regulation analysis, their localisation or labelling of specific cellular organelles. Limitations of this reporter are its low turnover rate, 2-h lag time for autoactivation of its chromophore, improper folding at high temperatures (37 °C), resulting in non-fluorescent or insoluble forms of the protein and requirement for oxygen, often not present in sub-cellular locations or cell types (reviewed in Lorang *et al.,* 2001). These characteristics, however, have not been limiting factors for many applications. Furthermore, mutant forms of GFP have been developed that possess the ability to fold correctly at high temperatures or with increased fluorescence and reduced photobleaching. Coupled with confocal microscopy, GFP is a very useful and highly informative tool for many biological investigations.

*Ustilago maydis was* the first filamentous fungus for which successful expression of GFP was reported (Spellig *et al.,* 1996). This was followed by *Aspergillus nidulans* and *Aureobasidium pullulans*. Since then many genera of true fungi have been transformed with GFP, for instance *Colletotrichum, Mycosphaerella, Magnaporthe,*

*Cochliobolus, Trichoderma, Podospora, Sclerotinia, Schizophyllum, Aspergillus* (reviewed in Lorang *et al.,* 2001) and *Leptosphaeria* (Sexton and Howlett, 2001).

Most recently, GFP was successfully introduced as a reporter molecule to *R. collo-cygni* (Thirugnanasambandam *et al.,* 2011). They showed for the first time in this fungus that GFP can be used as vital marker for studies of the symptomless infection by *R. collo-cygni* in its host plant, *Hordeum vulgare.*

#### 1.3.2.2. Red fluorescent protein reporter as a useful alternative to GFP.

The discovery of a red fluorescent protein DsRed from reef coral *Discosoma* spp. and its derivative, monomeric red fluorescent protein (mRFP1) (Matz *et al.,* 1999; Campbell *et al.,* 2002 respectively; reviewed by Nguyen *et al.,* 2007) has broadened significantly the utility of fluorescence microscopy in biological investigations. This innovation provided important tools for simultaneous imaging with GFP, permitting visualisation of protein-protein interactions in living cells. Nguyen *et al.* (2007) showed that mRFP1 is comparable to eGFP for cell biological research in most organisms. Since the development of mRFP1, other more intensely red fluorescent proteins have been developed, such as tdTomato fluorescent protein (Shaner *et al.,* 2004).

DsRed expressing stable *R. collo-cygni* transformant colonies were most recently obtained (Thirugnanasambandam *et al.,* 2011) however these isolates have not been used in any studies of pathogen infection to date.

#### 1.3.2.3. Confocal microscopy (CLSM) as a powerful tool for a wide range of biological investigations

Confocal laser scanning microscopy (CLSM) has become a truly invaluable tool for a wide range of applications in biological and medical investigations (Claxton *et al.,* 2005, unpublished). The microscopes are coupled with photomultipliers with high quantum efficiency in the near-ultraviolet, visible and near-infrared spectral regions. These instruments therefore, are able to examine fluorescence emission ranging from 400 to 750 nm.

The great advantage of confocal microscopy is that it allows a living specimen to be examined at greater resolution than conventional light microscopes. There is no need of lengthy preparation and the specimen can simply be fixed to a microscope slide using double-sided sticky tape. The essential feature of confocal imaging is that the illumination and detection are confined to the same spot in the specimen at any one time. Fluorescence from the specimen is registered by the detector and is converted into a digital image. These instruments capture in-focus images only, unlike standard light and fluorescence microscopes. The emitted light is focussed through a small pinhole in front of the detector at a fixed focal distance from the object. Therefore, only light emitted from particular focal point can pass through to the detector, eliminating out-of-focus information and collecting images of thin layers within the specimen. Furthermore, the confocal microscope can collect a series of images at different depths throughout the specimen, which then allows creation of 3-dimensional images (a Z-stack). The disadvantage however, is that confocal microscope can obtain information only from a relatively thin layer into the specimen, especially at higher magnification, and therefore sometimes the collected signal can be low.

Confocal microscopes use highly focused, high energy, laser light sources to provide distinct wavelengths of powerful illumination deep into the specimen. Different wavelengths of light can be used to excite different fluorophores (fluorescent molecules) or fluorochromes (fluorescent dyes) which in turn emit light of a distinct wavelength. The detectors in the confocal microscope separate them to produce images that show the distribution of fluorescent sources present in examined tissue. In general, confocal microscopy has a clear potential to produce very precise images and can be used in many different biological investigations.

## 1.4. Aims and objectives:

Overall aim of this project is to increase the understanding of the fundamental biology and life cycle of *R. collo-cygni.*

### 1.4.1. Analysis of infection development using GFP expressing isolate and CLSM

Relatively little is known about the infection strategy and development of Ramularia leaf spot disease. The study will utilise the transgenic *R. collo-cygni* isolates expressing GFP and DsRed fluorescent reporter markers to visualise the infection progression in living host tissues by confocal microscopy. The role of rubellin in symptom development and the structure of putative molecular machinery involved in rubellin biosynthesis will also be addressed. Understanding how the fungus colonises the host plant barley should help in the development of future strategies of RLS management.

### 1.4.2. Investigating the mode of a seed-borne transmission in *R. collo-cygni*

By using GFP expressing strain of the fungus, the mode of the seed-borne transmission will be investigated. The understanding of this important part of the pathogen's life cycle should help in disease control by the initiating the development of new specific seed treatments.

### 1.4.3. Analysis of sexual reproduction

Recent development of fungicide resistance in *R. collo-cygni* (Foutaine and Fraaije, 2009) has instigated research into the forces that may facilitate its rapid evolution. We will therefore aim to induce reproduction *in vitro* and analyse the potential resting stage in this important plant pathogen.

#### 1.4.3.1. Cell biological approaches

In order to verify the existence of sexual reproduction, the aim is to induce the sexual development and undertake comprehensive analysis by correlative use of light-, confocal- and low temperature scanning electron microscopy. Should sexual development be found, wax-embedded tissue samples of the obtained ascocarps will be prepared and analysed by light microscopy. This should help enhance our current poor understanding of sexual reproduction in *Mycosphaerella* species.

#### 1.4.3.2. Characterisation of MAT loci by PCR and sequencing

Sexual reproduction frequently results in genetic recombination and this has a major impact on the dynamics and fitness of a species. The teleomorphs of the *Ramularia* plant pathogens are presumed to be of *Mycosphaerella* type, however this is largely unknown as they have thus far not been successfully induced by crosses in the laboratory. As a first step to understanding the reproduction cycle in the apparently

asexual species, an objective is to identify which mating type(s) are present in the genome of this fungus and to study their frequency in defined field populations. To achieve this objective, an attempt will be made to: (1) sequence and characterise the mating type genes of *R. collo-cygni* using PCR-based techniques, (2) develop a multiplex PCR method for rapid identification of the *MAT1-1-1* and *MAT1-2* genes to determine the frequencies of the mating types in different *R. collo-cygni* populations.

# Chapter 2

# Analysis of infection strategy and development of Ramularia leaf spot

# 2. Analysis of infection strategy and development of Ramularia leaf spot

## 2.1. Introduction

The phytopathogenic fungus *R. collo-cygni* (Sutton & Waller) initiates a leaf spot disease on barley (RLS) and other cereals and grasses, and due to loss of green leaf area and subsequent early ripening of infected plants, the pathogen causes yield losses of up to 20 per cent, with an average loss in Scotland at 0.4 tonnes per hectare (Oxley, 2007). The development of PCR-based methods for detection of the fungus in barley tissue (Havis *et al.,* 2006a; Frei *et al.,* 2007; Taylor *et al.,* 2009) and the application of scanning electron microscopy (Stabentheiner *et al.,* 2009) have expanded our understanding of the *R. collo-cygni* life cycle. A recent report of the first successful stable genetic transformation of *R. collo-cygni* with fluorescent protein markers (Thirugnanasambandam *et al.,* 2011) has now provided an excellent tool for studying pathology of this economically important fungus. This chapter will discuss specific elements of the biology and life cycle of *R. collo-cygni* in order to achieve a better understanding of infection and subsequent stages of RLS development.

### 2.1.1. Infection characteristics with reference to the related pathogenic ascomycetes

*R. collo-cygni* conidia germinate on the leaf surface under moist conditions and start an early development of the fungus. The typical weather conditions that induce the rapid sporulation of the pathogen have been suggested (Sutton & Waller, 1988; Huss, 2004) and are described previously (Chapter 1, Section 4). The fungus enters

through open stomata within 24 hours after spore germination on the leaf surface (Sutton & Waller, 1988; Walters *et al.,* 2008) which is common with other closely related stealth plant pathogens such as *Zymoseptoria tritici* (Goodwin *et al.,* 2011). Although the apparently directional growth of young hyphae towards stomata has been observed *in planta*, it remains unclear how the pathogen detects the presence of stomatal pores (Stabentheiner *et al.*, 2009). As *R. collo-cygni* develops, it establishes a hyphal network on the leaf surface (Thirugnanasambandam *et al.,* 2011). This growth of mycelium usually extends above the infection site connecting the colonised stomata on the leaf surfaces. It has been reported that the pathogen can complete its life cycle without producing any symptoms during the entire barley growing season (Nyman *et al.,* 2009).

Sutton and Waller (1988) suggested that once inside the leaf, the fungus grows intercellularly, forming branched hyphae which colonise the mesophyll tissue although no evidence was presented to support this statement. Recently, Stabentheiner *et al.* (2009) showed the presence of fungal hyphae in the mesophyll of naturally infected samples from the field however it has not been shown that the observed hyphae indeed belonged to *R. collo-cygni*. Although molecular methods of detection now combined with microscopy approaches have enhanced the understanding of life cycle, some important aspects of infection biology still require in-depth analysis.

The asymptomatic infection of barley using the transgenic *R. collo-cygni* expressing GFP reporter marker has been studied previously (Thirugnanasambandam *et al.,* 2011) however the transition of the fungus from symptomless to its symptomatic phase remains poorly understood. In the closely related hemibiotroph, *Z. tritici*,

infection development on wheat by this fungus resembles *R. collo-cygni* as it also consists of an extended period of symptomless infection that is followed by necrotrophic growth (Goodwin *et al.,* 2011).

GFP expressing pathogen isolates have proved an excellent tool to visualise the full infection progression *in planta* (Rohel *et al.,* 2001). Confocal microscopy confirmed the penetration of *Z. tritici* through stomata, but also showed for the first time that the fungus was capable of infecting wheat leaves between the epidermal cells. This research also demonstrated the colonisation of the mesophyll during the transition to symptomatic phase confirming the findings of the previous histological study of *Z. tritici* infection of wheat using light microscopy (Kema *et al.,* 1996).

Besides barley, *R. collo-cygni* has been isolated from other cereal crops such as wheat, oat, rye and maize (Huss, 2004). According to this report, RLS symptoms may appear regularly on rye whereas on wheat they developed only under favourable conditions. Huss *et al.* (2004) also noted that infection of maize was mainly asymptomatic however certain cultivars may develop characteristic disease symptoms.

An important source of inoculum may come from annual and perennial grass species such as common couch grass (*Elymus repens*), annual wild barley (*Hordeum murinum*), annual grass *Echinochloa crus-galli* (Huss, 2004) and silky bent-grass, *Apera spica-venti* (Frei, 2004). In New Zealand, *R. collo-cygni* has also been recorded on several grass species such as *Agrostis* spp., *Bromus cartharticus* and *Glyceria fluitans* (Cromey *et al.*, 2004).

Huss (2004) concluded that the regular occurrence of *R. collo-cygni* on barley has led to a considerable infection pressure on other cereals and grasses. For example, RLS symptoms were only observed on false oat (*Arrhenatherum elatius*) if barley was heavily infected. Most recently, Peraldi *et al.* (2014) have demonstrated that the fungus is also capable of infecting a model grass species, *Brachypodium distachyon*. Perhaps the most intriguing example of a potential host is the report of RLS on *Cannabis sativa* (Scheuer, 1999). To date, this is the only dicot species shown to be colonised by *R. collo-cygni*.

Additional studies of the host- and non-host interactions could provide further insights into the potential *R. collo-cygni* host range in the field that this fungus may have evolved to colonise and exploit as inoculum sources. The characterisation of the fungal behaviour during non-host interactions could then be used for screening a range of barley cultivars for resistance sources using microscopy. Interesting research on non-host behaviour has been undertaken in closely related species of *Mycosphaerella* pathogens that cause Black Sigatoka disease of banana (Balint-Kurti *et al.,* 2001). To examine the *Mycosphaerella* banana pathogens on non-host species, tomato and tobacco plants were inoculated with spore suspension of GFP expressing transformants of *M. fijiensis* and *M. eumusae*. Although conidia of both species germinated and formed stomatopodia over the stomata of both non-host plants, subsequent penetration of substomatal cavities was not observed. Approximately 6 weeks post-inoculation the *M. eumusae* transformant was observed growing within a large necrotic spot that had developed occasionally on tobacco leaf however it was likely a saprophytic growth on already dead or severely senescent tissue (Balint-Curti and Churchill, 2004).

This ability of *M. fijiensis* and *M. eumusae* to locate stomata on the very distinct surfaces of banana, tobacco and tomato leaves could indicate that these pathogens are not guided by some host-specific topography of the leaf surface as is the case in some other plant pathogens (Hoch *et al.,* 1987; Tucker and Talbot, 2001). Subsequent failure to establish infection on the non-hosts is not yet understood. Some of the lesions observed on tomato leaf cells were located directly under stomatopodia which could suggest a classical hypersensitive response. On the other hand, on tobacco leaves and in many cases on tomato, no clear response was present (Balint-Curti and Churchill, 2004).

### 2.1.2. Objectives

Utilisation of the genetically transformed isolates expressing fluorescent protein genes in combination with CLSM offers tremendous potential for in-depth analysis of the infection process in living host tissue as demonstrated in many studies of fungal and oomycete pathogens (Spellig *et al.,* 1996; Maor *et al.,* 1998; van West *et al.,* 1999; Balint-Kurti *et al.,* 2001; Sexton and Howlett, 2001; Skadsen and Hohn, 2004; Linsell *et al.,* 2010). Most recently, live-tissue imaging of the asymptomatic phase of *R. collo-cygni* infection using a GFP expressing isolate on barley leaves has been reported (Thirugnanasambandam *et al.,* 2010). Although DsRed expressing stable *R. collo-cygni* transformant colonies were also generated, this isolate has not been used in any studies of pathogen infection to date.

The aim of this study was to elucidate the infection biology of *R. collo-cygni* on barley and other potential host- and non-host plant species in much greater detail than previously attempted and analyse the symptom development by the live cell

visualisation of fluorescent marker tags stably expressed in pathogen cytoplasm.

## 2.2. Materials and methods

### 2.2.1. Isolates

#### 2.2.1.1. Wild type isolates

Two *R. collo-cygni* wild type isolates were used in this study: Scottish isolate B1 and the recently sequenced, Danish isolate DK05Rcc001 (SRUC, unpublished). Both strains originate from barley cv. Braemar.

For cultivation of fungal cultures *in vitro*, several types of solid media have been tested, such as potato dextrose agar (PDA), Sabouraud agar, V8 juice agar and malt extract agar (MEA). Both isolates appeared to perform similarly during vegetative growth on all types of media. The cultures were maintained in controlled environment in darkness at 15$^{o}$ C.

#### 2.2.1.2. *R. collo-cygni* isolates expressing fluorescent reporter markers

Transgenic *R. collo-cygni* isolates 8B9 (Rcc-8B9-GFP) and Stratego (Rcc-ST-DsRed) expressing GFP and DsRed fluorescent proteins, respectively (Thirugnanasambandam *et al.*, 2011) were kindly provided by Dr Adrian Newton, The James Hutton Institute. Fungal cultures were maintained on clarified V8 juice agar (10 mM $CaCO_3$ in 20 % (v/v) V8 juice, 1.5 % agar) at 15$^{o}$ C in the dark.

### 2.2.2. Plant material

Barley seeds (*Hordeum vulgare*) cvs. Optic, Belgravia, Garner and Cocktail were germinated in pots and maintained in a glasshouse under 16 h light at 18$^{o}$C (day) and 8 h dark at 16$^{o}$C (night). In order to ensure the use of only *R. collo-cygni*-free kernels

in this study, the absence of the fungal DNA in seed material was determined by quantitative real time PCR (Taylor *et al.,* 2009).

In the early infection comparative study between barley and possible alternate hosts, winter wheat (*Triticum aestivum*) cultivar Alchemy and two additional perennial grasses, cock's foot (*Dactylis glomerata*) and Italian ryegrass (*Lolium multiflorum*) were germinated and grown under the same conditions as described for barley. In addition, a dicot model wild legume species, *Lotus japonicus* MG20, was also tested for compatibility with *R. collo-cygni*. The setup for this experiment was slightly different than for monocot species. Here, seeds were germinated directly in compost placed at the bottom of magenta boxes (Sigma Aldrich) and grown until 5 - 6 cm tall.

### 2.2.3. Detached leaf assay

Seeds of barley (*Hordeum vulgare*) cv. Optic were germinated and maintained in a glasshouse under 16 h light at 20°C (day) and 8 h dark at 16°C (night) for up to 30 days. Detached-leaf assays were performed as described in Thirugnanasambandam *et al.* (2011) and Newton *et al.* (2001) with some modifications. Briefly, leaf sections approximately 3-5 cm in length were taken from the 2nd and 5th – 6th leaf, gently abraded near the centre of the adaxial surface with a soft paintbrush to disrupt the surface wax structure, and placed with the abaxial surface down on 0.5 % distilled water agar containing 150 mg/L benzimidazole (Aldrich) in sealed polystyrene boxes (79 x 47 x 22 mm; Stewart-Solutions). The abraded area of each leaf was inoculated with 10 µL of mycelial fragment suspension (Figure 2.1) and the boxes incubated in a controlled environment cabinet (Leec, model LT1201) at 17°C, light intensity 200 $\mu mol.m^{-2}.s^{-1}$

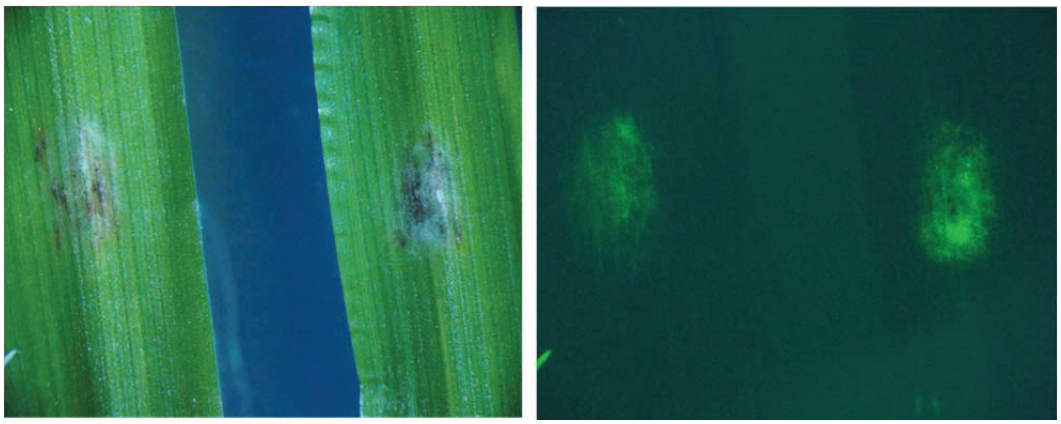

Figure 2.1
Detached leaf segments incubated on 0.5% water agar inoculated with Rcc-8B9-GFP isolate. Image taken using Olympus fluorescence stereo microscope equipped with gfp3 filter. Normal view (left) and corresponding fluorescence view (right)

### 2.2.4. Whole plant inoculation assay

Spot-inoculation of whole barley leaves was performed as described for detached leaf assays (Thirugnanasambandam *et al.*, 2011; Section 2.3) with some modifications. Mycelial fragments of GFP-expressing transformed isolates from 2-week-old spread-plates were prepared by scraping the colony surface with a sterile spatula, homogenising and then filtering through sterile glass wool in the neck of a sterile glass funnel. It was not possible to accurately quantify a fungal mycelial fragment inoculum suspension due to the apparent problem with obtaining spores in culture as discussed earlier (Chapter 2, Section 1). The mycelium harvested from a single spread plate was diluted in 5 mL sterile distilled water to drop-inoculate 10 µL onto each of up to 10 inoculation sites per leaf. For younger leaves, inoculum was places in the central region of a leaf blade whilst older leaves were inoculated on opposite sides of a midrib. Once inoculated, to maintain necessary high humidity to promote fungal growth and infection, the plants were gently covered with transparent

plastic bags for 48 hours without disturbing the drops of inoculum on leaves. Leaf segments 2 - 3cm long with the inoculation zone in the centre were then mounted and analysed microscopically on subsequent days throughout the live span of each infected barley plant. At least 5 inoculated leaves were studied for each time point. The experiment was repeated three times with different preparations of inoculum and separately cultivated plants.

For the inoculation experiments with *Lotus japonicus* MG20 grown in isolated environment facilitated by two connected magenta boxes, random leaves were drop-inoculated with Rcc-8B9-GFP however due to much smaller size of *L. japonicus* leaves in comparison with barley and other grasses leaf blades, only a 5µl drop of suspension of homogenised mycelium was used per leaflet (Figure 2.2)

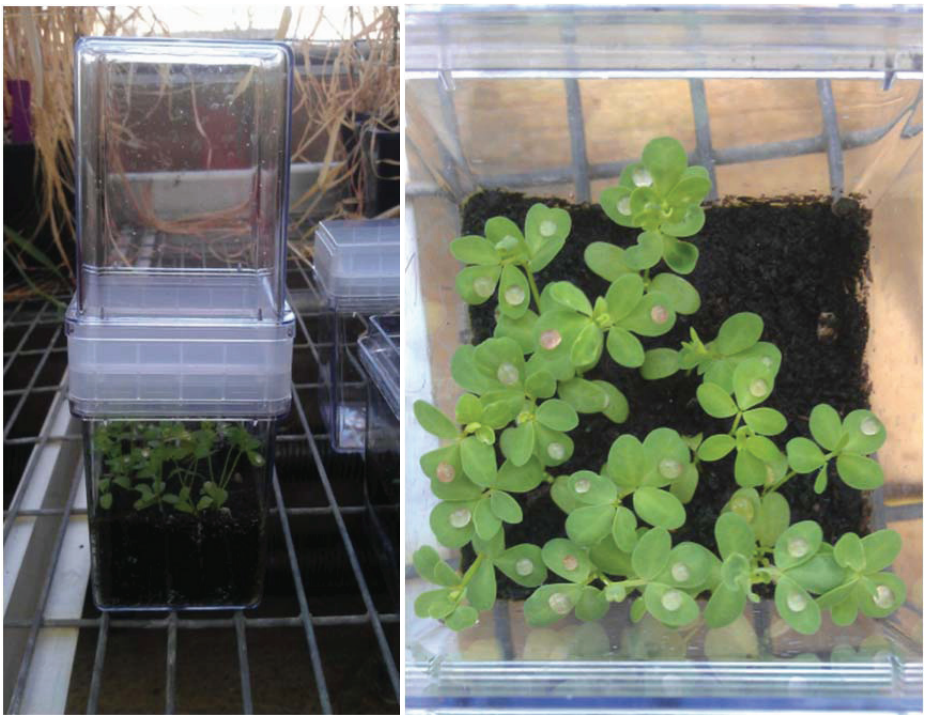

Figure 2.2
The connected 'Magenta' boxes setup used for the experiment with inoculation of *L. japonicus* MG 20. Right: drop-inoculated leaflets with the isolate Rcc-8B9-GFP.

### 2.2.5. Confocal microscopy (CLSM) conditions

To examine the plant material inoculated with transgenic *R. collo-cygni* isolates, we used a Leica SP2 CLSM on a DM6000 microscope fitted with a FI/RH filter block (excitation filter BP 490/15, dichroic mirror 500, emission filter BP 525/20; excitation filter BP 560/25, dichroic mirror 580, emission filter BP 605/30) and Leica water-dipping lenses (HCX APO L10x /0.30 W U-V-1, L20x /0.50 W U-V-1, L40x /0.80 W U-V-1 or L63x /0.90 W U-V-1). GFP fluorescence was imaged at the excitation wavelength of 488 nm and emission was collected at 500–530 nm. The autofluorescence signal from chlorophyll was collected simultaneously at light wavelengths between 650 and 700 nm. Transmission images (non-confocal) were captured using the transmission detector of the microscopes to collect 488-nm light passing through the leaf. Unless otherwise stated, images are overlay projections of z-stacks presented as maximum intensity projections and were assembled and edited using image editing software MacBiophotonics® ImageJ or Adobe Photoshop® CS5 Extended Edition.

### 2.2.6. Light microscopy conditions

Light microscopy was performed either using a Reichert-Jung Polyvar Photomicroscope with brightfield (BF) or differential interference contrast (DIC) optics, and 40x (1.0 NA) plan apochromat objective, or using a Nikon Eclipse TE2000 inverted microscope with DIC optics and a 40x (1.0 NA) plan fluor objective. Images from the Polyvar microscope were acquired by Canon EOS 600d SLR camera whilst images from the Eclipse microscope were captured with a DXM1200F camera and ACT-1 software.

### 2.2.7. Aniline blue staining

To examine leaf material from the field exhibiting typical RLS symptoms, leaves were destained and fixed in Petri dish with 1:1 v/v solution of glacial acetic acid and absolute ethanol, and kept for 48 hours until chlorophyll was completely removed from the leaves. Fixed leaf samples were then submerged twice for 30 minutes in sterile distilled water to remove acetic acid/ ethanol solution, and subsequently dehydrated with a series of increasing concentration of ethanol (25, 50, 75, 85, 95 and 100 %). Samples were stained with aniline blue stain (aniline blue/ ethanol 1:1) for a range of times, specifically 15, 30 and 60 minutes. To remove excess of aniline blue, leaves were briefly destained with absolute ethanol prior to mounting on a microscope slide.

## 2.3. Results

### 2.3.1. Symptomless infection characteristics

During asymptomatic stage, the infection was clearly restricted to the leaf surface and substomatal cavities. A thin spider web-like network of hyphae, driven by frequent hyphal fusion, radiated from inoculation site and colonised leaf surface. This epiphytic hyphal network appeared well organised as the pathogen used epidermis cell junctions and topography of the phylloplane for colony establishment (Figure 2.3 a). Pathogen covered substantial areas of the leaf at 3 dpi (Figure 2.3 b).

Similarly to the related ascomycete plant pathogens, such as *Z. tritici* and *Pseudocercospora fijiensis* (syn. *Mycosphaerella fijiensis*), *R. collo-cygni* gained entry into the host tissue through stomata by direct penetration of open stomatal pores. However, in many cases, the development of a morphologically distinct

structure called stomatopodium or infection peg was observed at the hyphal tip (Figure 2.3a). The existence of this structure has not been reported previously in *R. collo-cygni.* It appeared spherical or cylindrical in shape, somewhat swollen, with the diameter of approximately 4 - 5 µm, much thicker that surface colonising hyphae. It was often observed facilitating penetration of closed stomatal pores. In many instances, stomatopodia also developed as side branches of the epiphytic hyphae (Figure 2.3c). The swollen stomatopodia started branching after the entry into substomatal cavities (Figure 2.3d). They became multibranched thick conidiogynous basal aggregates at 7 dpi and remained connected and 'fed' by the epiphytic hyphal network spreading on the leaf surface (Figure 2.3e). Subsequently, an increasing number of coniodiogenous aggregates was observed in substomatal cavities (Figure 2.3 f).

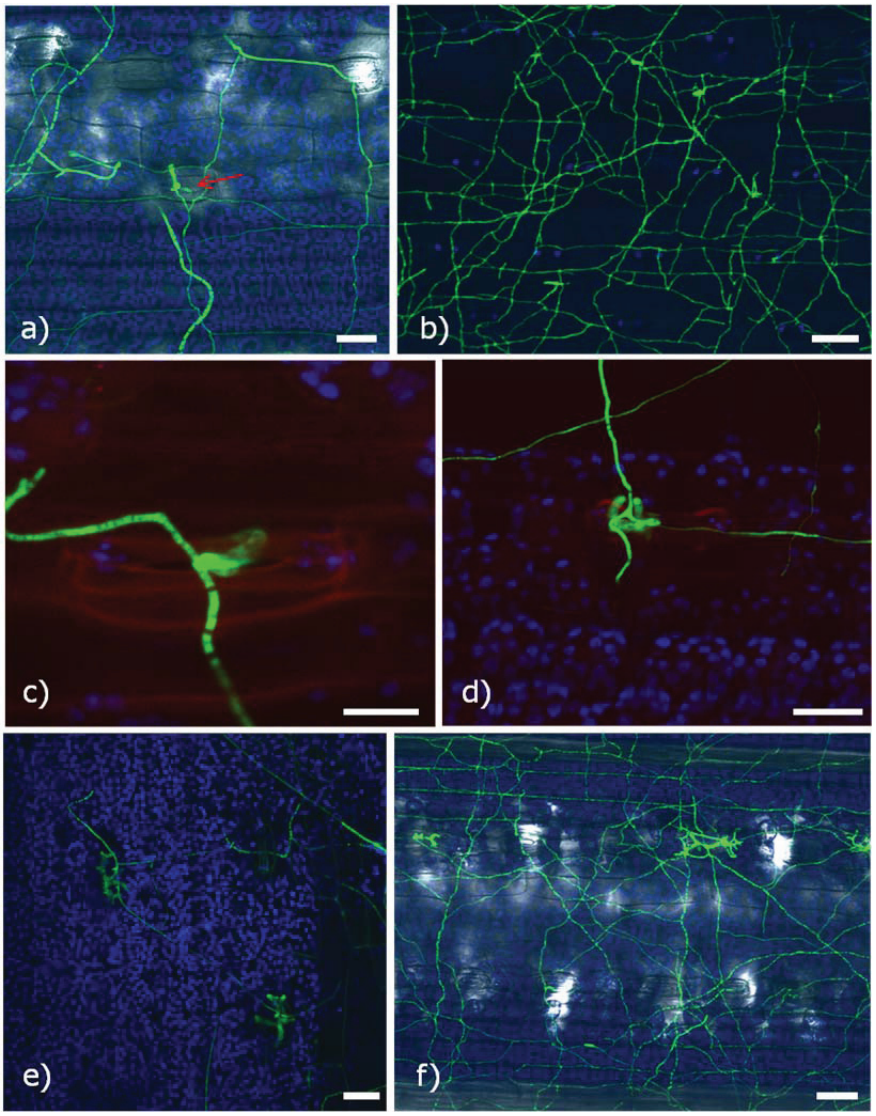


Figure 2.3
Confocal images of infection development on barley cv. Optic by the transgenic isolate Rcc-8B9-GFP. Green channel represents fungal cytoplasm expressing GFP; Blue channel – chlorophyll autofluorescence; Grey channel: non-confocal transmission background image; Red channel oversaturated red spectrum autofluorescence of plant cell walls. Unless otherwise stated, all confocal images are presented as maximum projections of corresponding z-stacks: a) Penetration of a stoma by stomatopodium produced at the hyphal tip (red arrow). The pathogen appears to use cell junctions for organised, directional growth. Bar = 50 µm; b) single image of a spider web-like network of epiphytic hyphae on the leaf surface. Bar = 50 µm; c) Stomatopodium produced by side branching of a leading hypha entering the stoma. Bar = 10 µm. d) early development of substomatal aggregate. Bar = 20 µm; e) Conidiogynous aggregates of swollen hyphae in substomatal cavities, connected by epiphytic hyphae. Bar = 100 µm; f) Image of the side of infection showing numerous fungal aggregates. Note organised growth pattern of epiphytic hyphae Bar = 50 µm.

Characteristic swan neck conidiophores rising from mycelial aggregates developed from 14 dpi onwards (Figure 2.4). The epiphytic hyphal network gradually disappeared from the centre of the infection site after the fungus had sporulated from 14 dpi onwards. The leaves remained asymptomatic until approximately 4 weeks pi.

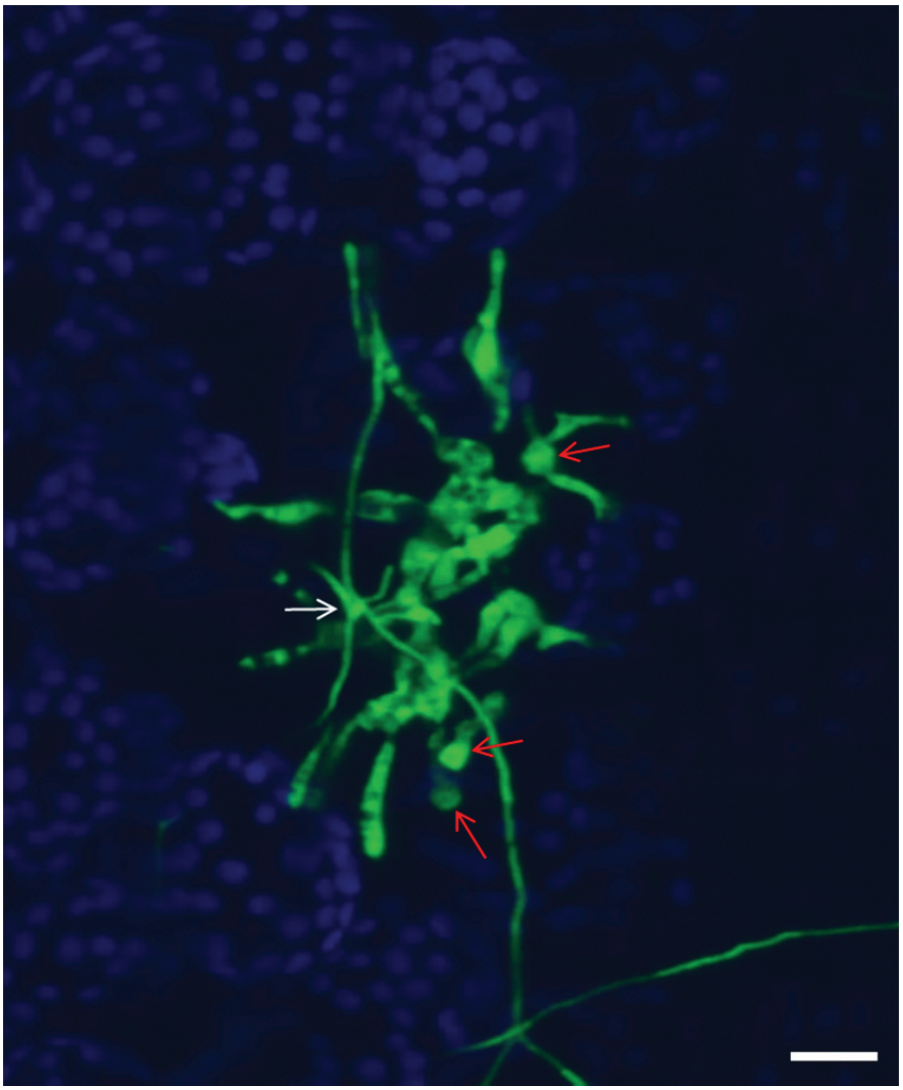

Figure 2.4
A typical fascicle of conidiophores rising from a colonised stoma. Red arrows indicate ripened spores, still attached to conidiophores. Note the presence of a stomatopodium above the stoma indicating the site of initial infection (white arrow).

### 2.3.2. Transition of the fungal life style and symptomatic phase

The transition of fungal behaviour was observed from 20 dpi at which point fungal behaviour changed progressing into the symptomatic phase of barley infection. *R. collo-cygni* exhibited an invasive growth into the mesophyll layer of the leaf (Figure 2.5 a). This mesophyll colonisation remained intercellular and appeared to start from infected stomata where thick endophytic hyphae radiated outwards from stomatal cavities (Figure 2.5 b). Such invasive hyphae were much thicker than those growing on the surface and subepidermal space, and were usually highly vacuolated (Figure 2.5a, 2.6a). The diameter of such invasive hyphae had a range of approximately 3 - 5 µm, compared to epiphytic hyphae with an average diameter of 1.2 µm. The intercellular 'brickwork-like' growth pattern appeared somewhat organised and intentional (Figure 2.5 c). For instance, long hyphae extended parallel to the leaf axis and were connected by side branches every 2 - 3 rows of mesophyll cells.

The development of a lesion around the infected stomata usually occurred only 5 - 7 days after the first observation of the aggressive colonisation of palisade mesophyll, indicated by the loss of chlorophyll fluorescence signal suggesting collapse of the cells in the affected areas (Figure 2.6 b). The newly formed, small lesions, called pepper spots were clearly visible from 25 dpi. At the edge of infection, outside the heavily colonised area of a leaf, the pathogen progressed into the mesophyll tissue directly after penetrating a stoma, without establishing a strong basal aggregates and sporulation (Figure 2.6 c).

Once the lesion had expanded encompassing the branched endophytic mycelium, the fungus appeared to develop long but less branched hyphae and actively grew away from necrotic area. This behaviour was observed within a chlorotic halo surrounding the developing lesion. Interestingly, no penetration of vascular bundles was observed at any stage of infection progression (Figure 2.5c, 2.6d).

Within heavily colonised collapsed mesophyll, the previously reported spore-like large hyphal swellings were observed (Figure 2.6e). At this stage, long chains of conidiophores emerged between anticlinal walls of collapsed epidermis (Figure 2.6f).

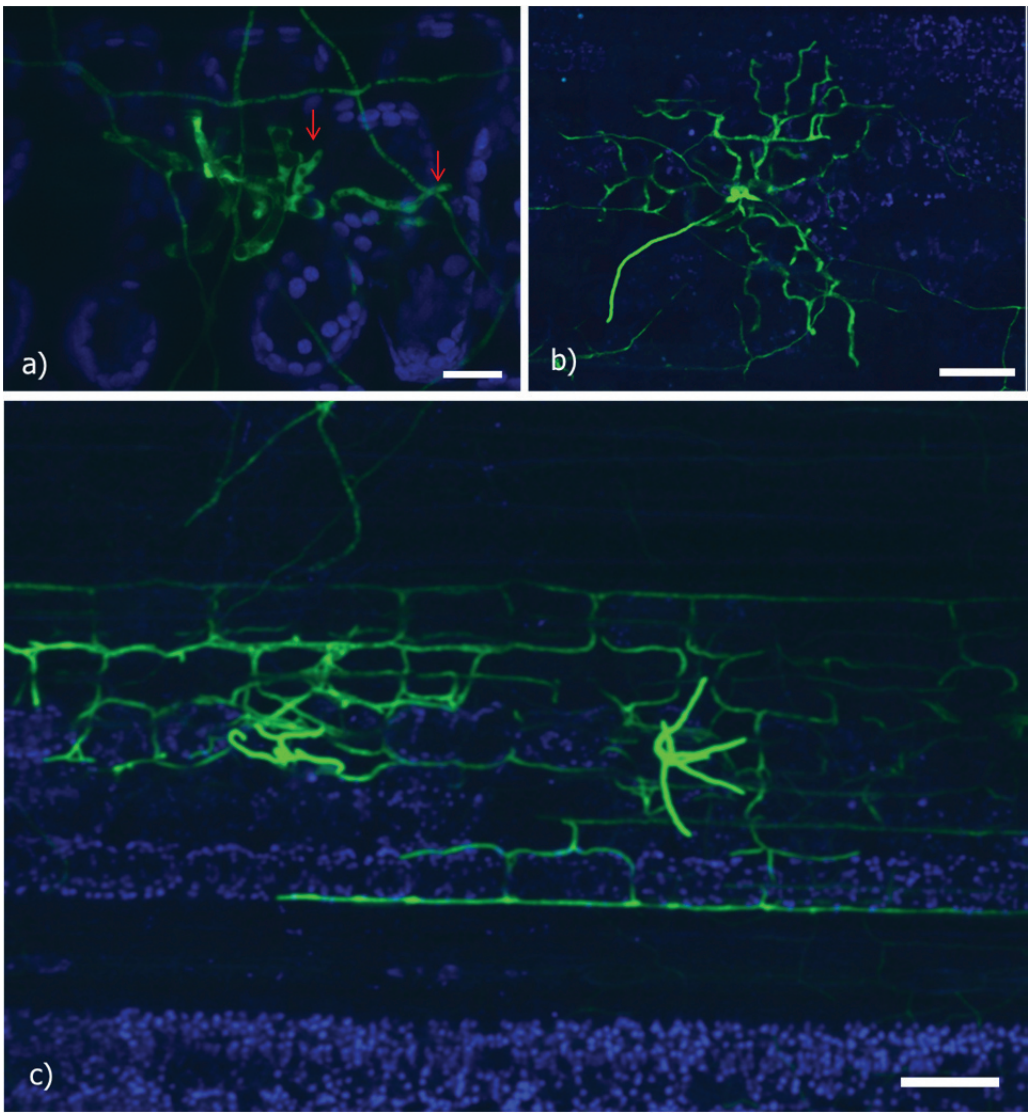


Figure 2.5

Confocal images of the transition of fungal lifestyle from symptomless to symptomatic phase of barley cv. Optic: a) the beginning of mesophyll colonisation; red arrows indicate the development of thick hyphal extensions from the basal aggregate. Bar = 20 µm; b) an endophytic hyphal network progression into palisade mesophyll layer, 'radiating' outwards from stomatal cavity. Bar = 50 µm; c) an endophytic 'brick work-like' growth pattern of branched intercellular hyphae, observed within the yet asymptomatic region of the leaf. Note conidiophores rising from stomata. Bar = 50 µm

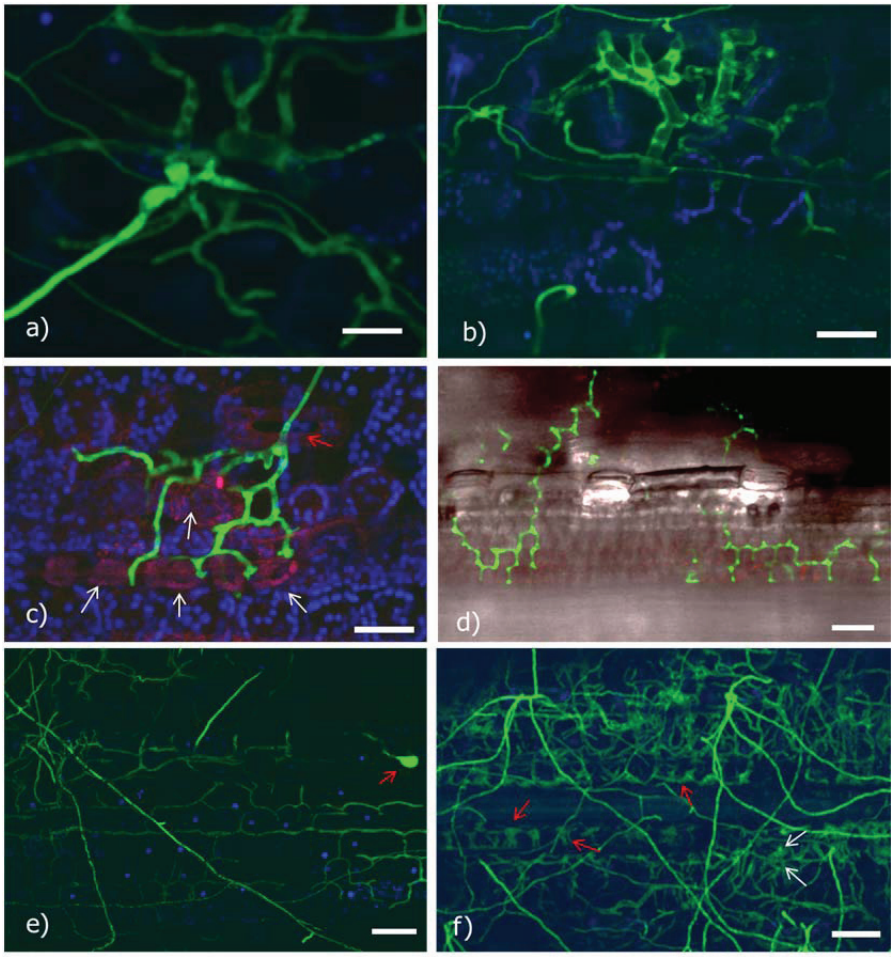


Figure 2.6

Confocal images of a dramatic transition of the pathogen's behaviour and the nature of symptomatic infection. Unless otherwise stated, bar = 20 µm: a) highly vacuolated fungal aggregate establishing endophytic growth of invasive hyphae; b) the development of lesion around an infected stoma, indicated by the gradual fading of chlorophyll autofluorescence in bottom right; c) the edge of an infection, outside the heavily colonised area of a leaf. The pathogen progressed into the mesophyll tissue directly after penetrating a stoma, without establishing a basal aggregate; red arrow indicate damaged mesophyll cells emitting red spectrum autofluorescence; d) rapid growth of intercellular hyphae outwards from the developing lesion. GFP channel superimposed onto brightfield non-confocal transmission image of the leaf surface. Note an apparent lack of the penetration into vascular bundle. Bar = 50 µm; e) heavy infection of presumably dead mesophyll by organised endophytic network. Note the development of spore-like hyphal swelling, indicated by the arrow; f) complete collapse of barley tissue after complete colonisation of mesophyll. Conidiophores rising in linear manner from endophytic hyphae, indicated by red arrows; white arrows show the developed spores. Lesions were clearly visible by the unaided eye at this stage. Bar = 50 µm.

### 2.3.3. Analysis of naturally infected leaf samples by light microscopy

In order to fully understand what happens to the fungus after leaf senescence and to validate the results obtained from artificial inoculation experiments, an additional analysis of the latest stages of fungal development was carried out using a staining procedure with naturally infected barley field samples (Section 2.7). The aniline blue method proved reliable for staining of fungal tissue present on the leaf surface. However the deep-seated intercellular hyphae colonising the mesophyll layer of leaves remained unstained and it could not be readily visualised by conventional light microscopy.

Microscopy revealed a mass sporulation encompassing the centre of the necrotic spot (Figure 2.7a). Here, the majority of observed spores developed in association with the fungal aggregates and infection of stomata. Towards the edge of the necrotic lesion, instances of sporulation associated with the infection of stomata became much less frequent. Instead, conidiophores were observed erupting through the epidermis anticlinal walls. Furthermore, long continuous chains of conidiophores also developed in large numbers in grooves between epidermal cells directly adjacent to vascular bundles (Figure 2.7b). Such chains of conidiophores were also observed previously during the inoculation experiments with the transgenic isolate Rcc-8B9-GFP (Figure 2.6f) and could therefore be linked directly to intercellular mycelium in the mesophyll that was clearly restricted by vascular bundles. At the edge of the lesion, within a chlorotic area, sporulation was rarely associated with substomatal cavities, but developed mainly by bursting through the anticlinal grooves of adjacent epidermis cells, whilst many stomatal pores appeared free of fungal structures (Figure 2.7c).

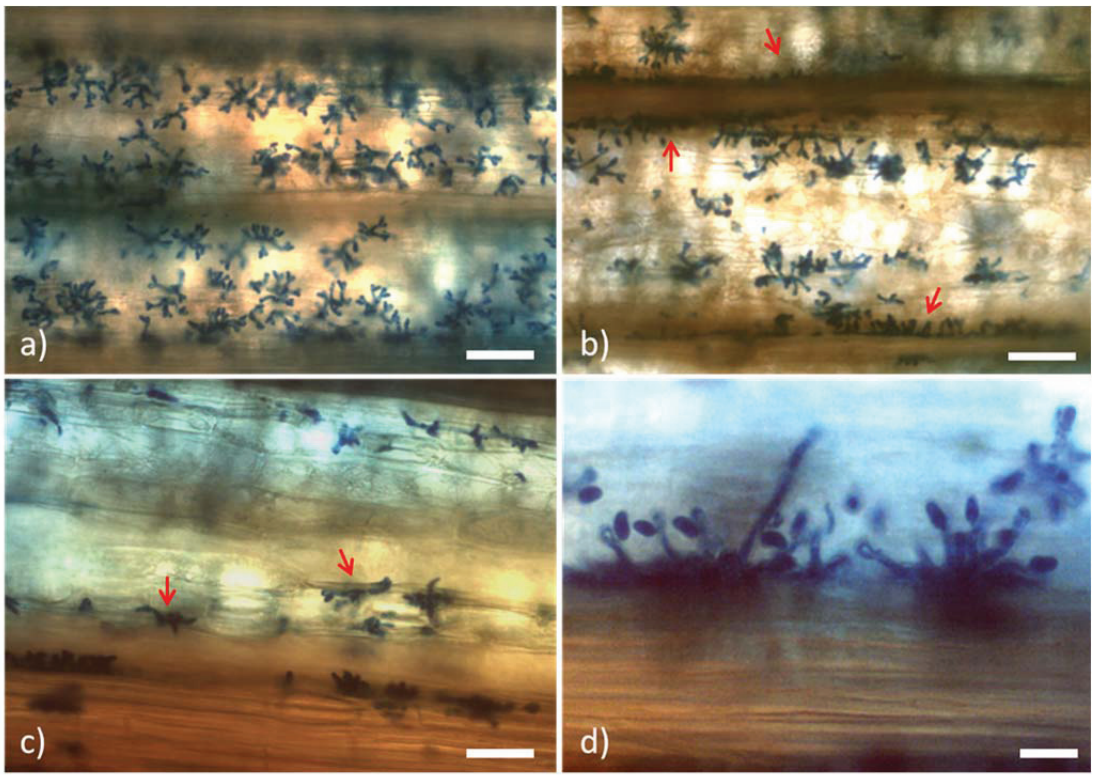


Figure 2.7
Light micrographs of barley leaves cv. Cocktail after harvest, naturally infected by *R. collo-cygni* under field conditions. Unless otherwise specified, bar = 50 µm: a) low magnification image of the central area of a necrotic lesion. Note characteristic swan neck conidiophores and a large number of still attached conidia, despite undergoing prior multistep staining procedure; b) decreasing number of fascicles in stomata and intriguing chains of conidiophores adjacent to vascular bundles at the egde of necrosis indicated by arrows; c) chlorotic halo region of the lesion. Note conidiophores rising in anticlinal grooves of adjacent epidermis cells indicated by red arrows. Many stomatal pores appear clean; d) zoomed-in image of chain of swan neck conidiophores bearing conidia. Bar = 20 µm.

### 2.3.4. Simultaneous infection by Rcc-ST-DsRed and Rcc-8B9-GFP isolates

Spring barley cultivar Optic was challenged with two transgenic isolates Rcc-8B9-GFP and Rcc-ST-DsRed to test their fitness *in planta* and to observe whether these isolates could coexist and simultaneously establish infection on one leaf.

Prior to the co-inoculation experiment, since the transgenic Rcc-ST-DsRed isolate had not been used in any *in planta* study to date, a brief experiment testing its pathogenic viability was performed (Figure 2.8 a, b). The behaviour of the transgenic Rcc-ST- DsRed was identical to the infection of barley by the isolate Rcc-8B9-GFP. Infection began with establishing an organised spider web-like network of hyphae on the leaf surface (figure 2.8a). An entry into stomata was observed from 24 hours pi. As observed earlier, for the GFP expressing isolate, such infection of stomata was facilitated by two modes of action, either by hyphal tip or infection peg branching from a leading hypha (Figure 2.8b).

Subsequent co-inoculation experiments revealed that both isolates were able to coexist within a small area of the leaf. Interestingly, a simultaneous infection of one stoma by both isolates was frequently observed (Figure 2.8c). However, both isolates during the establishment of their epiphytic networks appeared to avoid exploring the same grooves between epidermis cells (Figure 2.8d). Although, the sporulation of both fungal strains developed at 10 dpi, no instance of simultaneous formation of spores of both genotypes at one stoma was noted, possibly suggesting competition for the niche (Figure 2.8e-f).

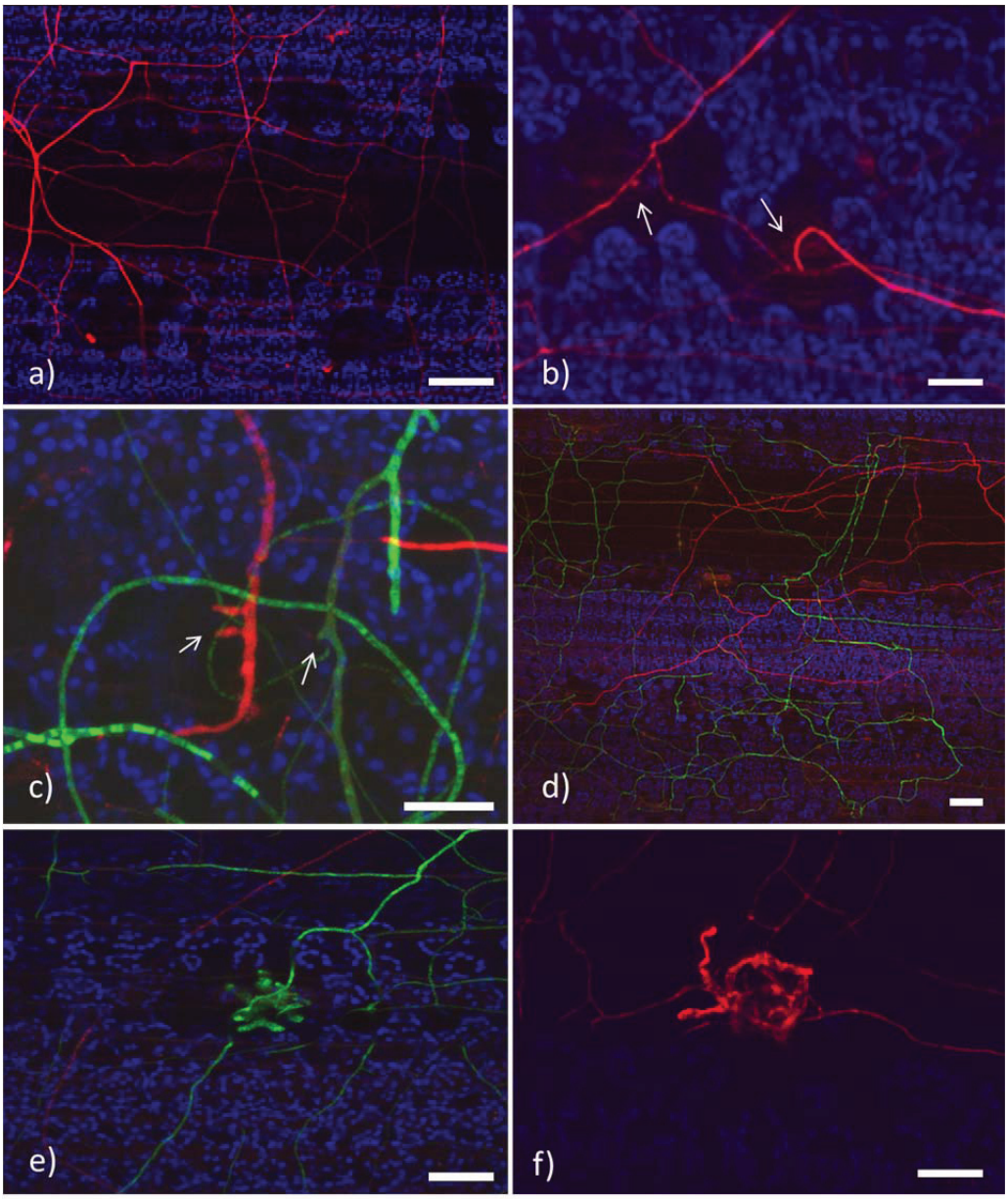


Figure 2.8

DsRed isolate pathogenicity test and subsequent co-inoculation experiment with two *R. collo-cygni* genotypes expressing two different fluorescent marker tags: a) Rcc-ST-DsRed establishing epiphytic network of hyphae on the leaf surface. Bar = 50 µm; b) two different modes of entry into stomata by Rcc-ST-DsRed isolate indicated by white arrows, i.e. laterally branching stomatopodium and direct penetration of a stoma by the hyphal tip. Bar = 50 µm; c) Simultaneous infection of a stoma by both transgenic isolates. Stomatopodia indicated by white arrows. Note Rcc-ST-DsRed that developed two infection pegs simultaneously. Bar = 20 µm; d) co-existing spider web-like epiphytic network. Note distinct spatial separation of isolates. Bar = 50 µm; e-f) sporulation of GFP and DsRed expressing isolates, respectively. Bar = 50 µm.

In all examined plant material, the number of substomatal aggregates appeared higher for Rcc-8B9-GFP than for Rcc-ST-DsRed. In order to verify the statistical significance, numbers of stomatal aggregates as a mean of successful infection were counted for both isolates across ten previously collected low magnification images of infection development at 7 dpi. T-test analysis showed that there was a significant difference between the numbers of the observed basal aggregates, i.e. Rcc-8B9-GFP produced significantly more aggregates than Rcc-ST-DsRed (P value = 0.004721; mean values 5.3 and 2.8, for Rcc-8B9-GFP and Rcc-ST-DsRed infected samples, respectively).

### 2.3.5. Whole plant inoculation experiment using a range of spring barley cultivars

Four cultivars of spring barley, namely Belgravia, Gardner, Optic and Cocktail that differ in their official HGCA resistance ratings for RLS, were used for inoculation experiments using confocal microscopy to compare if different levels of resistance are exhibited during asymptomatic infection. For instance, resistance ratings for these cultivars were 7, 4 and 5, respectively with no official rating available for Cocktail which in Scottish trials was as susceptible as Optic (Neil Havis, SRUC, personal communication). Cultivars were challenged with Rcc-8B9-GFP isolate using the whole plant inoculation assay (Section 2.2.4) in order to test if there were any differences in pathogenic behaviour of the fungus that could account for varietal resistance or tolerance.

Although the same batch of inoculum was used in the experiment and repeated twice, there were no apparent differences in the growth and development of the fungus during early stages of colonisation. The isolate was able to infect each of these cultivars with approximately the same pace, starting from establishing organised hyphal network and infecting stomata. However, the first instance of a mature form of conidiogenous aggregates and sporulation was on Cocktail as early as 8 dpi (Figure 2.9 a). The slowest development of these structures was found on Belgravia at 12 dpi (Figure 2.9 d). The remaining three cultivars, i.e. Optic and Gardner, exhibited an intermediate level of susceptibility to isolate Rcc-8B9-GFP, with the first observation of typical sporulation at 10 dpi (Figure 2.9 b, c; respectively).

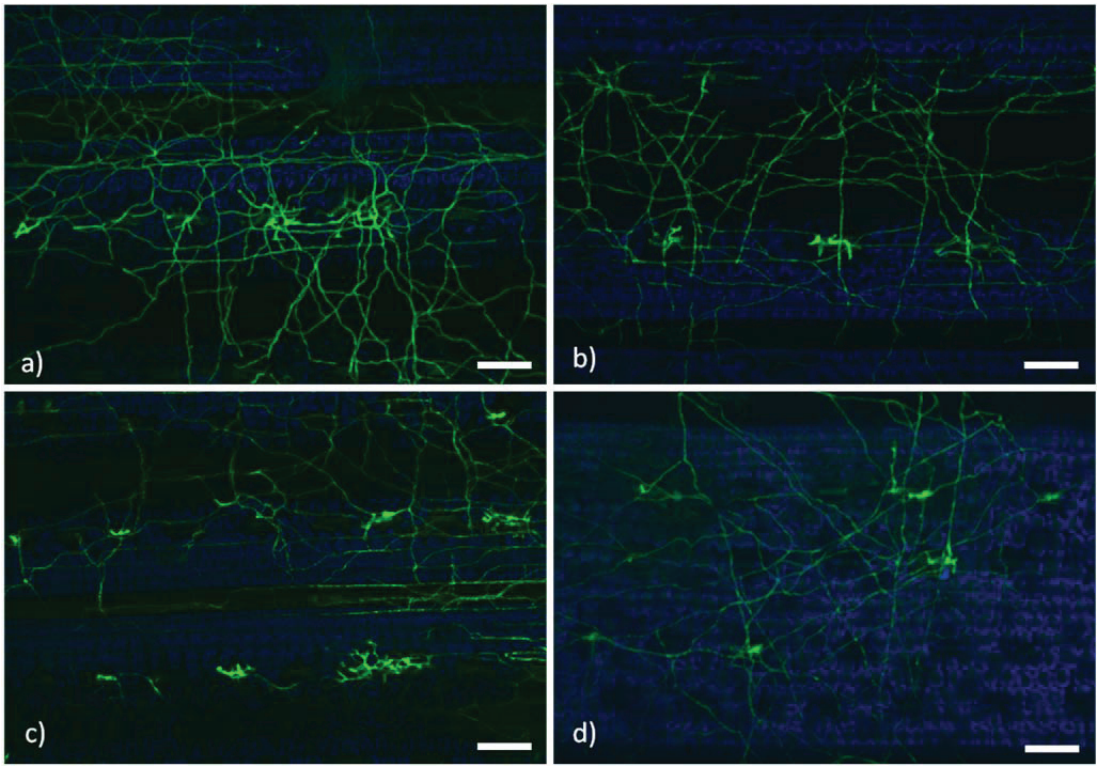


Figure 2.9
Infection time-course comparison between 4 different spring barley cultivars. Note the development of fascicles as evidence of successful infection without triggering immune response of the host. Bar = 50 µm: a) Cocktail; b) Optic; c) Gardner; d) Belgravia.

### 2.3.6. Analysis of alternate host range by confocal microscopy

#### 2.3.6.1. Infection of wheat (*T. aestivum*)

Similar to the previous observation of infection development on barley, *R. collo-cygni* isolate Rcc-8B9-GFP gained entry into plant tissue via stomata without triggering any resistance response from wheat, suggesting a compatible interaction (Figure 2.10a). The fungus developed an organised hyphal network and as infection progressed, the typical hyphal aggregates were observed in stomatal cavities which subsequently gave rise to conidiophores and conidia (Figure 2.10b, c).

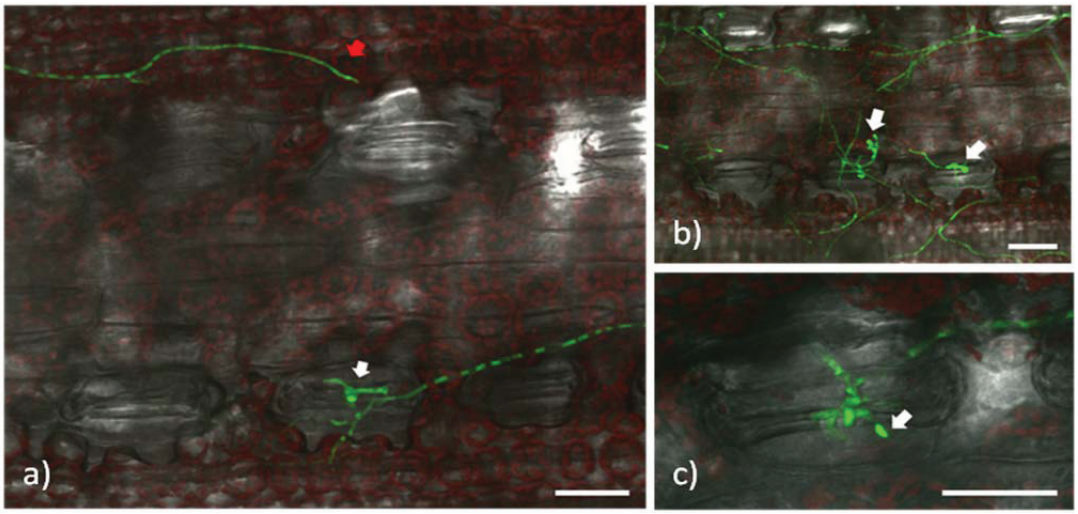


Figure 2.10
Confocal images of infection development in wheat (*T. aestivum*) cv. Alchemy. Green channel: GFP expressing isolate; red channel: chlorophyll autofluorescence; grey channel: BF transmission image. Bar = 50 µm: a) infection of a stoma by a swollen hyphal structure, the stomatopodium (white arrow). Note change to the directional growth of hyphae towards the stoma (red arrow); b) emergence of conidiophores with conidia indicated by the arrows; c) Close up image of the typical sporulation erupting through a colonised stoma. Developed conidium is indicated by the white arrow.

### 2.3.6.2. Italian ryegrass (*L. multiflorum*)

Initial infection of Italian ryegrass occurred in identical manner as for those observed in barley and wheat plants, with penetration of stomata by stomatopodia (Figure 2.11a) and establishing spiderweb-like network. However, in this system colonisation of subsequent stomata followed by sporulation appeared to be more rapid and abundant, i.e. spore formation in barley and wheat was observed at the earliest at 8 dpi and 10 dpi respectively, whereas in Italian ryegrass it occurred as early as at 5 dpi (Figure 2.11b). This therefore suggests that Italian ryegrass might be a very important inoculum sources for the fungus.

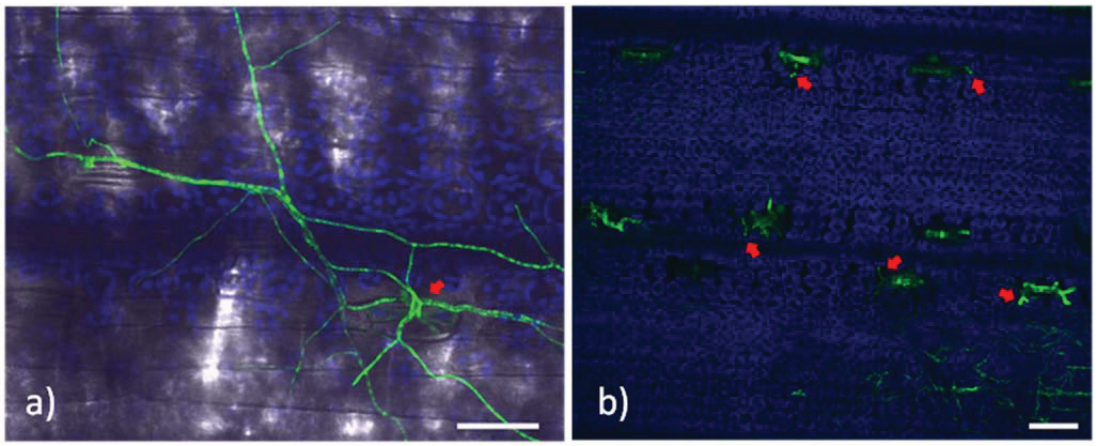


Figure 2.11
Confocal images of the infection development on Italian ryegrass (*L. multiflorum*). Unless otherwise specified, bar = 50 µm. a) maximum projection of a z-stack showing an early establishment of hyphal network and penetration of a stoma at 24 hpi, indicated by the red arrow; b) hyphal aggregates and abundant sporulation at 5 dpi. Red arrows show conidia still attached to swan neck conidiophores

#### 2.3.6.3. Cocksfoot (*D. glomerata*)

The infection characteristics in *D. glomerata* system suggested an incompatible interaction with the transgenic isolate Rcc-8B9-GFP. Although stomatopodia formation and the attempts to infect seemed to occur (Figure 2.12a, b), no further development such as substomatal aggregates was observed in this host. An initial epiphytic hyphal network formed, however, and leading hyphal growth appeared to be much less organised compared to that observed on other hosts, and often resembled snake's trails (Figure 2.12 a).

*R. collo-cygni* hyphae appeared to rapidly collapse as indicated by the loss of GFP expression. Dead hyphae had certain degree of autofluorescence observable in the red spectrum (Figure 2.12 b), with peak intensity present in numerous large vacuole-like vesicles. However it was also detectable around dead inoculum. In the region of the leaf where such hyphae were prevalent, the development of a lesion had occurred. Lesion formation was indicated by gradual fading and subsequent loss of detectable chlorophyll autofluorescence signal (Figure 2.12b).

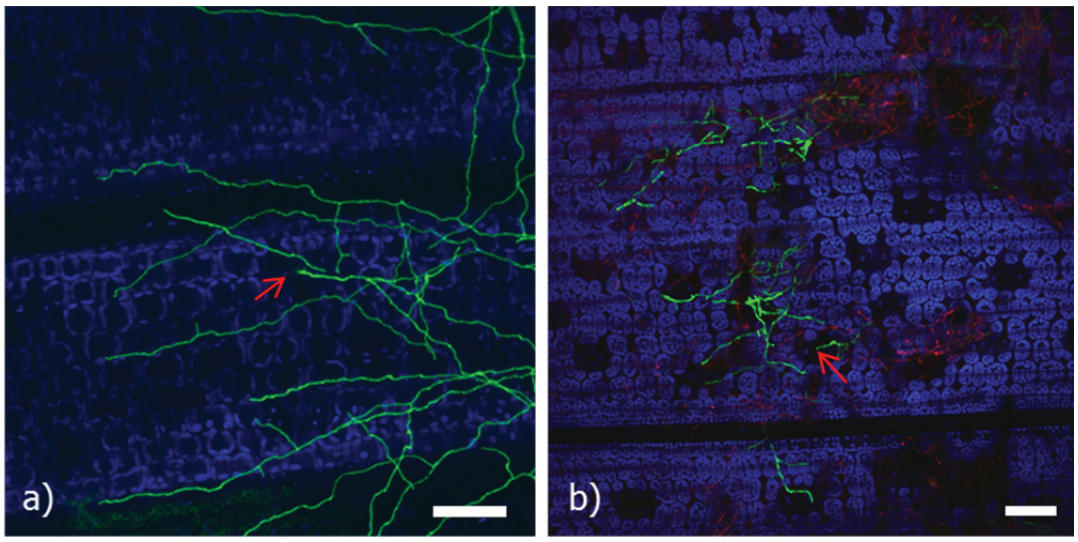


Figure 2.12
Confocal images of cocksfoot (*Dactylis glomerata*) challenged with *R. collo-cygni,* isolate 8B9-GFP. Bar = 50 µm: a) epiphytic hyphal network at 3 dpi. A sporadic attempt to colonise stoma is indicated by the red arrow; b) failure to establish infection. Despite attempts to colonise stomata (red arrow), no further development was observed. Note the emergence of symptoms in the regions of red fluorescing hyphae.

### 2.3.6.4. *Lotus japonicus*

Inoculation of *L. japonicus* with *R. collo-cygni* isolate Rcc-8B9-GFP resulted in hypersensitive response (HR) to the pathogen as in incompatible/ non-host interactions. Recognition of *R. collo-cygni* as a pathogen by *Lotus* plants resulted in typical programmed cell death lesions on the leaf tissue, observed from 2-3 dpi (Figure 2.13a). Subsequent examination of leaf samples using CLSM confirmed the HR to the pathogen, clearly suggesting an incompatible interaction between the fungus and *L. japonicus*. The characteristic 'wave' of cell death response was observed at the edge of the developing sharp lesion (Figure 2.13 b, c). It was detectable by the channel set up to collect the chlorophyll signal. GFP signal

disappeared towards the centre of lesion indicating the rapid death of the fungal hyphae (Figure 2.13 b).

Interestingly, *R. collo-cygni* seemed to perceive *Lotus* as a potential host and attempted to colonise the stomata by producing stomatopodia (Figure 2.13d). The fungal behaviour however, was fundamentally different to that observed on its host plant barley. For instance, no attempt to establish an organised spider web-like hyphal network was observed. Fungal growth was rather chaotic, although it did show some directionality towards stomata. This disorganised hyphal development still appeared to be driven by the different topography of dicot *Lotus* leaves compared with monocot plants. Swollen conidiogynous hyphae, similar to those which colonise mesophyll on barley were prevalent on the plant surface at the edge of HR symptoms (Figure 2.13 b, c, e). Such development differs from that seen on barley, where surface colonising hyphae are much smaller in diameter. Some budding off the conidiophores and spore development was observed however these were produced exclusively on the leaf surface rather than in stomata (Figure 2.13 e).

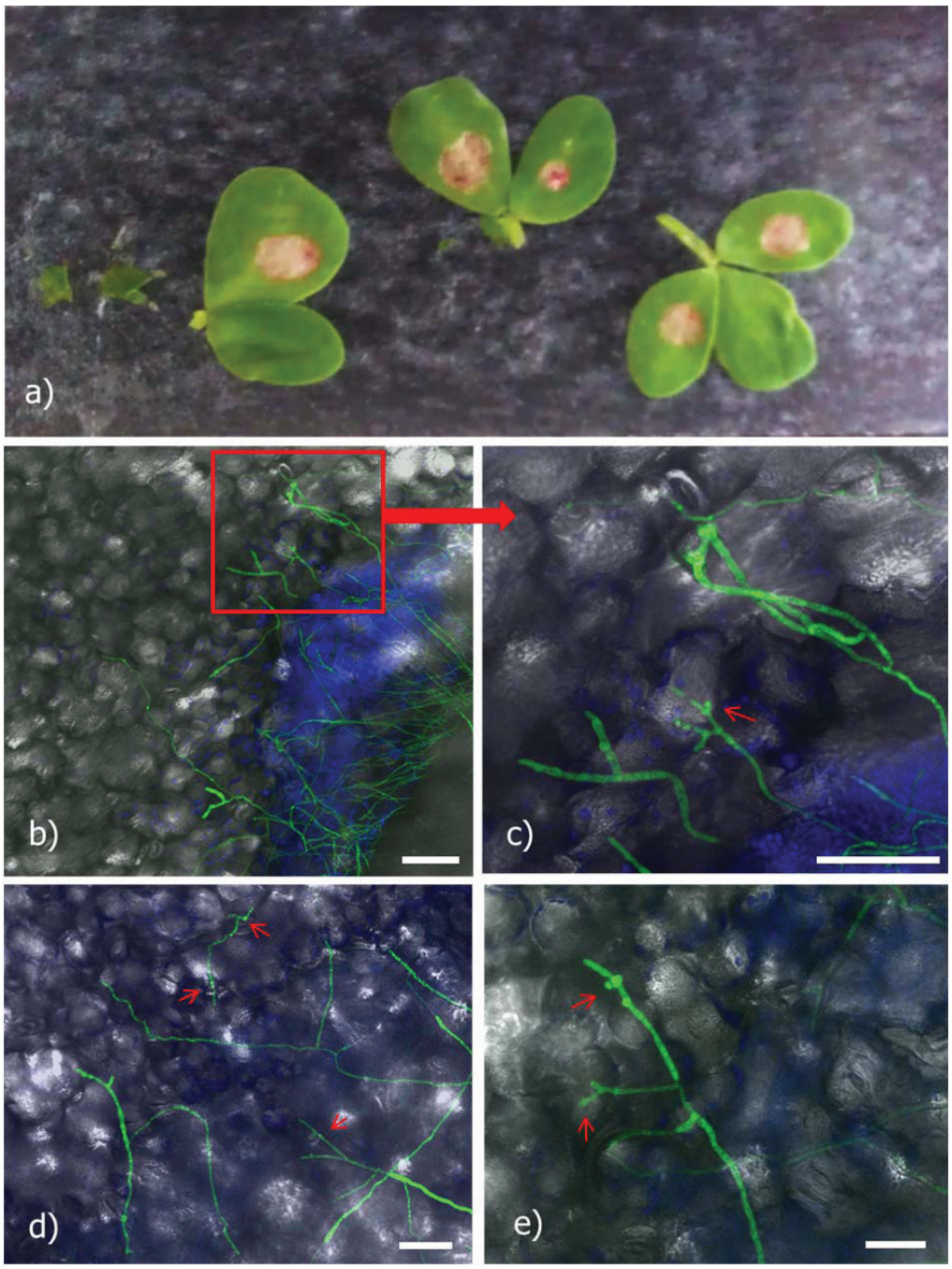


Figure 2.13
Inoculation experiment with *L. japonicus* MG 20: a) leaflets of *L. japonicus* inoculated with the transgenic isolate Rcc-8B9-GFP, ready for examination under CLSM. Note sharp lesions, characteristic to programmed cell death; (b-e) fungal development time-course. Bar = 50 µm: b) Low magnification image showing the edge of inoculation site. Note strong homogenous autofluorescence; c) zoomed in image of conidiogenous hyphae present at the edge of hypersensitive response lesion. Red arrows indicate the development of conidium, also observed on figure e); d) attempts to colonise stomata by the development of infection pegs (red arrows).

## 2.4. Discussion

Chapter 2 describes the horizontal transmission of *R. collo-cygni* on barley and other selected hosts. Both field and transgenic *R. collo-cygni* isolates expressing GFP and dsRed fluorescent reporter markers were utilised to visualise the infection progression in living host tissues by various light and confocal microscopy. The existence of a previously unknown structure called stomatopodium (infection peg), involved in the penetration of stomata, was demonstrated. The fungus initially exhibited symptomless epiphytic growth, extending above epidermis and connecting the hyphal aggregates inside substomatal cavities and subsequent initial sporulation. However, during the transition into symptomatic phase, the organised intercellular growth of hyphae into the mesophyll was observed. This hyphal network was involved in the production of asexual spores demonstrating that the raprture of epidermal layer was responsible for local necrosis observed for RLS. In addition to barley, several other speculated *R. collo-cygni* hosts have been used to verify their compatibility to the pathogen. Winter wheat (*T. aestivum*) and Italian Rygrass (*L. multiflorum*) proved to be compatible hosts and similar patterns of colonisation by the GFP expressing isolate observed in both species. On the other hand, cock's-foot (*D. glomerata*) and dicot model species, *Lotus japonicas* showed clear incompatible reaction responses.

In *R. collo-cygni,* initial observations with regard to its fundamental biology and life cycle came from the application of molecular methods of detection (Havis *et al.,* 2006a, 2014; Taylor *et al.,* 2009). Although these methods have proven useful, the question remains whether they are indeed the best way to describe the development of the fungus compared to that seen under the microscope. Molecular studies are just

based on amplification of the ribosomal internal transcribed spacer region (rDNA ITS). However, this region is very well conserved amongst ascomycetes, especially within species, therefore they might not distinguish all *Ramularia* spp. isolated from barley (Sutton & Waller, 1988 and references therein). For example, in *Zymoseptoria*, a newly described genus that includes the prominent wheat pathogen *Z. tritici* (syn. *M. graminicola* and *Septoria tritici*), several species have found on uncultivated grasses in the Middle East and in addition to *Z. tritici*, two new species were isolated from *Elymus repens*, *D. glomerata* and *L. perenne*, and named *Z. ardabiliae* and *Z. pseudotritici*. Both species were separated from *Z. tritici* by means of morphological characteristics and phylogenetic analyses of a seven-gene DNA dataset. One of the two new *Zymoseptoria* populations called S1 was recognised as the closest known relative of *Z. tritici*. The two species share the same sequence for the ITS region that often is used to distinguish ascomycete species (White *et al.,* 1990; Seifert, 2009), and it would therefore not be possible to separate them into two different species only by using the ITS approach. It is also important to remember that DNA is extracted from total mycelium present within the plant, from both viable and dead hyphae, which certainly provides noise and can compromise the overall picture. It was therefore desirable to verify the findings by cell biological approaches that enable a more direct observation of fungal development within the host plant.

Only a few detailed microscopic studies have been undertaken on *R. collo-cygni* infections and life cycle. Recent scanning electron microscopy (SEM) examinations of naturally infected leaves from the field provided an initial insight into *R. collo-cygni* development on barley (Stabentheiner *et al*., 2009). The successful stable genetic transformation of the fungus with fluorescent marker tags is useful for studying

asymptomatic infection on barley under confocal microscope (Thirugnanasambandam *et al.,* 2011). Studies on *R. collo-cygni* are challenging due to its sparse or even lack of sporulation *in vitro*. The inoculation of detached leaves was carried out here using mycelial fragments as inoculum, as was not possible to produce sufficient *R. collo-cygni* spores in axenic culture, which was also suggested earlier by Makepeace *et al*. (2008) and Thirugnanasambandam *et al.* (2011). The latter study proved that *R. collo-cygni* homogenised mycelium could be used to inoculate barley plants to initiate infection and observe the typical RLS symptom expression and demonstrated that mycelial fragments are a valid substitute for spores in infection assays. The work with Rcc-8B9-GFP hyphal fragment suspension is also supported by SEM analysis of *R. collo-cygni* spore germination on barley leaves (Stabentheiner *et al*., 2009) which showed that germ tubes and hyphae that developed from germinating spores behave in a similar manner and enter leaf tissue via stomata.

This study supports the previous microscopic observations of *R. collo-cygni* infection. The rapid formation of a mycelial network on the surface of the inoculated leaf has also been observed. Penetration of leaf tissue occurred always through the stomatal pore. This mode of entry may be less likely to trigger defence reactions caused by the damage of host tissues during infection of stomata. However, it is known that host plant responds on different levels that are not visually apparent and can often only be tested by the specific analysis of plant pathogen interaction at the molecular level (Jones & Dangl, 2006). The observation that the host epidermal cells remained intact during the early stages of infection is consistent with this hypothesis.

Both Stabentheiner *et al*. (2009) and Thirugnanasambandam *et al.* (2011) stated that no specialised penetration structures were formed by *R. collo-cygni* during

penetration of stomatal pores. In this study, although the invasive hyphae were observed to enter open stomata without producing any morphologically distinct structure, we have also determined the existence of a separate feature in *R. collo-cygni*. Our results clearly show that the penetration of a stoma was often facilitated by the structure called stomatopodium, an infection peg, which is a thickening of the invasive hypha that forms above the stomatal pores and pushes its entry between the guard cells (Figure 2.3 a, c). This was frequently, but not exclusively, the case for closed stomata (Figure 2.3a, 2.10a, 2.11a). Furthermore, it has also been observed that this structure formed on the leading tip of hypha but also could develop as side branches extending from hyphal network. Similar structure has been reported previously in the closely related fungal species, *Pseudocercosporella fijiensis* (teleomorph: *M. fijiensis*), the pathogen that causes Black Sigatoka disease of banana (Balint-Kurti *et al.,* 2001).

The development of an apparently organised network of epiphytic hyphae during asymptomatic infection was correlated with junctions between epidermis cells that the fungus used to colonise large areas of leaf surface. Our results also confirm the previous observation that the invasive hyphae exhibit directional growth towards stomata. It remains to be determined which mechanisms are involved in this growth habit. One possible explanation is that the topography of the leaf surface and cell layout could act as morphological clues for the pathogen to identify the presence of stomata in the near vicinity. However, it could also be hypothesised that the fungus is able to detect very subtle changes in the microclimate and humidity that exist around stoma due to transpiration.

We have observed that infection pegs once inside substomatal cavities develop into thick conidial bases (Figure 2.3d, 2.4) also observed by Thirugnanasambandam *et al.* (2011). This study supports their findings that the substomatal aggregates remain connected by the epiphytic hyphal network on the leaf surface. In this study, we observed that these aggregates comprised a group of swollen, often highly vacuolated cells from which the characteristic *R. collo-cygni* swan-neck conidiophores are produced. Initially, the typical sporulation rising from subsequent stomatal pores was associated with some local necroses of tissue surrounding stomata that were probably caused by mechanical damage during conidiophore emergence but RLS macroscopic symptoms were not observed until at least 25 dpi. However, we have determined that during later stages of development, from 20 dpi (Figure 2.5a, b), the substomatal aggregates begin expansion into mesophyll tissue surrounding the cavities and produced an organised endophytic network of swollen, heavily branched hyphae that explore intercellular space between mesophyll cells.

Intercellular growth was suggested by Sutton & Waller (1988) but no clear evidence was provided. Stabentheiner *et al.* (2009) showed the presence of fungal mass in the infected field samples, it was not possible however to determine beyond any doubt that it belonged to *R. collo-cygni.* In this study, it was observed that after 25 dpi, the aggregates that developed at the edge of the infection did not immediately produce spores, but instead they directly expanded into the mesophyll layer (Figure, 2.6 c, d). Interestingly, the leaves still appeared asymptomatic up to a week after the initial colonisation of the mesophyll occurred in the same batch of inoculated leaf samples. This endophytic mycelium then gave rise to mass sporulation that occurred in stomata and by conidiophores erupting through the epidermis, but appeared to rupture only at

the cell junctions. This caused a massive collapse of the tissue and subsequent symptom expression and can explain why macroscopic symptoms on infected leaves did not appear earlier. The conidiophores rising between cells caused the epidermal cells to collapse, which was quickly followed by heavy colonisation of the intercellular space between mesophyll cells.

It has been speculated that *R. collo-cygni* is an opportunistic saprophyte that is able to recognise and respond to the switch from vegetative to reproductive phase in the host by becoming a necrotrophic pathogen (Schutzendübel *et al.,* 2008). It has also been stated that sporulation usually occurs from the necrotic lesions (Walters *et al*., 2008). This study shows that the fungus can actually sporulate within stomata during early stages of the infection cycle without causing any significant damage, thus remaining asymptomatic which confirms the observations made previously by Thirugnanasambandam *et al.* (2011). This signifies that pathogen inoculum may spread within a barley crop during the growing season without apparent symptoms, until the plants move into the reproductive phase.

The results from these experiments suggest that the likely process of RLS symptom development could be slightly different than previously thought. The typical necrotic symptoms are actually caused by the combination of stomatal and mesophyll infection and subsequent eruption of conidiophores through the epidermis. Furthermore, no penetration of vascular tissue was observed during endophytic infection (Figure 2.5 c, 2.6 d, f). Hyphae often changed the direction of growth when they encountered vascular bundles and the intercellular hyphal network remained restricted between the leaf veins, within the mesophyll tissue. Such a growth habit could explain the

characteristic rectangular shape of symptoms that appear to be sharply delineated by the leaf veins (Walters *et al*., 2008).

The frequent lack of disease symptoms that do not develop usually during infection time course experiments poses a question regarding the current disease scoring system. Currently, the cultivars that are included in the Home Grown Cereals Authority (HGCA; www.hgca.com) recommended cultivars list are scored against *Ramularia* based on the percentage of visible symptoms. If a cultivar that is currently considered as "resistant" to *R. collo-cygni* still allows completion of the pathogen's lifecycle, then the term resistance is not entirely correct. Susceptibility of a cultivar increases disease symptoms, which in turn reduces the amount of green leaf area, thereby increasing loss of grain quality and yield. Perhaps the term "disease tolerance" is actually more appropriate in the case of RLS*,* as is the case for another major barley pathogen with asymptomatic phase, *Rhynchosporium commune* (Thirugnanasambandam, 2011). The tolerant cultivars enable survival of the pathogen, that perhaps still causes some loss of nutrients, but its influence on the grain quality and quantity is significantly reduced, and negligible.

The detached leaf assay has proved to be useful method for studying early stages of infection however it is often not possible to maintain quality leaf sections for longer than three to four weeks without compromising the results due to natural degradation of leaf tissue, not associated with fungal infection. In order to study using prolonged time series, a whole plant assay based on drop inoculation method, was developed (Section 2.4). A whole plant drop-inoculation was used to test a range of barley cultivars with different HGCA recommended list scores against *R. collo-cygni*. The results showed that the fungus was able to develop on all tested cultivars, although

there was a variation in speed and pattern of infection which correlated with official HGCA resistance ratings. The number of stomatal aggregates appeared similar for all observed asymptomatic interactions. It would now be necessary to verify the findings using statistical approaches.

For the first time since its development, DsRed expressing *R. collo-cygni* isolate (Rcc-ST-DsRed; Thirugnanasambandam *et al.,* 2011) was employed in the experiments using *in planta* assays. The development of Rcc-ST-DsRed was essentially the same as this observed in Rcc-8B9-GFP isolate, however we have detected significant differences in the speed of infection development on the same cultivar. Since the parental isolates for both transgenic strains were different, this suggested that there are differences in the level of aggressiveness between isolates. As expected, some are more pathogenically fit than other. Isolate x cultivar interactions would also need to be considered. However, there could also be that the Rcc-ST-DsRed isolate, since it had never been used in any *in planta* studies before, its pathogenicity level could have decreased due to prolonged storage in culture over many generations of the fungus.

It has been shown that *R. collo-cygni* can infect a broad range of monocot species (Salamati & Reitan, 2006). Several authors have reported the isolation of the fungus from many crop and perennial grass species (Huss, 2004; Frei, 2004; Cromey *et al.,* 2004). Alternate hosts should therefore be considered as another important source of RLS within the growing season. They can also facilitate pathogen survival through the winter period thus becoming a major source of primary inoculum between the growing seasons. Despite this, recent research has concentrated on *R. collo-cygni* - barley system and other putative hosts have gained a very little attention to date.

In order to develop an understanding of the early phases of RLS on the selection of possible hosts and non-hosts and to compare the results with those described earlier for barley, the infection of monocot plants, such as wheat (*T. aestivum*), Italian ryegrass (*L. multiflorum*) and cock's foot (*D. glomerata*) was investigated. In addition, we used the model dicot species, *L. japonicus*. Winter wheat is one of the most important crops in the world and has been reported to a compatible host for *R. collo-cygni* (Huss, 2004). Our experiments describe the nature of asymptomatic infection of winter wheat, confirming that not only could wheat be a viable source of inoculum for its primary host, barley, it can potentially develop the disease on its own. The pathogen behaved in the same way and pace on wheat as in barley, and was able to sporulate therefore completing the life cycle. This could have serious implications for wheat production worldwide. It would therefore be necessary to draw much more attention to studying *R. collo-cygni* – wheat system in order to establish an understanding of the level of potentially negative impact the pathogen could have on wheat crops globally.

The investigation of infection development on Italian ryegrass (*L. multiflorum*) occurred in the same way however it appeared to be even more rapid than on barley. This was indicated by much faster development of substomatal aggregates and sporulation. Although it is not possible to demonstrate specific reasons for this difference, it could be speculated that ryegrass can actually be more natural host than barley. Perhaps *R. collo-cygni* originated from perennial grasses and subsequently evolved to be the pathogen of the main cultivated crops. Similar evolutionary adaptation and a host jump from native grasses to crops have previously been described for the wheat pathogen *Z. tritici* (Stukenbrock *et al.,* 2007; 2012). The

findings described here suggest that *L. multiflorum* could be a major primary inoculum source for *R. collo-cygni* as ryegrass species represent some of the most common perennial grasses, being both cultivated for grazing and animal feed, and present as natural component of the habitats in rural areas. It can often be seen growing next to crop field, therefore the fungus can overwinter on them and can easily be transferred by wind borne spores to the neighbouring barley or wheat crops.

Results from the inoculation experiments with *D. glomerata* showed that this grass species is not a host for *R. collo-cygni.* The fungus was not able to establish infection despite repeated attempts in independent inoculation experiments. Interestingly, the initial development of the fungus was similar to this described earlier for barley and other hosts, i.e. some directional growth towards stomata and attempts to penetrate were observed. However, no further development occurred suggesting that mechanisms of incompatibility could exhibit themselves only during the infection of stomata. It also suggests that perhaps at the point of penetration the plant defence response was successfully deployed, stopping the pathogen from further development. However, the growth of fungal hyphal network appeared unstructured from the beginning of the observation (24 - 48 hours pi). This could suggest that perhaps specific morphological characteristics or topography of the leaf surface in cock's foot could also be the reason for the failed interaction. In host species, the fungus utilises the grooves between epidermal cells, thus the epiphytic network appears very well organised. Such early development of RLS unspecific symptoms, could suggest a programmed cell death response from cocksfoot due to the fungus attempting to colonise the stomata. On the other hand, this could also indicate that early release of the toxin rubellin, produced by the fungus, had occurred due to stress

from being unable to establish compatible interaction with its host and therefore being unable to feed. The results of the inoculation experiments with and Rcc-8B9-GFP isolate on *D. glomerata* were replicated during independent experiments that followed up this project confirming *R. collo-cygni* incompatibility or non-host status of *D. glomerata* (April Armstrong, 2013, BSc thesis, SRUC and University of Edinburgh).

There has been an interesting report of the occurrence of *R. collo-cygni* on the dicot species *Cannabis sativa* (Scheuer, 1999). Since *C. sativa* is a controlled substance in the UK, a model legume species, *Lotus japonicus* was used instead to further examine the interaction between the pathogen and dicot plants. The results were dramatically different to previously described monocots in this study, revealing an incompatible interaction between the fungus and *L. japonicus* (Figure 2.13). The immune response was much more apparent than in *D. glomerata*. Striking macroscopic symptoms of HR clearly demonstrated that *L. japonicus* is not a host for *R. collo-cygni*. The autofluorescence emission from the affected plant tissue was likely caused by the deployment and accumulation of ROS, such as hydrogen peroxide that damaged the chloroplasts that consequently leads to chlorophyll liberation to cytoplasm.

Although, more research would be needed to verify pathogen's compatibility amongst several dicot species, it is most likely that the fungus is primarily associated with monocot species. Since there were no other reports of *R. collo-cygni* on any other dicot species, the isolation of the pathogen from *C. sativa* could have been coincidental as the fungus could also survive saprotrophically and sporulate within mycelial mass. Such solitary type of spores on the leaf surface was also seen on *L.*

*japonicus*, which was not associated with stomata as typically observed in this pathogen after successful infection, and perhaps could be considered as act of desperation in order to survive.

Using model plant species for investigation of susceptibility mechanisms offers many advantages as there are many useful tools readily available, such as genome sequence, large mutant collections etc. Recently, Peraldi *et al.* (2013) verified compatibility of the model monocot species, *Brachypodium distachyon*. It would be possible to utilise this pathosystem in the future fundamental studies of molecular *R. collo-cygni* – host interactions. Subsequently, mechanisms of non-host resistance could now be studied using *L. japonicus*. This could help increase our understanding of this poorly known area of *Ramularia* research.

More studies are needed for the emerging pathogenic fungi in order to react to growing concerns with regards to their devastating impact on unprepared agriculture and horticulture. For instance, a very recent outbreak of ash dieback disease caused by ascomycete fungus *Chalara fraxinea* (teleomorph: *Hymenoscyphus pseudoalbidus*) (Gross *et al.,* 2014) has instigated a significant attention and public awareness of the plausible scenarios if future uncontrollable outbreaks of diseases took place, especially on economically important crop species. RLS has now become a plant disease of major importance for barley growers, despite being known for over a century (Cavara, 1893). The factors that contribute to the increase in prevalence of RLS remain to be conclusively determined. It is therefore essential to employ all available tools and resources, such as the fluorescently tagged *R. collo-cygni* isolates (Thirugnanasambandam *et al.,* 2011), to increase our understanding of *R. collo-cygni* infection of barley and to study other potentially important sources of the disease,

such as alternate hosts. This could lead to the development of new approaches and control measures to combat the disease. Presently, there are no cultivated barley varieties with high levels of resistance to *R. collo-cygni*. The detached leaf assay experiments involving a large number of barley cultivars and the transgenic isolates could be used to support field trials in order to find and characterise new resistance sources perhaps present in barley germplasm and to determine microscopically how any resistance may act against the pathogen. As the knowledge of the mode of action of the pathogen has now been significantly increased, it is suggested here that *R. collo-cygni* inoculation experiments could now be used for quantification of pathogen's development as an indicator of different susceptibility levels in a similar manner to that described for *Rhynchosporium commune* (Thirugnanasambandam *et al.,* 2010). It was not possible to attempt such study in this project due to limited availability of resources. For determination of different stages of the lifecycle of this fungus, the transgenic *R. collo-cygni* isolates were also used to further investigate the spread of inoculum from seeds to plants and plants to seeds, and in addition, to address the question of whether *R. collo-cygni* is able to persist in barley as an endophyte. Coupled with the PCR based techniques that enable the quantification of *R. collo-cygni* in infected leaf and seed material (Taylor *et al.,* 2009), visual analysis of the infection could provide knowledge on inoculum pressure required on the host before disease symptoms are seen. The combination of the methods described above will provide much more robust approach to obtain meaningful data and this could be used in addition to visual assessment based disease scoring across wide range of cultivars.

# Chapter 3

## Seed-borne transmission in *R. collo-cygni*

# 3. **Seed-borne transmission in *R. collo-cygni***

## 3.1. Introduction

It is estimated that about 90 per cent of all food crops in the world are propagated by seed. Nine such crops are of the highest importance and these are: wheat, rice, maize, barley, sorghum, sugar beet, common (*Phaseolus*) bean, soybean and ground nut. Combined they represent the greater part of food production worldwide and all of them are subject to attack by devastating seed-borne diseases, including plant pathogenic fungi. Although widely spread, vertical transmission of these microorganisms remains poorly understood (Neergaard, 1977).

The direct impact of fungi on seed is considerable. Many are parasites of seed primordia and maturing seeds thus reducing yield both quantitatively and qualitatively. Among the common types of seed disease and disorders, often encountered in combination are: seed abortion, shrunken or reduced seed size, seed rot, sclerotisation or stromatisation of seed, necrosis and discoloration, reduction or complete elimination of germination capacity, and physiological alterations in seed (Neergaard, 1977).

### 3.1.1. Overview of the seed-borne fungi

Barley is one of the major cereal crops, predominantly used for malting and for livestock feeding. Several major fungal pathogens that may affect seed of both winter and spring barley varieties have been described. The most serious seed borne diseases observed on this crop are: leaf blotch (scald) (*R. commune*), loose smut (*Ustilago nuda*), covered smut (*U. hordei*), barley leaf stripe (*Drechslera graminea*), net form and spot form net blotch (*Pyrenophora teres.* f. *teres* and f. *maculata*,

respectively), seedling and head blight (*Fusarium* spp. including *F. culmorum*, *F. graminearum* and *Microdochium nivale*), common foot rot (*D. sorokiniana*). Generally, seed-borne diseases are usually divided into two categories based on the mode of transmission.

It was first proposed by Hauptfleisch (1929) that *R. commune* infection was seed-borne. Subsequently, it was suggested that seed infection could have played a very important role in the introduction of this fungus into new areas with no history of barley cultivation (Habgood, 1971; Lee *et al.,* 2001). The symptoms of leaf blotch generally occur on the lemmas and paleas producing characteristic irregular or elliptical lesions with dark brown edges and pale centres (Lee *et al.,* 2001). However, Habgood (1971) and Kay & Owen (1973) showed that leaf blotch could also develop from symptomless seeds. Using PCR, Lee *et al.* (2002) demonstrated that visual assessments correlate poorly with *R. commune* DNA levels from the same seed. Brunner *et al.* (2007) showed that UK *R. commune* populations are genetically very similar to those found in Australia and that the initial establishment of this population was probably due to the transportation of seed from old British cultivars during the early part of the last century. Recently, Fountaine *et al.* (2010) investigated seed-borne transmission in *R. commune* using qPCR detection method and suggested that this type of fungal spread should not be underestimated as the pathogen may produce no symptoms in the plant for several months, and currently almost all of the commercial seed treatments used by growers are not active against *R. commune* infection contained in the seed.

Loose smuts of barley and wheat, *U. nuda* and *U. tritici,* are the classic examples of seed-borne fungi of the embryo colonising type of blossom infection (Neergaard,

1977). It has been claimed that diploid hyphae, after conjugation between germinating teliospores, penetrate between the papilla of the stigma and grow intercellularly through the style (Lang, 1910; 1917). However, it was also observed that germ tubes could only penetrate when papillae of the stigma had started to wither and collapse (Lang, 1910). Subsequent reinvestigations did not confirm that the stigma is indeed a path of infection (Pedersen, 1956) and pointed at penetration through ovary wall as the only method of invasion (Neergaard, 1977).

Similarly to *U. nuda*, in barley leaf stripe and net blotch pathogens, *P. graminea* and *Pyrenophora teres*, respectively, the mycelium is located within the seed tissue, specifically in pericarp (Babadoost, 1997) which makes it more difficult to control these diseases.

Some fungi for survival predominantly rely on the sophisticated mechanism of transmission via seed. It is certainly true for seed-borne ascomycetous endosymbionts of perennial grasses such as *Neotyphodium* (teleomorph *Epichloe*) species. These fungi have been studied in great detail, revealing intriguing insights into their life history. The first important findings were reported at the beginning of the 20$^{th}$ Century. Freeman (1904) elucidated the location of the fungus as being between the pericarp and aleurone layer of the starchy endosperm and showed embryo infection. He also described in detail the colonisation of shoot apical meristem.

### 3.1.2. Confocal microscopy for studying seed-borne stage in fungi

Utilisation of GFP expressing transgenic isolates of plant pathogenic fungi offers good potential to study least known aspects of biology and lifecycle of these often

cryptic microorganisms. Recently, research conducted on the rice blast fungus *Magnaporthe oryzae* using transgenic strains of the fungus revealed important insights into its seed-borne stage (Faivre-Rampant *et al.,* 2012). The main overwintering and primary inoculum sources reported in this pathogen are infested residues and seeds. A systemic infection has been proposed (Marcel *et al.,* 2010) but the evidence was never demonstrated and furthermore, the subsequent steps of the fungal life cycle remain largely unknown. The study followed *M. oryzae* progression in infected seeds from germination to established seedling stage, using detailed microscopic observations of GFP-tagged rice blast fungus strains. It was demonstrated that spores which were produced on contaminated seeds can infect emerging seedling tissues (coleoptile and primary root) and produce mycelium that colonizes the newly formed primary leaf and secondary roots. Furthermore, by using different rice cultivars, exhibiting distinct levels of resistance or susceptibility to *M. oryzae*, it was observed that resistance or susceptibility of a considered genotype is already established at the seedling stage. The results also showed that when plants are inoculated either at ripening stage (mature panicles), heading stage (flowering/ immature panicles) or even before heading (flag leaf fully developed), they produce infested seeds. These seeds produce contaminated seedlings that mostly die and serve as an inoculum source for healthy neighbouring plants, which gradually develop disease symptoms on leaves. This paper demonstrated that the seed-borne stage is not systemic in *M. oryzae* as the fungus is preferentially located on the seed coat and spreads onto neighbouring plant from infested material.

### 3.1.3. Current understanding of the seed-borne stage in *R. collo-cygni*

Evidence exists that *R. collo-cygni* may overwinter as a seed-borne stage (Havis *et al.,* 2006a, b; Frei, 2007; 2009; Matusinsky *et al.*, 2011; Havis *et al.,* 2013). First reports using developed PCR-based diagnostic method for the rapid detection of *R. collo-cygni* confirmed the transmission of the pathogen via seed (Havis *et al.,* 2006a, b). During field experiments in 1999 and 2004 in Scotland, the pathogen was indeed detected in harvested barley grain. Microscopic examination of seedlings cultivated from these seed samples revealed the presence of *R. collo-cygni* within leaves, although it was not present on the leaf surface (Havis *et al.,* 2013; Havis *et al.,* unpublished results, cited in Walters *et al.,* 2008). Nyman *et* al. (2009) have observed by using PCR diagnostics that plants with no visible RLS symptoms often produced kernels infected by *R. collo-cygni*. More recently, Matusinsky *et al.* (2011) have studied the impact of seed-borne *R. collo-cygni* infection on the intensity of RLS symptoms under field conditions using methods for the quantitative detection of the fungus. An important aim was determining the location of *R. collo-cygni* in the kernel by dissecting seeds into individual parts and quantifying *R. collo-cygni* DNA. The highest *R. collo-cygni* DNA concentration was observed in lemma, lower in the pericarp and embryo and negligible in the testa and endosperm. Presence of *R. collo-cygni* DNA was also detected in the water that was used for washing the kernels.

Most recently, Havis *et al.* (2013) confirmed that Rcc DNA could indeed be detected in the lemma of seed, with lower amounts found in the embryo and pericarp. However, in contrast to Matusinsky *et al.* (2011), a nested PCR diagnostic tool (Havis *et al.,* 2006a) indicated that colonisation of endosperm did take place. In fact, amongst seven barley cultivars used in the study, only the cultivar Concerto gave

negative endosperm infection results. Interestingly, during the investigation using light microscopy, Havis *et al.* (2014) reported that fungal mycelium was not observed on the leaf surface using light microscopy and staining techniques, whereas the presence of fungal structures in substomatal cavities was described.

The existence of a *R. collo-cygni* seed-borne stage could have serious implications for barley cultivation as the fungus may be present in the majority of crops prior to symptom expression. It was therefore necessary to study the process of fungal transmission via seed to understand the mode of infection as it could allow the development of more successful strategies of RLS management. This chapter describes the nature of the seed-borne stage by correlative use of light and confocal microscopy, and transgenic and field isolates of the fungus. The pathogen was followed from seed formation stages after flowering through dormancy. This work also demonstrates the development of the fungus after seed germination up to the first leaf stage. Furthermore, the potential impact of different levels of infection on seed germination is also addressed.

## 3.2. Materials and methods

### 3.2.1. Whole plant inoculation assay

#### 3.2.1.1. Plant material

Barley seeds (*Hordeum vulgare*) cvs. Optic and Belgravia were germinated in pots and maintained in a glasshouse under 16 h light at 18 °C and 8 h dark at 16 °C. To avoid interference with the potential natural *R. collo-cygni* infection, the material was tested for the presence of fungal DNA using qPCR based diagnostic method described by Taylor *et al.* (2007). Only seed batches with no detected fungal contamination or infection were selected for germination and subsequently used in this study.

#### 3.2.1.2. Fungal isolates

The transgenic isolate Rcc-8B9-GFP was cultured on potato dextrose agar medium (PDA) at 15 °C in darkness as previously described (Chapter 2, Section 2.1).

#### 3.2.1.3. Drop-inoculation assay

Drop-inoculation of barley leaves was performed as described for detached leaf assays (Thirugnanasambandam *et al.*, 2011 after Newton *et al.*, 2001) with some modifications. Mycelial fragments of GFP-expressing transformed isolates from 2-week-old spread-plates were prepared by scraping the colony surface with a sterile spatula, homogenizing, washing with sterile distilled water twice and then filtering through sterile gauze. It was not possible to accurately quantify a fungal mycelial fragment inoculum suspension due to the apparent problem with obtaining spores in culture. The mycelium harvested from a single spread-plate was diluted in 5 mL sterile distilled water to drop-inoculate 10 µL onto each of 8 - 10 places of the flag

leaves prior to head emergence. Some of the stems were also punctured with pipette tips to transfer inoculum onto the developing head inside the pseudostem surrounded by a leaf sheath. The experiment was repeated twice with different preparations of inoculum and plants.


Figure 3.1
Whole plant inoculation procedure: a) high humidity levels post inoculation maintained by placing flag leaves and emerging awns in sterile zip-bags; b) drop inoculated flag leaf and awns, indicated by arrows; c) 15 days post inoculation; note the presence of surprisingly early symptoms developing on flag leaf (red arrows).

### 3.2.2. Examination of the infected seeds, coleoptiles and seedlings

#### 3.2.2.1. Preparation of material for confocal microscopy

Barley ears derived from inoculated plants were examined at several different developmental stages of ripening, from ear emergence through to mid flowering, watery ripe and hard dough stages. Developing kernels were dissected using a sterile vibratome blade to obtain thin longitudal sections. It was not possible to embed seed material prior to sectioning without compromising GFP expression due to potential heat or chemical damage of fungal hyphae.

To observe the transmission of *R. collo-cygni* into the seedlings, seeds derived from plants previously inoculated with the transgenic strain Rcc-8B9-GFP were washed several times with sterile distilled water for approximately 30 minutes and then placed in petri dishes on soaked sterile paper towels for germination (Figure 3.2).

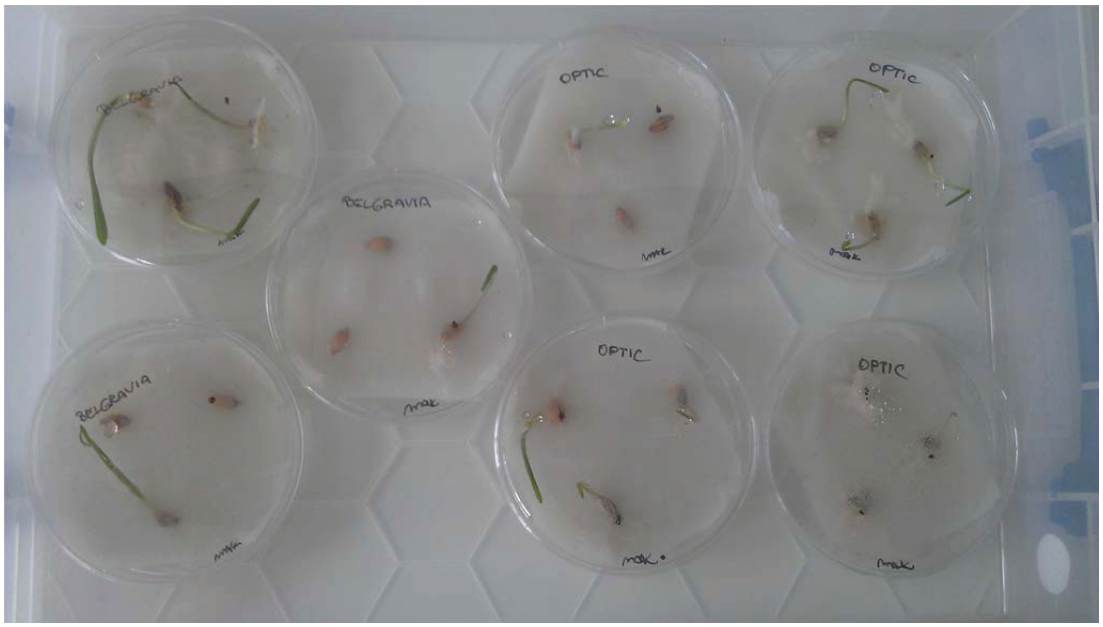


Figure 3.2
Infected seeds of spring barley cultivars Optic and Belgravia germinated *in vitro* for subsequent examination by confocal microscopy.

#### 3.2.2.2. Confocal microscopy conditions

Transverse sections of the emerging coleoptiles and first true leaves were examined for the presence of viable fungal hyphae using Leica SP2 CLSM on a DM6000 microscope fitted with a FI/RH filter block (excitation filter BP 490/15, dichroic mirror 500, emission filter BP 525/20; excitation filter BP 560/25, dichroic mirror 580, emission filter BP 605/30) and Leica water-dipping lenses (HCX APO L10x / 0.30 W U-V-1, L20x /0.50 W U-V-1, L40x /0.80 W U-V-1 or L63x /0.90 W U-V-1). GFP fluorescence was imaged at the excitation wavelength of 488 nm and emission was collected at 500–530 nm. The autofluorescence signal from chlorophyll was collected simultaneously at light wavelengths between 650 and 700 nm. Transmission images (non-confocal) were captured using the transmission detector of the microscopes to collect 488-nm light passing through the leaf. Unless specified, the images are overlay projections of z-stacks at maximum intensity and were assembled and edited using MacBiophotonics® ImageJ or Adobe Photoshop® CS5 software.

### 3.2.3. Embedding on naturally infected seed

Seed samples determined to contain *R. collo-cygni* DNA (Taylor *et al.,* 2007) were fixed and embedded using Paraplast® embedding as described earlier (Chapter 4, Section 4.2.7) according to Weigel & Glazebrook (2008) with some modifications. Seeds were fixed in 10 ml of formaldehyde: glacial acetic acid fixative (FAA) in 20 ml scintillation vials and incubated overnight. Fixative was then replaced with 50% ethanol and moved through ethanol series (60, 70, 85 and 95%) for 45 min at each concentration. This was followed by counterstaning in 0.1% eosin Y in 95% ethanol

overnight. Eosin Y solution was then washed off with 100% ethanol, and then gradually replaced by a series of xylene : ethanol (25:75, 50:50, 75:25%, respectively) and finally by 100% xylene. Paraplant chips were then added and incubated at 42 ºC (around 20 each time, after the previous had dissolved, until 100 chips per vial). Finally, xylene : Paraplast solution was replaced by molten Paraplast chips at 60°C. Molten Paraplast was replaced every 12 hours at least three times to ensure deep and uniform penetration of dense seed tissues. Individual impregnated seeds were then placed in plastic molds and sunk in molten Paraplast. Samples were then allowed to set at room temperature and subsequently stored in a fridge at 4 ºC until needed.

### 3.2.4. Preparation of embedded material for light microscopy

Sectioning was performed using a metal microtome knife mounted on a Leica Microtome. The set depth of each section was between 5 and 10 μm, connected in ribbons comprising 5 to 6 sections. Ribbons were then placed on microscope slide and washed in xylene to remove Paraplast. Individual sections were then stained with aniline blue for subsequent microscopy.

### 3.2.5. Impact of *R. collo-cygni* infection on germination

In the experiments assessing the impact of fungal infection/ contamination on the germination of seeds containing different levels of *R. collo-cygni* DNA, seeds of spring barley Belgravia and Garner were placed in 96 well germination blocks, with 2 seeds in each of the 4 corners, giving the total of 100 per seed batch (Figure 3.3). Plants were maintained in growth chamber (Snijders Scientific Ltd.) under the same conditions as described above and allowed to develop until second leaf stage. All

germinated plants were then counted for subsequent analysis of variance (ANOVA) using GenStat version 11.1 (VSN International Ltd).

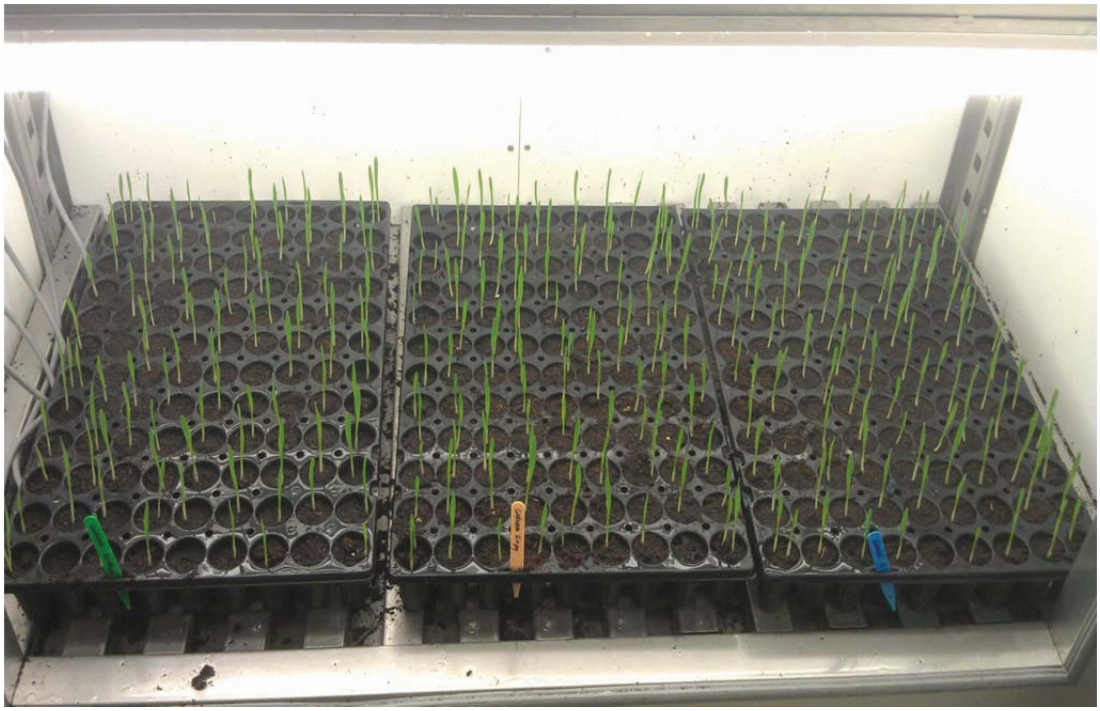

Figure 3.3
Germination experiment using 100 seeds of spring barley cultivar Garner. Three different batches were used, from clean seeds (0 pg DNA), through medium infection at 5.11pg DNA, to highly infected seed (30.66 pg DNA).

## 3.3. Results

### 3.3.1. Confocal examination of vertical transmission

In order to study the mode of vertical transmission via seed in *R. collo-cygni* - barley system, host plants were inoculated with the transgenic isolate Rcc-8B9-GFP prior to head emergence and infection progress was frequently monitored using visual assessment and confocal microscopy. On flag leaves symptoms developed much more rapidly than previously observed on younger plants (see Chapter 2). Typical RLS lesions were observed forming from 2 weeks after inoculation (Figure 3.4 a).


Figure 3.4
Rcc-8B9-GFP-infected ears used in this study: a) head after flowering; note typical symptoms developed on the leaf at 21 dpi indicated by red arrow; b) harvested ear subsequently used for sectioning of the seeds. Red arrow indicates fungal mycelium with the characteristic rubellin pigment on the seed coat.

Plants were allowed to mature and kernels were collected for further studies at different developmental stages. Size and morphology of the ears and seeds on heavily infected plants appeared the same as on healthy control plants. In some cases fungal mycelium was visible with unaided eye (Figure 3.4b).

Confocal examination of seeds at milky stage of development showed accumulation of hyphae between the pericarp and aleurone layer of the endosperm (Figure 3.5 a). No visible signs of damage to seed tissue caused by fungal infection at this early stage were observed. The plant appeared to tolerate the presence of the pathogen under the seed coat. Interestingly, numerous hyphal swellings were also seen in some seeds.

In dissected mature seed, a thick layer of interwoven fungal hyphae just outside the aleurone layer was detected (Figure 3.5 b-c). It appeared much denser than previously observed for earlier stages of kernel development. In some instances, fungus penetrated the aleurone layer, but growth remained intercellular (Figure 3.5 b). Hyphal size appeared very similar to that observed for mesophyll colonising hyphae during endophytic growth in leaves, i.e. up to 4 μm in diameter (Figure 3.5 c).

This dense fungal layer under the seed coat initially appeared uniformly distributed around the lumen of dissected kernels however, in a few cases after many repeated observations it tended to become more concentrated near the space between endosperm and scutellum. This led to further investigation into a possible embryo infection.

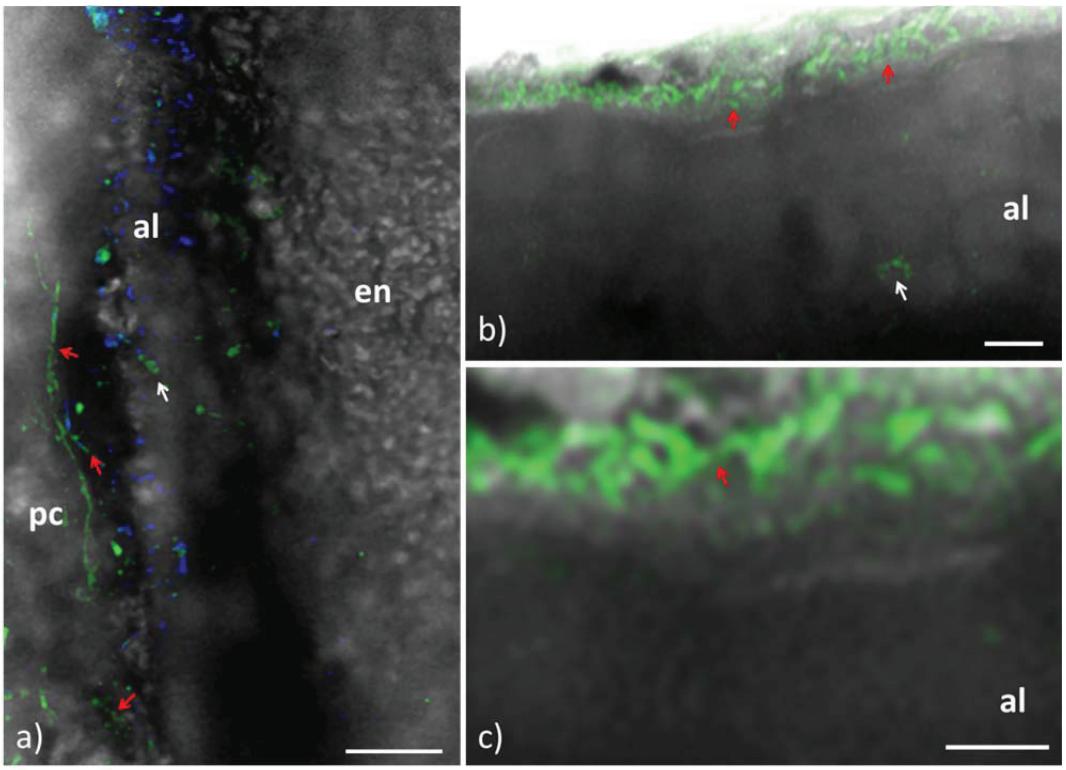


Figure 3.5

Confocal images of the longitudinal section of a kernel (cv. Optic) showing location of the transgenic isolate Rcc-8B9-GFP within the seed tissue. Green channel represents GFP expressing transgenic isolate 8B9; blue channel – chlorophyll; grey channel – bright field transmission: a) low magnification image of the longitudinal section of barley cv. 'Optic' seed at milky stage showing accumulation of hyphae between pericarp (pc) and aleurone layer (al) of endosperm (en), indicated by red arrows. Note swollen segments of hyphae (white arrow). Bar = 100 µm; b) a very dense layer of highly branched hyphae (arrows) is present between the pericarp and aleurone layer (al) of the endosperm in a fully ripened kernel (red arrows). Note presence of hypha between aleurone cells (white arrow). Bar = 50 µm; c) high magnification image of the interwoven hyphae outside the aleurone layer (al). Bar = 10 µm.

*R. collo-cygni* hyphae were subsequently found to be able to colonise the scutellum (Figure 3.6 a). Interestingly however, within dry seed, the pathogen remained outside the coleoptile and did not progress any further into the embryo at this stage.

In order to study the process of vertical transmission during germination, seeds were placed in humid environment. Initial examination after 16 hours revealed that some hypha started to penetrate through the coleoptile (Figure 3.6 b). This was followed by the observation of several viable hyphae within the embryonic tissues at 24 hours into germination. Fungal growth still appeared extracellular as in all previous stages (Figure 3.6 c). However, the longitudinal sections of the seed, performed manually, did not allow complete verification of this observation. It was therefore necessary to confirm this by preparing cross transverse sections as well. This procedure showed that indeed, tissue penetration is intercellular. A heavy infection of leaf primordia had a rather complex nature. A dense hyphal layer was observed under the coleoptile within the tissue of a young shoot (Figure 3.7 a). However, after careful excision of the coleoptile, a hyphal network was also observed on abaxial surface of the membrane, suggesting that hyphae were both on the surface of young leaves and within inner tissues (Figure 3.7 b).

Some of hyphae were found very deep and appeared evenly distributed across the developing leaf (Figure 3.7 c). The observed hyphae were clearly intercellular. Despite the heavy and rather aggressive nature of fungal colonisation, no apparent damage or symptoms due to plant infection was ever observed. The examined seeds germinated successfully, in a normal way as would be expected from healthy seed material.

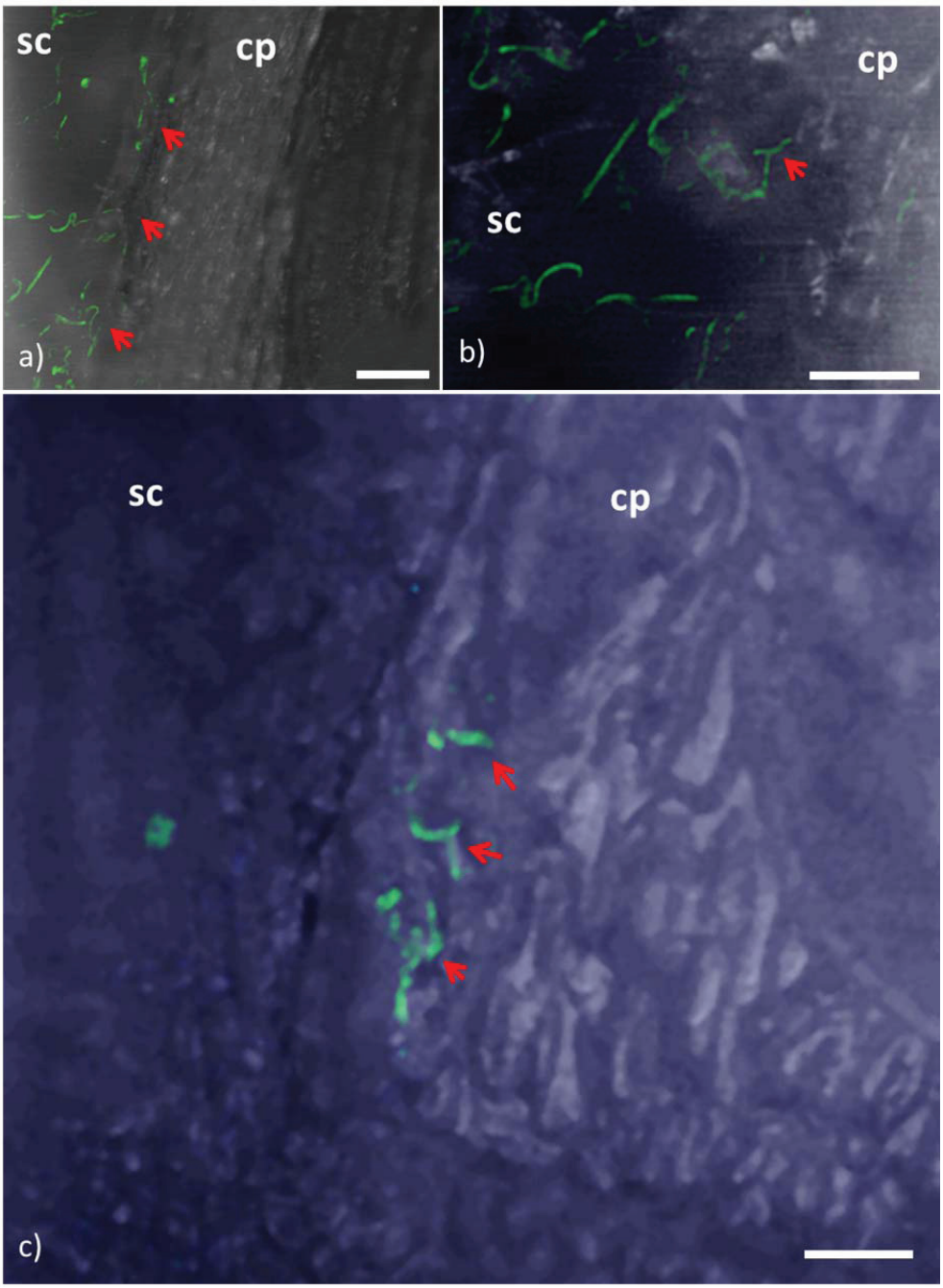


Figure 3.6
Confocal images of embryo infection in barley Optic: a) longitudinal section through scutellum (sc) and coleoptile (cp) before germination. Hyphae (red arrows) infected sc but did not penetrate cp (arrows). Bar = 100 µm; b) hypha (red arrow) penetrating cp at 16 hours after transferring into humid condition for germination. Bar = 50 µm; c) infection of cp at 24 hours into germination. Hyphal growth appears intercellular (red arrows). Bar = 20 µm.

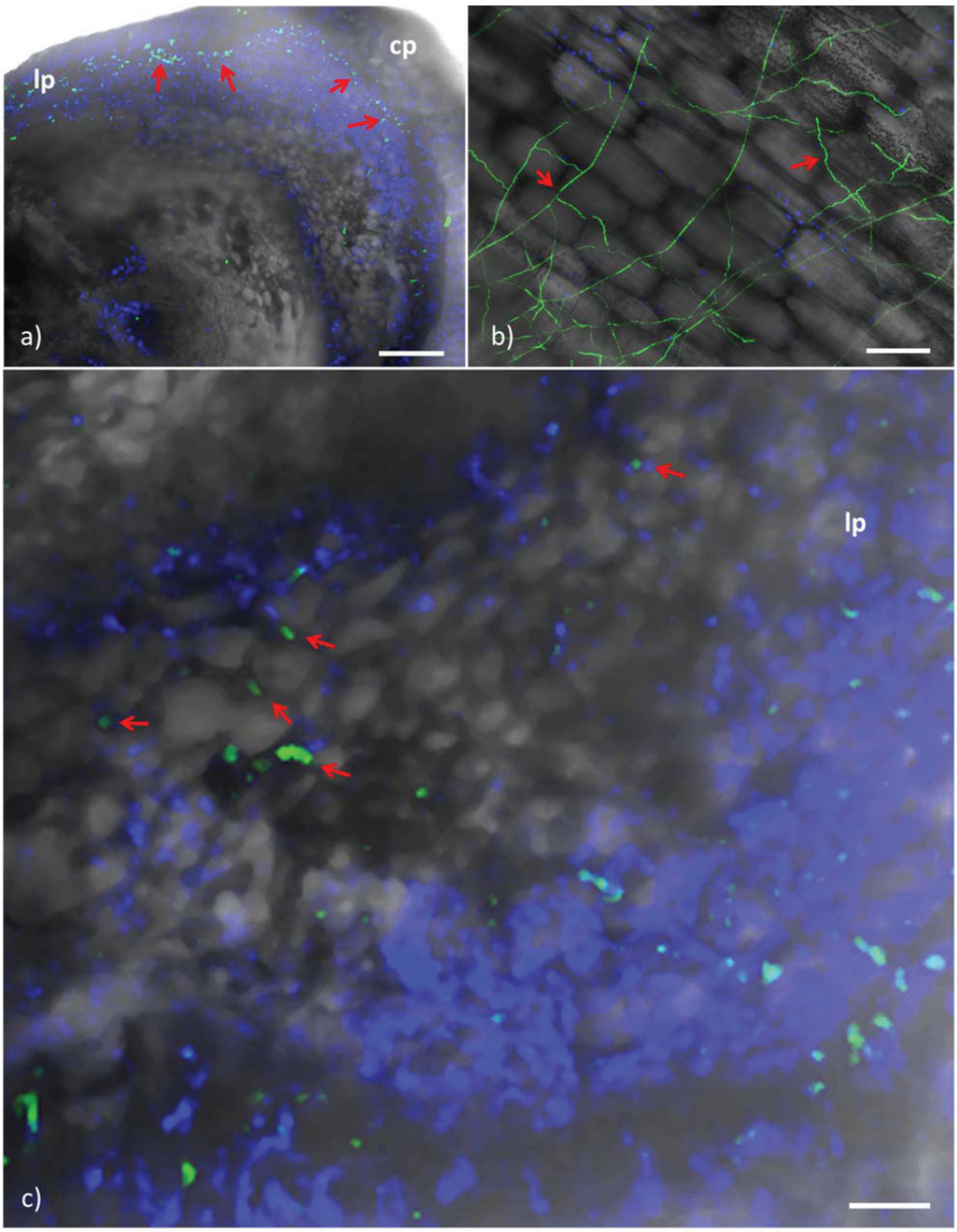


Figure 3.7
Confocal images of infected embryo: a) transverse section through the coleoptile (cp). Note heavy infection of the leaf primordia (lp) indicated by red arrows. Bar = 200 µm; b) abaxial side of shoot sheath surrounding embryo infected by *R. collo-cygni* hyphae (red arrows). Bar = 20 µm; c) transverse section through the coleoptile. Red arrows indicate the intercellular endophytic hyphae. Bar = 50 µm.

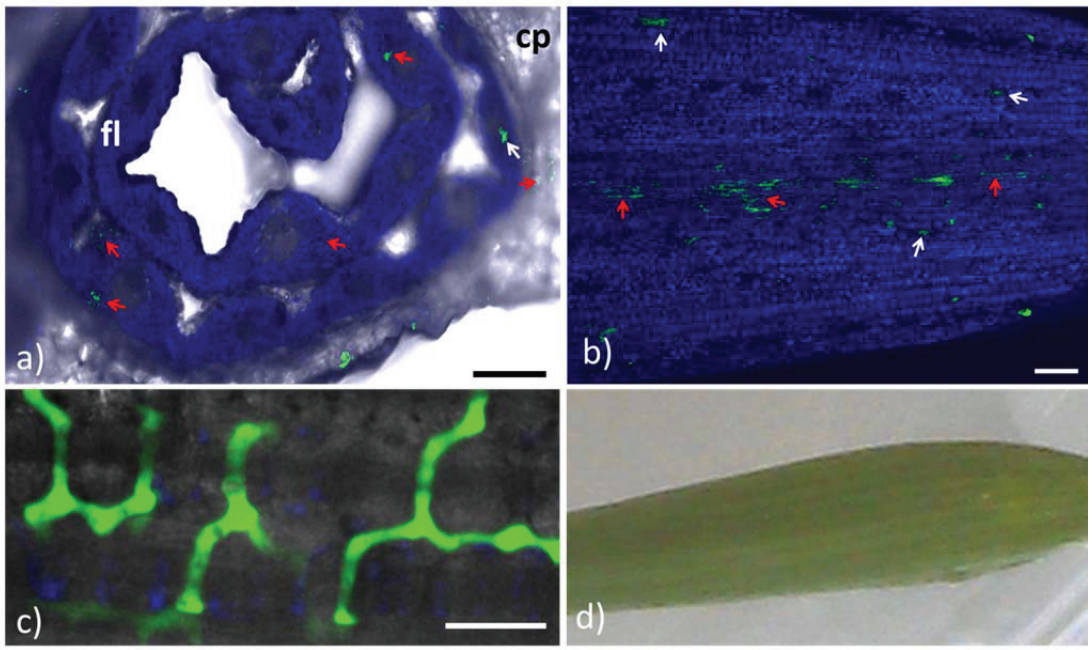


Figure 3.8
Confocal images of barley cv. Belgravia germination process showing the development of Rcc-8B9-GFP isolate in barley seedling. Green channel represents GFP expressing transgenic isolate 8B9; blue channel – chlorophyll; grey channel – bright field transmission: a) transverse section through the coleoptile (cp) and first 'rolled' developing leaf (fl). Red arrows indicate presence of fungal hyphae. Note penetration of vascular bundle (white arrow). Bar = 200 µm; b) dissected and flattened first leaf corresponding to (a). The pathogen is present throughout the leaf but is clearly concentrated around the midrib (red arrows). White arrows show conidiogynous aggregates within substomatal cavities. Bar = 200 µm; c) High magnification image of intercellular mesophyll colonising hyphae. Bar = 20 µm; d) completely symptomless leaf at 5 days post germination, despite heavy infection of mesophyll tissue by endophytic hyphae.

The pathogen remained present in intercellular space of the mesophyll in the developing first leaf as well as under the coleoptile (Figure 3.8 a). After flattening of the leaf, a brick work-like endophytic growth pattern was observed (Figure 3.8 b-c). Despite the systemic infection of the mesophyll layer, the leaf developed normally, and no symptoms were observed either with the unaided eye (Figure 3.8 d) or under the microscope.

### 3.3.2. Anatomy of naturally infected seed material using light microscopy

In order to verify the findings, seed material harvested in the field was tested for the presence of *R. collo-cygni* DNA. Heavily infected seed batches were embedded in Paraplast and sectioned. For control purposes, the seed that came back *Ramularia* negative were also used (Figure 3.9 a). Lemma and pericarp were clean and deeply-stained hyphae were not observed. In comparison, in infected seed pericarp, gradual accumulation of a hyphal layer was immediately visible (Figure 3.9 b-c) and a thick fungal network remained outside aleurone layer (Figure 3.9 c). The staining procedure was very useful as hyphae could be easily distinguished from plant tissue due to much higher accumulation of aniline blue in fungal structures. The growth was intercellular (Figure 8.9 d) which confirmed the findings from inoculation experiments. In most cases hyphal growth was present just above the scutellum (Figure 3.9 e) which confirmed this mode of entry and subsequent colonisation of embryo.

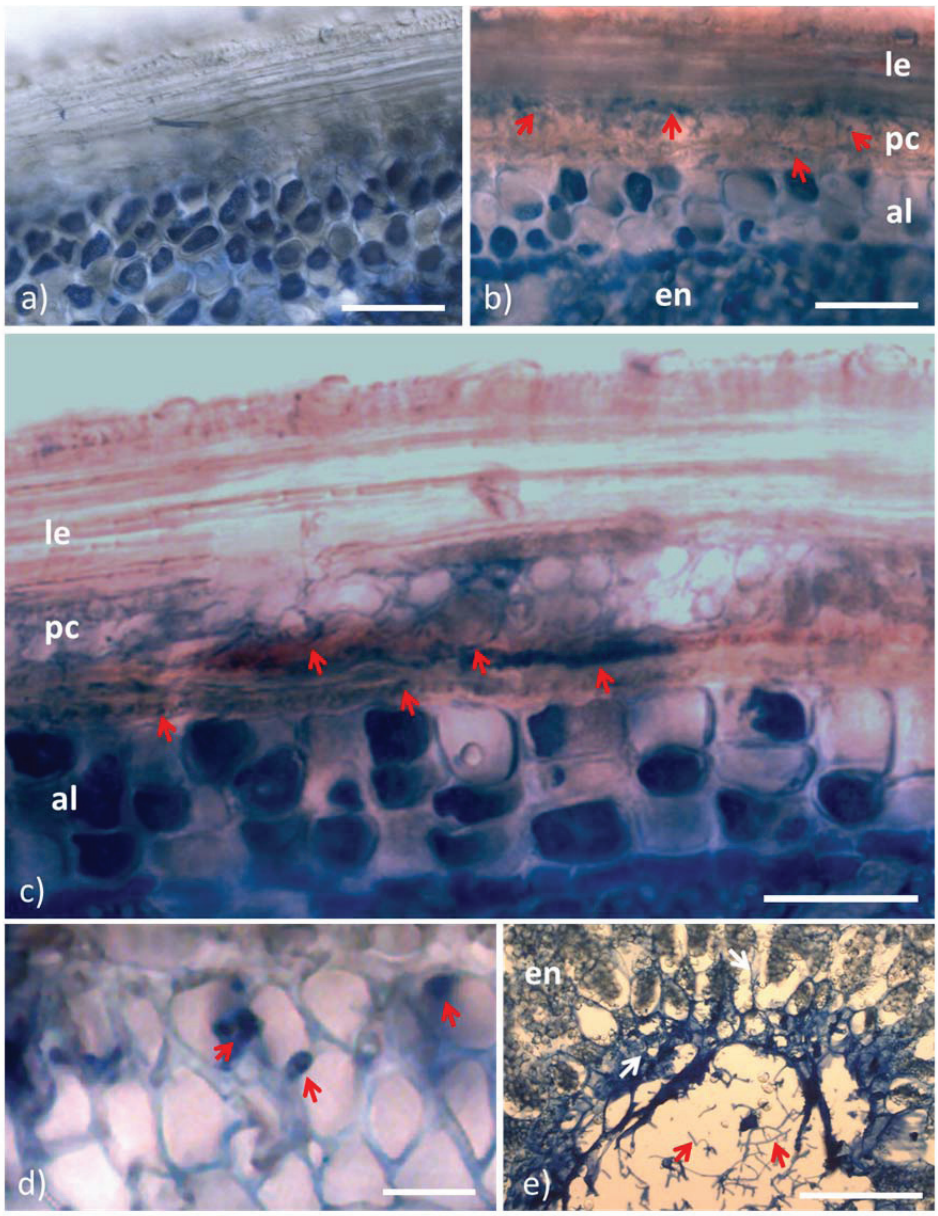


Figure 3.9
Bright field images of microtome sections (depth ~ 5 µm) of Paraplast-embedded seed material of cultivar Belgravia, stained with aniline blue; le – lemma; pc – pericarp; al – aleurone layer; en – endosperm. High level of *R. collo-cygni* DNA determined to be present in seeds used for sections b-e); a) image of a 'clean' seed of the same cultivar. Bar = 100 µm; b) *R. collo-cygni* hyphae (red arrows) present in pc and le, just under seed coat. Bar = 100 µm; c) Heavy infection of pc by accumulated layer of interwoven fungal hyphae, indicated by red arrows. Some hyphae present between pc and al. Bar = 50 µm; d) high magnification image of deeply stained intercellular hyphae (red arrows). Bar = 10 µm; e) infection of en by branched hyphae (white arrow) and likely point of embryo infection just above scutellum (red arrows). Bar = 50 µm

### 3.3.3. Impact of *R. collo-cygni* infection on seed germination

Since *R. collo-cygni* colonisation did not appear to impair germination or have any other negative impact on seed morphology and anatomy in all infected plant material, a simple experiment was attempted to address this in a more analytical way.

The seeds of two different spring barley cultivars with medium and high level of *R. collo-cygni* DNA were germinated. Additionally, seed batches with no detectable fungal DNA were used as controls. After repeating the experiments four times for 100 seeds per cultivar per DNA level each time, the subsequent analysis of variance (ANOVA) did not show any significant differences, therefore demonstrating that the seed infection has no impact of germination capability and establishing the crop. The total means are presented in Table 3.1 below.

Table 3.1

The assessment of the impact of *R. collo-cygni* on germination of barley

| Variety | DNA level | | |
|---|---|---|---|
| | High | Low | Zero |
| Belgravia | 92.75 | 92.5 | 92.25 |
| Garner | 92.75 | 92 | 90.5 |

## 3.4. Discussion

In chapter 3, a whole plant inoculation assay was developed to investigate the mode of the fungal seed-borne transmission by using GFP expressing strain of the fungus. It is shown here for the first time that the vertical transmission is systemic, involving symptomless colonisation of embryo and closely resembled the mode of dissemination observed for *Neotyphodium* species, mutualistic fungal endosymbionts on grasses. These results were compared by histological study of naturally infected seed material. The impact of fungal infection on seed germination ability was also examined that revealed no significant difference between clean, moderate and high levels of *R. collo-cygni* DNA.

Many pathogenic and mutualistic fungi use the plant seed as a means of dissemination and transmission between growing seasons. Recent studies indicated that it is also the case for *R. collo-cygni,* which may overwinter as a seed-borne stage (Havis *et al.,* 2006a, b; Frei, 2007; 2009; Matusinsky *et al.*, 2011; Havis *et al.,* 2014). Recent development of PCR-based diagnostic methods for the rapid detection of *R. collo-cygni* was successfully applied to confirm that such transmission takes place (Havis *et al.,* 2006 a, b). During field experiments in 1999 and 2004 in Scotland, the pathogen was indeed detected in harvested barley grain (Walters *et al.,* 2008). Subsequent qPCR diagnostic tool (Taylor *et al.,* 2009) allowed the quantification of the fungal DNA in the seed. Furthermore, Nyman *et* al. (2009) using PCR diagnostics observed that plants with no visible RLS symptoms often produced kernels infected by *R. collo-cygni*.

Several important questions remained which could not be answered using DNA-based methods. For instance, what is the real nature of the *R. collo-cygni* seed-borne stage? Is this vertical or horizontal mode of fungal transmission? Does the fungus colonise the seed in a systemic way or contaminate the seed coat? Matusinsky *et al.* (2011) and Havis *et al.* (2014) verified the presence of DNA within seed however the results were inconclusive as the fungus appeared to be in all types of seed tissue as well as in the water used for washing the plant material for subsequent dissection.

In order to develop a better understanding of the seed-borne stage and answer the questions listed above, it was necessary to apply microscopy to directly observe the fungus on the plant surface and within host tissues. Therefore this study further utilised the developed whole plant inoculation assay and genetically transformed *R. collo-cygni* isolate expressing GFP reporter molecule to initially observe and characterise the mode of fungal transmission via seed. This approach proved useful to generate seed infected with Rcc-8B9-GFP strain. The seed collected from infected plants appeared normal in terms of their morphology. No apparent necrotic symptoms were observed on the grain which suggested that the seed health has not been compromised. This contradicts the notion that yield losses due to RLS are caused by a significant decrease of kernel size and quality (Greif, 2002; Harvey, 2002; Hjorshoj *et al.,* 2013).

The dissected seeds revealed the infection of lemma and pericarp and partially confirmed observations made by Matusinsky *et al.* (2011). The fungus was indeed observed colonising the pericarp and more specifically the space between the pericarp and the aleurone layer of the endosperm (Figure 3.5) from which it also infected the embryo (Figure 3.6). The infection of embryo involved penetration of

scutellum (Figure 3.6 c). This demonstrated a systemic mode of transmission. Most recently, Havis *et al.* (2014) also confirmed these observations, however, in contrast to Matusinsky *et al.* (2011), the nested PCR diagnostic tool (Havis *et al.,* 2006a) used in the study indicated that colonisation of endosperm took place. In fact, amongst seven barley cultivars used in the study, only in the endosperm of cultivar Concerto were the results negative. In the current study, the fungal hyphae were also observed within the endosperm on several occasions which confirm the results reported by Havis *et al.* (2014). However, the hyphae seen in the endosperm appeared rather sporadic and their presence could have been coincidental (Figure 3.5 b). There was no damage caused by the fungus and host tissue remained asymptomatic. Since seeds were washed prior to sectioning, only some fungal hyphae could be observed on the seed coat (Figure 3.4). It was also present on the head axis. This could have been artificial and a direct result of the inoculation of developing heads inside the leaf sheath. The fungus could then have survived as saprophyte for a period of time.

In order to initially test germination percentage and to observe if the fungus remained viable during dormancy in dry kernels, barley seeds were germinated *in vitro*. At 12 hours post germination, the infection of leaf primordia was observed demonstrating that the fungus survived within dry host tissue. At four weeks after harvest, GFP signal was weak on many occasions which suggested slow metabolism of fungal cells. This could suggest the strategy that is employed for survival during seed storage periods.

Fungal progression in the developing coleoptile, leaf primordia and seedling was then followed. Fungal growth within barley tissues remained intercellular at all

times. A dense hyphal layer was concentrated under the coleoptile within the tissue of young shoot (Figure 3.7 a). Havis *et al.* (2014) have recently reported use of light microscopy for the examination of seedlings cultivated from field seed samples tested for the presence of *R. collo-cygni* DNA. During the investigation, it was reported that fungal mycelium were never observed on the leaf surface whereas the presence of fungal structures in substomatal cavities was noted. However, no evidence such as microscopic images was produced by these authors to support these statements. Our findings indicated that a majority of fungal mass was embedded in the mesophyll layer, although some mycelium was also present on the leaf surface. After careful removal of the coleoptile, a hyphal network was detected on the abaxial surface of the membrane suggesting that some hyphae grew on the surface of young developing leaves (Figure 3.7 b). Despite the prolific and aggressive nature of fungal colonisation, no apparent damage or symptoms on plant tissue was ever observed. All examined seeds germinated successfully as would be expected from healthy seed material. At the first leaf stage, the infection remained strictly endophytic showing the typical brick work- like growth pattern, which concentrated near the midrib and appeared evenly distributed throughout the length of the leaf. This suggested that the fungal hyphae under the coleoptile surrounding the developing leaf could have been coincidental and since the fungus was observed on the seed coat, it could colonise this space after coleoptile emergence. Most importantly, all the leaf material generated and used in this study was asymptomatic (Figure 3.8 d).

The location of *R. collo-cygni* in naturally infected seed was also investigated using histological approaches, i.e. embedding, sectioning and staining procedure. The results confirmed the findings from inoculation experiments, demonstrating the

systemic mode of fungal transmission. The Paraplast embedding method proved useful but it was very challenging to obtain good quality sections due to the hardness of seed material, despite extended periods of infiltration. It would therefore be desirable to use resin embedding rather than paraplast in future histological studies of the seed-borne stage of *R. collo-cygni*.

The findings clearly show striking similarities to the observed symbiotic associations between endophytes of *Epichloe/ Neotyphodium* species (epichloe endophytes; family *Clavicipitaceae*) and cool season grasses (family *Poaceae*, subfamily *Pooideae*). In these associations (symbiota), the fungus occupies a specialised niche within grass leaf tissues, in which it has access to nutrients in the apoplastic space, and also has a means of dissemination by transmission through the host seeds (Schardl *et al.,* 2004). In return, the endophyte promotes host growth and persistence through improved nutrient acquisition and facilitates protection from a range of biotic and abiotic stresses, including drought, disease, and animal herbivory. It has been demonstrated that protection from herbivory is associated with fungal synthesis of various biologically active metabolites, such as peramine, lolines, indole-diterpenes, and ergot alkaloids (Schardl *et al.*, 2013).

Intercellular space as the endophytic niche that offers a unique habitat for *R. collo-cygni* has been described in this study. The fungus is contained within the seed and is not subject to the direct influence of the environment when colonising intercellular spaces during barley growth. The pathogen accumulates along the plant axis. The endophytic features of *R. collo-cygni* are due to the reproductive modes used by this apparently pathogenic species that could be both vertically and horizontally transmitted. The fact that *R. collo-cygni* is transmitted in a very similar manner to

*Neotyphodium* endosymbionts on grasses and that the fungus is able to maintain asymptomatic infection throughout a majority of its life cycle on the barley host poses a question with regard to the current definition of parasitism and mutualism. Ascomycetous endophytes that live within host grass tissues are viewed as strong mutualists on the basis of theory and empirical studies of introduced agronomic grasses. Evolutionary theory predicts that microbial symbionts should evolve to benefit their hosts and normally lose sexuality and rely on propagules of their hosts for transmission (Faeth & Sullivan, 2003). The assumption of mutualism has recently been tested in native grasses, which often harbour high but variable frequencies of systemic asexual endophytes. In a 3-year field experiment, Faeth and Sullivan (2003) tested the effect of *Neotyphodium* infections on the native fescue species in Arizona, USA. Their findings demonstrated that infection generally decreased host growth in terms of plant volume, number of tillers, and dry mass of shoots and roots, contradicting previous assumptions and challenged the notion that systemic asexual endophytes must be plant mutualists for infections to persist in nature.

In *Epichloe* endophyte-grass associations, hyphae display a highly restricted growth pattern, systemically colonising all aerial host tissues but remaining within host intercellular spaces, aligned parallel to the leaf axis (Christensen *et al.,* 2002, 2008). Hyphal growth is closely coordinated with host growth. For instance, hyphae remain metabolically active throughout the life of the host, but their growth is observed only during periods of host leaf growth (Tan *et al.,* 1997; Christensen *et al.,* 2002, 2008). This apparently regulated control of endophyte growth within the grass is indicative of underlying sophisticated signalling between host and fungus. Recent work using

the *Epichloe festucae*-perennial ryegrass (*L. perenne*) association as a model experimental system has highlighted how finely balanced the interaction is between mutualism and antagonism. Disruption of components of the reactive oxygen species (ROS)-generating NADPH oxidase (Nox) complex, including NoxA, NoxR, and RacA, led to a breakdown of the mutualistic interaction, with endophyte mutants displaying unrestricted growth in planta and inducing host stunting and premature senescence (Takemoto *et al.,* 2006; Tanaka *et al.,* 2006, 2008). More recently, it has been shown that disruption in signalling pathway in fungal grass endophyte led to pathogenesis (Eaton *et al.,* 2010). In the *E. festucae* - perennial ryegrass (*L. perenne*) association as a model symbiotic experimental system, an essential role for the fungal stress-activated mitogen-activated protein kinase (sakA) in the establishment and maintenance of this mutualistic interaction was demonstrated. Deletion of sakA switched the fungal interaction with the host from mutualistic to pathogenic. Infected plants exhibit loss of apical dominance, premature senescence, and dramatic changes in development, including the formation of bulb-like structures at the base of tillers that lack anthocyanin pigmentation. Furthermore, the transcriptome of sakA mutants in comparison with wild-type showed dramatic changes in fungal gene expression consistent with the transition from restricted to proliferative growth, including a down-regulation of several clusters of secondary metabolite genes and up-regulation of a large set of genes that encode hydrolytic enzymes and transporters. Corresponding analysis of the host *L. perenne* transcriptome revealed up-regulation of host genes involved in pathogen defence and transposon activation as well as dramatic changes in anthocyanin and hormone biosynthetic/ responsive gene expression. These results clearly highlighted the fine balance between mutualism and

antagonism in a plant-fungal interaction and suggest similar future studies to be undertaken in *R. collo-cygni* – barley association at molecular level. This could allow further our understanding of the fungal transition from endophytic to pathogenic stage (Eaton *et al*., 2010).

The nature of the seed-borne stage has now been described by correlative use of light and confocal microscopy, and transgenic and field isolates of the fungus in much greater detail than in any previous studies. The pathogen was followed from seed formation stages after flowering through dormancy. This work for the first time demonstrates the location of *R. collo-cygni* within the seed and its subsequent development after seed germination up to the first leaf stage. Furthermore, the potential impact of different levels of infection on seed germination was also addressed showing that the presence of the pathogen in the seed material did not have any negative impacts on germination ability thus suggesting that crop could establish in the field environment despite fungal infection (Table 3.1). The existence of *R. collo-cygni* seed-borne stage could have serious implications for barley cultivation as the fungus may be present in the majority of crops prior to symptom expression. This current study of histology and infection pathways in the process of fungal transmission via seed should therefore be used for the development of more successful strategies of RLS management. Perhaps the new systemic seed treatments could eliminate the pathogen from being present in the field from the very beginning of growing season.

# Chapter 4

## Sexual reproduction in *R. collo-cygni*

# 4. Sexual reproduction in *R. collo-cygni*

## 4.1. Introduction

Detailed analysis of sexual development in filamentous fungi using microscopy has been mainly undertaken in well studied model organisms such as *N. crassa* (Raju, 2008)*, Podospora tetrasperma* and *P. vesticola* (Bell and Mahoney, 1996), and *S. macrospora* (Lord and Read, 2011). In the latter study, the authors used state-of-art microscopy to demonstrate 'step by step' morphogenesis of the perithecium to enhance our general understanding of the sexual development in filamentous fungi. On the other hand, studies of sexual reproduction in plant pathogenic fungi, especially in *Mycosphaerella* species are much less frequent. Higgins (1920, 1929, 1936) was first to provide an analysis of these fundamental processes, and he demonstrated the role of spermatia as 'male' donors' in *Sphaerella bolleana, M. personata* and *M. tulipiferae* (Figure 4.1) respectively, using microtomed lesion samples. Relatively little has been done to expand knowledge of sexual reproduction in *Mycosphaerellaceae* step by step since then, despite numerous reports of *Mycosphaerella* teleomorph stages of major plant pathogenic fungi such as *Septoria, Cercospora* and related genera (Barr, 1956; Keiser and Crous, 1998; Davis, 1938; Gilman and Wadley, 1952; Ware *et al.,* 2007). Most recently, Niyo *et al.* (1986) used TEM and SEM microscopy to provide fascinating insights into ultrastructure of the ascocarps, asci and ascospores of *M. populorum* (anamorph: *Septoria musiva*), the pathogen causing leaf spots and stem and branch canker of *Populus* species. Nevertheless, such studies are still rare in modern mycology and plant pathology.

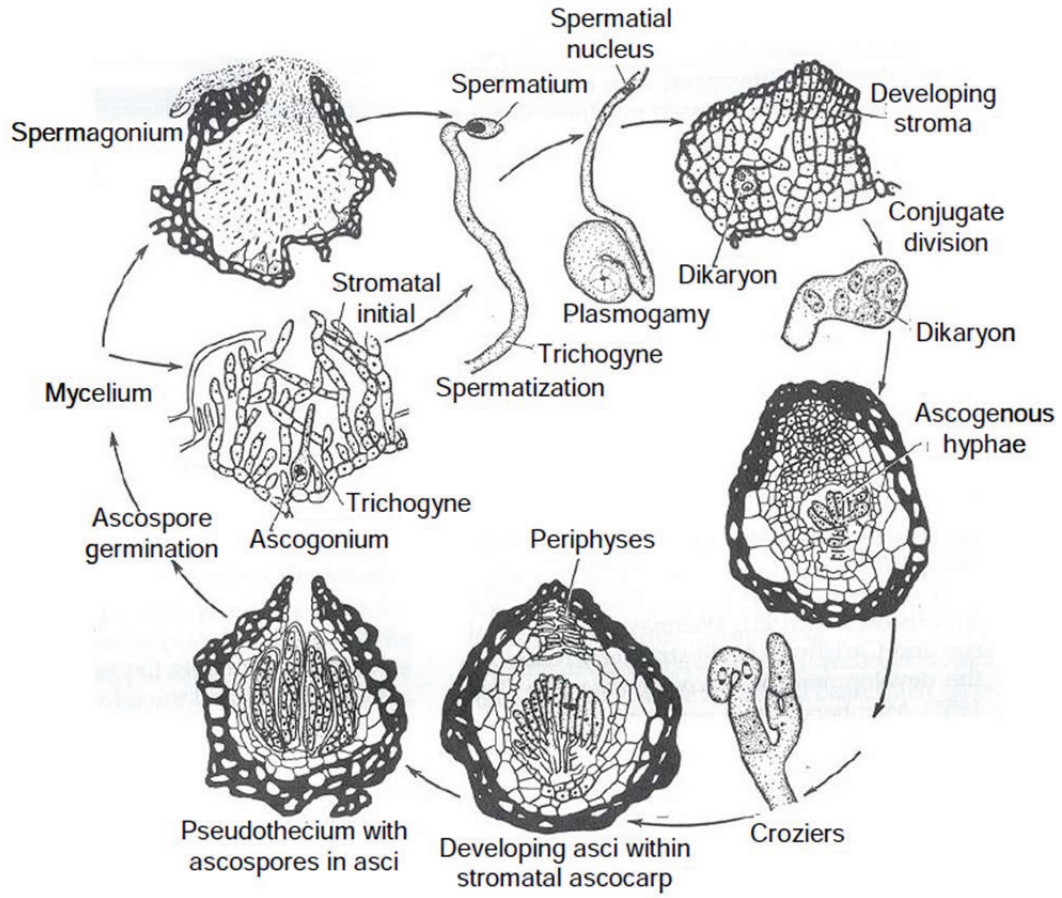


Figure 4.1
Assumed process of sexual reproduction in *Mycosphaerella tulipiferae* (Higgins, 1936; adapted from Alexopoulos *et al.,* 1996)

### 4.1.1. Sexual development in filamentous ascomycete fungi

Traditional classification of the filamentous ascomycetes based on fruiting-body structure has been largely supported by molecular phylogenetic studies, except for the loculoascomycetes (Taylor, 1995). Depending on their morphology, fruiting bodies are called perithecia (pyrenomycetes), apothecia (discomycetes), cleistothecia (plectomycetes), or pseudothecia (loculoascomycetes, e.g. *Mycosphaerellaceae*). Despite several morphological differences between these ascomata, what happens inside them is very similar in all the filamentous ascomycetes (Coppin *et al.,* 1997).

During their vegetative stage of the development, the filamentous ascomycetes form a network of partially septate hyphae containing haploid nuclei. In most filamentous ascomycetes that undergo sexual development, the sexual cycle begins with the differentiation of female reproductive structures called the ascogonia. This occurs under appropriate environmental conditions that include light and starvation for specific nutrients (Coppin *et al.,* 1997). It was also noted that ascogonia arise as lateral coiled hyphae with an apical receptive hyphal element, the trichogyne. Ascogonia can be naked or quickly enclosed by nearby hyphae, forming a protoperithecium. In heterothallic, self-sterile species such as *Neurospora crassa*, the trichogyne fuses with a male element of the opposite mating type (Lord and Read, 2011). Here, the 'male' cells are usually macroconidia however it may be also microconidia and hyphae. The fertilization requires entry of the 'male' nucleus into the primary ascogonium cell (Coppin *et al.,* 1997). The fusion of these two elements is necessary for any further development of protoperithecium into mature perithecium stage. This occurs via migration of nuclei through the trichogyne. Within the protoperithecium, nuclei of opposite mating type are grouped together and pair-up to form a dikaryon in the ascogenous hyphae of the developing perithecium (Lord and Read, 2011). Therefore, in heterothallic *N. crassa* effectively, the fertilization events initiate the development of the fruiting bodies inside which asci and ascospores form through a complex developmental process. On the other hand, in homothallic self-fertile species such as *Sordaria macrospora*, mating is not required thus protoperithecia can develop directly into perithecia. In fact, despite conidia and trichogynes being absent, the nuclei still pair-up to form a dikaryon (Read and Beckett, 1996; Lord and Read, 2011). Ultimately, ascomycetes can

produce hundreds of asci from a single fertilization event. For example, in *N. crassa*, between 200 and 400 asci develop from the ascogenous hyphae in each perithecium (Raju, 2008).

In *Mycosphaerellaceae,* one of the largest genera in Ascomycetes and some of the most prolific plant pathogens (Crous *et al.,* 2009), sexual reproduction has now been described for many species (Higgins, 1920, 1929, 1936; Keiser and Crous, 1998) with several stages of the development being very distinct from the model ascomycete species described earlier. There are however, many important questions that remain poorly understood or require further analysis or clarification. For example, in *Mycosphaerella* pathogens responsible for Black Sigatoka disease complex on banana, such as *M. fijiensis*, *M. musicola* and *M. eumusae*, the production of spermatia (Liberato *et al*., 2009), which are considered as the male gametes, occurs in multicellular structures called spermagonia. Their development begins in the substomatal chambers primarily on the abaxial leaf surface. Spermatia are hyaline, single-celled and rod-shaped, and are released through the ostiole of the spermagonium, which protrudes through the stomatal pore. However, the cytological details of spermatisation and ascospore development have not yet been described for any of these species. Although ascospores of *M. fijiensis* are produced abundantly in the field, the production of fruiting bodies (Etebu *et al*., 2003; Mourichon and Zapater, 1990) and ascospores (Etebu *et al*., 2003) *in vitro* has met with limited success as methodologies for efficient and reliable sexual crossing are not routine. Furthermore, the teleomorphs are believed to be largely similar (reviewed in Carlier *et al*., 2000a-c; Crous and Mourichon, 2002; Jones, 2000b). Despite this work, contradicting descriptions for the three species that comprise Black Sigatoka disease

of banana still exist. The early literature refers to the fruiting structures of *M. fijiensis* as perithecia (Jones, 2000a; Meredith and Lawrence, 1969) or, more generally, ascostroma (Pons, 1987). However, placement of the *Mycosphaerella* banana pathogens in the family *Mycosphaerellaceae* should actually be at least partially defined by the production of pseudothecia which are morphologically distinct from perithecia. They contain bitunicate (two-layered) asci (reviewed in Crous *et al*., 2009). The *M. eumusae* teleomorph has been described as producing pseudothecia (Crous and Mourichon, 2002), and the same description would be expected to apply to the teleomorph stages of the closely related *M. fijiensis* and *M. musicola* banana pathogens (Crous *et al*., 2003).

Some multicellular bodies have been previously reported and described in several species of *Ramularia*, such as *R. vallisumbrosae* (Gregory, 1939; Figure 4.2)*, R. onobrychidis* (Hughes, 1949), *R. deusta* (Baker *et al.,* 1950) and *R. armoraciae* (Dring, 1961; Figure 4.3). In their extensive studies, the authors presented the detailed analysis of these organs. However, they could not draw solid conclusions on their definite function. For example, the sclerotium-like stage of *R. vallisumbrosae* was first reported by Beaumont (1926; cited in Gregory, 1939), who observed numerous very minute black bodies on withered leaves which probably represented the resting stage of the fungus, but which contained no spores. Gregory (1939) also noted the presence of these roughly spherical structures in *R. vallisumbrosae* which developed in great numbers on the dying leaves after conidial formation had ceased. Furthermore, he observed the production of filiform spores in the neck of the body. Similarly, in *R. armoraciae* on horseradish, the overwintering sclerotia germinated in spring to give conidia (Dring, 1961). In some sclerotia of *R. vallisumbrosae*

however, the hyaline hyphae within the body remained thin-walled and apparently discrete throughout the summer and winter (Gregory, 1939). Although the fate of these sclerotia is not yet known, during the investigations, Gregory (1939) detected organs strongly resembling trichogynes, present in the centre and neck of the bodies. This suggested therefore that the structures might represent the fundaments of yet undiscovered perithecial stage.

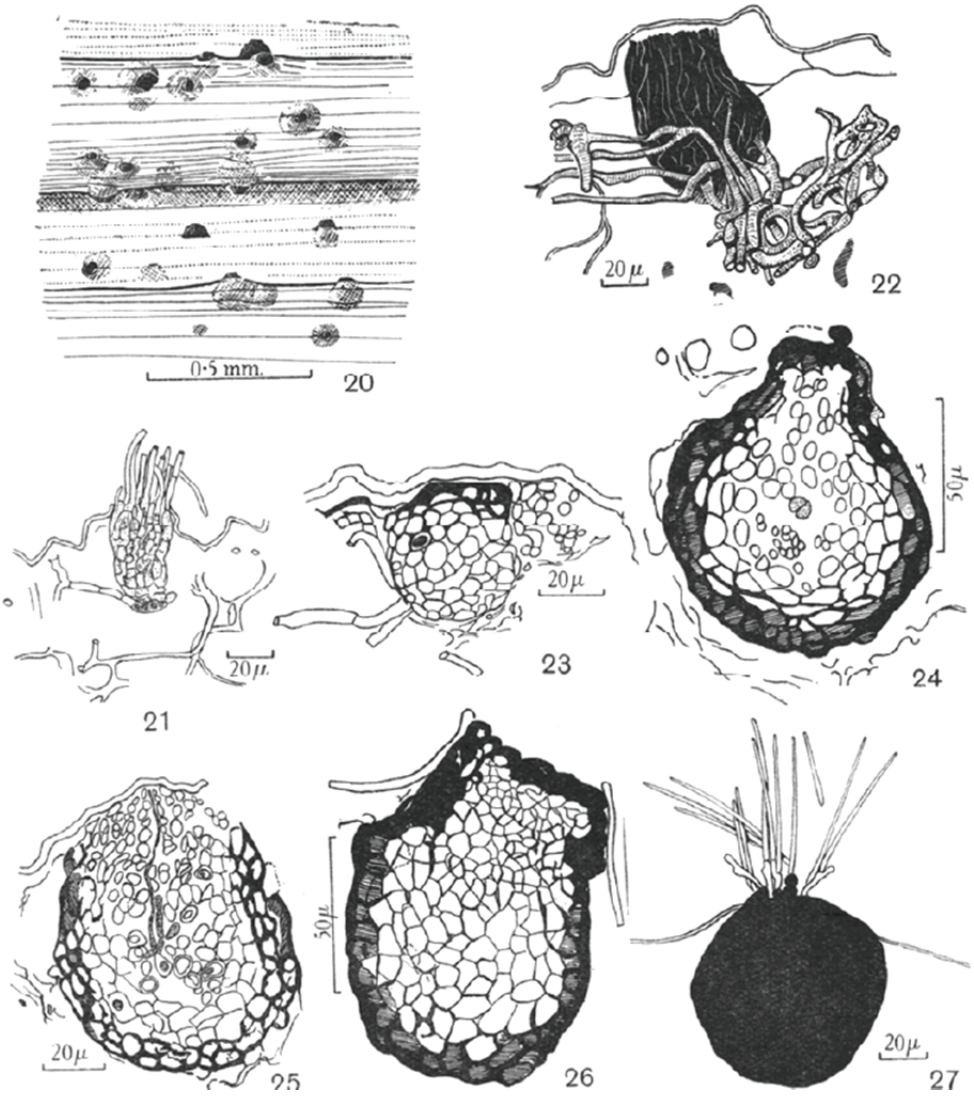


Figure 4.2
Original drawings of sclerotia in *R. vallisumbrosae* (adopted from Gregory, 1939)

Hughes (1949) observed similar structures in *R. onobrychis*. He suggested however that the sclerotia are more probably the vegetative organs of aestivation as no internal differentiation had been found. It is also important to note that Gregory (1939) mentioned that in some sclerotia of *R. vallisumbrosae*, the development was similar to this observed for pycnidia. These seemed to contain minute phialospores. Nevertheless, all the authors did not disregard the hypothesis that the sclerotia could be an intermediate state that may further develop into perithecium.

The perfect state of *Ramularia* species is presumed to belong to the ascomycete genus *Mycosphaerella.* For instance, the existence of a functional teleomorph has been determined in *R. grevilleana,* syn. *R. brunnea* (teleomorph *M. fragariae*) on strawberry (Dring, 1961). Most recently, it has been suggested that the genus *Mycosphaerella* should be restricted only to taxa related to *Ramularia* anamorphs due to very close phylogenetic relationship of these genera (Crous, 2009).

Although the complete sexual development in *Ramularia* appears to be rarely discovered, in species such as *R. armoraciae* on horseradish (Dring, 1961) and *R. deusta* on sweet pea (Baker *et al.,* 1950), the existence of a spermatial state has been previously noted. In *R. armoraciae,* the spermogonia measured 30-45-70 μm in diameter and contained rod-shape spermatia (2.5-4.5 x 08-1.0 μm), produced endogenously in flask-shaped mother cells (Figure 4.3). They were discharged through pores into the lumen of the spermogonium and then the mass of spermatia and mucus escaped through the ostiole. Furthermore, Dring (1961) also observed more or less spherical sclerotia-like bodies of *R. armoraciae*, 25-45 μm in size, that were embedded in the dead mesophyll tissue within the lesions, accompanied by

spermogonia. They were composed of brown pseudoparenchyma with the largest and thinnest-walled cells on the inside and were surrounded by a peridium of one to two cell layers (Dring, 1961).

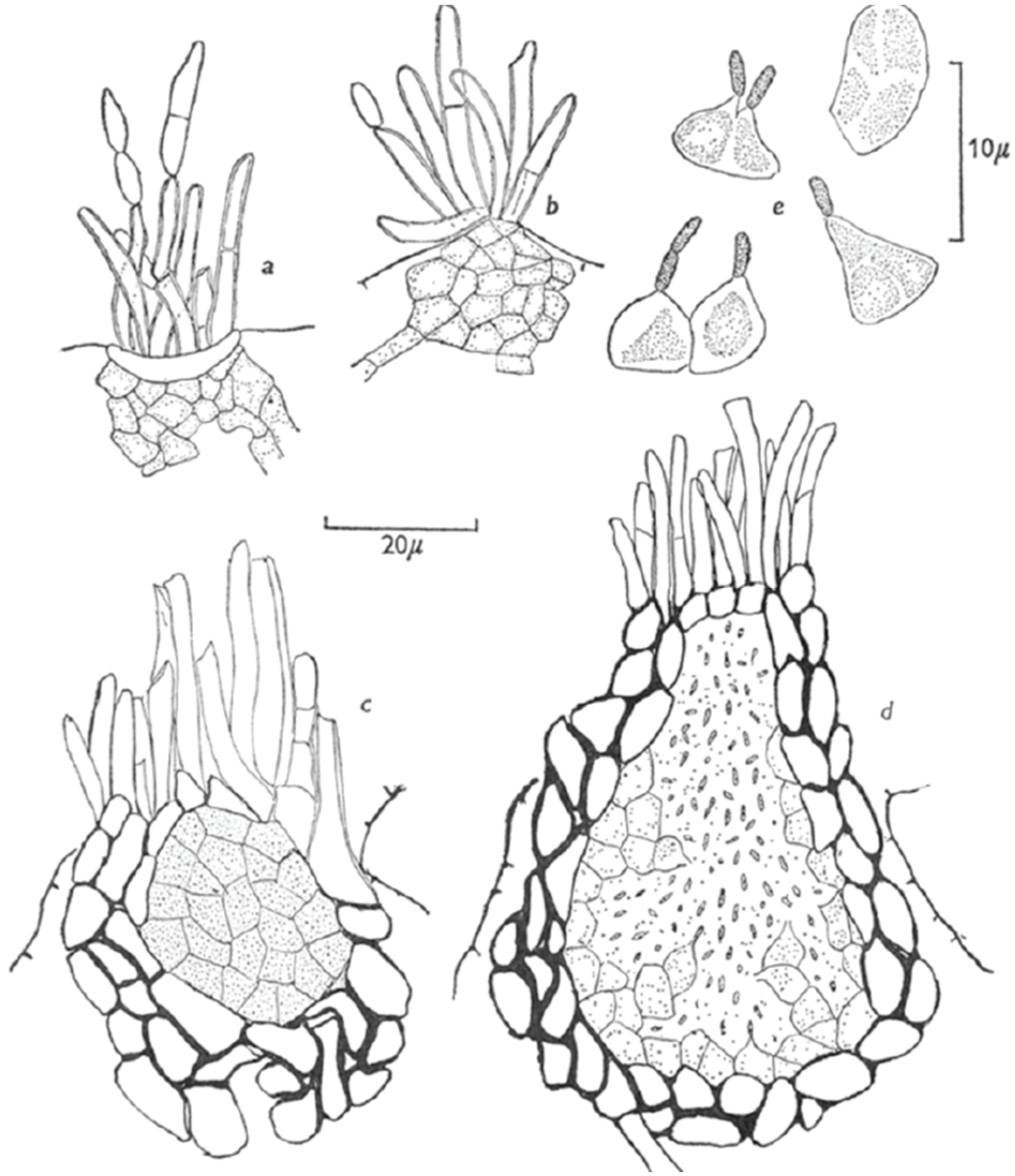


Figure 4.3
Asexual conidia, spermogium and spermatia of *R. armoraciae* (original drawings adopted from Dring, 1961)

In a study on *R. deusta,* Baker *et al.* (1950) searched for the perfect stage of the fungus in California for several years. Spermogonia were present on old perennial pea leaves in winter. However, it was not demonstrated that they belong to *R. deusta*. Nevertheless, their presence suggested the possible existence of a perfect stage of the *Mycosphaerella* type. During the winter months the fungus also produced sclerotia-like structures in substomatal cavities. These bodies also carried conidiophores on the upper surface. They resembled the bodies observed in *R. vallisumbrosae* by Gregory (1939) and similarly may represent immature perithecia. Good (1947; cited in Baker *et al.,* 1950) also reported spermatia and perithecial initials in culture. However, cultural studies and examination of field material over various seasons failed to provide more than a suggestion that the perfect stage exists.

There is some indirect evidence suggesting the existence of a yet undescribed resting stage of *R. collo-cygni.* Recently, the spermogonial stage (*Asteromella*) has been potentially identified in *R. collo-cygni.* The first report that *Asteromella*-like structures had been observed on barley, in close association with *R. collo-cygni*, came from Argentina (R. Delhey; cited by Braun, 2002). Although Braun (2002) suggested that these structures could be the microsporidial state of the fungus, it was not proven experimentally that the spermogonia indeed belong to this pathogen. Since then, there has been an attempt to induce *Asteromella* in culture (Salamati & Reitan, 2006). The authors were able to observe spermogonia-like structures that formed on barley straw introduced to old *R. collo-cygni* cultures *in vitro*, however no evidence of the presence of spermatia was demonstrated. Most recently, Thirugnanasambandam *et al.* (2011) noted the presence of some morphologically distinct structures (hyphal-swellings), approximately 5 µm wide and 7 µm long that

formed during asymptomatic infection of barley, at 7 dpi. These structures were produced either at the apical tip of growing hyphae or within the hyphae. They also observed similar structures in cultures *in vitro* in the transgenic GFP and DsRed expressing isolates. The authors suggested that they could possibly be the *Asteromella* stage.

### 4.1.2. Molecular analysis of mating type loci (MAT)

The discovery of heterothallism in fungi introduced a whole new topic in mycological research, which was later termed 'mating types' (Coppin *et al.,* 1997). Blakeslee (1904) showed that mating in *Rhizopus* (*Mucorinae;* zygomycetes) was only possible between two different single-spore strains. Such isolates could therefore be assigned to two different sexually compatible groups that could not be distinguished by their morphological comparison. These groups were defined into two signs, 1 and 2. Shortly after these observations, heterothallism was characterised also in other fungi, in particular in filamentous ascomycetes. The determinants of mating type had since become a subject of genetic analysis.

The first direct evidence of mating type corresponding to two allelic forms of a single locus came from the study of *Ascobolus magnificus* and *Ascobolus carbonarius* (Dodge, 1920). This was followed by the study of several *Neurospora* species (Shear and Dodge, 1927). It was also shown by Gwynne-Vaughan and Williamson (1932) that heterothallism was independent of sexual differentiation. The authors concluded that strains of each mating type produced both elements i.e. receptor and donor (the equivalent of female organs and fertilizing elements). In addition, the two strains contributed a compatible pair of organs which were always

of opposite mating types. The experimental proof that heterothallism was indeed bipolar was finally demonstrated by Whitehouse (1949).

In the apparent absence of known teleomorph state structures, there are several genetic approaches that can be used to obtain the evidence of sexual reproduction. It has been determined that populations undergoing regular sexual reproduction should have many more genotypes which result in higher levels of genotypic diversity compared to those with only asexual reproduction (Milgroom, 1996; Groenewald *et al.,* 2006). A good example comes from the studies carried out on the *M. graminicola* population, in which it has been found that the genetic structure is indeed very diverse (Linde *et al.,* 2002; Zhan and McDonald, 2004; Zhan *et al.,* 2002, 2003). There is also another method for testing the possibility of sexual reproduction, which is based on determining the occurrence and frequency of the mating type genes (Groenewald *et al.,* 2006). For instance, although only asexual reproduction has been observed in many filamentous ascomycetes such as *Alternaria alternata* and *Fusarium oxysporum*, it was possible to characterise both of their mating types (Arie *et al.,* 1997, 2000). On the other hand, the presence of the mating type idiomorphs in a given species alone is insufficient to prove the existence of a sexual stage (Groenewald *et al.,* 2006). However, if the two mating types occur in approximately equal frequencies within a population, the probability of functional sexual reproduction is high (Halliday *et al.,* 1999; Linde *et al.,* 2003; Milgroom, 1996; Waalwijk *et al.,* 2002).

*Saccharomyces cerevisiae* was the first fungus in which the molecular analysis of the mating type idiomorphs was demonstrated (Astell *et al.,* 1981). In filamentous

ascomycetes, the first cloning and sequencing of mating type genes (*MAT1-1-1* and *MAT1-2*) was achieved in *Neurospora crassa* (Glass *et al.,* 1988). The direct target genes of the mating type proteins have not yet been demonstrated however, there is some evidence that they control pheromone genes (Bobrowicz *et al.,* 2002).

Typically, the DNA and amino acid sequences of mating type genes don't show obvious similarities, although the mating type locus is surrounded by common flanking regions (Turgeon *et al.,* 1993). The similarity of homologous mating type genes is usually very low between different species, except for the protein domains called high mobility group (HMG) and the alpha (Turgeon, 1998). In the former domain, the similarities can be up to 90% and these homologous regions have been used to design the primers for amplification and cloning of the *MAT1-2* gene (Arie *et al.,* 1997).

Four *MAT1-1* genes have been described in ascomycetes (Pöggeler, 2001). Three of these genes can be distinguished from one another by the specific domain they contain (Groenewald *et al.,* 2006). The *MAT1-1-1* gene contains an alpha domain, the *MAT1-1-2* gene has a MAT A-2 domain, and the *MAT1-1-3* gene has a HMG domain, whereas the *MAT1-1-4* encodes for a metallothionein protein (Kronstad and Staben, 1997; Turgeon, 1998). Only a single gene, *MAT1-2*, has been found to confer the MAT2 phenotype. This formal mating type gene nomenclature proposed by Turgeon and Yoder (2000) has been used to define the mating type locus and genes from the pathogens closely related to *Mycosphaerella*, such as *Cercospora* (Groenewald *et al.,* 2006) and *Dothistroma* (Groenewald *et al.,* 2007) species.

An important property of the *MAT1-2* nucleotide sequences is their high variability among species but low variability within species (Du *et al.,* 2005; Paoletti *et al.,* 2005). This property of sequences specifically in the *MAT1-2* HMG domain has been used to investigate the phylogenetic relationships among closely related species in the *Gibberella fujikuroi* complex (Steenkamp *et al.*, 2000), the *Ceratocystis coerulescens* complex (Witthuhn *et al.,* 2000), *Fusarium graminearum* (O'Donnell *et al.,* 2004), the *Ophiostoma ulmi* complex (Paoletti *et al.,* 2005), and *Colletotrichum* species (Du *et al.,* 2005). The major conclusion of the majority of these studies has been that the sequences of the HMG domain may give at least the same and sometimes even greater resolution than the sequences of the more frequently used internal transcribed spacer regions (ITS) of nuclear ribosomal DNA (Groenewald *et al.,* 2006).

## 4.2. Materials and methods

### 4.2.1. General *R. collo-cygni* culture conditions

#### 4.2.1.1. Wild type isolates

Several different artificial media have been used to maintain *R. collo-cygni* cultures, such as potato dextrose agar (PDA), Sabouraud agar, V8 juice agar and malt extract agar (MEA). Although the cultures seemed to perform similarly during vegetative growth, the latter medium was chosen to be most commonly used. The cultures were maintained in controlled environment in darkness with temperature set at 15 ºC.

#### 4.2.1.2. *R. collo-cygni* isolates expressing GFP and DsRed reporter markers

Transgenic *R. collo-cygni* isolates 8B9 and Stratego (isolated from barley in Scotland and Denmark, respectively), described by Thirugnanasambandam *et al.* (2011) were kindly provided by Dr Adrian Newton, The James Hutton Institute. The cultures were maintained on clarified V8 juice agar (10 mM CaCO3 in 20 % (v/v) V8 juice, 1.5 % agar) at 18 °C in the dark.

### 4.2.2. Straw inoculation assay

Mycelial plugs (2 per plate) of several wild type *R. collo-cygni* isolates were inoculated onto malt extract agar (MEA) plates on opposite sides and confronted to observe the possible sexual interactions (Figure 4.4). A fragment of autoclaved barley straw, approximately 5 cm long, was placed in the middle of the plate. Cultures were allowed to grow until they met on the surface of straw sections. After 2 - 3 weeks the

colonised straw segments were then initially inspected for the presence of multicellular bodies under Zeiss SR Stereo Microscope. Microscopic slides were then prepared by mounting the outer layers of colonised leaf sheaths on a cover slip.

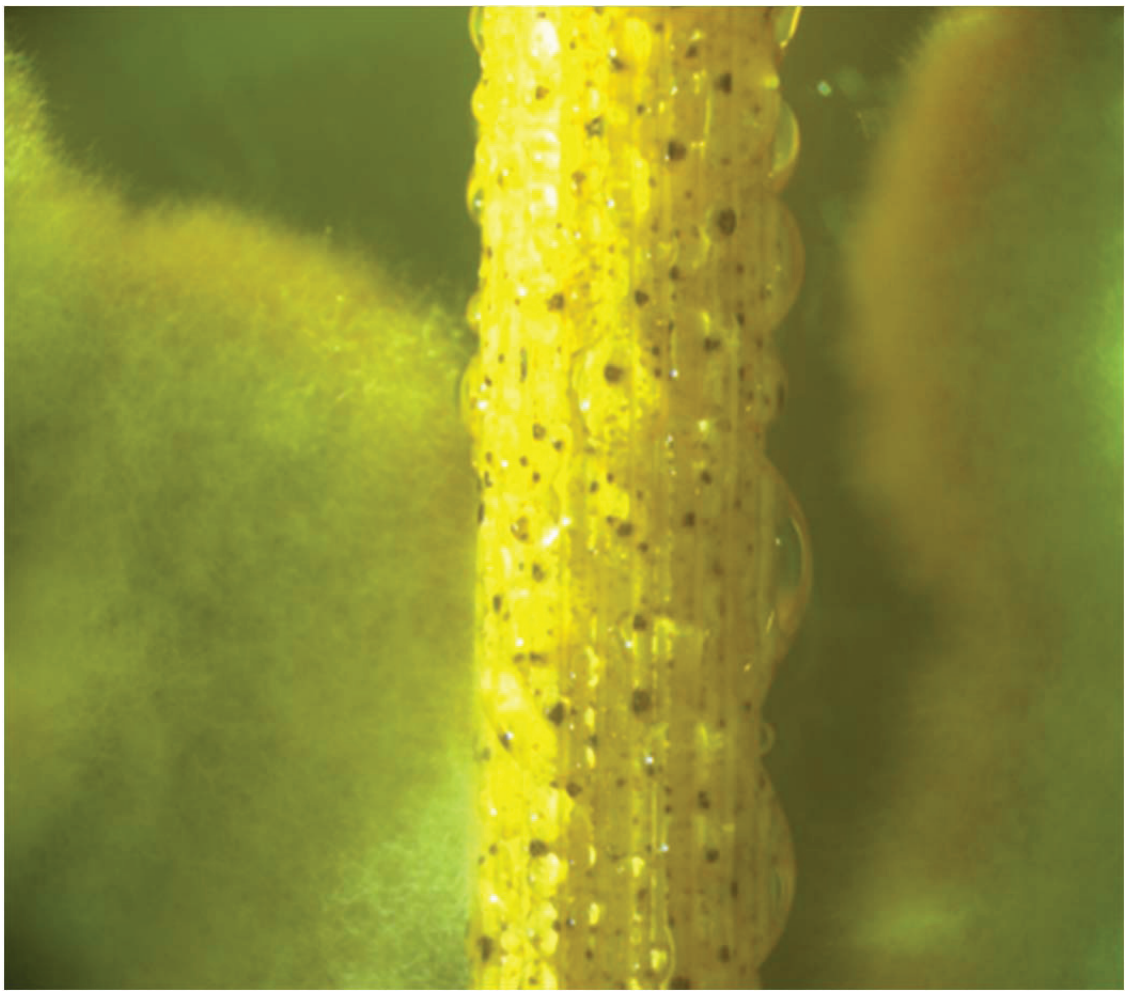

Figure 4.4
Straw inoculation assay. Two different isolates inoculated on opposite side of the autoclaved straw fragment. Note large number of multicellular bodies present of plant material at 6 weeks pi.

### 4.2.3. Molecular analysis of mating type loci

#### 4.2.3.1. DNA extraction procedure

DNA of all isolates used in this study was extracted using Illustra Nucleon Phytopure Genomic DNA Extraction Kit (GE Healthcare UK Limited, Little Chalfont, UK), according to manufacturer's instructions. Fungal material was freeze-dried overnight and stored in -80 ºC until used for extraction procedures. Isolated DNA was resuspended in 1% TE buffer (10 mM Tris, 1 mM EDTA-ethylenediaminetetraacetic acid, Sigma-Aldrich). The concentration of DNA was measured using NanoDrop spectrophotometer ND1000 (Thermo Fisher Scientific, Wilmington, USA). In the case of any obtained sample which showed a high protein contamination, a second step of DNA purification using a mixture of chloroform-phenol-isoamyl alcohol (Sigma-Aldrich) was performed. Briefly, two volumes of chloroform-phenol-isoamyl alcohol were added to each sample, then mixed and centrifuged at maximum speed (14800 rpm) for ten minutes. The upper liquid fraction containing DNA was transferred to a fresh Eppendorf tube and precipitated for ten minutes at room temperature in an equal volume of isopropanol. DNA was then spun down at maximum speed (14800 rpm) for ten minutes, and isopropanol was replaced by 500 µl of 70% ethanol. The samples were centrifuged for five minutes at maximum speed, and the DNA pellet was then air dried and resuspended in 1% TE buffer. Prior to PCR, samples were diluted to final concentration of 2.5 ng/ µl.

#### 4.2.3.2. Primer design

In order to identify fragments of the *R. collo-cygni* mating-type *mat* genes by their PCR amplification, several primer sets were designed to target the conserved regions of *mat* loci, namely domains Alpha1 (of *mat*1-1) and HMG Box (of *mat*1-2) (Table 4.1). The recently sequenced genome of *R. collo-cygni* isolate DK05 was initially examined for the presence of any of these genes. Only one component of a mating system, *mat*1-1, was identified and this sequence was used to design several specific primer sets. The most reliable set, i.e. ALPHA1_F1 and ALPHA1_R4 was used in this experiment. In order to develop primers for HMG Box region of *mat*1-2, the design was based on the sequence alignment of known *mat* loci in several related ascomycetes. The *mat*1-2 sequences of *Z. tritici* (syn. *M. graminicola*) (GenBank Accession No. AF440398), *S. passerinii* (GenBank Accession No. AF483194) and *M. fijiensis* (Abeln, *unpublished data*) were exported in FASTA format and the alignments were generated using Geneious software, version 5.6 (Biomatters Limited). Several sets of degenerate *mat*1-2 primers were designed. In addition, the recently published primer sets for rapid identification of *MAT* genes in the closely related ascomycete *Septoria passerinii* (Ware *et al.,* 2007) were also tested in this study. The primer sequences are presented in Table 4.1.

Table 4.1

Primers used for indentification and characterisation of *R. collo-cygni* mating system

| Name | Sequence | Purpose |
|---|---|---|
| ALPHA1_F1 | TAGGACCACTCGGGACGCGG | ALPHA1 domain (*mat*1-1) - specific forward primer |
| ALPHA1_R3 | CAGGCAGTCATCCCGACCGC | ALPHA1 domain (*mat*1-1) - specific reverse primer |
| MAT1-2_F4 | CRAAGAAYGCRTTCMTGATCTAYCG | HMG Box domain (*mat*1-2) - degenerate forward primer |
| MAT1-2_R3 | TTCTTCTCGGATGGCTTGC | HMG Box domain (*mat*1-2) - degenerate reverse primer |
| HMG_F5 | TCAAGGCCGCGAACCCTGAC | HMG Box domain (specific forward primer) |
| HMG_R5 | TCTCGGATGGCTTGCGGGGT | HMG Box domain (specific reverse primer) |
| MT-F | CTTCTTGCCTGCGCCACAGG | *Mat*1-2 forward primer (Goodwin *et al.,* 2003) |
| HMG(849)R | TAGTCGGGACCTGAAGGAGTG | *Mat*1-2 reverse primer (Goodwin *et al.,* 2003) |

#### 4.2.3.3. PCR conditions

For the designed degenerate primers, several different PCR condition regimes were initially tested. The best results, in terms of different product bands, were obtained using the following protocol. The reaction mixtures had a total volume of 25 µl and contained 5 µl of diluted gDNA, 12.5 µl of Go Taq® Green Mastermix 2x (Promega Corporation, USA), 5 µl of sterile distilled water and 1.25 µl of each degenerate primer. The amplification reactions were performed either using a GeneAmp® PCR System 9700 (Applied Biosystems, Foster City, CA) or Biometra® T3000 (Biometra Biomedizinische Analytik GMBH, Göttingen, Germany). The initial denaturation step was done at 94 °C for 5min, followed by 40 cycles of 94 °C for 20 seconds, 52 °C for 20 seconds, and 72 °C for 50 seconds. A final elongation step at 72 °C for 5 minutes was included in the run. The obtained PCR products were separated by electrophoresis at 50 V for 1h on a 1% (w/v) agarose gel containing Gel Red stain in

1x TBE buffer (0.4M Tris, 0.05M NaAc, and 0.01M EDTA, pH 7.85) and visualized under UV-light. Products of expected approximate size were cloned using *E. coli* plasmid vector pGEM-T Easy (Promega, UK) or sent for direct sequencing after DNA clean up using MinElute PCR Purification Kit (Qiagen). Successful inserts were confirmed by additional PCR reaction using appropriate primers. Plasmid DNA was then purified using Plasmid DNA Extraction Kit and sequenced in both directions. The obtained sequences were aligned and analysed using Geneious® software package and then blasted against NCBI database.

PCR conditions for amplification of both mating type genes using specific primer sets, the initial denaturation step at 94 °C for 5 minutes was followed by 40 cycles of 94 °C for 30 seconds, 60 °C (30 seconds) and 72 °C (45 seconds) and finished by the final elongation step at 72 °C (5minutes).

For the mating-type analysis using primers developed by Goodwin *et al.* (2003) and successfully used by Ware *et al.* (2007), the instructions specified by these authors were followed.

### 4.2.4. Low-temperature scanning electron microscopy (LTSEM) conditions

The multicellular bodies which had developed on straw fragments inoculated with *R. collo-cygni* were imaged in the frozen-hydrated state by low-temperature scanning electron microscopy (LTSEM) using method described by Lord & Read (2011). All samples were prepared and incubated in the same way. Sections of straw approximately 3 cm x 1 cm were transferred from crossing cultures and adhered to the cryospecimen carrier (Gatan, Oxford, UK) with 10.2% polyvinyl alcohol, mixed with 4.3% polyethylene glycol (Tissue Tek® Sakura Finetek, Torrance, CA, USA),

then immediately cryofixed by plunging into subcooled liquid nitrogen (-210 °C) . The specimen carrier was transferred under low vacuum to the cold stage (-120 °C) of a 4700II field-emission scanning electron microscope (Hitachi, Wokingham, UK), where the samples were partially freeze-dried at -80C to remove surface ice by sublimation. Specimens were then cooled down to -120 °C; sputter-coated in a Gatan Alto 2500 cryopreparation system at -180 °C and coated with approximately 10 nm of 60:40 gold-palladium alloy (Testbourne Ltd., Basingstoke, UK) in an argon gas atmosphere. Each specimen was examined at -160 °C with a beam accelerating voltage of 10 kV, a beam current of 10 mA, and working distances of 12–15 mm. All collected digital images were captured at a resolution of 2560x1920 pixels using in most cases the signal from the lower secondary electron detector, and then saved as TIFF format.

### 4.2.5. Confocal microscopy (CLSM) conditions

Confocal laser scanning microscopy was performed using either a Bio-Rad MRC600 system equipped with an argon ion laser and mounted on either a Nikon Diaphot TMD or TE300 inverted microscope (all supplied by Bio-Rad Microscience, Hemel Hempstead, UK). Simultaneous, brightfield images were captured using a transmitted light detector, which collected the light from behind the microscope condenser. GFP and DsRed fluorescent proteins were excited with the 488 and 514nm laser lines, respectively, and their fluorescence was detected at > 550nm. Oil immersion 60 x (N.A. 1.4) or dry 20 x (N.A. 0.75) plan apochromatic objective lenses were used for imaging. The laser intensity and laser scanning of individual hyphae were kept to a minimum to reduce photobleaching and phototoxic effects.

For imaging of co-inoculated plant material with both transgenic *R. collo-cygni* strains *in planta* under Leica SP2 CLSM, a multi-laser approach was employed to sequentially excite GFP and DsRed fluorescent proteins using HeNe laser and solid state lime laser, respectively.

### 4.2.6. Light microscopy conditions

Light microscopy was performed either using a Reichert-Jung Polyvar Photomicroscope with brightfield (BF) or differential interference contrast (DIC) optics, and 40 x (1.0 NA) and 100 x (1.32 NA) plan apochromat objectives, or using a Nikon Eclipse TE2000 inverted microscope with DIC optics and a 100 x (1.4 NA) plan fluor objective. Images from the Polyvar microscope were recorded on Canon DSL-R camera, whilst images from the Eclipse microscope were captured with a DXM1200F camera and ACT-1 software.

### 4.2.7. Preparation of tissue samples for Paraplast® embedding and sectioning

Straw samples inoculated with *R. collo-cygni* isolates, which carried the multicellular bodies of interest, were fixed and embedded using Paraplast® embedding. The procedure was performed according to Weigel & Glazebrook (2008) with some modifications. Briefly, several pieces of colonised plant tissue were placed in 10 ml of formaldehyde: glacial acetic acid fixative (FAA) in 20 ml scintillation vials and incubated for at least four hours, until the tissue sunk to the bottom of the vial. Fixative was then replaced with 50% ethanol and moved through ethanol series (60, 70, 85 and 95%) for 30 min at each concentration. This was followed by counterstaining in 0.1% eosin Y in 95% ethanol overnight. Eosin Y solution was

then washed with 100% ethanol, and then gradually replaced by a series of xylene : ethanol (25:75, 50:50, 75:25%, respectively) and finally by 100% xylene. Paraplant chips were then added and incubated at 42 ºC (around 20 each time, after the previous had dissolved, until 100 chips per vial). Finally, xylene : Paraplast solution was replaced by molten Paraplast chips at 60°C.

## 4.3. Results

### 4.3.1. Molecular analysis of *R. collo-cygni* mating system

The experiments concentrated on genetic aspects of the *R. collo-cygni* mating system. In order to assess the possibility of sexual reproduction, the molecular structure of MAT loci needs to be determined by the targeted PCR amplification and sequencing. These loci are determined by two genes called idiomorphs which are functionally complimentary but structurally different, i.e. each carry a specific conserved domain. For instance, *Mat* idiomorphs can be characterised by Alpha1 domain (for *mat*1-1) and HMG-box domain (for *mat*1-2). Sequences of *mat* 1-1 and *mat* 1-2 genes from *Z. tritici* (accession numbers) were blasted against the contigs of the recently sequenced *R. collo-cygni* genome (James Fountaine, personal communication, SRUC) using tBlast X tool showed the presence of only Alpha1 domain in the 454 sequence data that was characteristic to *mat*1-1 (Figure 4.5). Based on the obtained data, specific primers ALPHA1_F4 and ALPHA1_R3 targeting Mat_Alpha1 domain were designed and applied in this study.

The primers produced a PCR product with an expected size of approximately 650 bp (Figure 4.7). The highest sequence identity was shared with the red band needle blight pathogens of pine, *D. pini* (ABK91355.1) (Table 4.2) and *M. pini*, (ABK91356.1) at 42 and 40 per cent, respectively. This was followed by the *Mycosphaerella* pathogens of banana, *Pseudocercosporella fijiensis, Mycosphaerella eumusae* and *Pseudocercospora musae* (XP_007922387.1, ADB11107.1 and ADB11119.1, respectively). Interestingly, *Z. passerinii* (AAO49357.1) showed only 27 per cent query coverage, suggesting major structural differences between these homologues.

Table 4.2

NCBI Blast results showing similarity of *R. collo-cygni mat*1-1 protein to other related fungal species.

| Description | Query cover [%] | E value | Identity [%] | Accession |
|---|---|---|---|---|
| putative mating type 1-1-1 protein [Mycosphaerella pini] | 95 | 5e-27 | 40 | ABK91356.1 |
| putative mating type 1-1-1 protein [Dothistroma pini] | 95 | 3e-26 | 42 | ABK91355.1 |
| putative alpha1 mating-type protein [Passalora fulva] | 95 | 2e-24 | 42 | ABG45907.1 |
| alpha1 mating-type protein [Pseudocercospora fijiensis CIRAD86] | 96 | 1e-21 | 39 | XP_007922387.1 |
| mating-type 1-1 protein [Mycosphaerella eumusae] | 96 | 3e-21 | 37 | ADB11107.1 |
| mating-type 1-1 protein [Pseudocercospora musae] | 96 | 1e-20 | 38 | ADB11119.1 |
| putative MAT1-1 mating type-1 protein isoform A [Hortaea werneckii] | 99 | 3e-07 | 30 | AGT96071.1 |
| hypothetical protein W97_06800 [Coniosporium apollinis CBS 100218] | 38 | 2e-05 | 36 | EON67657.1 |
| MAT-1 protein [Zymoseptoria passerinii] | 27 | 6e-05 | 43 | AAO49357.1 |
| putative mating type 1-1 protein [Cercospora zeina] | 59 | 8e-05 | 35 | ABB83706.1 |

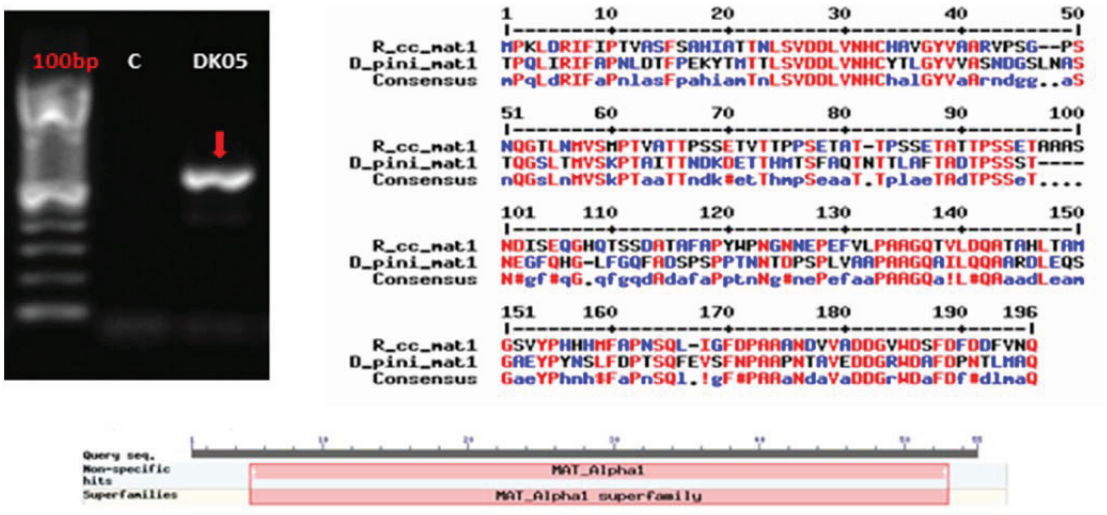


Figure 4.5

Identification of the Alpha1domain of *mat*1-1 gene in *R. collo-cygni* isolate DK 05. Left: gel electrophoresis showing a PCR product (red arrow) in the recently sequenced *R. collo-cygni* isolate DK05, obtained by using primers MAT1-1_F1 and MAT1-1_R3 (C=control). Right: Partial alignment of protein sequences of MAT1-1_ORFs of *R. collo-cygni* and *D. pini* (Genbank: ABK91355.1). Bottom: Graphical representation of t Blast X (NCBI) results of the sequenced PCR product showing the conserved domain of interest MAT_Alpha1.

It was necessary to find and characterise the HMG Box domain of *mat*1-2. To do this, several primers published by Goodwin *et al.* (2003) and Ware *et al.* (2007) were initially tested (Table 4.1). Despite the numerous DNA bands produced, subsequent cloning and sequencing indicated they were not the desired *mat*1-2 HMG Box. Therefore, degenerate primers were developed *de novo* for this gene in *R. collo-cygni*. A comprehensive alignment of *mat* 1-2 from closely related fungi was prepared and several different primer pairs were generated. Degenerate primers MAT1-2_F4 and MAT1-2_R3 proved successful for targeting conserved HMG Box domain and amplified a single product with an approximate size of 280 bp (Figure 4.6). The product was subsequently sequenced confirming that indeed it represents a desired fragment of *mat*1-2, specifically Alpha1 domain. The obtained data was then used to develop specific primers for the amplification of partial *mat*1-2 gene.

The primers were employed to amplify a PCR product of expected size of approximately 280 bp (Figure 4.6). Highest protein sequence identity was observed for *Cercospora* species, i.e. *Cercospora* cf. *modiolae* CPC 5115 (ABB83718.1) and *Cercospora* sp. F JZG-2013 (ABB83723.1) at 61 per cent (Table 4.3). This was followed by *Passalora fulva* (ABG49507.1) at 57 per cent. The amplified PCR fragment of *mat*1-2 was also similar to *Mycosphaerella* species complex responsible for Black Sigatoka disease of banana and red band needle blight pathogens of pine, *D. pini* ABK91353.1 and *D. septosporum* (syn. *M. pini*) (EME39094.1, ABK91354.1) which was also observed for the case of *mat*1-1 idiomorph.

Table 4.3

NCBI Blast results showing similarity of *R. collo-cygni mat*1-2 protein to other related fungal species.

| Description | Query cover [%] | E value | Identity [%] | Accession |
|---|---|---|---|---|
| putative mating type 1-2 protein [Cercospora cf. modiolae CPC 5115] | 58 | 7e-11 | 61 | ABB83718.1 |
| putative mating type 1-2 protein [Cercospora sp. F JZG-2013] | 58 | 1e-10 | 61 | ABB83723.1 |
| putative mating type 1-2 protein [Cercospora sp. P JZG-2013] | 58 | 1e-10 | 61 | ABB83707.1 |
| MAT1-2-1 mating-type protein [Passalora fulva] | 58 | 1e-10 | 57 | ABG49507.1 |
| putative mating type 1-2 protein [Dothistroma pini] | 91 | 1e-10 | 42 | ABK91353.1 |
| mating-type protein 1-2 [Pseudocercospora musae] | 58 | 1e-10 | 57 | ACA49542.1 |
| putative mating type 1-2 protein [Mycosphaerella pini] | 58 | 1e-10 | 55 | ABK91354.1 |
| mating type locus 1-2 [Dothistroma septosporum NZE10] | 58 | 2e-10 | 55 | EME39094.1 |
| MAT1-2 protein variant 3 [Cercospora beticola] | 58 | 2e-10 | 61 | AFH56913.1 |
| putative mating type 1-2 protein [Cercospora beticola] | 58 | 2e-10 | 61 | ABB01678.1 |

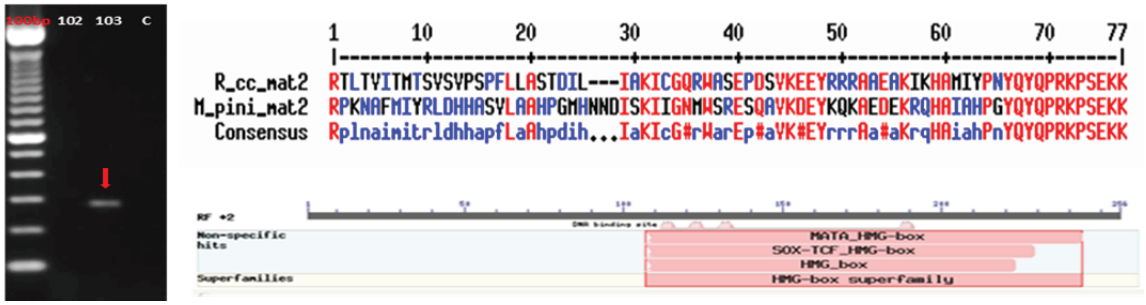


Figure 4.6

The identification of *mat*1-2-HMG Box using degenerate primers. Left: gel electrophoresis showing a PCR product (red arrow) in the isolate 103, obtained by using degenerate primers MAT1-2_F4 and MAT1-2_R3 (C=control; isolate 102 of known opposite mating type *mat1-1*). Top right: partial alignment of protein sequences of MAT1-1_ORFs of *R. collo-cygni* and *M. pini* (Genbank Accession: ABK91354.1). Bottom right: tBlast X (NCBI) results of the sequenced PCR product showing the conserved domain of interest HMG Box.

*R. collo-cygni* proved to be a heterothallic organism, i.e. each isolate carried only one of the two idiomorphs. In order to assess the frequency of mating type alleles in the defined population, a collection of forty *R. collo-cygni* strains isolated from the leaf samples with RLS symptoms was used (Marta Piotrowska, SRUC). Since the entire collection was obtained from one field it was possible to determine the likelihood of functional sexual recombination occurring in natural conditions.

To screen the population, specific primers for PCR amplification of *mat*1-2 HMG Box were developed, namely MAT1-2_F5 and MAT1-2_R5 and used together with the previously described specific *mat*1-1 primers MAT1-1_F4 and MAT1-1_R3.

Amongst the first twenty isolates, 18 produced mating type specific bands (Figure 4.7). The isolate 117 produced a weak but clear band and therefore was included in the total count. There were two isolates, i.e. 106 and 109, which did not produce any product, despite numerous repeats with different batch of DNA samples. Based on this partial result, mat1-1:mat1-2 ratio of 10:8 (n=18), pointed at potential frequent sexual reproduction amongst the tested isolates.

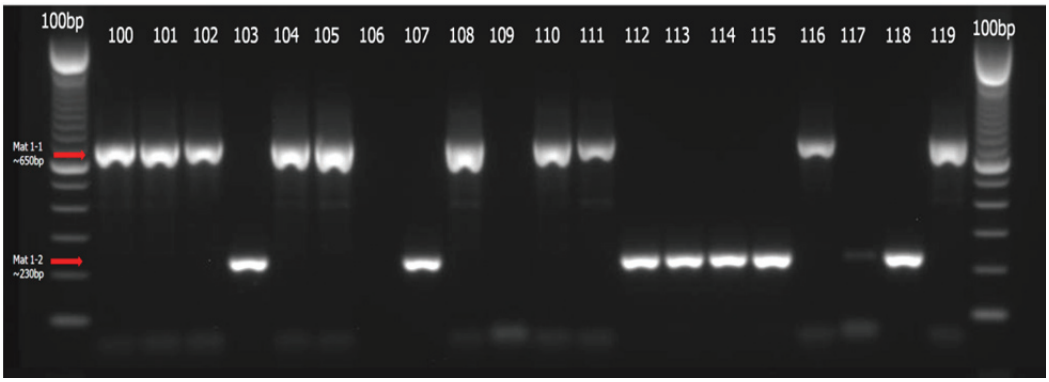


Figure 4.7
Gel electrophoresis of PCR amplified fragments of the two mating type idiomorphs described for *R. collo-cygni* amongs a subpopulation of 20 isolates (100 to 119). Note apparent lack of any bands produced in isolate 106 and 109. Isolate 117 produced a weaker but clear and size specific band.

The next subpopulation of twenty isolates, namely 120 to 139, yielded mating type specific bands that segregated into mat1-1:mat1-2 ratio of 11:8 (n=19) (Figure 4.8). The isolate 120 did not produce the band, similarly to previously described isolates 106 and 109.

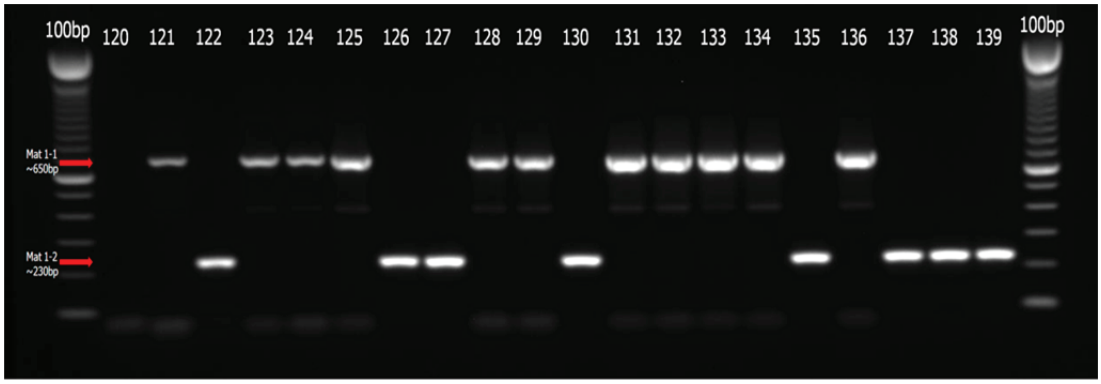


Figure 4.8
Gel electrophoresis of PCR amplified fragments of the two mating type idiomorphs amongst a subpopulation of 20 isolates (120 to 139). Note apparent lack of PCR product for isolate 120.

The overall ratio within the whole population (n=37) was therefore 21:16, thus close to 1:1 which is expected from fungal populations with a highly frequent sexual recombination. It is also important to note that when considering the radiating pattern of sampling within four separate circular patches of the field in which the isolates were collected, i.e. 10 per circle, mating type ratio was highly variable. For instance, for the first 10 isolates (100 to 109) the ratio was 3:1 (n=9) however in subpopulation of another 10 isolates (130 to 139), ratio was exactly 1:1 (n=10), typical for fungi with known frequent sexual reproduction.

### 4.3.2. The development of spore-like hyphal swellings

During the experiment of infection development on barley (see Chapter 2), the production of swollen hyphal segments and spore-like structures on the leaf surface which clearly differed from the typical *R. collo-cygni* conidia was noted (Figure 4.9). Their presence was also confirmed in culture conditions (Figure 4.9 b-f). At the earliest, they were found on cultivar 'Optic' at 9 dpi (Figure 4.9 b). Furthermore, the size of the smallest structures was approximately 5 μm in diameter. However, during the later stages of infection development some of them reached up to 30 μm (Figure 4.9 d, e). This suggested that their gradual maturation occurs over time.

These spore-like bodies were produced either at the apical tip of growing hyphae or within the hyphae (Figure 4.9 d). It was also noted that the bodies located at the hyphal tips were most often rounder and larger compared to those developing within the length of hypha, which were much more elongated, lemon-shaped and, in general, tended to be smaller. Despite their apparent differences in shape and size, both were unicellular. Often, the structures were observed forming chains separated by 20 - 40 μm long segments of hyphae (Figure 4.9 d, e). It was also observed that they could form at dichotomous extensions of epiphytic hyphae (Figure 4.9 e). *In planta,* the majority of these bodies were usually located alongside the midrib section of the leaves (Figure 4.9 f). Some of the structures appeared to germinate in a similar way to conidia (Figure 4.9 a, c, e). However, the newly produced hyphae had a smaller diameter than the germ tube (Figure 4.9 d). No further internal differentiation of these structures was observed.

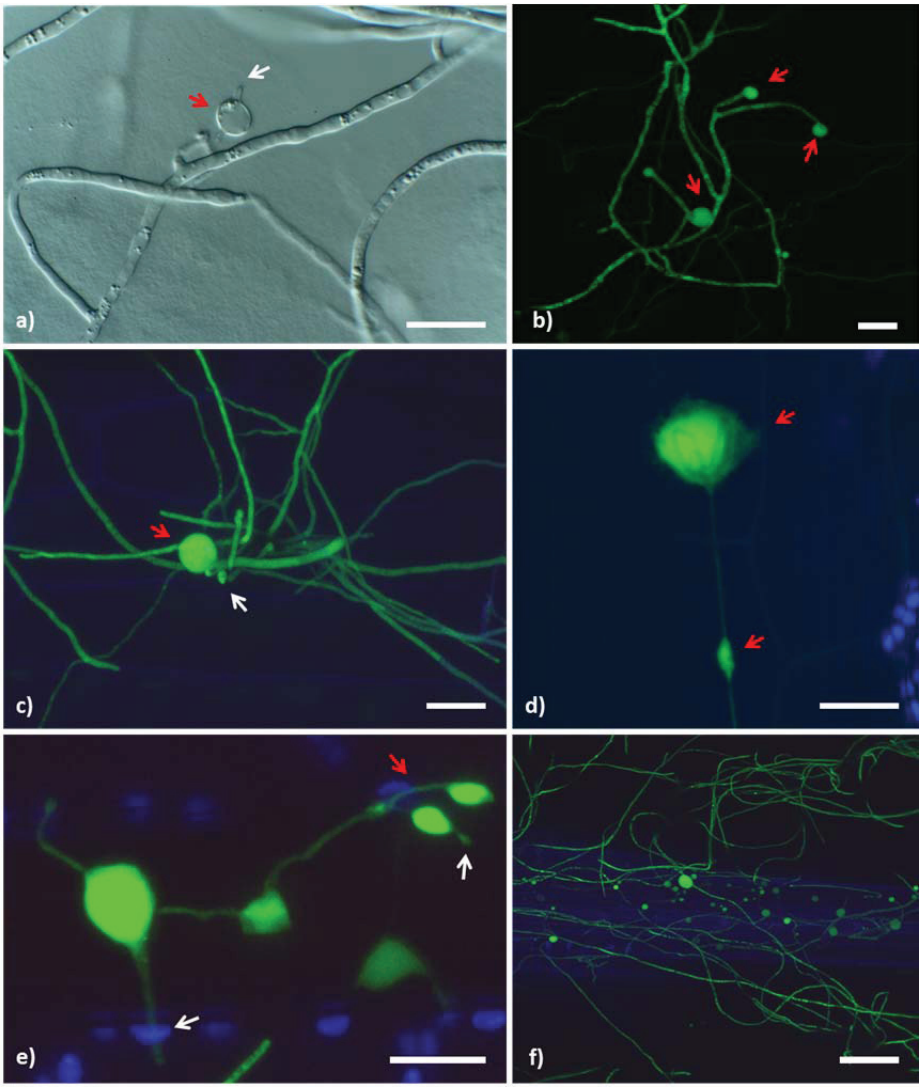


Figure 4.9
Production of spore-like structures by *R. collo-cygni* in culture and *in planta*. Unless otherwise stated, scale bar = 20 µm. a) DIC image of round spore-like structure (red arrow) developing in culture of the isolate DK05. Note continuous growth of hyphae extending from the body, indicated by white arrow; b – f) maximum projections of z-stacks acquired using Leica SP2 CLSM; b) production of hyphal swellings *in planta* during infection progression by the isolate *Rcc*-8B9-GFP on cultivar 'Optic' at 9 dpi. Note different sizes of these structures, indicated by arrows. c) globose-shaped body (red arrow) and extending hypha. Note its size compared to conidium (white arrow), still attached to swan-neck conidiophore; d) Two distinct types of the spore-like hyphal swellings (arrows) at different stages of development, arranged in chain on the leaf surface. Bar = 30 µm. Larger, round body located at hyphal tip whereas smaller, lemon-shaped is a swollen segment of vegetative hypha e) a chain comprising multiple structures of different shape and size. Note dichotomous branching (red arrow), distinct from typical sporulation in *R. collo-cyni.* Germination or hyphal extension is indicated by white arrows; f) abundant production of the structures appears to concentrate in the groove on the leaf surface where vascular bundle is located. Bar = 50 µm.

### 4.3.3. Straw inoculation experiments

#### 4.3.3.1. Induction of multicellular bodies *in vitro*

Different pairs of *R. collo-cygni* isolates, co-inoculated onto opposite sides of the autoclaved straw fragment in culture were able to coexist and simultaneously colonise the surface and sub-stomatal cavities. Additionally, Petri dishes inoculated with the same crosses were also prepared without adding the straw. Initially, crossing plates were checked with the unaided eye twice per week and the crosses that produced multicellular bodies were subsequently observed under stereo microscope at low magnification to confirm that the structures are indeed of fungal origin (Figure 4.10 a).

Although the colonies merged in the centre of Petri dishes, suggesting their compatibility, the potential resting bodies were not observed on the plates prepared without straw pieces. This suggested that these structures require host tissue for development. Interestingly, the structures were able to develop in large numbers on autoclaved barley kernels and were observed to concentrate around rachilla on the embryo side of the seed (Figure 4.10 b). It was also noted that the growth of basal aggregates, which give rise to conidiophores, occurred in similar manner as on leaving plant tissue during infection.

Several different combinations of isolates and the environmental conditions were tested. Firstly, the structures generally developed much faster and in larger numbers on the plates that were sealed with Milipore tape (Fisher Scientific UK Ltd, Loughborough, UK) which allowed air circulation (data not shown).

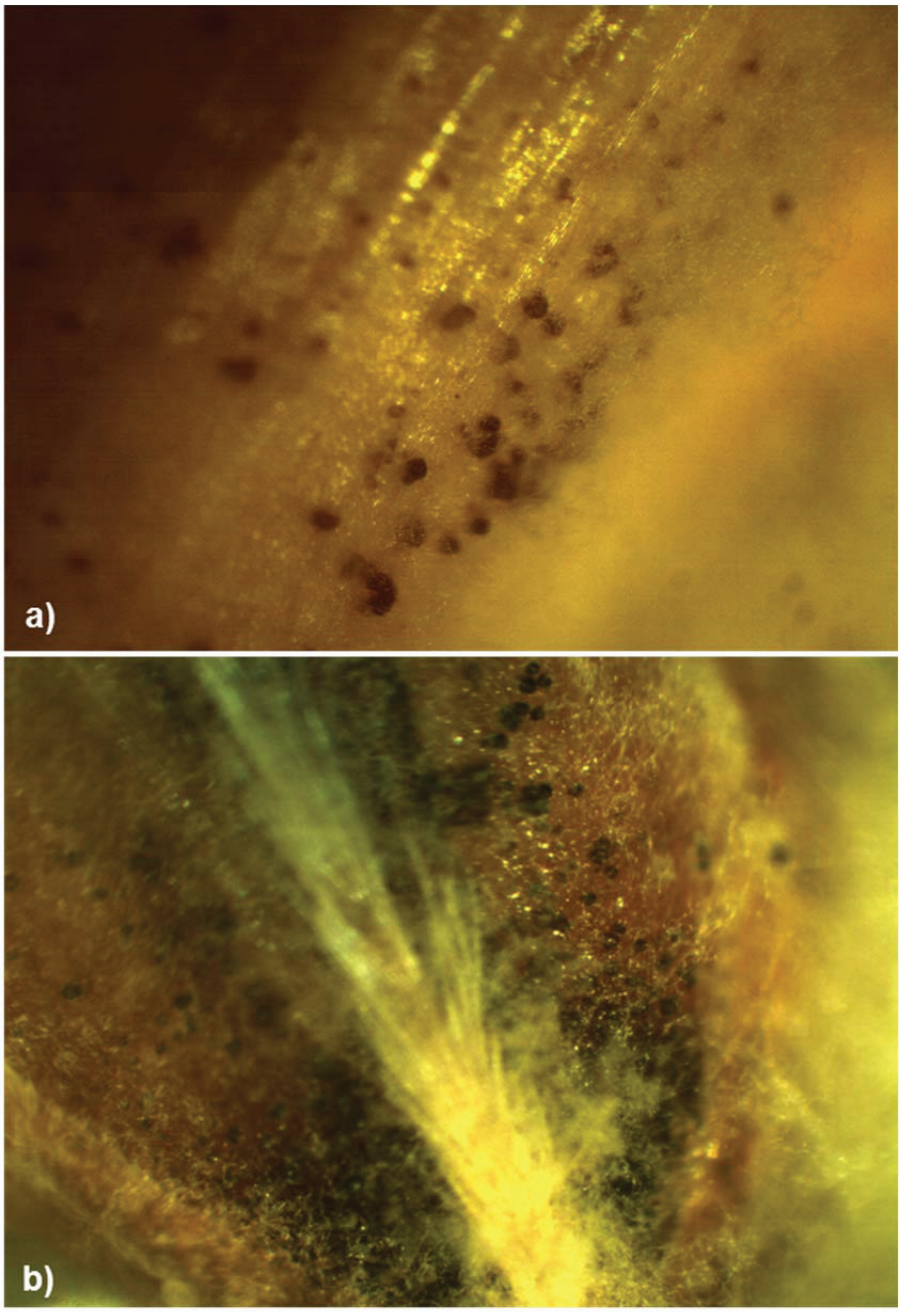


Figure 4.10
The development of fungal structures at 5-6 weeks pi on different parts of the autoclaved barley material, introduced to *R. collo-cygni* cultures: a) fragment of straw; b) barley seed.

An increase in numbers of multicellular bodies was observed for cultures exposed to blue-black light for 48 hours suggesting that their development can be stimulated by specific wavelengths of light (Table 4.4).

Table 4.4
Influence of blue-black light condition on observed quantity of multicellular bodies

| Cross | BB light + | BB light - |
|---|---|---|
| 102 x 103 (c) | +++ | + |
| 111 x 112 (c) | ++ | - |
| 121 x 122 (c) | +++ | + |
| 121 x 137 (c) | ++ | + |
| 110 x 111 (i) | ++ | + |
| 128 x 129 (i) | ++ | - |

A representation of the rough numbers of multicellular bodies based on visual assessment using stereomicroscope: +++ >50 bodies; ++ 25 - 50; + <25; - =0; (c) compatible; (i) incompatible.

#### 4.3.3.2. Analysis of multicellular bodies by correlated use of several microscopy techniques

The most successful crosses were then analysed in detail by correlated use of several microscopy techniques. Three to four weeks after inoculating the plates, the initially transparent aggregates gradually turned red-brown (Figure 4.11 a, b). Although first instances of the presence of these bodies on straw fragments suggested that their development is strictly linked with substomatal cavities (Figure 4.11 a), further observations showed that they can also develop on the leaf surface, or slightly submerged in the epidermis (Figure 4.11 b).

The size and morphology of the structures suggested that they could be the previously speculated spermogonia. Interestingly, the structures were able to develop independent of their mating compatibility but in much lower quantities than for isolates of opposite mating type (Table 4.4). After an additional two weeks of incubation, these structures became dark brown and this pigmentation did not change any further, therefore suggesting that they reached their maturity.

The presence of another kind of multicellular body that had different size and shape was also noted at this stage of experiments and since their function was completely unknown, they are initially described as sclerotium-like bodies. The study primarily concentrated on spermogonium-like structures to determine their function and confirm if they are indeed spermogonia. The detailed analysis undertaken here is described in this section.

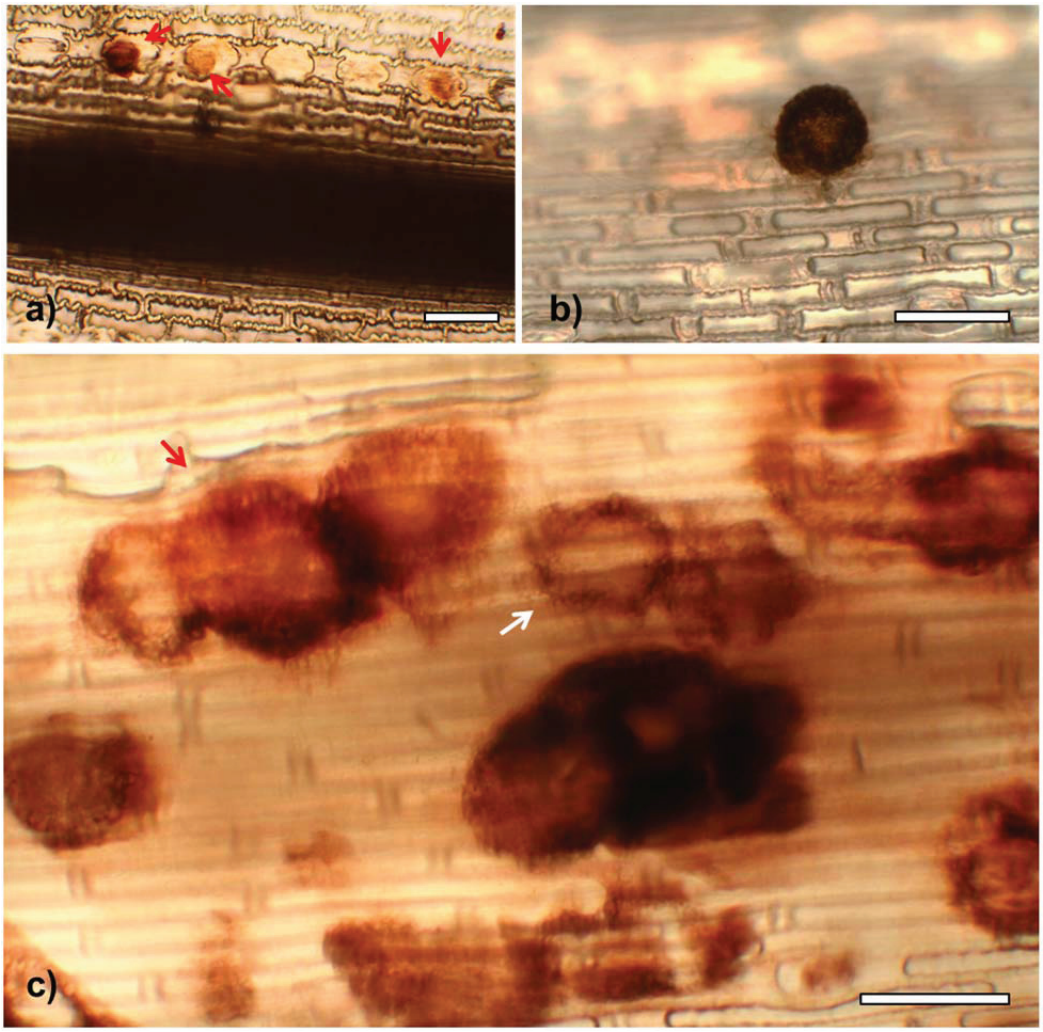


Figure 4.11
DIC microscopy images of the spermogonium stage development on autoclaved barley straw in culture. Bar = 100 µm: a) maturation of spermogonium inside substomatal cavities indicated by red arrows. Note changes in pigmentation suggesting maturation. Bar = 100 µm; b) matured spermogonium on the leaf surface. Bar = 100 µm; c) developing spermogonia on barley straw, forming clusters (red arrow). Note uni – bicellular wall surrounding the interior of spermogonium (white arrow).

The majority of these structures had an ellipsoidal shape and closely resembled a spermogonium (Figure 4.12 a, b), reported in related *R. armoraciae* (Dring, 1961). It was therefore considered that indeed they could represent the speculated spermogonial stage of *R. collo-cygni.* The size of the mature structure was approximately 60 - 70 x 40 - 50 µm in diameter. They were surrounded by the brown-pigmented wall (peridium) that was typically uni – to bicellular. The bodies often formed clusters of up to ten separate units.

To study the interior of these structures, i.e. if they carried any type of spores, and to confirm that they are indeed spermogonia rather than some other type of fungal developmental stage, the bodies were punctured with sterile needle and squashed to force the contents out of them (Figure 4.12 c). Furthermore, microtome sectioning of embedded fungal material containing a large number of multicellular bodies was also carried out in order to elucidate their function in the fungal lifecycle. Subsequent experimental procedures confirmed the existence of a yet undescribed spermatial stage *in vitro.* These structures had the form of minute small bacilliform microconidia, most likely produced by the elongated mother cells (Figure 4.12 b) within spermogonia (*Asteromella*). The size of a single spermatium was 3-5 x 0.5-1 µm (Figure 4.13 a, b). No germination ability for these spores was ever determined, despite frequent screening and time course observations of numerous samples at many separate occasions (Figure 4.13 b). However, they were observed to fuse with the distinct type of hyphae that appeared thinner than typical vegetative hyphae present on the surface of colonised straw (Figure 4.13 c). These observations suggested that spermatia could play their anticipated role in fertilisation.

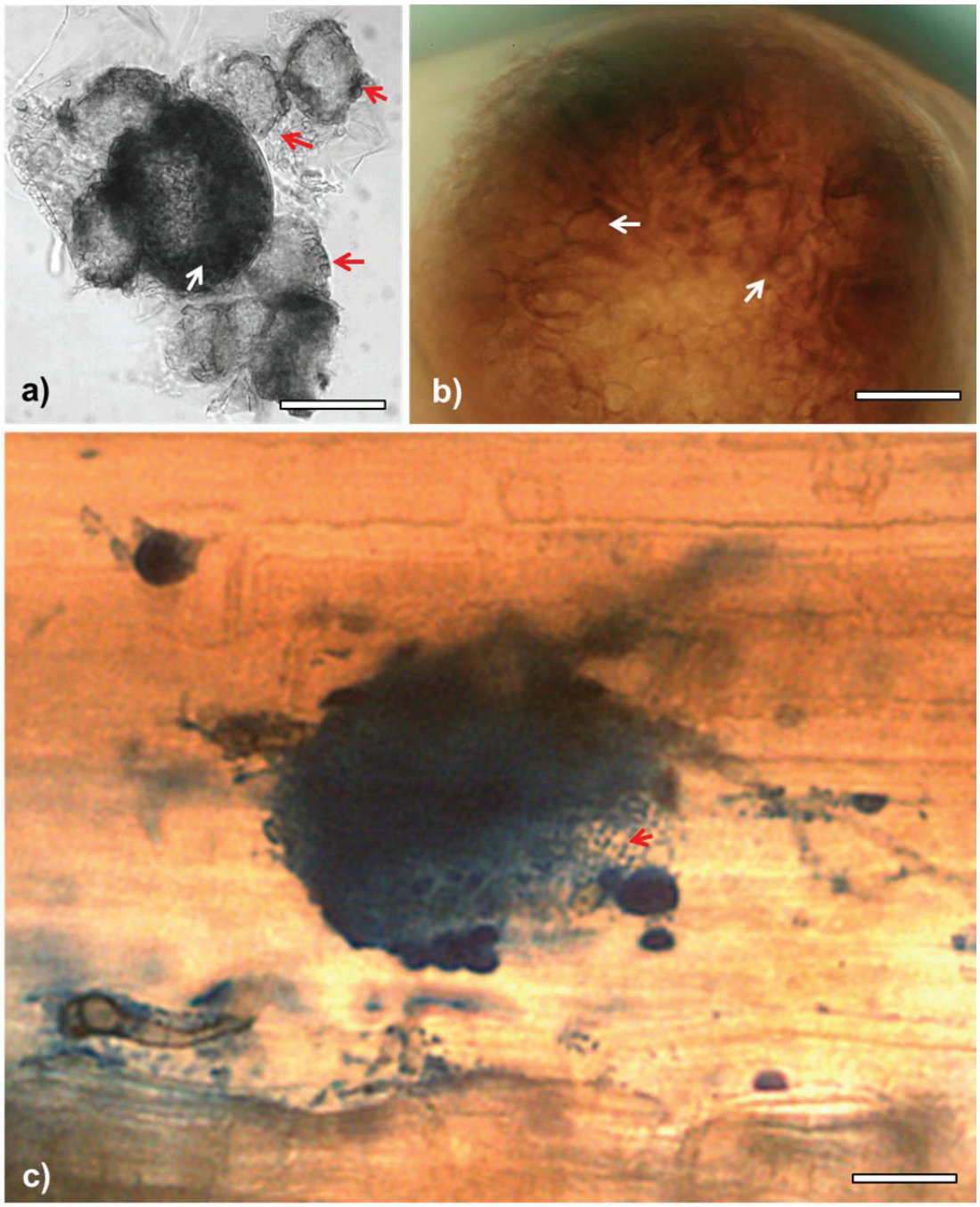


Figure 4.12
Bright field images of spermogonium stage in *R. collo-cygni*: a) black and white images of the cluster of spermogonia, excised from barley straw using sterile scalpel blade. Young spermogonia surrounded by unicellular walls, indicated by red arrows with mature spermogonium in the centre (white arrow). Bar = 50 µm; b) the interior of single ripening spermogonium showing several layers of elongated cells (arrows). Bar = 30 µm; c) aniline blue-stained sample of barley straw with spermogonium after mechanical puncturing with sterile needle, showing mass of small spore-like objects, oozing from its interior, indicated by red arrow. Bar = 30 µm.

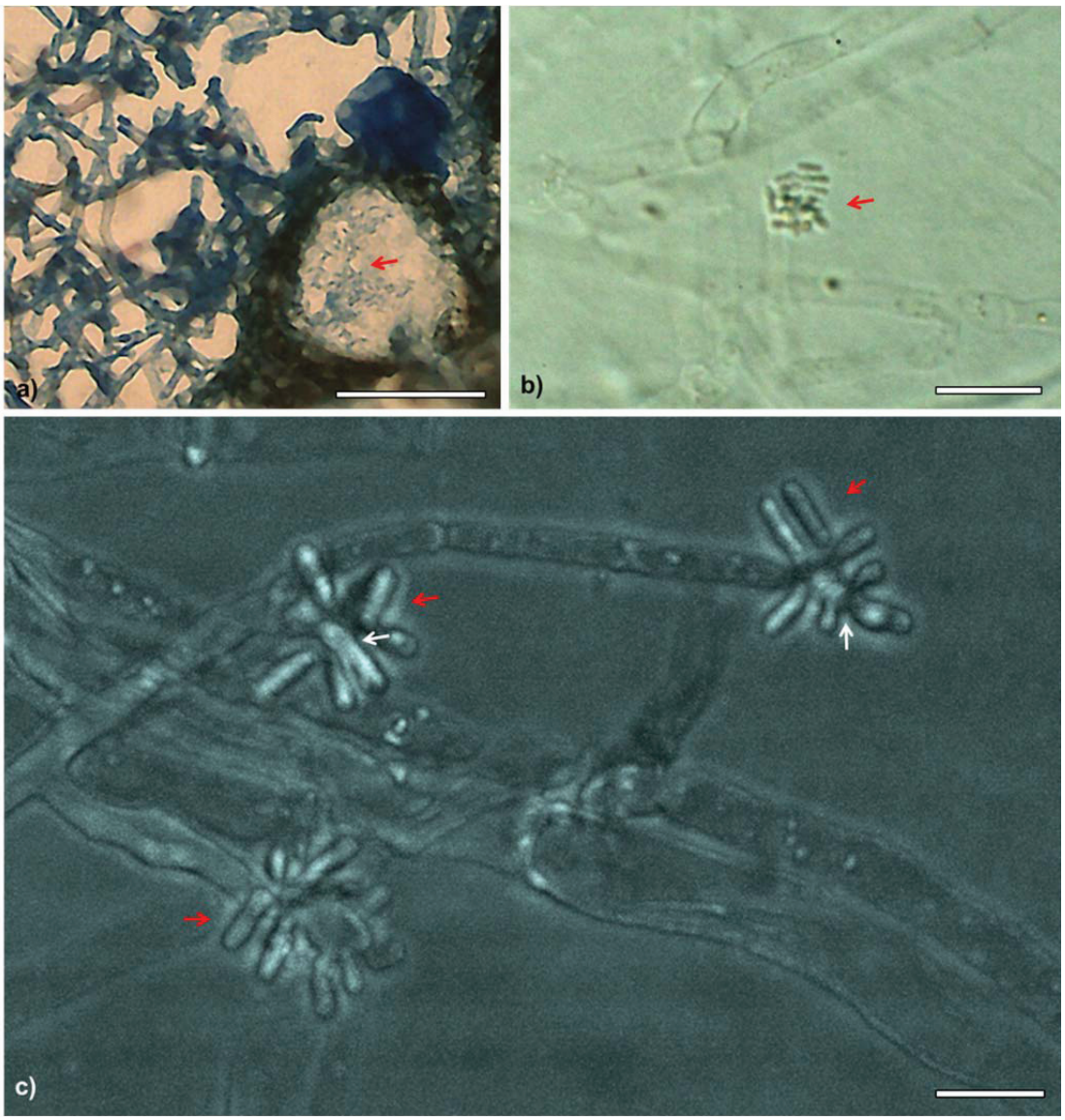


Figure 4.13
Spermatial stage (*Asteromella*) developed within spermogonium in *R. collo-cygni*: a) cross section through mature spermogonium, embedded in Paraplast and stained with aniline blue. Red arrow indicates the presence of bacilliform spermatia. Bar = 50 µm; b) a population of rod shaped spermatia that exhibited lack of ability to germinate. Bar = 20 µm. c) transmission image of fusion of hyphae (putative trichogynes) with single spermatium (white arrows). Red arrows point at spermatia not fused with the trichogyne. Bar 5 µm.

During the experiments, it became apparent that in fact two distinct types of fungal structures were present simultaneously on barley straw. Another type of multicellular body previously unreported in *R. collo-cygni*, which was morphologically different from the spermogonium was observed (Figure 4.14). It was much more heavily melanised, glossy black, with somewhat 'polished' metallic appearance. Although first structures of this type developed together with spermogonia (Figure 4.15 a), it persisted much longer and gradually became dominant when spent spermogonia had collapsed after mass release of spermatia. At approximately 10 weeks of incubation, they represented a vast majority of the two types of multicellular bodies that were present of colonised straw (Figure 4.15 b). After puncturing with needle, no spores were observed which also confirmed that they were not spermogonia, but rather of sclerotium type.

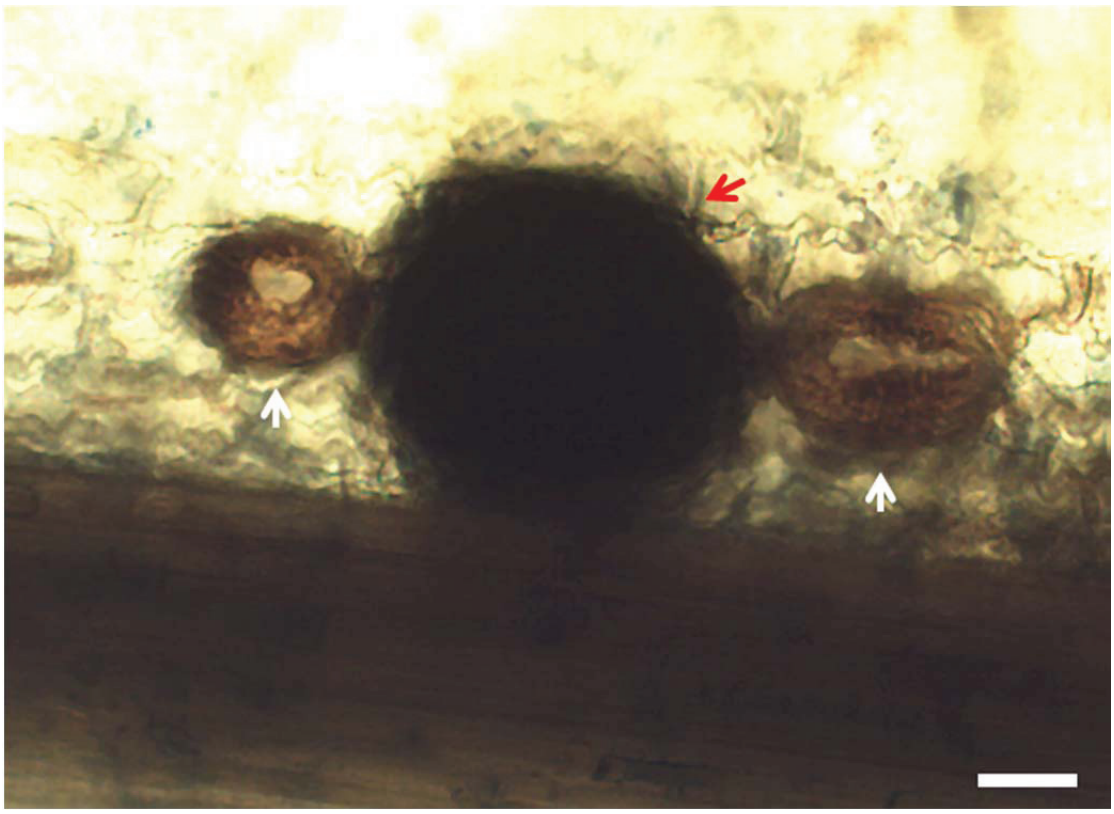

Figure 4.14
Two different types of multicellular bodies observed on inoculated barley straw in culture at 6 weeks of incubation. White arrows indicate spermogonia. Note the presence of much larger sclerotium-like body (red arrow). Bar = 30 µm

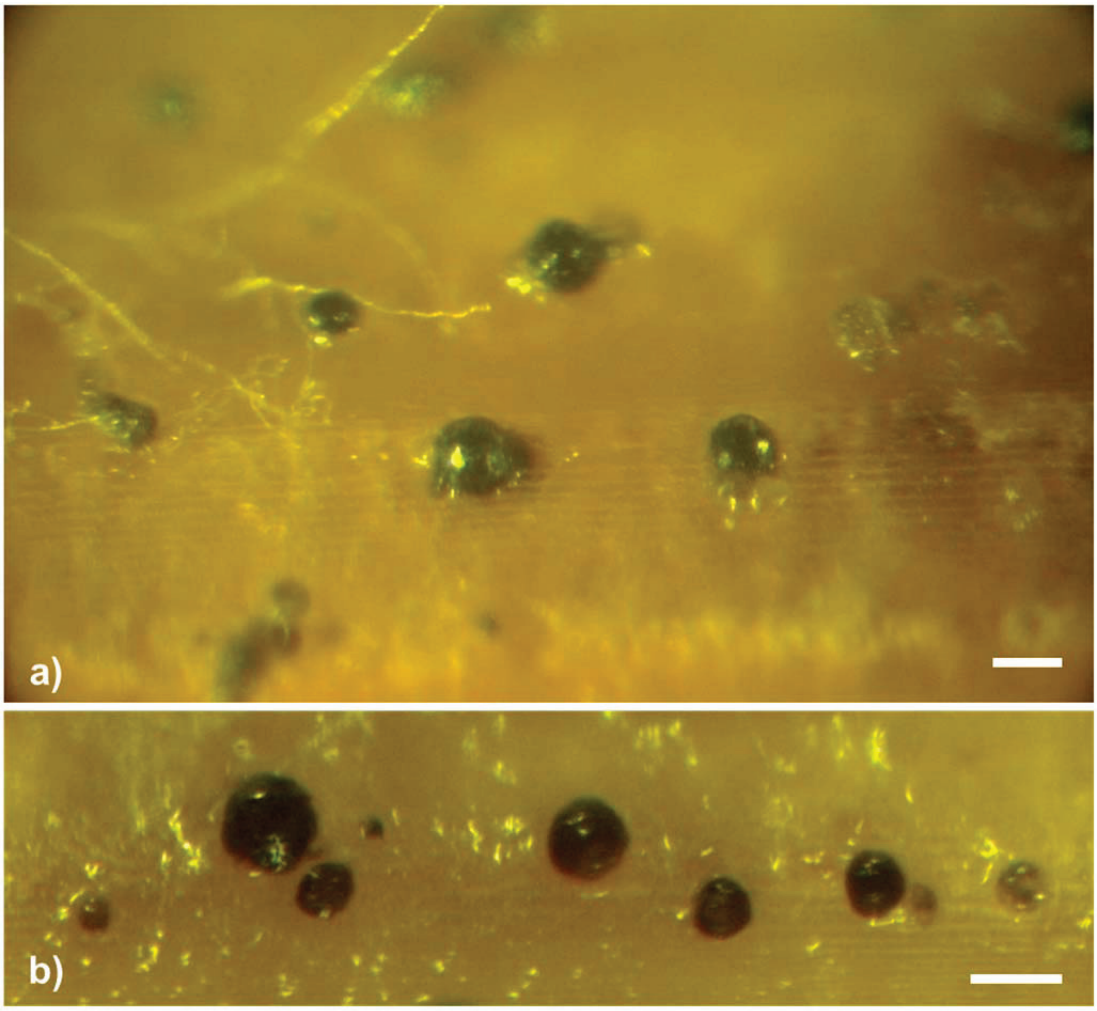


Figure 4.15
The potential resting stage of *R. collo-cygni* induced on barley straw *in vitro:* a) note different size and intensity of pigmentation, from translucent to deep black, as observed under stereomicroscope in 3-month old cross culture of the isolates DK05 and 8B9. Bar = 50 µm.

In order to initially observe their developmental process and morphology, low temperature scanning electron microscopy (LTSEM) was employed (Figure 4.16). Structures of different sizes were readily observed. The development involved gradual size increase by an aggregation of interwoven, highly branched enveloping hyphae (Figure 4.16). The presence of the potential initial stage was also noted (Figure 4.16 a). It resembled the globose spore-like swellings that were observed during infection development on barley by the GFP expressing isolate (Section 4.3.1). They appeared to be at the centre of the developing sclerotium- like bodies, surrounded by enveloping hyphae at their bases and subsequently rising up to produce dome-like structure. Many structures were embedded in plant tissue with the neck often protruding through epidermis and rising up whereas the main body appeared submerged into plant tissues (Figure 4.16 b). The more mature structures became pear shaped, approximately 80 µm diameter at their widest. The size and appearance resembled sexual fruiting bodies such as perithecium or pseudothecium described for related *Mycosphaerella* spp. such as *M. populorum* (Niyo *et al.,* 1986). At some instances, near the neck of a body, some elongated, bicellular spore-like structures were also observed that germinated producing short germ tube and vegetative hypha (Figure 4.16 c).

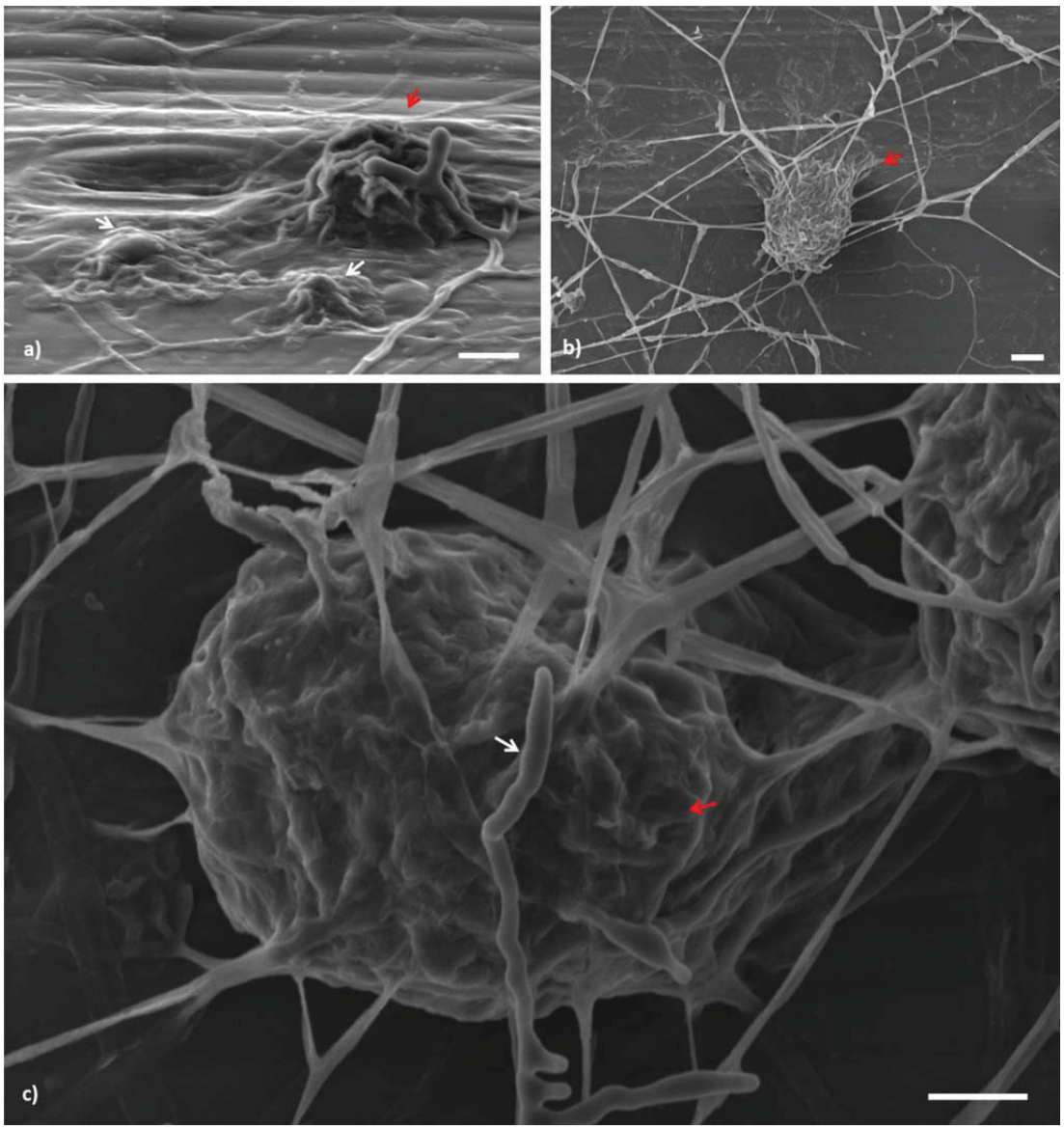


Figure 4.16
The development of sclerotium-like bodies on barley straw observed between 4 and 8 weeks of incubation. Bar = 20 µm: a) the developing structures at 4 weeks pi. Note the initial spore-like stage resembling the previously observed hyphal swellings (white arrows) gradually enveloped by highly branching hyphae (red arrow); b) ostiole of a large multicellular body rising from a stoma (red arrow); c) pear shape sclerotium-like structure (red arrow). Note the presence of elongated spore-like object that appears to germinate on the side of the neck (white arrow).

The next experiment employed a crossing strategy using two transgenic isolates expressing GFP or DsRed fluorescent protein to induce the development of this structure *in vitro* in order to determine if recombination had occurred. Optical sectioning of the dissected structures using sequential imaging under confocal microscopy revealed spore-like structures in their interior (Figure 4.17). The presence of yellow hyphae suggested that it was derived by recombination between both isolates (Figure 4.17 a). Subsequently, the spore-like cells were also observed to co-express both fluorescent proteins of the parental strains (Figure 4.17 b-1). This was further determined by co-localisation analysis (Figure 4.17 b-2).

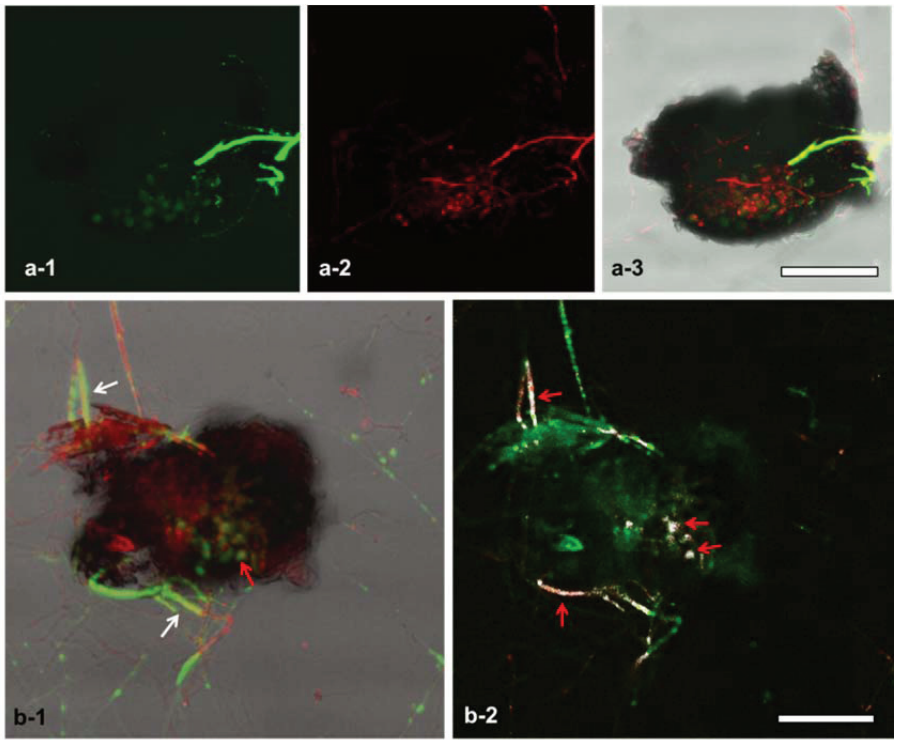


Figure 4.17
Sclerotium-like bodies dissected from barley straw, obtained by crossing Rcc-8B9-GFP and Rcc-ST-DsRed and imaged using confocal microscopy. Bar = 30 µm: a-1) green channel; a-2) red channel; a-3) merged red and green channels overlaid with transmission BF image; b-1) overlay projection of red and green channels superimposed on a transmission image; b-2) co-localisation analysis white colour indicates pixel both green and red. Green channel serves as a background.

Interestingly, microconidia were also observed in the near vicinity of the structure (Figure 4.18), which suggested that they may actually serve their potential role as spermatia in the process of fertilisation. This therefore indicated that the body may represent the functional teleomorph of *R. collo-cygni*.

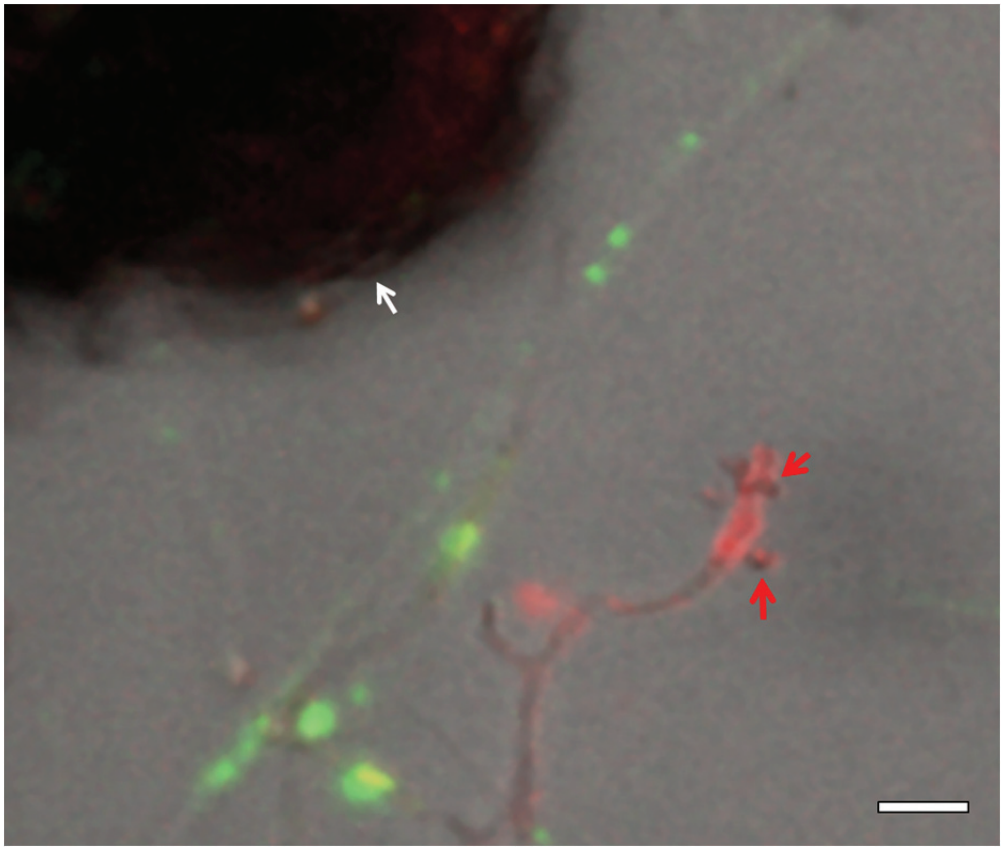

Figure 4.18
Presence of spermatia (red arrows) close to sclerotium-like body suggesting their potential role in fertilisation (white arrow)

In order to study the histology for determining the function of the sclerotium-like structures, straw material bearing large numbers of the bodies was embedded in Paraplast and sectioned using the microtome. Initial sectioning of 5 weeks old material revealed clumps of stroma, which comprised many single bodies (Figure 4.19 a) as observed earlier using LTSEM. At this stage however, no apparent differentiation was observed within the bodies. The interior consisted of pseudoparemchyma cells enveloped by dark stained perydium. This suggested their function as sclerotium, a vegetatively derived fungal resting structure. Some of the bodies appeared empty of internal tissue.

However, from 8 weeks pi, in some of the structures some internal reorganisation was observed (Figure 4.19 b-c). For instance, whilst the vast majority remained undifferentiated, some the central region took the shape of a rosette made of a group of elongated cells. These cells appeared to stain deeper than pseudoparenchyma cells. Furthermore, in a few cases a distinctly thin hypha was observed growing out of the central region towards the neck (Figure 4.19 b). Sectioning of samples embedded at 10 - 12 weeks pi showed that this rosette-like formation became much larger and filled up almost all the interior of the multicellular body. The structure resembled an elongated ascus (Figure 4.19 c-1) with further internal organisation, i.e. it enveloped a group of ellipsoidal spore-like cells. They measured approximately 10 x 5 μm (Figure 4.19 c-2). It was not possible to determine their viability as the material underwent invasive fixation, embedding and staining procedures. Examination of bodies after 15-18 weeks of incubation showed no further development suggesting that the described structures had reached maturity at around 12 weeks pi.

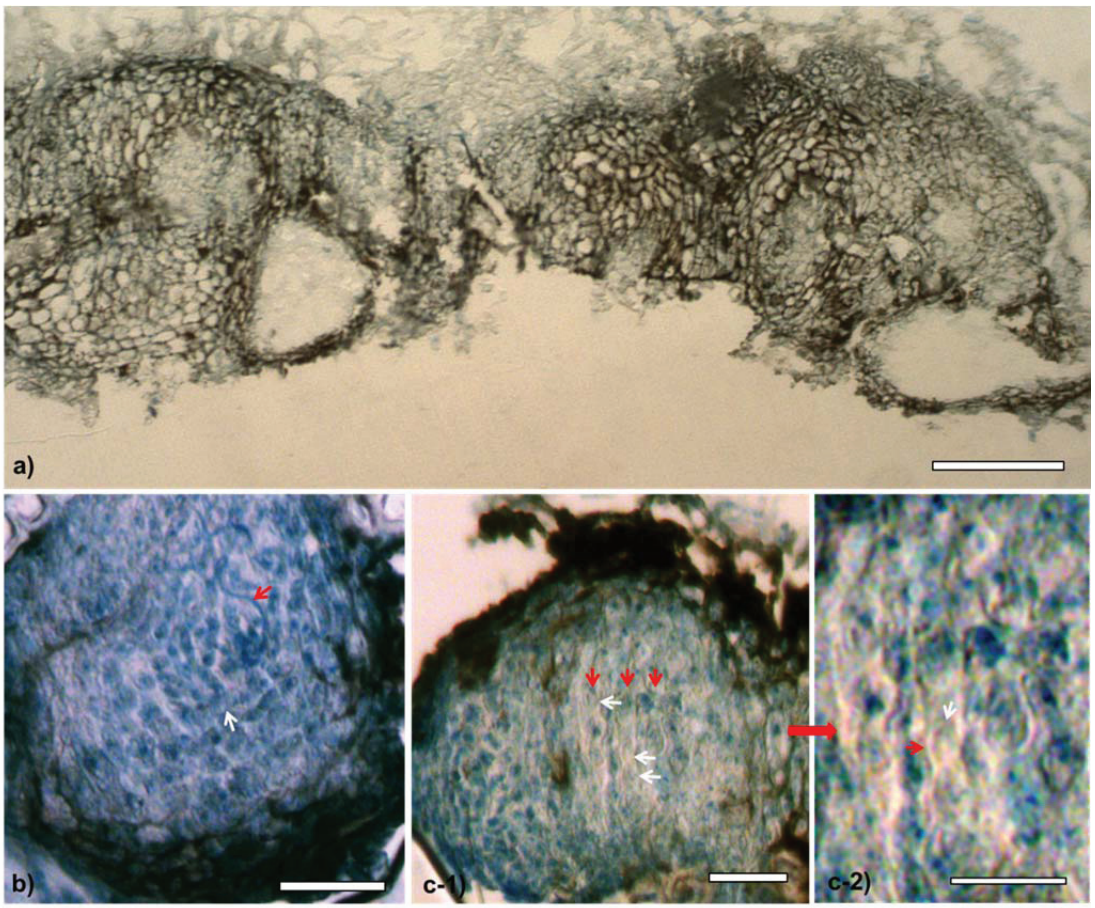


Figure 4.19
Microtome sections (depth ~ 5 µm) of Paraplast-embedded sclerotium-like multicellular bodies: a) large stroma composed of clumped sclerotia, composed of pseudoparenchyma cells. Note some of the structures appear empty; these were considered spermogonia after release of spermatia. Bar = 50 µm; b) differentiating interior of potential ascoma, with rosette of developing ascogynous hyphae (white arrow). Note presence of hyphae, possibly trichogyne, connected to ascogynous hyphae (red arrow). Bar = 20 µm; c) Potential ascoma with elongated ascus-like structures (c-1, red arrows), surrounding ascospores (c-2, white arrow). Bar = 20 µm.

An important finding came from inoculated straw fragments that were not exposed to the period of low temperature. For instance, a secondary function of the sclerotium-like bodies has been observed during incubation of infected straw segments at higher temperature (above 18 ºC) and humidity. In such conditions, the interior of the structures did not differentiate, but sprouted in similar manner to typical sclerotia (Figure 4.20).

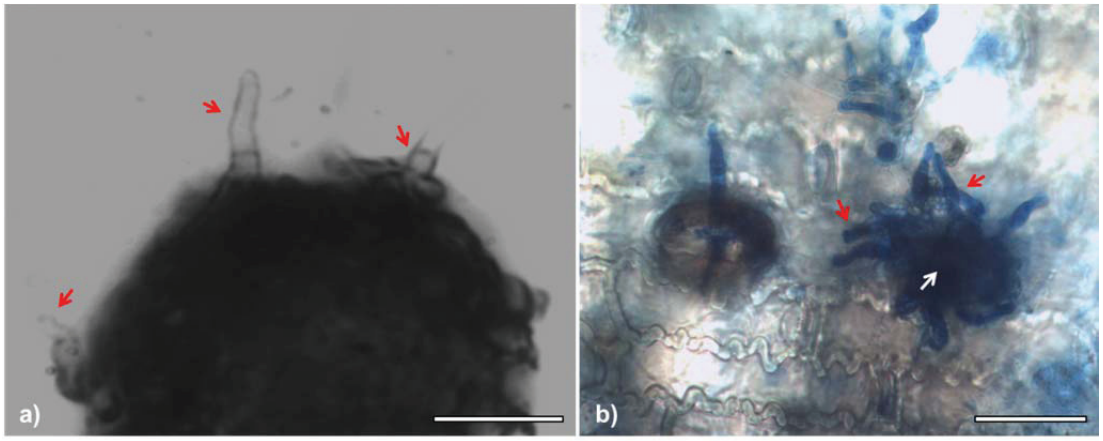


Figure 4.20
Sprouting sclerotium under high humidity and 20 ºC: a) small sclerotium beginning to sprout producing conidiophores (red arrows). Bar = 20 µm; b) sclerotium embedded in stoma (white arrow) accompanied by conidiophores (red arrows) rising from the envelope of the structure. Bar = 50 µm.

## 4.4. Discussion

Chapter 4 characterises the genetic structure of the mating system by using PCR-based techniques which demonstrates the heterothallic nature of the fungus. The defined population of *R. collo-cygni* field isolates was screened for the presence of the discovered mating type idiomorphs (*mat*) to determine the frequencies of the mating types in the defined *R. collo-cygni* populations. The segregation ratio of *mat1-1* and *mat1-2* was close to 1:1 which indicated a frequent sexual reproduction. In order to verify the existence of functional sexual stage in *R. collo-cygni*, sexual development was studied using the potentially compatible isolates and a comprehensive analysis was undertaken by correlative use of light-, confocal- and low temperature scanning electron microscopy. Two types of multicellular bodies were observed and described. First was the speculated *Asteromella* stage (male donor) that carries spore-like spermatia. The second structure initially resembled sclerotia that in only a few instances developed into perythecium/ pseudothecium that appeared to carry the sexual spores, ascospores enveloped in asci.

The life cycle of filamentous fungi is a complex developmental process that often comprises several different stages. It involves morphological, histological and even changes in ploidy level over time. Sexual reproduction in Ascomycetes is an important part of their life histories and development. However, at the same time it is one of the least studied. This is certainly true for one family of plant pathogenic species, *Mycosphaerellaceae*.

Despite numerous studies in early and mid- 20$^{th}$ century, only a few brief reports of the discovery of *Mycosphaerella* teleomorphs exist in *Ramularia* spp, many of

which are crop pathogens, such as *R. collo-cygni,* the subject of this project. Although *Mycosphaerella* is generally accepted to represent one of the largest genera of ascomycetous fungi, it has been recently demonstrated that this could be well overestimated, and that *Mycosphaerella* should be restricted to taxa linked to *Ramularia* anamorphs (Crous *et al.,* 2009). It is therefore necessary and desirable to characterise sexual development in this fungus, in order to advance knowledge of *Mycosphaerella* plant pathogens in general.

To characterise the mating system in *R. collo-cygni,* the obvious experimental approach was the molecular analysis of mating type loci. To our best knowledge, such studies have not been previously attempted for any *Ramularia* species. Therefore this chapter represents the first ever report of the nature of the mating system in this taxon. In order to examine mating behaviour and compatibility, PCR amplification of mating type genes was attempted. To do this, we developed a specific primer set for both mating type idiomorphs in *R. collo-cygni* as the use of primers previously developed for related genera of *Mycosphaerella* species (Goodwin *et al.,* 2003; Ware *et al.,* 2007) did not yield any results. This is most likely due to the fact that, although the specific domains targeted by these primers, such as Alpha1 and HMG Box in *mat*1-1 and in *mat*1-2 genes, respectively, are usually well conserved within certain species, the actual level of synteny is low for mating type loci across different genera of ascomycetes (Crous *et al.,* 2009).

*R. collo-cygni* has shown to be a heterothallic species with each isolate carrying one of the two mating type idiomorphs. In such system, only strains of opposite mating types are compatible. The related *Mycosphaerella* species of known mating systems are heterothallic species such as *M. fijiensis, M. eumusae, M. musicola, Z. tritici* and

many others. It was therefore anticipated that this pathogen may share these characteristics. In the case of *R. collo-cygni*, many previous authors suggested its close relationship to *Z. tritici*. Although that could be true for well conserved genomic regions such as internal transcribed spacer (ITS-rDNA) used in molecular RLS diagnostics, this study suggests that this speculated similarity could actually be overestimated. The sequence of the conserved regions of MAT locus studied here, i.e. Alpha1 and HMG Box (*mat*1-1 and *mat*1-2 genes, respectively) suggests otherwise and shows much closer relationship with other fungal species such as *D. septosporum* (teleomorph *M. pini*) as well as the *Mycosphaerella* banana species complex, such as *Pseudocercosporella fijiensis* (teleomorph *M. fijiensis*), *Pseudocercosporella musae* (*M. musicola*) and *M. eumusae* (Table 4.2, 4.3). Furthermore, one of the highest similarities in both studied genes was also observed for several *Cercospora* species and *Passalora fulva* (syn. *Cladosporium fulvum*). *Z. tritici* (syn. *M. graminicola*) and *Z. passerinii* (syn. *Septoria passerinii*) were classified far below the abovementioned species, with the latter sharing only 29 per cent coverage for HMG Box (Table 4.3). These observations support recent separation of *Zymoseptoria* species from *Septoria* with typical *Mycosphaerella* teleomorphs (Quaedvlieg *et al.*, 2011).

A collection of 40 isolates was used to determine the frequency of *mat* idiomorphs within the defined population of the fungus. The distribution of mating idiomorphs across in this population that originated from a single spring barley field indicated with a good confidence that *R. collo-cygni* could have a cryptic teleomorph stage (Figure 4.7 and 4.8). For instance, the ratio between *mat*1-1 and *mat*1-2 isolates was close to 1:1 which is a typical scenario for the species with very frequent sexual

reproduction such as *Z. tritici*. This result is supported by the recent population genetic analysis undertaken on the same collection of isolates using SSR markers (Marta Piotrowska *et al.,* unpublished). However, it is also important to acknowledge that the existence of functional sexual reproduction relying exclusively on mating type genes ratio should not be assumed. For instance, mating type genes have been identified in many other fungal species in which a sexual cycle has not yet been characterised. In another barley pathogen, *Rhynchosporium commune* (syn. *R. secalis*), phylogenetic analysis suggested the existence of a teleomorph in the genus *Tapesia* (Goodwin, 2002). Subsequently, in two separate studies in which mating type genes of this fungus were cloned using degenerate primers designed from sequences of *Tapesia yallundae* and *Pyrenopeziza brassicae* (Foster and Fitt, 2003; Linde *et al.*, 2003), natural populations of *R. commune* showed a high level of genetic diversity and a 1:1 ratio for *mat*1-1: *mat*1-2 in most populations sampled (Linde e*t al.*, 2003). Similarly, in *Fusarium oxysporum*, a well-studied plant pathogen with a wide host range (Armstrong and Armstrong, 1981), mating type genes have been cloned by Arie *et al.* (2000) however, attempts to cross isolates of *F. oxysporum* with opposite mating types have not yielded sexual spores (Ware S., unpublished), nor have these spores been found in nature, although high genotypic diversity in natural populations of *F. oxysporum* also suggests the possibility of a sexual cycle (Baayen *et al.,* 2000; Bao *et al.,* 2002).

Since we have determined only partial sequences of mating type genes, it would be necessary to clone and characterise the entire *mat* locus in the future. The obtained data could be useful for phylogenetic relationships within *Ramularia* species as has been done for related ascomycetous fungi. Conserved domains within the mating

type genes have been used to study the phylogeny of different fungal species and families such as *Colletotrichum* and *Cercospora* species complex and *Dothistroma* needle blight pathogens (Du *et al.,* 2005; Groenewald *et al.,* 2006, 2007, respectively).

The desired outcome of the analysis of mating system in *R. collo-cyni* was the ability to distinguish between isolates according to their mating type and to identify potentially compatible pairs for further mycological study. The candidate mating pairs were used in the attempts to induce the putative functional teleomorph and to characterise the potential sexual development in this fungus by employing a range of mycological and cell biological approaches.

During the examination of disease development using GFP expressing isolate, the presence of so called 'hyphal swellings' *in planta* was noted which confirms previous reports of similar structures found in *R. collo-cygni* (Salamati & Reitan, 2006; Thirugnanasambandam *et al.,* 2011). These studies suggested that the spore-like structures could in fact be the speculated *Asteromella* stage. Salamati & Reitan (2006) first observed the hyphal swellings in six month old cultures that were stored at 4 °C. They also demonstrated the development of much larger structures on autoclaved pieces of barley straw. They concluded that the observed hyphal swellings later developed to the spermogonium stage. Thirugnanasambandam *et al.* (2011) showed that the structures were produced as early as 7 days post inoculation *in planta* and after 2 weeks of incubation *in vitro* suggesting that these spore-like bodies are not necessarily produced only on crop debris in the field but can also be produced at early stages of infection. Both studies did not demonstrate that the spore-

like hyphal swelling and the reported much larger bodies on the straw represented the same structures at different stages of development.

During this study, the spore-like structures at the earliest were found on cultivar Optic at 9 dpi (Figure 4.9). Furthermore, the size of the smallest bodies was approximately 5 µm, similar to those previously reported by Thirugnanasambandam *et al.* (2011). However, at three weeks post inoculation some of them were up to 30 µm in diameter, therefore much larger than previously described. This suggests their gradual maturation occurs over time (Figure 4.4 c). It was also observed that they appear to germinate producing hyphae. This could suggest they have a function in the spread of the disease. This fact and the morphological characteristics and their ability to germinate, giving rise to hypha suggest that they can be a secondary asexual spore type produced by *R. collo-cygni,* which could have a role during infection. There is report of several distinct types of conidia produced at different environmental conditions in *R. vallisumbrosae* (Gregory, 1939), the closely related *Ramularia* species that causes necrotic spotting of narcissus. The lack of apparent internal differentiation in the structures observed in this study could therefore support the argument that these spore-like hyphal swellings have a different function than the suggested spermogonium which is a complex multicellular body.

We have tested the hypothesis that near UV light could be an important factor necessary for the development of sexual reproduction-related structures in *R. collo-cygni*. Initial study using bright field (BF) and DIC microscopy of inoculated fragments of barley straw in culture has confirmed the formation of stromatal knots embedded in stomata (Figure 4.11 a). Our results showed that the exposure of crossing cultures to blue-black lamp caused an increase in numbers of observed

multicellular bodies on straw fragments (Table 4.4). The phenomenon of light-induced sporulation in fungi was first reported during the 20th century (Smith, 1936). Stevens (1928a, 1928b) first observed that ultraviolet (UV) radiation stimulated both sexual and asexual reproduction of *Glomerella cingulata*. Mycologists recognised that reproduction of many fungi can be stimulated by light (Carlile, 1965; 1970). Leach (1972) conducted extensive study on the influence of light on peritheciuim production in the Loculoascomycete fungus *Leptosphaerulina trifolii*. He observed that ascostromata were much more abundant in colonies exposed to specific light conditions. Only UV wavelengths (<350 nm) stimulated perithecium formation when colonies were exposed to filtered light from a combination of near- ultraviolet and daylight fluorescent lamps. Extensive monochromatic radiation studies were conducted using wavelengths from 240-360 nm at 5 nm intervals (5 nm bandwidth). Results of these studies indicated that only wavelengths <370 nm (approx.) stimulated perithecium formation.

The straw inoculation assay, used previously by Salamati & Reitan (2006) to show the development of multicellular bodies, identified as the potential spermogonium stage, *Asteromella*, proved useful for determining the role of these structures in *R. collo-cygni* lifecycle. We have been able to verify the nature of these bodies (Figure 4.12, 4.13). This study reports the existence of spermatia (*Asteromella*) produced by these structures (Figure 4.13) thus confirming that indeed they represent the speculated spermogonial state. Similar development was observed previously in the related *Ramularia* species, i.e. *R. armoraciae* (Dring, 1961) and *R. deusta* (Baker *et al.,* 1950). The latter authors reported the presence of spermogonia on old perennial pea leaves in winter.

We have been able to identify yet another type of multicellular bodies that develop on the inoculated barley straw (Figure 4.14). Their interior consisted of undifferentiated pseudoparenchyma cells (Figure 4.19 a). We observed that these structures could sprout to produce conidiophores (Figure 4.20) which led to the initial conclusion that they could be sclerotia, i.e. the vegetative 'organ' of aestivation. This was supported by previous studies of life history in related *Ramularia* species, specifically *R. vallisumbrosae* (Gregory, 1939)*, R. onobrychidis* (Hughes, 1949), *R. deusta* (Baker *et al.,* 1950) and *R. armoraciae* (Dring, 1961). In these extensive studies, detailed analysis of these organs was presented however the authors could not agree on their definite function. For instance, Gregory (1939) studied this sclerotium-like stage of *R. vallisumbrosae* and observed the production of filiform spores in the neck of the body. Similarly, in *R. armoraciae* on horseradish, the overwintering sclerotia germinated in spring to give conidia (Dring, 1961). Hughes (1949) also observed similar structures in *R. onobrychis* for which no internal differentiation had been found. Nevertheless, all the authors did not disregard the hypothesis that the sclerotia could be an intermediate state that may further develop into perithecium.

During the course of our examination, several different temperature conditions have been tested in order to verify if sclerotia could serve their presumed function of overwintering. Interestingly, in 8 - 12 week old cultures exposed to the temperature of 4 ºC for a period of a week, we found a small number of the structures in which internal differentiation had taken place. Furthermore, we observed some hyphae in the interior that could be trichogynes, a specialised type of receptive hyphae. The initially spherical structures also became pear shaped and were reminiscent of sexual

fruiting bodies of related ascomycetous species, such as *M. fijiensis* (Meredith and Lawrence, 1969). In fact, in some sclerotia of *R. vallisumbrosae*, the hyaline hyphae within the body remained thin-walled and apparently discrete throughout the summer and winter months (Gregory, 1939). The author also detected hyphae present in the centre and neck of the bodies that strongly resembled trichogynes (Figure 4.2). This suggested therefore that the structures might represent the fundaments of a yet undiscovered perithecial stage. Good (1947; cited in Baker *et al.,* 1950) also reported spermatia and perithecial initials in culture. However, the subsequent examination of field material at various seasons failed to provide more than a suggestion that the perfect stage exists.

In order to detect a potential recombination, two transgenic isolates expressing either GFP or DsRed were crossed, which proved successful in producing sclerotium-like bodies which carried spore-like structures that appeared to co-express both fluorescent protein markers. This proved that the recombination had occurred between these isolates. It is important however, to consider other potential mechanisms that may have facilitated this recombination. For instance, parasexual recombination is thought to play an important role in increasing the diversity amongst fungal populations (Roca *et al.*, 2005a, b; Read & Roca, 2006; Ishikawa *et al.*, 2010).

The perfect state of *Ramularia* species is presumed to belong to the ascomycete genus *Mycosphaerella.* For instance, the existence of a functional teleomorph has been determined in *R. grevilleana,* syn. *R. brunnea* (teleomorph *M. fragariae*) on strawberry (Dring, 1961). Most recently, it has been suggested that the genus

*Mycosphaerella* should be restricted only to taxa related to *Ramularia* anamorphs due to very close phylogenetic relationship of these genera (Crous, 2009). We have been able to observe within some of the described structures a formation of cylindrical asci, which appeared to carry ascospores (Figure 4.19 c, d). However, this has only occurred for three of several hundred sectioned bodies. Unfortunately, it was not possible to obtain viable ascospores to observe if these spores could produce typical *R. collo-cygni* colonies. Although our findings could be of great importance, we cannot formally describe the sexual stage as required by the International Code of Botanical Nomenclature due to the lack of well-preserved ascospore material. In order to confirm beyond any doubt that indeed these bodies represented the teleomorph of *R. collo-cygni,* it is suggested here that the subsequent studies were attempted using samples that were exposed to natural environment as *in vitro* induction of sexual stage in *Mycosphaerella* species so far yielded a very limited success in the banana pathogen *M. fijiensis* (Etebu *et al*., 2003), or failure in the barley pathogen *Z. passerinii* (Ware *et al.* (2007).

Sexual reproduction facilitates the increasing diversity within fungal species and could lead to rapid development of fungicide resistant strains of the fungus. It is therefore suggested here that potential sexual stage in *R. collo-cygni* should remain as one of the most intensely studied aspect of its biology to monitor the risk of future outbreaks by new virulent strains and the future impact on barley production as well as the development of fungicide resistance in general.

# Chapter 5

# Cell biology and genetics of rubellin biosynthesis

# 5. Cell biology and genetics of rubellin biosynthesis

## 5.1. Introduction

*R. collo-cygni* produces photodynamically active phytotoxins, specifically the anthraquinone derivatives rubellins such as rubellin D (Heiser *et al.,* 2003a, b), rubellin B (Miethbauer *et al.,* 2003) and rubellin C (Heiser *et al.,* 2004). Rubellins had previously been described for *Mycosphaerella rubella*, the pathogen that causes a necrotic spot disease of the medicinal plant *Angelica sylvestris* (Arnone *et al.,* 1986, 1989).

The biochemical structure of additional sister metabolites has also recently been elucidated. These are rubellin A and two new rubellins: 14-dehydrorubellin D and rubellin E. The latter is related to rubellins B and D but does not possess a lactone ring (Miethbauer *et al.,* 2006). In this study they also identified the presence of rubellins in *R. uredinicola*, suggesting that this could be common across this genus. By incorporating [1-$^{13}$C]-acetate and [2-$^{13}$C]-acetate into the rubellins, they showed that the anthraquinone derivatives were biosynthesised via the polyketide pathway. Furthermore, the labelling pattern after feeding [U-$^{13}C_6$]-glucose demonstrated the existence of the fungal folding mode of the poly-β-keto chain. Most recently, Miethbauer *et al.* (2008) reported the isolation, structural elucidation and bioactivity of novel similar compounds such as uredinorubellin I, II and caeruleoramularin.

Although the accumulation of the toxin in *R. collo-cygni* hyphae has previously been demonstrated (Miethbauer *et al.,* 2006), research on rubellins in *R. collo-cygni* has so far concentrated on identification and biochemical structure of these important anthraquinone-derived toxins. It would now be necessary to expand this knowledge

and gain understanding of the fundamental cell biological processes and genetics behind biosynthesis of these necrosis inducing toxins. A crucial step in order to characterise its mode of action would be the identification of gene candidates involved in the synthesis of rubellins.

Important insights into the genetics of secondary metabolite biosynthesis pathway have been provided for the structurally similar secondary metabolite, anthraquinone-derived toxin dothistromin produced by the related ascomycete pathogen responsible for the red band needle blight of pine, *Dothistroma septosporum* (teleomorph *Mycosphaerella pini*) (Bradshaw *et al.,* 2002). The biochemical structure of dothistromin appears to be also similar to that of versicolorin B, a precursor of aflatoxin and sterigmatocystin (Bradshaw and Zhang, 2006). Both toxins, rubellin (Miethbauer *et al.,* 2008) and dothistromin (Stoessl *et al.,* 1990; Jones *et al.,* 1995) are toxic not only to plant tissue, but also to a wide range of other eukaryotes and bacteria, and hence are considered host-nonspecific toxins (Bradshaw *et al.,* 2009).

Although the precise mode of action is not known, dothistromin can be reductively activated leading to the formation of the reactive oxygen species superoxide ($O_2$-) and $H_2O_2$. Similarly, the perylenequinone toxin cercosporin also absorbs light and reacts with oxygen molecules to generate reactive oxygen species, including singlet oxygen ($^1O_2$) and $O_2$- (Daub and Hangarter, 1983). These reactive oxygen species therefore cause peroxidation of cell membranes and leakage of electrolytes in host plant tissue (Daub, 1982b; Daub and Briggs, 1983; Daub and Ehrenshaft, 2000). It has been demonstrated that cercosporin is able to damage major cellular components such as nucleic acids, proteins and lipids. It is also toxic to bacteria, many fungi and mice (Yamazaki *et al.*, 1975; Ito, 1981; Daub, 1982 a). Accumulation of cercosporin

in culture is affected by environmental and developmental factors (Jenns *et al.*, 1989; Daub and Ehrenshaft, 2000). It has been shown that light is the most critical factor, not only for toxicity, but also for biosynthesis of cercosporin as the toxin was only produced in the light and this process was completely suppressed in darkness. However, immediately after only a brief exposure to light, the production of the toxin was initiated (Ehrenshaft and Upchurch, 1991).

Most recently, dothistromin has been demonstrated to be a virulence factor that may play a major role in the development of the red band needle blight of pines (Kabir *et al.,* 2014). Interestingly, Schwelm *et al.* (2009) presented the evidence that dothistromin-deficient mutants of *D. septosporum* generated by disruption of the dothistromin polyketide synthase gene (*pksA*) were pathogenic to *Pinus radiata*. This showed that dothistromin was not required by the pathogen to complete its lifecycle. The results of competition studies *in vitro* indicated that the toxin may have a role in competition against other microorganisms in the needle environment. However, most recent evidence showed that dothistromin could be in fact a virulence factor in *D. septosporum* (Kabir *et al.,* 2014). Cercosporin has also recently been demonstrated to play a crucial role in pathogenicity of *C. nicotianae* and lesion formation on tobacco (Choquer *et al.*, 2005; 2007; Dekkers *et al.*, 2007).

A number of fungal secondary metabolites, including aflatoxins, compactin, ergot alkaloids, fumonisins, gibberellins, gliotoxin, HC toxin, indole-diterpenes, loline alkaloids, penicillin, sterigmatocystin, sirodesmin and trichothecenes, and dothistromin are synthesized by genes found in clusters within fungal genome (Hohn *et al.*, 1993; Brown *et al.*, 1996; 2004; Brakhaage, 1998; Young *et al.*, 2001; 2006; Abe *et al.*, 2002; Ahn *et al.*, 2002; Proctor *et al.*, 2003; Gardiner *et al.*, 2004; 2005;

Yu *et al.*, 2004; Haarmann *et al.*, 2005; Spiering *et al.*, 2005; Tudzynski, 2005, Bradshaw *et al.,* 2002).

The aflatoxin (AF) synthesis pathway has been described in a great detail and comprises a series of highly organised oxidation-reduction reactions (Bhatnagar *et al.,* 1992; Minto and Townsend, 1997). AF and related sterigmatocystin (ST) are produced predominantly by species within the Orders Eurotiales and Sordariales (Klich *et al.,* 1995). In *Aspergillus*, AF is made by section Flavi species such as *A. parasiticus* and *A. flavus*, as well as by non- Flavi, *A. ochraceoroseus* (Cary and Ehrlich, 2006).

The AF biosynthesis requires around 25 genes which encode enzymes as well as some regulatory proteins (Figure 5.1), clustered together in a 70-kb region of the genome (Yu *et al.,* 2004; Bhatnagar *et al.,* 2003). Biosynthesis begins with conversion of malonyl-CoA to a condensed polyketide noranthrone by the products of two fatty acid synthase genes (*fas-1* and *fas-2*) and a polyketide synthase gene (*pksA*) (Cary *et al.,* 2000a, b). No specific enzyme has yet been coupled with this conversion of noranthrone to norsolorinic acid (NOR) which is the first stable metabolite. Some enzyme candidates have been suggested, such as a monooxygenase (possibly *cypA*) and a dehydrogenase (possibly *norB*) (Bhatnagar *et al.,* 2003). Subsequent conversion to averantin (AVN) involves a dehydrogenase, encoded by the gene *nor-1* (Chang *et al.,* 1992; Trail *et al.,* 1994), but Cary and Bhatnagar (1995) demonstrated that the reaction can also be catalysed by the dehydrogenase encoded by *norA*. There are still some steps in the conversion of AVN to versicolorin B (VERB) that remain not assigned to a specific gene in the cluster. Three genes are possible candidates for individual steps: *cypX*, *moxY*, and *avfA*

(Bhatnagar *et al.,* 2003). Two genes: *ver-1* (encoding a ketoreductase; Skory *et al.* 1992) and *verA* (encoding a cytochrome P-450 monooxygenase) are required for the conversion of versicolorin A (VERA) to demethylsterigmatocystin (DMST). The final step in the formation of aflatoxins is the conversion of O-methylsterigmatocystin (OMST) or dihydro-O-methylsterigmatocystin (DHOMST) to aflatoxins B1, B2, G1 and G2, requiring the presence of a NADPH-dependent monooxygenase, ordA (Prieto and Woloshuk 1997; Yu *et al.*, 1998). The formation of the G toxins involves an additional step, possibly involving the enzyme encoded by *ordB*. Another gene, *aflT*, encodes an ABC transporter protein that may be necessary for aflatoxin efflux from the cells (Yu *et al.* 1998; Yabe *et al.* 1999).

Keller and Hohn (1997) characterised the ST cluster in *A. nidulans* and demonstrated that most of the ST genes are orthologs of AF genes, although they are arranged in a different order. Subsequent analyses of gene clusters from a range of section and non-section Flavi species suggested the ST cluster could be an ancestral to the AF-type. Therefore an ancestral core cluster has been proposed that comprised genes *pksA*, *hexA*, *hexB* and *nor-1*, possibly along with some regulatory genes such as *aflR*, *aflJ* (Cary and Ehrlich, 2006). These genes are required to form the initial polyketide product. The authors then speculated that duplication and recruitment of genes encoding polyketide-modifying enzymes subsequently took place. This was possibly followed by purifying selection and some gene loss. To support this speculation, there is considerable evidence for duplication of genes in metabolic gene clusters (Cary and Ehrlich, 2006; Chang and Yu, 2002) as well as for the occurrence of transposable elements and/or repeated sequences. This then suggests a mechanism of

the movement of sets of genes during the evolution of gene clusters (Tanaka *et al.,* 2006; Young *et al.,* 2006).

The synthesis of secondary metabolites such as AF is affected by environmental and nutritional factors such as temperature, pH, carbon and nitrogen source, stress factors, lipids, and certain metal salts (Cary *et al.*, 2000a). Some of these factors may control the expression of the components in aflatoxin biosynthetic pathway by responding to nutritional and environmental signals (Tag *et al.*, 2000) Amongst 23 genes so far isolated that code for proteins involved in aflatoxin biosynthesis, one gene, *aflR*, encodes a putative transcription factor (Ehrlich *et al.,* 1999).

Isolation of the pathway-specific regulator gene, *aflR* was first achieved by its cloning from an *A. flavus* cosmid library by showing that it could restore AF-producing ability to a mutant blocked in all steps of AF biosynthesis (Payne *et al.,* 1993). A homolog was subsequently isolated from *A. parasiticus* transformed with a DNA fragment containing *aflR* that caused the transformants to become orange-pigmented due to overproduction of AF biosynthetic intermediates (Chang *et al.* 1993). Overexpression of *aflR* in *A. flavus* up-regulated biosynthesis pathway gene transcription and AF accumulation in a fashion similar to that found in *A. parasiticus*, but pigmented colonies were not observed, a result suggesting that subtle differences in biosynthesis occur in the two fungi (Flaherty and Payne, 1997). These results suggested that an increase in the copy number of *aflR* somehow altered normal regulation of AF biosynthesis. Metabolite feeding studies showed that a functional *aflR* allele is required for accumulation of NOR, the first stable intermediate in the AF biosynthetic pathway (Payne *et al.*, 1993). When *aflR* was disrupted, the fungi were incapable of aflatoxin metabolite production or

transcription of *nor-1*, but otherwise grew normally. Interestingly, *aflR* homolog with only 31% identity to that of *A. parasiticus* or *A. flavus* was also found in the cluster of sterigmatocystin (ST)- producing *A. nidulans* (Yu *et al.*, 1996). Induced expression of *A. flavus* aflR in *A. nidulans*, under conditions in which ST biosynthesis is normally suppressed, activated the genes in the ST biosynthetic pathway. These studies demonstrated that aflR function is conserved in widely different *Aspergillus* spp. Homologs of aflR have been identified from all aflatoxin and ST-producing *Aspergilli* so far examined (Watson *et al.*, 1999; Ehrlich *et al.*, 2002).

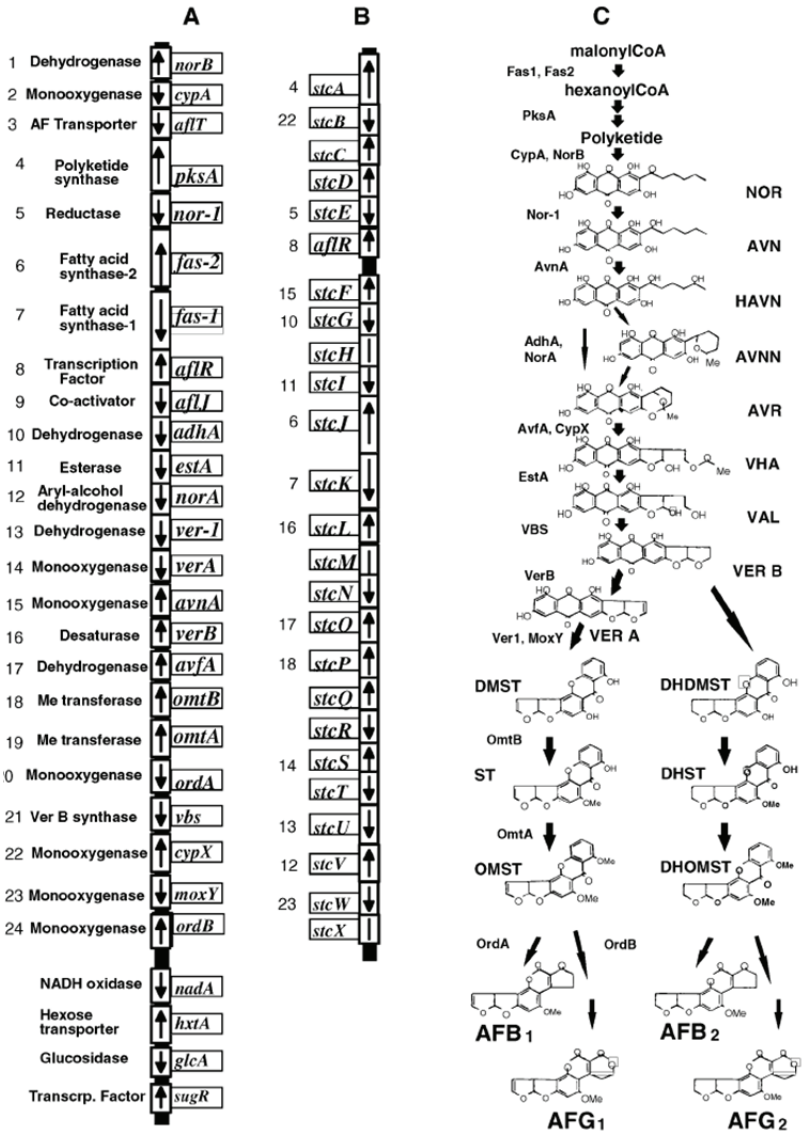


Figure 5.1
Widely accepted representation of aflatoxin (A) and sterigmatocystin (B) clusters with their biosynthesis pathway (C) (Bhatnagar *et al.,* 2003).

An interesting aspect of *Dothistroma* biology is the close similarity of its secondary metabolite dothistromin (DS) to the AF precursor, versicolorin B (Zhang *et al.,* 2007). The availability of the *D. septosporum* genome sequence (deWit *et al.,* 2012) enabled identification of putative dothistromin genes. The genome contains

orthologs of AF genes that are located on a 1.3-Mb minichromosome. For example, the *dotA* and *pksA* genes encode versicolorin reductase and polyketide synthase, respectively, which have 80 % and 57 % amino acid identity to their *A. parasiticus* orthologs, namely *ver-1* (AflM) and *pksA* (AflC). Subsequent targeted gene knockout of *dotA* and *pksA* confirmed that both genes are essential for DS production and are surrounded by several other AF-like genes (Bradshaw *et al.,* 2002, 2006). Due to the close structural similarity of DS and versicolorin B, it was expected that a cluster of AF gene homologs would be present in the *D. septosporum* genome. Interestingly, DS genes were shown to have other (non-DS) genes alongside and were not the elements of only one cluster, but most of the genes were spread over six separate regions (loci) on chromosome 12 (1.3 Mb) (Schwelm and Bradshaw, 2010; deWit *et al.,* 2012). These findings showed that in contrast to the complete clusters of AF and ST, DS is synthesised by a highly fragmented group of genes.

An ortholog of the aflatoxin regulatory gene *AflR* has recently been identified and studied in a great detail (Chettri *et al.,* 2012). This study demonstrated that levels of expression of the widely dispersed genes in *D. septosporum* are not correlated with gene location with respect to their distance from a telomere, but that the expression is regulated by *aflR*. The production of DS by *D. septosporum* mutant in which the *aflR* gene was knocked out was drastically reduced, but still detectable. This is in contrast to orthologous aflR mutants in *Aspergillus* species that lack any AF or ST production (Payne *et al.,* 1993; Price *et al.,* 2006).

A large body of research has been generated on cercosporin (CR) toxicity and resistance, which then drifted towards studying a putative biosynthetic pathway and

its regulation. A Zn(II)Cys6 transcription factor, *crg*1, has been identified with a role in regulating both CR resistance and production (Chung *et al.*, 1999; 2003a), however the mechanism of *crg*1 regulation and its relation to signalling pathways and environmental signals is not yet understood. Most recently, Chen *et al.* (2007) also reported a core cluster of six genes involved in CR synthesis in addition to *ctb1* and *ctb3* that were co-ordinately regulated and highly induced under CR-producing conditions. In addition, they also confirmed the function of two genes, *ctb2* and *ctb8*, in cercosporin biosynthesis using targeted gene disruption and genetic complementation.

### 5.1.1. Objectives

An important aim of this study was to elucidate the role of rubellin in *R. collo-cygni* infection biology and symptom development on barley by live cell imaging of rubellin biosynthesis and discharge during the infection development using detached leaf inoculation assay and confocal microscopy.

The role of rubellin toxin in RLS symptom induction and the biochemical structure has previously been demonstrated (Heiser *et al.,* 2004; Miethbauer *et al,* 2006). However, the putative molecular processes that could facilitate rubellin synthesis remained unknown. The recently sequenced *R. collo-cygni* genome (SRUC, unpublished) has now provided an excellent tool for studying the complex genetics and molecular biology of this increasingly important barley pathogen.

The biochemical structure of rubellin molecules suggested its close relationship with aflatoxin and dothistromin, toxins produced by *Aspergillus* spp. and *D. septosporum*, respectively, for which biosynthesis at the fundamental genetics level has been

characterised. An important objective of this study was therefore to identify the structure of putative molecular machinery that may be involved in rubellin production in *R. collo-cygni* by comparative genomic appraches using the findings in the abovementioned closely related fungi.

## 5.2. Methods

### 5.2.1. Plant material, *R. collo-cygni* isolates and detached leaf assay

Fungal isolates, methods for inoculation and the preparation of plant material used in this study been described in detail in Chapter 2.

### 5.2.2. Live-cell imaging of rubellin vesicles using autofluorescence

The 2 - 3 months old cultures of the *R. collo-cygni* wild-type isolates B1 and Stratego were used in the initial analysis of the fluorescence spectra of putative rubellin. A lambda scan across wide range of light wavelengths, from 488 nm up to 720 nm, was performed using Leica SP2 confocal equipped with HeNe laser.

These isolates were subsequently used for imaging vesicles using confocal laser scanning microscopy (CSLM). This was performed using a Bio-Rad MRC600 system equipped with an argon ion laser and mounted on either a Nikon Diaphot TMD or TE300 inverted microscope (all supplied by Bio-Rad Microscience, Hemel Hempstead, UK). Simultaneous, brightfield images were captured using a transmitted light detector, which collected the light from behind the microscope condenser. GFP fluorescent protein was excited with 488 nm laser line and their fluorescence was detected at > 550nm. Oil immersion 60 x (N.A. 1.4) or dry 20 x (N.A. 0.75) plan apochromatic objective lenses were used for imaging. Putative rubellin autofluorescence signal was detected at light wavelength between 535 and 605 nm and bright-field transmission images were simultaneously collected using transmission detector on inverted Nikon TE300.

Similar imaging conditions were used for the imaging of rubellin vesicles during experiments on the infection development by the transformant strain Rcc-8B9-GFP *in planta* under Leica SP2 CLSM, however to reduce potential cross-talk between the channels, GFP and rubellin autofluorecence spectra were collected sequentially by HeNe laser and solid state lime laser lines, respectively. The obtained z-stacks were then assembled into maximum projections using ImageJ and Leica Confocal Suite software.

### 5.2.3. Bioinformatics approaches

Ketoreductase encoding *dotA* gene (Bradshaw *et al.,* 2002) from *D. septosporum* (Gen Bank accession AF448056.2) was chosen as a starting point. The nucleotide sequence was blasted against *R. collo-cygni* genome sequence (SRUC, unpublished) using the translated nucleotide query tblastx tool provided by The GenePool, University of Edinburgh.

In order to identify other ORFs surrounding putative dotA orthologous sequence, a large contig that contained the selected gene was analysed by StarORF application (HTML version) (Massachusetts Institute of Technology, USA). The putative ORFs were blasted against known protein sequences (NCBI blastp) and their corresponding proteins were aligned using the Multalin sequence alignment tool (Corpet, 1988).

## 5.3. Results

### 5.3.1. Cell biology of rubellin synthesis and discharge

*R. collo-cygni* produces large quantities of a red pigmented toxin, called rubellin, in both solid and liquid cultures. The pigments are clearly visible by the naked eye and by conventional microscopy as a red coloration of the colony (Figure 5.2 a). Further investigation into the origin of the toxin revealed that mature hyphae hold many vacuole-like vesicles that contain this heavily pigmented substance (Figure 5.2 b). The toxin was subsequently observed to be released from hyphae presumably by some form of exocytosis (Figure 5.2 c)

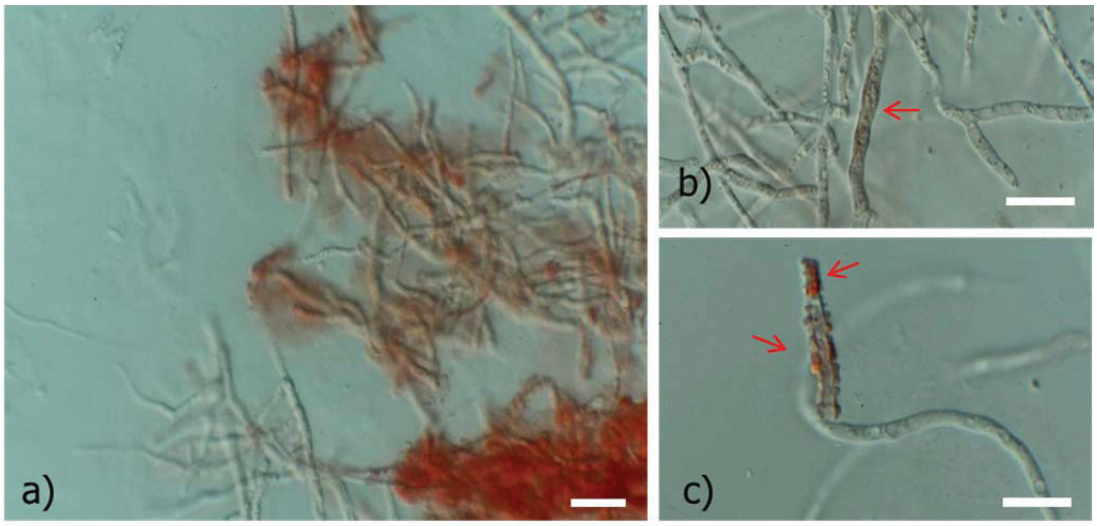


Figure 5.2
Rubellins as observed in a culture using DIC microscopy. Bar = 10 µm: a) large volume of rubellins released by field isolate DK05 cultivated on PDA medium; b) formation of vacuole-like vesicles, filled with toxin (red arrow); c) hyphae releasing the toxin from the vacuole-like vesicles presumably via exocytosis, indicated by red arrows

Based on the anthraquinone properties and the known biochemistry of rubellin (Miethbauer *et al.,* 2003, 2006), a new method of direct visualisation of the toxin *in vivo* by confocal microscopy was developed. In order to determine the fluorescence emission wavelengths specific for rubellin vesicles, a lamdba scan under a confocal microscope was used. The obtained spectra matched the biochemical predictions of previous studies. Intensity of emission increased dramatically at 520 nm and reached top fluorescence intensity at wavelengths between 555 and 605 nm. Two distinguishable peaks of highest intensity suggested a mixture of at least two compounds of similar pigmentation (Figure 5.3 a). The wavelengths suggested a possible domination of rubellin D in fungal hyphae.

Rubellin was found inside the vacuole-like vesicles of various sizes as previously observed under light microscopy (Figure 5.3 b). This visualisation of rubellin autofluorescence was subsequently used in direct observations of vesicle formation during live-cell imaging of GFP expressing *R. collo-cygni* isolate (Figure 5.3 c) and inoculation experiment *in planta.* It was possible to separate GFP, chlorophyll rubellin autofluorescence channels by sequential imaging using multi-laser approach (Figure 5.3 d)

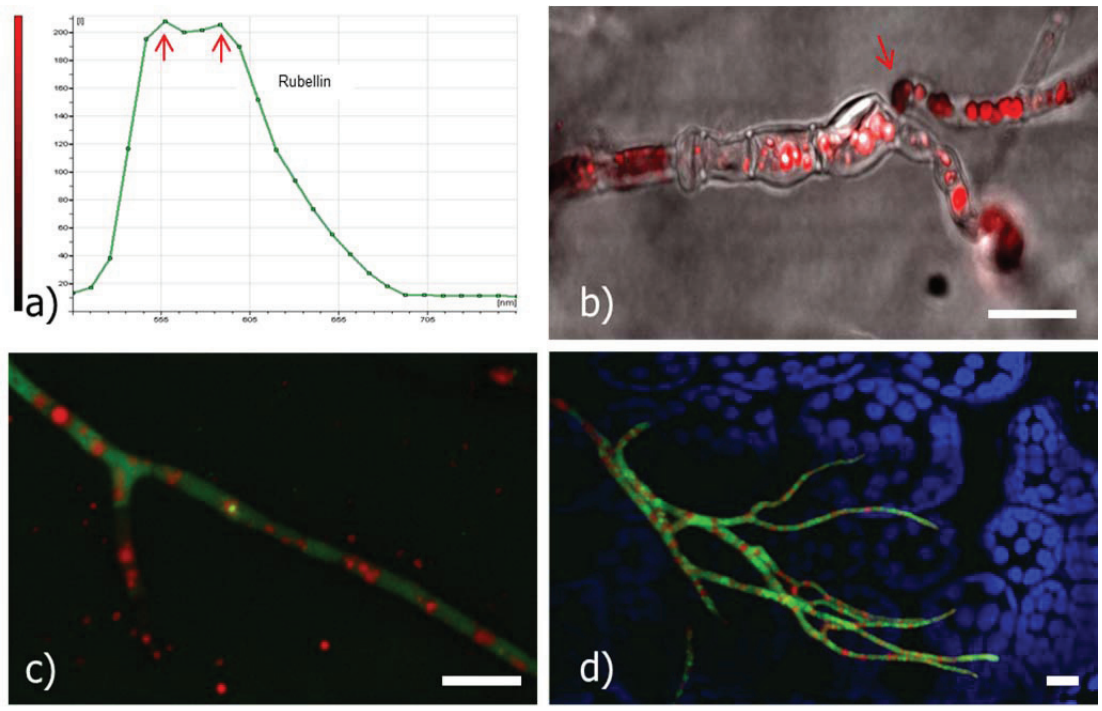


Figure 5.3

The development of a method for direct observation of rubellin *in planta* using CLSM: a) analysis of the emission spectra of the putative rubellin autofluorescence signal collected using lambda scan; b) confocal image of rubellin autofluorescence in a wild type *R.collo-cygni* isolate B1, superimposed on brightfield transmission image. Note various sizes of vacuole-like vesicles within the collapsed hypha. Arrow indicates discharge of rubellin via hyphal tip. Bar = 5 µm; c) confocal image of a viable hypha of the transgenic isolate Rcc-8B9-GFP carrying rubellin vesicles. Note red autofluorescence also present outside living hyphae. Bar = 10 µm;d) the transgenic isolate Rcc-8B9- GFP inoculated on barley cv. Optic leaf. Maximum projection a z-stack sequentially collected using HeNe laser for GFP (green channel) and chlorophyll autofluorescence (blue channel), and lime laser for rubellin autofluorescence (red channel). Bar = 10 µm.

### 5.3.2. Imaging of putative rubellin *in planta*

Putative rubellin signal detection was incorporated into inoculation experiments with the transgenic isolate Rcc-8B9-GFP. Rubellin was initially observed in the dead hyphae that either failed to survive saprophytically and compete with other mycelia, but it is also possible that harvested inoculum used for inoculation contained already dead hyphal fragments. Although each of the prepared microscopic slides was frequently scanned within the developing infection away from inoculation site, rubellin was detected for the first time at earliest 23 to 25 dpi in heavily colonised plant material. First instances of rubellin discharge into plant tissue were determined for stomata that carried the substomatal aggregates after their expanding into surrounding palisade mesophyll layer (Figure 5.4 a). Here, a stoma became necrotic and a developing lesion expanded into neighbouring stomata (Figure 5.4 b).

During three independent time-course imaging experiments, rubellin was commonly localised to the regions of mesophyll colonisation by the thick highly vacuolated hyphae (Figure 5.4 c). Pepper spot symptoms could be observed on the leaf by the unaided eye that subsequently developed into typical RLS lesions.

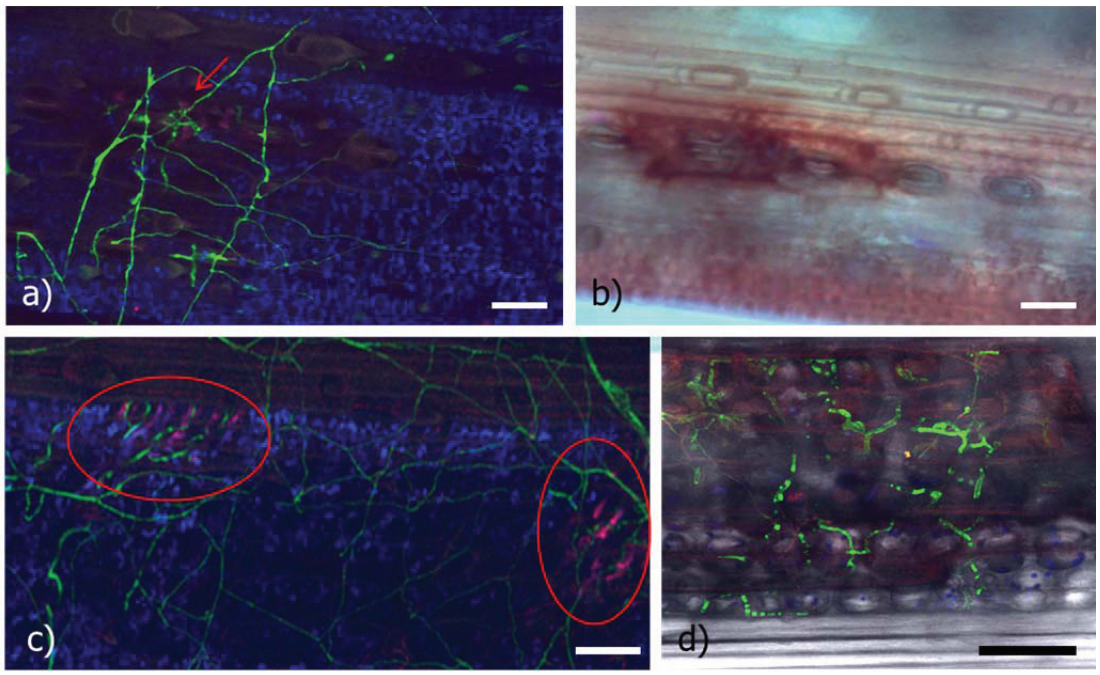


Figure 5.4
Confocal images of infection development by the transgenic isolate Rcc-8B9-GFP on barley cv. Optic: a) early stages of a lesion development following rubellin deployment by a vacuolated fungal aggregate in substomatal cavity (red arrow). b) corresponding overlay brightfield transmission image of RGB projections of a). Note the expansion of symptoms into the neighbouring stomata. Bar = 100 µm; c) rubellin signal (magenta) localised to the areas of mesophyll tissue colonised by endophytic intercellular hyphae. Developing symptoms have been circled red. Bar = 100 µm; d) maximum projection of fully developed lesion accompanied by rubellin signal present throughout the necrotic site. Confocal images of GFP and rubellin channels were superimposed on brightfield transmission image. Note a gradual degradation of intercellular hyphae in collapsed mesophyll tissue indicated by loss of GFP expression in fungal cytoplasm. Bar = 20 µm

A study of the vesicle formation was also carried out in order to identify a likely process of rubellin biosynthesis at the cellular level. A short, 2- to 3-minute exposure to UV lamp was sufficient to activate rubellin synthesis. The observation initially showed toxin autofluorescence across cytoplasm, which then started accumulating in small vesicles (Figure 5.5 a). The size of these vesicles gradually increased to reach in many instances the size of a typical vacuole. Subsequent observation also revealed strong autofluorescence of expected characteristics in the plant extracellular spaces surrounding the endophytic hyphae (Figure 5.5 b). Here, vacuoles appeared to no longer carry the toxin however the hyphae continued to express GFP which demonstrated that the fungus was alive and could tolerate the toxin.

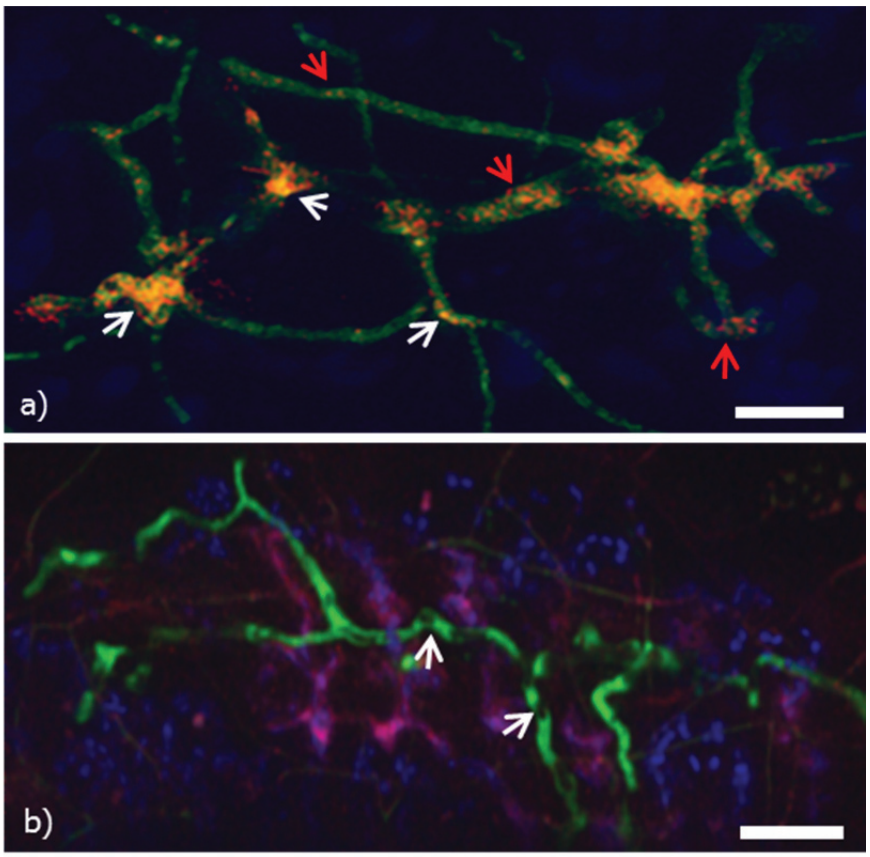


Figure 5.5
Cell biology of rubellin biosynthesis and discharge. Bar = 20 µm: a) rubellin appears to be synthesised in the cytoplasm and then transported into the vacuoles. Yellow colour demonstrates co-localisation of cytoplasmic GFP (green)- and rubellin (red) channels (white arrows). Note small red vesicles also present within thick hyphae suggesting gradual accumulation of toxin inside vacuole-like vesicles (red arrows); b) branched endophytic hypha surrounded by rubellin (magenta indicates co-localisation of rubellin in red and chlorophyll in blue) spreading into intercellular spaces of the mesophyll layer. Note hypha still viable but vacuoles no longer contain the toxin (white arrows).

### 5.3.3. The structure of a putative rubellin biosynthesis pathway

The initial study of *Aspergillus* spp. demonstrated the biosynthesis of aflatoxin, the secondary metabolite toxic to animals, produced by those species of higher Fungi. It was found that the production of this toxin is governed by enzyme encoding genes that were clustered in one place on one chromosome. Since then, the existence of aflatoxin-like gene cluster has also been demonstrated in closely related plant pathogens, *D. septosporum* and *Cladosporium fulvum*.

The recent *R. collo-cygni* genome sequencing project (Fountaine *et al.*, unpublished), accomplished with Scottish Government funding under RESAS Work Packages 1.4 (Barley Pathology) and 6.4 (Disease Epidemiology) has now provided an excellent tool for studying the putative molecular machinery required for rubellin production. The composition of the cluster closely resembles gene cluster described for *D. septosporum*, necessary for production of toxin dothistromin. The biochemical structure of both compounds, i.e. rubellin and dothistromin, is similar therefore it is possible to suggest that biosynthesis pathway of these secondary metabolites should remain similar. By using bioinformatics approaches, we have been able to determine the existence of aflatoxin-like gene cluster in the genomic data.

A defined metabolic island consisted of clustered genes determined to be involved in the synthesis of known toxins in the fungal kingdom such as aflatoxin and dothistromin in *Aspergillus* spp. and *Dothistroma septosporum*, respectively (Figure 5.6).

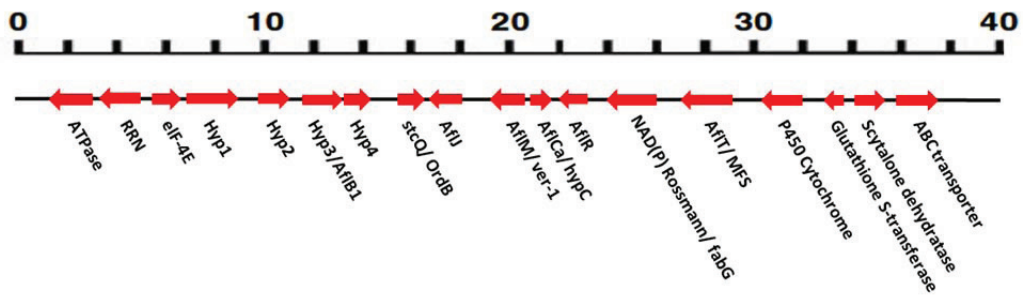


Figure 5.6
The composition of a putative metabolic gene cluster in *R. collo-cygni* with the predicted protein function (if known) based on the published genomes of related fungal species, mainly *D. septosporum* and several *Aspergillus* species.

A number of putative key genes present in the cluster were identified: *aflB*, *stcQ*, *aflJ*, *ver-1* (*aflM*), *aflR*, cytochrome P450 (*cypA*/ *X*) and two transporter genes, i.e. Major Facilitator Superfamily transporter (MFS) and ABC transporter. In addition, the above genes with a predicted role were surrounded by a range of hypothetical proteins with unknown function. These appeared to follow a specific order according to highest blast hits GenBank accession numbers that was identical to this found in *D. septosporum*. Many of these genes contained specific chemical binding domains that belong to the NAD(P) Rossmann protein superfamily. The biochemical composition and function is based on the description provided by Marchler-Bauer *et al.* (2009, 2011) and Marchler-Bauer & Bryant (2004).

The first two genes present in the cluster are the hypothetical proteins, namely Hyp1 and Hyp2. These are the first genes with unknown predicted function found that could play a role in rubellin biosynthesis. Protein blast results showed significant amino acid identity of 29 % and 40 % to *D. septosporum* genes with GenBank

accession numbers EME49365.1 (Figure 5.7 a) and EME49364.1 (Figure 5.7 b), respectively.

a)

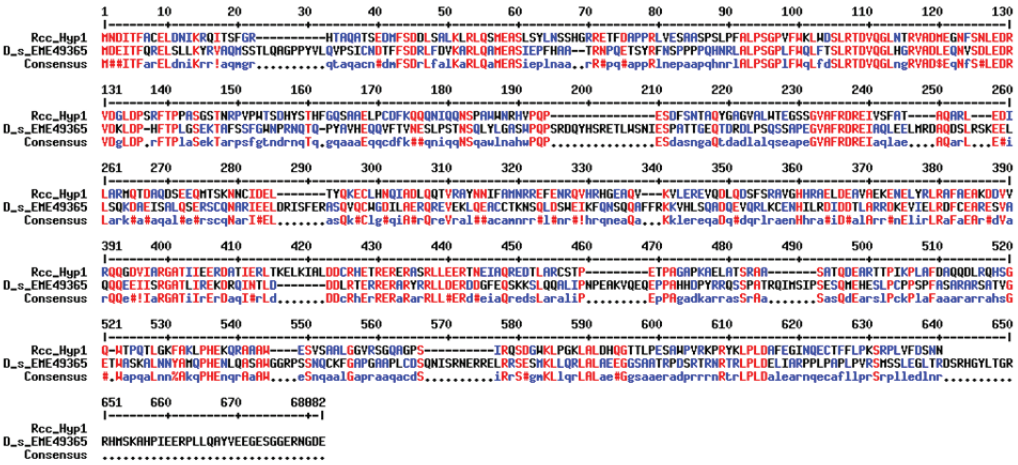

b)

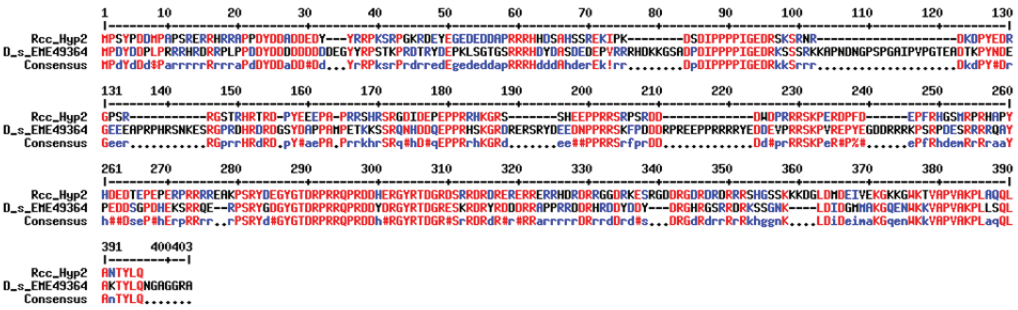

Figure 5.7
Alignment of a Hyp1 and Hyp2 ORFs and corresponding similar hypothetical proteins in *D. septosporum*: a) EME49365.1 and b) EME49364.1.

These are followed by *Hyp3*/ *aflB1* genes, similar to that with a predicted function in aflatoxin biosynthesis pathway. It showed amino acid identity to *D. septosporum* (EME49363.1) at 64 % (Figure 5.8). Furthermore, the obtained blast results also

indicated 37 % identity to *Taphrina deformans* AflB1 protein (CCG82151.1). These results pointed at the putative function of this protein to be as an aldo/ keto reductase (AKR).

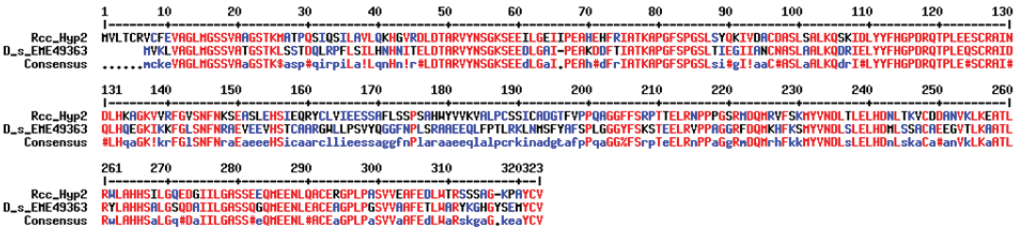

Figure 5.8
Alignment of Hyp3/ aflB1 ORF and corresponding similar hypothetical protein in *D. septosporum* (EME49363.1)

Hyp4 was the next gene found in the upstream sequence that encodes a hypothetical protein which had 36 % amino acid identity to *D. septosporum* protein (EME49362.1) of unknown function (Figure 5.9).

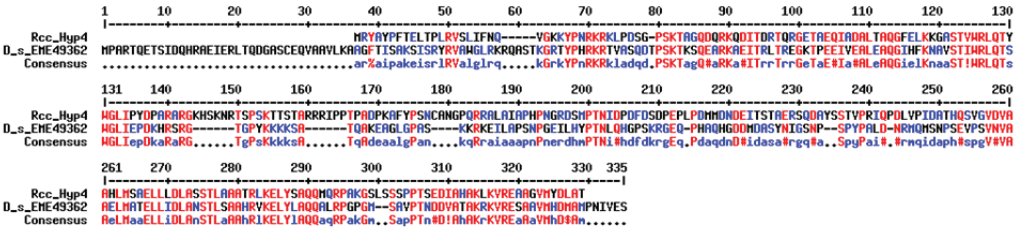

Figure 5.9
Alignment of a Hyp4 ORF and corresponding similar hypothetical protein in *D. septosporum* EME49362.1.

The next gene in the cluster showed significant 51 % amino acid identity to *Aspergillus nidulans* (CBF90090.1) and *Aspergillus fumigatus* (XP_001266598.1) which are known to be toxin biosynthesis proteins in these species (Figure 5.10). Blast results also indicated significant 49 % amino acid identity to stcQ and ordB proteins in *Arthroderma otae* (XP_002844732.1) and *Arthroderma gypseum* (XP_003169337.1), respectively. Furthermore, this protein containing NAD binding 10 multidomain found in NADB Rossmann superfamily also indicated its putative function, which was predicted to be nucleoside-diphosphate-sugar epimerases. The predicted function of these proteins is cell envelope biogenesis and, most importantly, outer membrane carbohydrate transport and metabolism.

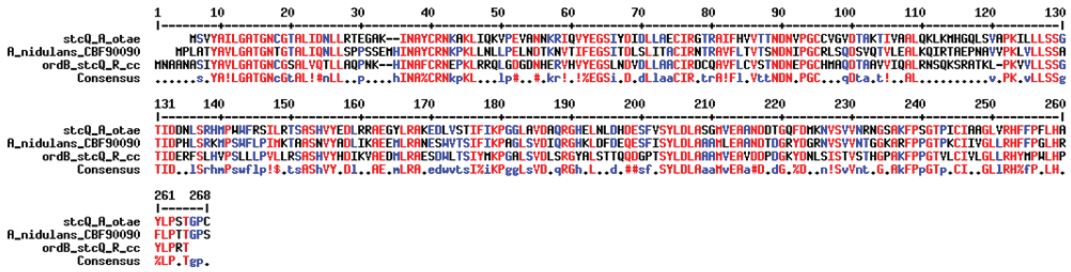

Figure 5.10
Alignment of ordB/ stcQ ORF and corresponding similar stcQ protein in *A. otae* and *Aspergillus nidulans.*

The key gene found to be adjacent to the previous component in the upstream sequence of the metabolic cluster was *aflJ*. It showed significant amino acid identity to the *D. septosporum* toxin biosynthesis regulatory- like protein (EME38896.1) at 36 % (Figure 5.11) and *aflJ* regulatory protein in *A. nidulans* (CBF90109.1) at 33 %. This protein belongs to o-methyltransferase superfamily proteins and primary

function of these enzymes is utilising S-adenosyl methionine. The examples of genes encoding these enzymes are the regulatory proteins in aflatoxin and sterigmatocystin-producing *Aspergillus* species (now called AflS in *A. parasiticus*).

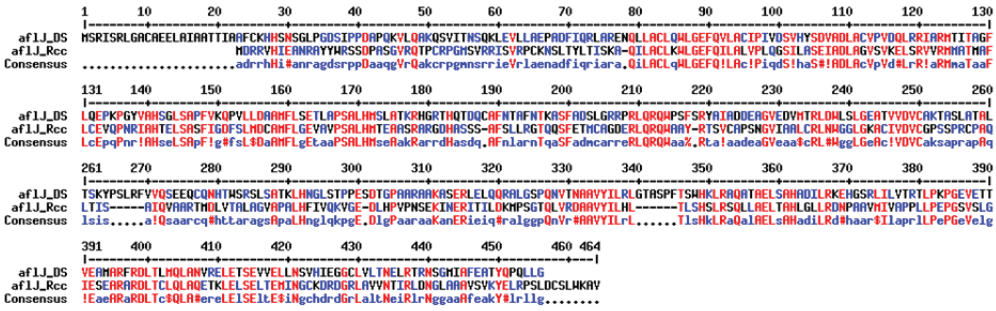

Figure 5.11
Alignment of aflJ/ aflS ORF and orthologous protein in *D. septosporum.*

Adjacent to *aflJ* gene was another key component of toxin biosynthesis cluster, a putative versicolorin reductase gene, *ver-1* (previously called *aflM*). The enzymes encoded by these genes belong to NADB Rossman superfamily with a characteristic domain fabG, 3-ketoacyl-(acyl-carrier-protein) reductase. It showed 63 % amino acid identity to *Sclerotinia borealis* versicolorin reductase (ESZ98970.1) and 69 % to 17-beta-hydroxysteroid dehydrogenase in *A. otae* (XP_002844741.1), but also shared 58 % identity with *ver-1* gene in *A. flavus* (AAS90076.1) (Figure 5.12).

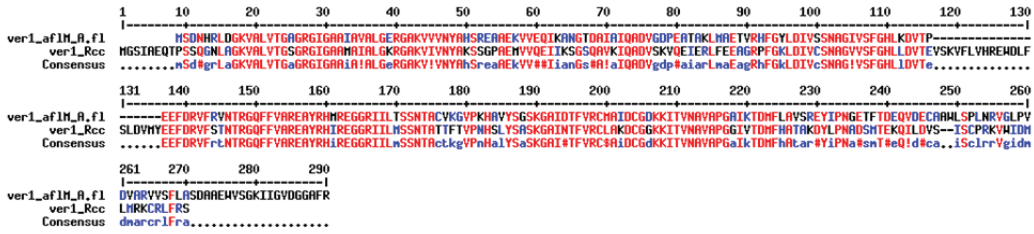

Figure 5.12
Alignment of ver-1/ aflM ORF and corresponding ver-1 protein in *A. flavus.*

The next potential gene present in the metabolic cluster was identified to be a putative protein encoding gene called aflCa/ hypC. It contains a conserved domain DUF1772 and produces significant alignments with *D. septosporum* arthrone oxidase-like protein (EME39098.1) and norarthrone monooxygenase in *A .flavus* (XP_002379950.1) with 44 at 41 % similarity, respectively.

An important key component of known toxin biosynthesis clusters in fungi, called *aflR*, was found adjacent to the putative *R. collo-cygni* gene *aflCa/ hypC*. It showed significant amino acid identity to several known transcription factors in diverse ascomycetes. For instance, it shared 28 % identity to *Neosarthoria fischeri* aflatoxin regulatory protein (XP_001266596.1) (Figure 5.13), 27 % to *A. parasiticus* aflR (AAM02998.1), 24 percent to *D. septosporum* AflR-like (EME38895.1) and 27 % to *Cercospora nicotianae* cercosporin biosynthesis regulatory transcription factor *cbr1* (ABK64185.1). All these examples have been described and functionally analysed showing that these genes encode the toxin biosynthesis regulatory protein. They contain a conserved GAL4-like Zn2Cys6 binuclear cluster DNA-binding domain found in transcription regulators. This domain consists of two helices organised around a Zn(2)Cys(6 ) motif.

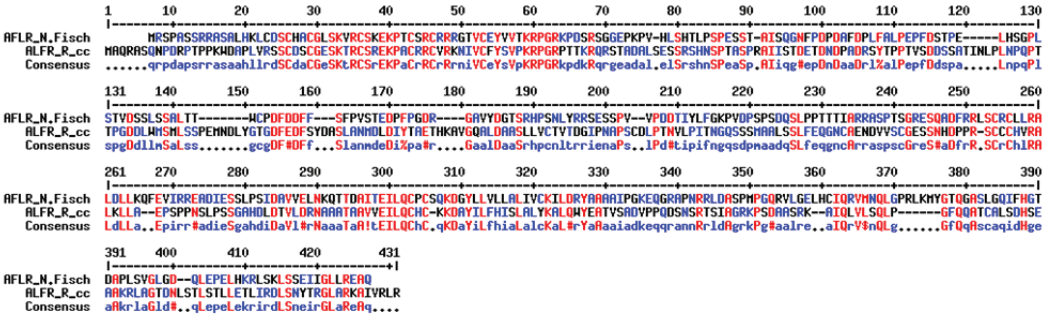


Figure 5.13
Alignment of aflR ORF and corresponding aflR protein in *N. fischeri.*

The next genetic component of the metabolic island was a predicted gene called Hyp5 that was similar to short chain dehydrogenase/ reductase in *Aspergillus* sp. MF297-2 (ADM34148.1) (Figure 5.14). *Hyp5* contain NADB Rossmann superfamily / fabG multidomain that is also present in *ver-1* (*aflM*) gene, described earlier.

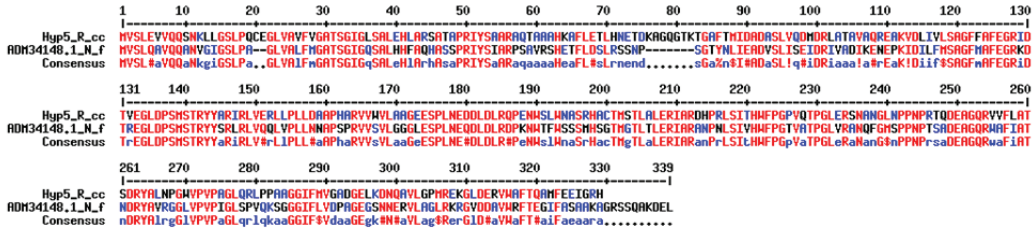

Figure 5.14
Alignment of Hyp5 ORF and corresponding highest blast hit in *Aspergillus* sp. MF297-2.

Another closely related neighbouring gene (*Hyp6*) was identified as a putative short chain dehydrogenase with NAD(P) chemical binding domain with a characteristic Rossmann-fold protein superfamily. A specific conserved domain similar to WcaG multidomain was identified, suggesting that this protein belongs to nucleoside-diphosphate-sugar epimerases which have functions in cell envelope biogenesis, outer membrane / carbohydrate transport and metabolism. This putative gene produces significant alignment with *N. fischeri* hypothetical protein XP_001265817.1 (Figure 5.15) which is 52 % identical, however the ORF in *R. collo-cygni* genome data is in fact much shorter than its ortholog in *N. fischeri*.

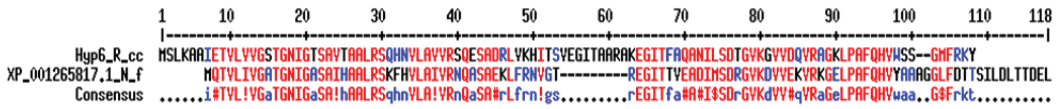


Figure 5.15
Partial alignment of Hyp6 ORF and its ortholog in *N. fischeri.*

Another potentially important gene in the cluster was identified as the Major Facilitator Superfamily (MFS) transporter. It produces significant protein alignment with *N. fischeri* MFS transporter (XP_001265322.1) at 60 % amino acid identity (Figure 5.16), and MFS aflatoxin efflux pump in *Aspergillus flavus* (XP_002377524.1) at 39 % identity. MFS is a large and diverse group of secondary transporters that includes uniporters, symporters, and antiporters.

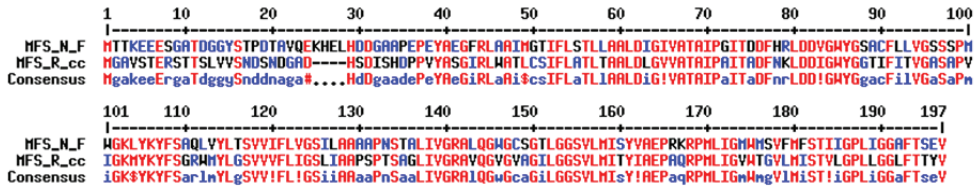


Figure 5.16
Partial alignment of putative MFS transporter ORF and its ortholog in *N. fischeri.*

A cytochrome P450 was identified within the cluster as a potentially important protein, known to be a component of aflatoxin, sterigmatocystin and dothistromin biosynthesis pathways. Blast P analysis revealed a high similarity to *Myceliophthora thermophila* (XP_003663607.1) at 43 % and also to *Colletotrichum gloeosporioides* (EQB43691.1) at 31 % (Figure 5.17). It is also important to highlight the similarity to o-methylsterigmatocystin oxidoreductase in *Fusarium fujikuroi* (CCT72382.1) at 30 %.

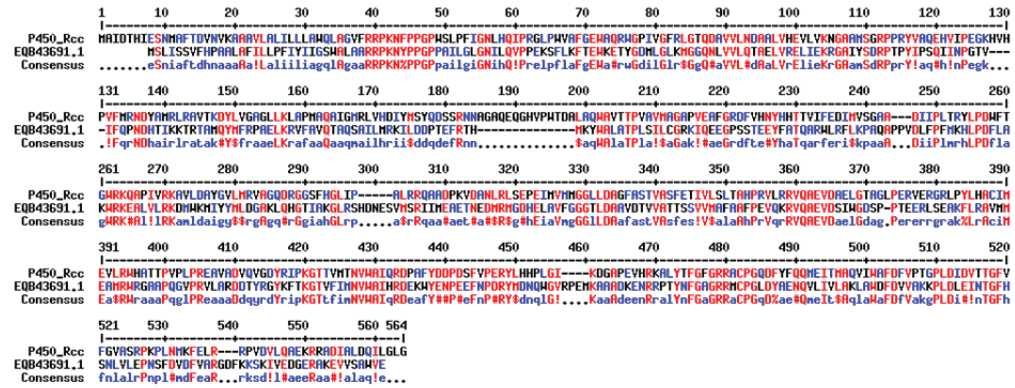

Figure 5.17
Alignment of cytochrome P450 ORF and its ortholog in *C. gloeosporioides.*

Interestingly, a second gene encoding for another type of transporter proteins, i.e. ABC transporter, was found located in the vicinity of aflatoxin biosynthesis gene orthologs described earlier. Blast P results revealed several domains within the ORF such as ABC_membrane2, ABCD peroxisomal ALDP/ ABC ATPase Superfamily and Multidomain 3a01203. Translated sequence showed significant amino acid identity to ABC transporters characterised in closely related fungal plant pathogens *Z. tritici* (XP_003857231.1) (Figure 5.18), *M. fijiensis* (EME87750.1) and *D. septosporum* (EME49183.1) at 87, 84 and 83 %, respectively.

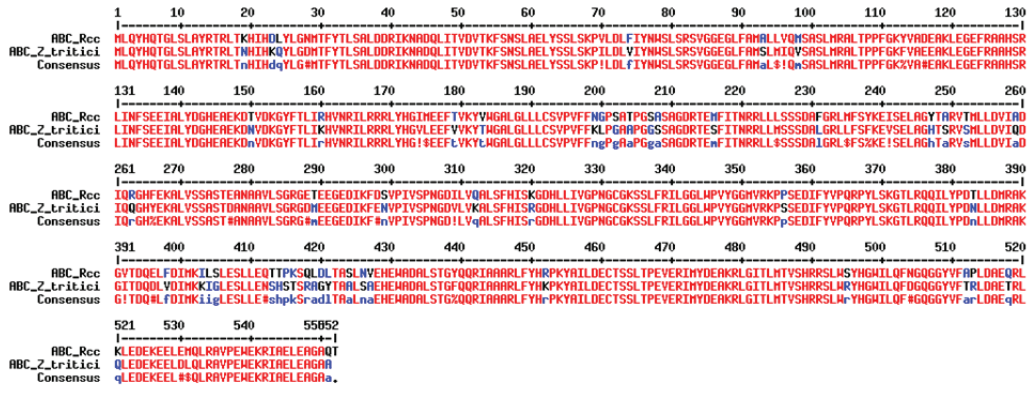

Figure 5.18
Partial alignment of putative ABC transporter ORF and its ortholog in *Z. tritici.*

The organisation of metabolic gene cluster found in *R. collo-cygni* genome with the key members of the cluster described above is presented in Table 5.1.

Table 5.1

List of ORFs within the cluster with the corresponding amino acid identity and the putative function if known.

| Gene name | Homologous Genes (NCBI GenBank accession numbers) | | Amino acid identity [%] | Predicted conserved domains/ putative function |
|---|---|---|---|---|
| **Hyp1** | *D. septosporum* | EME49365.1 | 35 | Multidomain protein COG2433/ unknown |
| **Hyp2** | *D. septosporum*<br>*M. fijiensis*<br>*Z. tritici* | EME49364.1<br>EME88037.1<br>XP003856253.1 | 40<br>39<br>45 | unknown |
| **Hyp3/ aflB1** | *D. septosporum*<br>*M. fijiensis*<br>*Z. tritici*<br>*T. deformans* | EME49363.1<br>EME88036.1<br>XP003856254.1<br>CCG82151.1 | 65<br>68<br>68<br>37 | Aldo/ keto reductase superfamily<br>Aflatoxin B1-like aldehyde reductase |
| **Hyp4** | *D. septosporum* | EME49362.1 | 41 | unknown |
| **stcQ/ ordB** | *A. nidulans*<br>*A. fumigatus*<br>*A. otae* | CBF90090.1<br>XP_001266598.1<br>XP_002844732.1 | 51<br>51<br>49 | stcQ/ ordB protein<br>ST/ AF biosynthesis |
| **AflJ** | *D. septosporum*<br>*A.fumigatus*<br>*E. lata* | EME38896.1<br>XP_751378.1<br>EMR67229.1 | 44<br>37<br>45 | o-methyltransferase family<br>AflJ AF/ ST-like regulatory protein |
| **Ver-1/ aflM** | *A. otae*<br>*A. flavus*<br>*D. septosporum*<br>*M. pini* | XP_002844741.1<br>BAA34393.1<br>EME39778.1<br>AAL87045.1 | 82<br>63<br>58<br>62 | NAD(P) binding<br>17-beta-hydroxysteroid dehydrogenase<br>Versicolorin reductase<br>Elsinochrome reductase-like protein/ ketoreductase |
| **aflCa/ hypC** | *D. septosporum*<br>*A. flavus* | EME39098.1<br>XP_002379950.1 | 44<br>41 | Domain DUF1772<br>arthrone oxidase-like protein<br>norarthrone monooxygenase<br>with |
| **aflR** | *N. fischeri*<br>*D. septosporum*<br>*C. nicotianae* | XP_001266596.1<br>EME38895.1<br>ABK64185.1 | 28<br>24<br>27 | aflR toxin regulatory transcription factor protein |
| **Hyp5** | *Aspergillus* sp. MF297-2 | ADM34148.1 | 65 | fabG multidomain<br>short chain dehydrogenase/ reductase<br>NADB Rossmann superfamily |
| **Hyp6** | *N. fischeri* | XP_001265817.1 | 52 | NAD(P) binding<br>short chain dehydrogenase Rossmann<br>WcaG multidomain nucleoside-diphosphate-sugar epimerase |
| **MFS** | *N. fischeri*<br>*A. flavus* | XP_001265322.1<br>XP_002377524.1 | 60<br>39 | Major Facilitator Superfamily (MFS) transporter<br>Toxin efflux pump |
| **P450** | *M.thermophila*<br>*C.gloeosporioides*<br>*F. fujikuroi* | XP_003663607.1<br>EQB43691.1<br>CCT72382.1 | 43<br>31<br>30 | Cytochrome P450 oxidase<br>o-methylsterigmatocystin oxidoreductase |
| **ABC** | *Z. tritici*<br>*M. fijiensis*<br>*D. septosporum* | XP_003857231.1<br>EME87750.1<br>EME49183.1 | 87<br>84<br>83 | ABC_membrane2,<br>ABCD peroxisomal ALDP/ ABC<br>ATPase, Multidomain 3a01203 |

## 5.4. Discussion

Chapter 5 investigates the potential biological processes that may be responsible for rubellin biosynthesis at cellular level and the role of this toxin in symptom development by using autofluorescence phenomenon. The structure of putative molecular machinery involved in rubellin biosynthesis was addressed by using bioinformatics approaches and the complete *R. collo-cygni* genome sequence. A gene cluster encompassing several components of other known secondary metabolite biosynthesis pathways, such as that of dothistromin and aflatoxin, was found and putative protein function of the genes is hypothesised.

An important aspect of research on RLS has been the discovery and biochemical studies of polyketide toxins, produced by the fungus. These studies identified a number of very similar compounds, present in culture filtrates, called rubellins (Heiser *et al.,* 2003, 2004). These authors presented some preliminary evidence suggesting the role of these toxins in the necrotrophic phase of RLS development. Furthermore, Miethbauer *et al.* (2006) showed the presence of these coloured compounds within fungal hyphae. These findings were used to develop a method of direct observation of rubellin *in planta* based on the properties of aromatic rings that are the backbone of the biochemical structure of rubellins as predicted by Miethbauer *et al.,* 2006). Determination of the autofluorescence spectra by applying a lambda scan using CLSM (Figure 5.3 a) confirmed previous physiochemical predictions of rubellin molecules (Miethbauer *et al.*, 2006). This finding allowed the development of a new toxin detection and visualisation method *in planta.* Analysis of infection development from the angle of rubellin production by the fungus and its release into plant tissue showed that toxin could have a role in symptom development as its presence in plant tissues

co-localised with the collapsed epidermis and mesophyll cells, and subsequent rapid symptom development. Our findings demonstrated that rubellin production occurs late in the infection cycle as was usually observed from 3 - 4 weeks pi.

The production of vacuole- like vesicles was a distinct feature of intercellur hyphae, which initially was observed to be unusually highly vacuolated. Dothistromin production by the red band needle blight pathogen of pine, *D. septosporum* has also been shown to be synthesised and stored by this fungus in vacuole-like organelles (Bradshaw *et al.*, 2009). Such a mechanism could facilitate detoxification of cytoplasm thus reducing potential self-toxicity of rubellin to the cells. Therefore, both dothistromin and rubellin produced by these closely related fungi share biochemical similarities, but also aspects of cell biology as demonstrated by this study. Our observations of the location and mode of putative discharge of the rubellin into the lumen of intercellular space in the mesophyll layer suggest that the transport of rubellin into vacuole-like vesicles which is then unloaded into the intercellular spaces in the mesophyll tissue, most likely via the process of exocytosis.

Research on dothistromin has also concentrated on the genetics behind its synthesis. Bradshaw *et al.* (2003) reported the existence of gene orthologs that were determined to be involved in aflatoxin production by *Aspergillus* spp. The authors demonstrated that the dothistromin biosynthesis involves genes arranged in a metabolic cluster. Following these findings, we tested the hypothesis that rubellin biosynthesis could also be governed by similar gene cluster as those found in *D. septosporum* and *Aspergillus* spp. Our data confirms the existence of gene orthologs in the recently sequenced *R. collo-cygni* genome (SRUC, unpublished) and suggests the putative molecular machinery that could be involved rubellin.

Although function of the first two predicted proteins, i.e. *Hyp1*, *Hyp2* was not characterised due to the unknown functions for the orthologs in the related fungal species, it is likely that the encode proteins that could be involved in rubellin synthesis as suggested by their presence within the metabolic cluster. Despite these two genes, function of the majority of the putative rubellin synthesis proteins that comprised the cluster has been identified.

For example, Hyp3/ aflB1 gene was predicted to encode an aldo/ ketoreductase. AKRs are a superfamily of soluble NAD(P)(H) oxidoreductases whose purpose is to reduce aldehydes and ketones to primary and secondary alcohols. Members of this family have very distinct functions that comprise aflatoxin aldehyde reductases, aldose reductases, hydroxysteroid dehydrogenases, steroid 5beta-reductases and potassium channel beta-subunits among others (Marchler-Bauer *et al.,* 2009, 2011; Marchler-Bauer & Bryant, 2004).

Another gene, ver-1 with the predicted function of versicolorin reductase could be a key component of rubellin biosynthesis pathway. These conserved THN-reductase-like domains called tetrahydroxynaphthalene/ trihydroxynaphthalene reductase-like, called classical SDRs are typical members of the SDR family containing the canonical glycine rich NAD(P)-binding site and active site tetrad, and function in fungal melanin biosynthesis. SDRs are a functionally diverse family of oxidoreductases that have a single domain with a structurally conserved Rossmann fold (alpha/beta folding pattern with a central beta-sheet), an NAD(P)(H)-binding region, and a structurally diverse C-terminal region. Classical SDRs are typically about 250 amino acids long, while extended SDRs consist of approximately 350 amino acids. Sequence identity between different SDR enzymes are typically in the

15-30 % range, however the enzymes share the Rossmann fold NAD-binding motif and characteristic NAD-binding and catalytic sequence patterns. Complex (multidomain) SDRs such as ketoreductase domains of fatty acid synthase have a GGXGXXG NAD(P)-binding motif and an altered active site motif (YXXXN). Fungal type ketoacyl reductases have a TGXXXGX(1-2)G NAD(P)-binding motif. Some atypical SDRs have lost catalytic activity and/or have an unusual NAD(P)-binding motif and missing or unusual active site residues. Reactions catalysed within the SDR family include isomerization, decarboxylation, epimerisation and oxidoreduction amongst other functions (Marchler-Bauer *et al.,* 2009, 2011; Marchler-Bauer & Bryant, 2004).

Another example of the predicted protein found in the cluster was Cytochrome P450s encoding gene. P450s are haem-thiolate proteins involved in the oxidative degradation of various compounds. They are particularly well known for their role in the degradation of environmental toxins and mutagens. They can be divided into 4 classes, according to the method by which electrons from NAD(P)H are delivered to the catalytic site. Sequence conservation is relatively low within the family - there are only 3 absolutely conserved residues - but their general topography and structural fold are highly conserved. While prokaryotic P450s are soluble proteins, most eukaryotic P450s are associated with microsomal membranes. Their general enzymatic function is to catalyse oxidation of non-activated hydrocarbons at physiological temperatures. Cytochrome P450 protein was an essential component in other known toxin biosynthesis gene clusters such as in AF (*CypX* gene) in *Aspergillus* spp. (Bhatnagar *et al.,* 2003) and DS biosynthesis (deWit *et al.,* 2012).

Function of another gene, *Hyp6* has been predicted to be a short chain dehydrogenase however no orthologous sequence in known toxin synthesis genes was identified by Blast analysis. Short chain dehydrogenases play diverse roles in secondary metabolites biosynthesis and transport (Marchler-Bauer *et al.,* 2009, 2011; Marchler-Bauer & Bryant, 2004) which suggested that this gene could have a function in rubellin synthesis.

Interestingly, two different types of transporter protein were found within *R. collo-cygni* cluster. These were MFS and ABC membrane transporters and had also been identified within AF and DS gene clusters. MFS transporters facilitate the transport across cytoplasmic or internal membranes of a variety of substrates including ions, sugar phosphates, drugs, neurotransmitters, nucleosides, amino acids, and peptides. They do so using the electrochemical potential of the transported substrates. Uniporters transport a single substrate, while symporters and antiporters transport two substrates in the same or in opposite directions, respectively, across membranes. (Marchler-Bauer *et al.,* 2009, 2011; Marchler-Bauer & Bryant, 2004). It has been reported that *dotC* that encode MFS is involved in dothistromin transport in *D. septosporum* (Bradshaw *et al.,* 2009), that further suggests the putative function of the ortholog in *R. collo-cygni*.

Second putative ABC transporter protein encoding gene was also identified in the cluster. In contradiction with *D. septosporum* in which *dotC* encoding MFS transporter is thought to play a function is DS transport (Bradshaw *et al.,* 2009), in *Asperigillus* spp., it has been suggested that *aflT* gene encoding ABC transporter protein which may be necessary for aflatoxin efflux from the cells (Yu *et al.* 1998; Yabe *et al.* 1999). Generally, peroxisomal ATP-binding cassette transporter (Pat) is

involved in the import of very long-chain fatty acids (VLCFA) into the peroxisome. The peroxisomal membrane forms a permeability barrier for a wide variety of metabolites required for and formed during fatty acid beta-oxidation. To communicate with the cytoplasm and mitochondria, peroxisomes need dedicated proteins to transport such hydrophilic molecules across their membranes (Marchler-Bauer *et al.,* 2009, 2011; Marchler-Bauer & Bryant, 2004). It would be interesting to establish the function of both genes present in putative rubellin cluster which could also have implication in further general understanding of DS and AF toxin biosynthesis cluster.

Two putative regulatory genes have also been found within the cluster. These were *aflJ* and *aflR* homologues. It is strongly suggested to include these genes for functional analysis using gene knock out approach, similar to this undertaken in *D. septosporum* (Chettri *et al.,* 2012). The study demonstrated that levels of expression of the widely dispersed genes in *D. septosporum* are not correlated with gene location with respect to their distance from a telomere, but that the expression is regulated by *aflR*. The production of DS by *D. septosporum* mutant in which *aflR* gene was knocked out was drastically reduced, but still detectable. This is in contrast to orthologous aflR mutants in *Aspergillus* species that lack any AF or ST production (Payne *et al.,* 1993; Price *et al.,* 2006).

Direct imaging of rubellin during the infection process is an important aspect of RLS research. Using rubellin autofluorescence proved useful to expand our knowledge of cell biological processes that may be involved in rubellin production and discharge. Thirugnanasambandam *et al.* (2011) reported the method for the genetic transformation of *R. collo-cygni* with fluorescent protein markers. This method

combined with the results from the study on putative rubellin cluster could be used to fluorescently tag the selected candidate genes, especially the transporter proteins found within the cluster. This approach has been previously used in *D. septosporum* to visualise the process of biosynthesis and transport of DS in the cells (Bradshaw *et al.,* 2009).

The recently sequenced *R. collo-cygni* genome (SRUC, unpublished) has provided an excellent tool to study fundamental processes such as those described in this chapter and should now be used more effectively to develop new methods for RLS management. This work proposes a genetic framework for better understanding of the metabolic pathway and regulation of rubellin biosynthesis. The structure of the molecular machinery that may be involved in rubellin production has now been characterised. Future studies should therefore involve the analysis of gene expression to identify candidates for functional studies by generating knock out mutants to observe if rubellin production is impaired or lost. This fundamental understanding could have major implications for the future development of the new breeding programmes that could incorporate screening for rubellin tolerant cultivars.

# Chapter 6

# General discussion

# 6. General discussion

Fungal plant pathogens pose a serious economic threat to agriculture at any stage of crop production, i.e. during crop establishment in the field or by impairing the harvested yield (Agrios, 2005). Due to their ability to produce a large number of spores, fungi can be easily distributed by air or water and thus can cause substantial levels of disease which often contributes to the reduction of crop yield and subsequent economic loss. An important aspect of the negative impact of some plant pathogenic fungi is mycotoxin production. One of the most prolific cases is the production of toxins by *Fusarium* spp. that can make the resulting harvest unsuitable for food, feed or malting (Skadsen & Hohn, 2004). It is therefore of great importance to study the biology of fungal plant pathogens to develop strategies that will help reduce crop losses and sustainably produce food for an increasing human population in ever more demanding environment, due to climate variability.

Barley (*Hordeum vulgare* L.) is one of the world's oldest and most cultivated cereal crops (Nevo, 1992; FAO, 2007) and is therefore a frequent target for constantly evolving fungal pathogens. In addition to the existing array of economically important fungal barley diseases worldwide, such as mildew, net blotch, leaf scald and brown rust, a new threat called Ramularia leaf spot (RLS) has appeared. It is now considered as a major disease and has been added to the UK cultivar resistance scoring (HGCA, 2013). Although first identified in the late 1890s, relatively little is known about the biology and life cycle of the causal agent, the filamentous fungus *R. collo-cygni.* In order to develop an effective and durable strategy of RLS

management, a more complete understanding of pathogen's fundamental biology is required.

The development of the molecular methods of detection (Havis *et al.,* 2006a, Taylor *et al.* 2010) has proven useful for initial studies on the fundamental biology and life cycle of *R. collo-cygni*. These techniques allowed the tracking and quantification of fungal build up during disease development and also during the asymptomatic phase. However, more direct visual detection of the fungus to determine its exact location both internally and externally on the host plant could only be possible by the application of microscopy. Two recent studies have used microscopy to study *R. collo-cygni* infection and life cycle. The examination of naturally infected leaves using scanning electron microscopy (SEM) has provided the initial insight into *R. collo-cygni* development on barley (Stabentheiner *et al*., 2009). However, the most important breakthrough was the successful stable genetic transformation of the fungus with fluorescent marker tags (Thirugnanasambandam *et al.,* 2011).

Studies on *R. collo-cygni* are challenging due to its sparse or even complete lack of sporulation *in vitro* and therefore unreliable symptom expression following inoculation on plants as suggested earlier by Thirugnanasambandam *et al.* (2011). This study proved that using *R. collo-cygni* mycelial fragments to infect barley plants was sufficient to initiate infection and observe the typical RLS symptom expression thereby confirming an earlier report by Makepeace *et al.* (2008) which showed that hyphal fragments are a valid substitute for spores in infection assays.

*R. collo-cygni* infection biology and life cycle has been investigated in this project in much greater detail than previously attempted. The detached leaf assay described by

Thirugnasambandam *et al.* (2011) has proved a very useful method to contain barley tissue infected by the genetically modified pathogen isolates. It is suggested that in any future detailed analysis of the behaviour of the fungus, the detached leaf approach should be the method of choice as spray inoculation of the leaf (Makepeace *et al.,* 2008) will inevitably add a large amount of noise, in the form of a mycelial mat present on the leaf surface. Behaviour of the fungus after using this form of inoculation could therefore be misinterpreted.

Our study largely supports the previous observations of *R. collo-cygni* asymptomatic infection. It confirms the rapid formation of a mycelial network on the surface of the leaf and the entry into leaf tissue exclusively through the stomatal pore. Such mode of invasion may be less likely to trigger defence reactions caused by the damage of host tissues during direct penetration through cuticle. However, it is important to remember that host plant responds on many different levels that are not always visually apparent. For instance, the immune response could be supressed at molecular level stopping the development of histological symptoms of resistance on plant tissue (Jones & Dangl, 2006). The observation that the host epidermal cells remained intact during the early stages of infection is consistent with this hypothesis. It would therefore be essential to examine the expression pattern during early stages of infection to determine the molecular machinery likely to be involved in avoiding the recognition of the fungus entering the stomatal pore.

In contrast with both previous microscopic analysis which concluded that no specialised penetration structures were formed by *R. collo-cygni* during penetration of stomatal pores (Stabentheiner *et al*., 2009; Thirugnanasambandam *et al.,* 2011), this study reports and describes for the first time the existence of a distinct structure

in the form of infection peg that facilitates the penetration of a stoma. Our results clearly show that it was frequently but not exclusively produced by the fungus to enable penetration of closed stomata. Since a morphologically similar structure called stomatopodium has been reported previously in the closely related fungal species, *Pseudocercosporella fijiensis* (Balint-Kurti *et al.,* 2001), it is reasonable to propose the same nomenclature in *R. collo-cygni*. Stomatopodia that entered the substomatal cavities develop into thick hyphae, reported earlier by Thirugnanasambandam *et al.* (2011). Perhaps the term 'conidiogenous aggregates' would be a more appropriate for these structures as it has been shown in the current study that they comprise a group of large conidiophore- and conidia-producing cells.

The development of an apparently organised network of epiphytic hyphae during asymptomatic infection appeared defined by utilising the epidermal cell junctions that fungus uses to colonise the leaf surface. The results also confirm previous observation that the invasive hyphae exhibit directional growth towards stomata (Stabentheiner *et al.,* 2009). It is yet to be determined experimentally what could involve the apparent ability to detect stomata by the fungus. Although it was not the subject of this project, several possible mechanisms that could govern such behaviour are hypothesised. Firstly, the topography of the leaf surface and cell layout clearly explored by *R. collo-cygni* hyphae during compatible interactions with the host could act as morphological clues to identify the presence of stomata in the near vicinity. This hypothesis is supported by the interaction of *R. collo-cygni* with non-host dicot plant, *L. japonicus*, in which the structured organisation of epiphytic hyphae is lost as described in this study. Secondly, it could also be that attraction of the fungus to stomata could be facilitated by hydrotropism and gas exchange through stomata as is the case for the

related plant pathogenic fungus *C. beticola* on sugar beet (Rathaiah, 1977). Interestingly, in *C. zeae-maydis* that is able to detect very subtle changes in the microclimate and humidity that exist around a stoma, regulation of stomatal tropism and infection has also been linked to the responses to photoperiod of both pathogen and host (Kim *et al.,* 2011). It is also possible that the combination of these processes could explain the fungal behaviour during the initial colonisation of the leaf surface and subsequent infection. It would certainly be an interesting topic to verify these hypotheses as a part of any research on *R. collo-cygni* biology as it could have some important implications in the search for potential sources of resistance to RLS.

An important aim of this project was to study *R. collo-cygni* biology throughout the whole disease cycle encompassing the symptomless and symptomatic phase to establish a basic understanding of the transition of the fungal behaviour and symptom development. Our results showed the dramatic change in the nature and severity of colonisation apparently only restricted to substomatal cavities. Initially, the conidiophores rising from stomatal pores in some cases caused local necroses of the tissue surrounding stomata. This could be possibly due to the mechanical damage of guard cells during conidiophore emergence. However, any further development of macroscopic size lesions that could be correlated with the substomatal aggregates and the first sporulation was not observed. Actually, in the majority of cases no damage to the stomata was detected. The change in the aggressiveness of *R. collo-cygni* was observed at three to four weeks post-inoculation. Prior to RLS symptom development, the fungal growth radiated from conidiogenous aggregates into mesophyll tissue surrounding the cavities. The swollen, heavily branched hyphae that comprised the local networks around each stoma merged producing an organised, large endophytic

network that explored intercellular space between the cells. Although heavily colonised at this stage, the mesophyll layer still appeared asymptomatic. Furthermore, this endophytic network shared similar function to the fungal aggregates in substomatal cavities and was responsible for the prolific production of spores. It has been observed that 7 days after colonisation of the mesophyll, conidiogenous aggregates that developed at the edge of the infection did not immediately produce spores. In contrast, they began the establishment of intercellular network. This endophytic mycelium then gave rise to mass sporulation. The majority of conidiophores erupted directly through the epidermis and furthermore, they appeared to rupture only through the cell junctions. This caused a subsequent massive collapse of the plant tissue and necrosis. Such behaviour could explain why macroscopic symptoms on infected leaves do not appear earlier.

It has been speculated that *R. collo-cygni* is an opportunistic saprophyte that is able to recognise and respond to the switch from vegetative to reproductive phase in the host by becoming a necrotrophic pathogen (Newton *et al.,* 2010). Walters *et al*. (2008) also stated that sporulation usually occurs from the necrotic lesions. This study shows that the fungus can actually sporulate within stomata during early stages of the infection cycle without causing any significant damage, thus remaining asymptomatic. This confirms the observations by Thirugnanasambandam *et al.* (2011) and signifies that pathogen inoculum may increase and spread within a barley crop during the growing season, but without visible symptoms, until the plants move into the reproductive phase (Havis *et al.,* 2014). It has previously been suggested that *R. collo-cygni* could detect the change of plant growth from vegetative to reproductive and react by the increase in aggressiveness and subsequently cause RLS symptoms (Schützendubel *et*

*al.,* 2008). To pinpoint the exact genetic mechanism employed by the pathogen to detect the plant morphogenetic stages, it would now be necessary to study the changes in the plant gene expression pattern during the shift from vegetative to reproductive phase that could also be correlated with the changes in fungal gene expression.

The results from the current study suggest that the process of RLS symptom development could be slightly different than previously thought. The typical necrotic symptoms are not caused by the damage of conidiophores that disrupt the stomatal functionality but by the combination of both, stomatal sporulation and possibly even more importantly, the extensive mesophyll infection and subsequent eruption of conidiophores directly through epidermis. Furthermore, the observation of the mesophyll colonising hyphae that did not penetrate vascular tissue as if they encountered a barrier could be directly linked to the appearance of typical RLS lesions. The extensive intercellular network remained restricted between the main vascular bundles and this could explain the characteristic rectangular shape of symptoms that appear to be sharply delineated by the leaf veins (Walters *et al*., 2008).

It is known that *R. collo-cygni* on barley can remain asymptomatic throughout the entire plant life cycle (Nyman *et al.,* 2009). In these experiments, it was observed that on many detached leaf sections typical RLS lesion did not develop. Although the detached leaf assay is a useful method for studying early stages of infection, in many cases it was not possible to maintain quality leaf sections for longer than three to four weeks without compromising the results due to natural degradation of leaf tissue, not necessarily associated with fungal infection. In order to study a prolonged time series, the whole plant assay was developed, based on drop inoculation method. This allowed testing a range of barley cultivars with different HGCA recommended list resistance

scores against *R. collo-cygni*. The results showed that the fungus was able to develop on all tested cultivars. However, there was some variation in speed and pattern of infection, which in three out of the four varieties tested, correlated with official HGCA resistance ratings. The number of stomatal aggregates was considered as an indicator of successful infections and appeared similar for all observed asymptomatic interactions. However, statistical analysis was not attempted in this study. It is therefore suggested that further experiments be carried out in order to verify the differences between susceptibility of cultivars using analytical approaches. Currently, the recommended list of cultivars published by the Home Grown Cereals Authority (HGCA; www.hgca.com) is based on the percentage of visible RLS symptoms. It is a known fact that *R. collo-cygni* could be easily confused with other diseases and abiotic physiological spotting complex (Walters *et al.,* 2008) making the scoring difficult and could even lead to significant errors. The findings also highlight the necessity to develop a more reliable disease scoring system. If a cultivar that is currently considered as resistant to *R. collo-cygni* still allows completion of the pathogen's lifecycle, then the term resistance is not entirely correct. Perhaps the term disease tolerance (or symptom tolerance) is actually more appropriate in the case of RLS*,* as is the case for another major barley pathogen with asymptomatic phase, *Rhynchosporium commune* (Thirugnanasambandam A., PhD Thesis, University of Dundee, 2011). The tolerant cultivars enable survival of the pathogen, that perhaps still causes some loss of nutrients, but its influence on the grain quality and quantity is significantly reduced, and negligible.

In this study, for the first time since its development (Thirugnanasambandam *et al.,* 2011), DsRed fluorescent protein expressing *R. collo-cygni* strain (Rcc-ST-DsRed)

was also was employed in the experiments using *in planta* assays. Our results showed that although the mode of the behaviour was essentially the same as that observed in barley infected by Rcc-8B9-GFP isolate, significant differences in the speed of infection were observed, depending on the cultivar. This suggested that the level of aggressiveness of *R. collo-cygni* may vary across a range of isolates and some will be more pathogenically fit than others.

*R. collo-cygni* infection of several monocot species, including many cereal crops and perennial grasses has been reported (Huss, 2002; Frei, 2002; Cromey *et al.,* 2002; Salamati & Reitan, 2006). This suggested a potentially very important role of alternate hosts as a primary inoculum source of RLS that could facilitate the spread of the pathogen between growing seasons. Despite these reports the infection of putative hosts has gained a very little attention to date. Therefore, in order to develop an understanding of the early phases of RLS, a selection of plants such as wheat (*Triticum aestivum*), Italian ryegrass (*Lolium multiflorum*), cock's foot (*Dactylis glomerata*) and also the model dicot species, *Lotus japonicus* was chosen for investigation using the isolate Rcc-8B9-GFP.

Huss (2002) reported that wheat is a compatible host for *R. collo-cygni,* however only limited evidence was provided to support this claim. As one of the most important crops in the world, it was very important to verify the previous findings. The results clearly showed that *R. collo-cygni* could indeed infect and colonise winter wheat. This confirms the presence of the fungus on this crop and indicates that its isolation was not coincidental. Wheat could therefore be a viable source of inoculum for its primary host, barley. Further studies should be attempted in order to determine if RLS could also develop on wheat, which may lead to yield losses.

Similarly, *R. collo-cygni* colonisation of Italian ryegrass occurred at a previously observed rate. However, the pathogen appeared to develop the epiphytic network more rapidly compared to barley. Much faster development of substomatal aggregates and sporulation was noted. These findings suggest that *L. multiflorum* could be a major primary inoculum source for RLS. One possible explanation for more rapid development of infection is that ryegrass can actually be a more natural, perhaps a primary host. It could also be speculated that *R. collo-cygni* originated from perennial grasses and subsequently evolved to become the pathogen of the domesticated cultivated crops. Similar evolutionary adaptation and a host jump from native grasses to crops have previously been described for of the wheat pathogen *Z. tritici* (Stukenbrock *et al.,* 2007; 2012).

The inoculation experiments with *D. glomerata* showed that this grass species may not be a compatible host for *R. collo-cygni.* Although the initial behaviour of the pathogen up to 24 hours after inoculation was similar to previously described for barley, i.e. the fungus exhibited stomatal tropism and attempted to penetrate, no further development occurred. This suggested that mechanisms of incompatibility could act upon the pathogen attack on stomata. Perhaps at the time of penetration, the molecular interaction between *R. collo-cygni* and plant failed to establish stopping the pathogen from further development. On the other hand, since the growth of mycelium on the leaf surface appeared very chaotic at 24 - 48 hours after inoculation, this could also suggest that some morphological characteristics of the plant such as topography of the leaf surface in *D. glomerata* could facilitate this incompatibility. In a host species, the fungus uses grooves between epidermal cells therefore the epiphytic network appears very well organised. It would be interesting to study this potential mechanism of

incompatibility further. One possible approach would be to disturb the leaf surface to determine if cuticular features may play the role in stopping the fungus from colonisation. It would also be desirable to determine which genes may be involved in this incompatibility by gene expression analysis in *D. glomerata* at the point of expected penetration of stomata, i.e. 24-48 hours after inoculation.

The existence of potential alternate host species such as wheat and Italian ryegrass investigated here highlights the importance to verify the exact host range by challenging a much broader selection of perennial grasses and cereal crops with *R. collo-cygni*.

Many plant pathogenic and mutualistic fungi infect plant seed as means of dissemination and transmission between growing seasons (Neergard, 1977). Recent studies using PCR-based diagnostic methods for the rapid detection of *R. collo-cygni* have showed that the pathogen is also seed-borne (Havis *et al.,* 2006a, b; Frei, 2007; 2009; Matusinsky *et al.*, 2011; Havis *et al.,* 2014). During field experiments in 1999 and 2004 in Scotland, the pathogen was detected in harvested barley grain (Walters *et al.,* 2008). Subsequent qPCR tool (Taylor *et al.,* 2010) allowed the quantification of the fungal DNA in the seed. Interestingly, using these tools Nyman *et al. (*2009) observed that plants with no visible RLS symptoms often produced kernels infected by *R. collo-cygni*. Matusinsky *et al.* (2011) and Havis *et al.* (2014) verified the presence of DNA within seed. However the results were inconclusive. Although the results indicated that the majority of the *R. collo-cygni* DNA was present in the lemma, it was also detected in all types of seed tissue as well as in the water used for washing the plant material for subsequent dissection.

By using barley inoculatied with the Rcc-8B9-GFP isolate as well as field grown seed material naturally infected by the fungus, the nature of *R. collo-cygni* seed-borne stage has now been elucidated. The results showed the vertical mode of fungal transmission and addressed several important questions that could not be answered using DNA-based methods. The developed whole plant inoculation assay proved successful in generating seed infected with GFP strain. Interestingly, the seed collected from infected plants appeared normal in terms of their morphology which contradicted the notion that yield losses due to RLS is caused by a significant decrease of kernel size and quality (Greif, 2002; Harvey, 2002; Hjorshoj *et al.,* 2013). However, this could be due to the difficulty to replicate the exact environmental conditions that barley crops are exposed to in the field which could have an impact on RLS development. For instance, the presence of a large number of necrotic lesions on the leaves observed in the field causes a reduced photosynthetic area during grain filling. This in turn may cause yield loss rather than the fungal infection of kernels. Nevertheless, the lack of apparent necrotic symptoms on the grain obtained from the plant cultivated in controlled environment and the ability to germinate normally suggested that the seed health has been not compromised.

The dissected seeds revealed the presence of *R. collo-cygni* in the lemma and pericarp. This confirms results reported by Matusinsky *et al.* (2011) and Havis *et al.* (2014). Furthermore, colonising pericarp and more specifically the space between pericarp and aleurone layer of the endosperm enabled the fungus to infect the embryo following penetration of the scutellum. This demonstrated a potential systemic mode of transmission. We have also observed fungal hyphae within the endosperm on several occasions however it appeared rather sporadic and could have

been coincidental. Most recently, Havis *et al.* (2014) used nested PCR diagnostics (Havis *et al.,* 2006 a) and reported potential colonisation of endosperm, in contrast with findings of Matusinsky *et al.* (2011).

The infected barley seeds were germinated *in vitro* for subsequent observation using confocal microscopy. The infection progression in the developing coleoptile, leaf primordia and seedling was followed, revealing a strictly intercellular association of *R. collo-cygni* with barley. This is also consistent with the mode of the mesophyll layer infection in mature leaves. Despite the prolific and aggressive nature of fungal colonisation, no apparent damage or symptoms on plant tissue due to the infection was ever observed. At the first leaf stage, the infection remained endophytic showing the typical brick work- like growth pattern that concentrated near the midrib and appeared evenly distributed throughout the length of the leaf. All examined seeds germinated successfully as would be expected from healthy seed material and most importantly, all the fresh leaf material they produced remained asymptomatic.

The location of *R. collo-cygni* in naturally infected seed was also investigated using histological approaches, i.e. embedding, sectioning and staining procedure which confirmed the findings from inoculation experiments. Paraplast embedding method proved useful. However, it was very challenging to obtain good quality sections due to the hardness of seed material despite extended periods of infiltration. Perhaps the Spurr resin embedding method (Lord & Read, 2011) would be more suitable for any future detailed histological research on the seed-borne stage of *R. collo-cygni.*

An important feature of infection of barley by *R. collo-cygni* has been identified in this project, i.e. the endophytic colonisation of the intercellular space, a unique

habitat within plant tissue. This behaviour links the mode of seed infection and transmission into seedlings and subsequent long asymptomatic phase and describes the asexual life cycle of the fungus in its entirety. The endophytic nature of *R. collo-cygni* association with barley throughout the majority of the plant life cycle showed striking similarities to the observed symbiotic interactions between *Epichloe/ Neotyphodium* endophytes and cool season grasses. In these associations, the endophyte occupies a specialised niche within grass tissues, in which it has access to nutrients in the apoplastic space. It also provides an effective method of spread by transmission through the host seeds (Schardl *et al.,* 2004). The endophyte in return promotes host growth and persistence through improved nutrient acquisition. It also facilitates protection from a range of biotic and abiotic stresses, including drought, disease, and also animal herbivory. This has been associated with fungal synthesis of various biologically active toxic metabolites, such as peramine, lolines, indole-diterpenes, and ergot alkaloids (Schardl *et al.*, 2013).

The fact that *R. collo-cygni* is transmitted via seed in a very similar manner to *Neotyphodium* endosymbionts on grasses and it also exhibits prolific intercellular growth throughout the host plant life cycle, until the expression of first symptoms in the final stages of plant development, i.e. during flowering (Walters *et al.,* 2008) poses an important question with regard to the current definition of parasitism and mutualism. Ascomycetous endophytes are viewed as strong mutualists on the basis of theory and empirical studies of introduced agronomic grasses, which predict that microbial symbionts should evolve to benefit their hosts and rely on propagules of their hosts for transmission (Faeth & Sullivan, 2003). This apparent mutualism in *Neotyphodium*-grass association has been recently tested in native grasses. Faeth and

Sullivan (2003) demonstrated that infection generally decreased host growth in terms of plant volume, number of tillers, and dry mass of shoots and roots. This contradicts previous assumptions and challenged the notion that systemic asexual endophytes must be plant mutualists for infections to persist in nature.

*R. collo-cygni* has been shown to colonise barley leaves asymptomatically for a prolonged period of time that suggests a biotrophic or even a mutualistic relationship with the host (Newton *et al.*, 2010). RLS symptoms usually develop only after the emergence of ears (Stabentheiner *et al.*, 2009) and cause early senescence. This potentially regulated disease development within barley is indicative of underlying sophisticated signalling between host and fungus. It has been suggested that the pathogen recognises the reduction of the antioxidative defences of barley that occur during grain ripening stages (Schutzendubel *et al.*, 2008). Our results further support the hypothesis that the transition of fungal life style from symptomless to symptomatic phase is triggered by the changes in gene expression that could be linked to senescence. Indeed, inoculation of fully developed flag leaves prior to head emergence appeared to promote much earlier expression of symptoms compared to infection of younger leaves.

Recent work on the *Epichloe festucae-Lolium perenne* association as a model symbiotic experimental system showed a fine balance between mutualism and antagonism at molecular level. For instance, disruption of components of the reactive oxygen species (ROS)-generating NADPH oxidase (Nox) complex, including NoxA, NoxR, and RacA, led to a breakdown of the mutualistic interaction, with endophyte mutants displaying unrestricted growth in planta and inducing host stunting and premature senescence (Takemoto *et al.,* 2006; Tanaka *et al.,* 2006, 2008). More

recently, it has been shown that disruption in signalling pathway in fungal grass endophytes can lead to pathogenesis (Eaton *et al.,* 2010). In the *E. festucae* - perennial ryegrass (*L. perenne*) system, an essential role for the fungal stress-activated mitogen-activated protein kinase (sakA) in the establishment and maintenance of this mutualistic interaction was demonstrated. It is therefore suggested that similar future studies could also be undertaken in *R. collo-cygni* – barley system, especially since both, fungal and host genomes are available (SRUC, unpublished; The International Barley Genome Sequencing Consortium, 2012). This could expand our understanding of the fungal transition from endophytic to pathogenic stage.

The nature of the seed-borne stage has now been described by correlative use of light- and confocal microscopy, and the transgenic and field *R. collo-cygni* isolates. Furthermore, the potential impact of different levels of infection on seed germination was also addressed. The presence of the pathogen in the seed material did not have any negative impacts on germination ability thereby suggesting that the crop could establish in field environment despite fungal infection. Our results question the current definition of pathogenesis as the majority of *R. collo-cygni* development throughout barley growth is asymptomatic. More importantly, interesting results from controlled environmental study on infected barley suggested an increase in plant biomass compared to non-infected plants (Neil Havis, SRUC, personal communication). This evidence supports the hypothesis that subsequent disease symptoms late in the season could be a trade-off that has to be balanced with earlier benefits.

An important aspect of this project was to identify and characterise the existence of the potential sexual reproduction in *R. collo-cygni.* The sexual stage of a fungus is an important part of their life histories and development and it often represents major primary inoculum source by producing propagules called ascospores. Despite this fact, studies on sexual reproduction remain one of the least studied topics in modern plant pathology. This is certainly true for a large group of plant pathogenic fungi, family *Mycosphaerellaceae*. It is generally accepted that *Mycosphaerella* represents one of the largest genera of ascomycetous fungi, although it has recently been demonstrated that this could be well overestimated. Crous *et al.* (2009) suggested that *Mycosphaerella* should be restricted to taxa linked only to *Ramularia* anamorphs. It is therefore necessary and desirable to characterise sexual development in *R. collo-cygni*, which has a potential to advance knowledge of *Mycosphaerella* plant pathogens in general.

An essential objective of this research was characterisation of the mating system in *R. collo-cygni* by molecular analysis of the mating type loci. To our best knowledge, this chapter represents the first ever report of the nature of the mating system in any *Ramularia* species. In order to examine mating behaviour and compatibility, by PCR amplification of the conserved domains of mating type genes, a specific primer set for both mating type idiomorphs in *R. collo-cygni* was developed. The results showed that the fungus is a heterothallic species, with each isolate carrying one of the two mating type idiomorphs, and only strains of opposite mating types are compatible. Sequencing of the conserved domains of mating type genes and subsequent blast results showed a closer relationship with other fungal species such

as *D. septosporum* (teleomorph *M. pini*), as well as the *Mycosphaerella* banana species complex.

The development of mating type-specific primers provided an excellent tool for predicting the occurrence of functional sexual recombination taking place within defined populations and was essential for subsequent attempts to induce ascosporogenesis *in vitro*. The distribution of mating type genes across defined field population of isolates (n=40) clearly indicated that *R. collo-cygni* could have a cryptic teleomorph stage. The ratio between *mat*1-1 and *mat*1-2 isolates was maintained at the ratio close to 1:1, which is a typical scenario for species with very frequent sexual reproduction, such as *Z. tritici*. This supports the results of recent population genetic analysis undertaken on the same collection of isolates using SSR markers (Marta Piotrowska *et al.,* unpublished). Although our results suggested a frequent recombination in *R. collo-cygni*, relying exclusively on mating type genes ratio and microsatellite markers is not sufficient for determining the existence of the functional sexual stage. A good example of this is another barley pathogen, *Rhynchosporium commune* (syn. *R. secalis*) in which mating type genes ratio was 1:1 for both, *mat*1-1: *mat*1-2 in most populations sampled (Linde e*t al.*, 2003). Although phylogenetic analysis suggested the existence of a teleomorph in the genus *Tapesia* (Goodwin, 2002), the sexual stage structures and ascospores have so far not been found and characterised.

The desired outcome of the analysis of mating system in *R. collo-cyni* was establishing the ability to distinguish between isolates, according to their mating type and to identify potentially compatible pairs for further mycological study. Only partial sequences of mating type genes were used to identify the candidate mating

pairs to induce sexual development *in vitro*. Therefore it is suggested that the next step in future research should be cloning and characterisation of the entire *mat* locus. The obtained data could be useful for determining the phylogenetic relationships within *Ramularia* species as has been done for related ascomycetous fungi such as *Colletotrichum* and *Cercospora* species complex and *Dothistroma* needle blight pathogens (Du *et al.,* 2005; Groenewald *et al.,* 2006, 2007, respectively).

In order to induce sexual reproduction *in* vitro, a straw inoculation assay was employed as previously described by Salamati & Reitan (2006). The authors showed the development of the potential spermogonium stage on barley straw. However, these observations did not provide the evidence of spermatia (*Asteromella*), i.e. spore-like bodies that act as male donors that develop within spermogonium. Adopting this method in the current study proved very useful for determining the role of these structures in *R. collo-cygni* lifecycle. This study reports the existence of spermatia (*Asteromella*) produced within the structures, thus confirming that indeed they represent the speculated spermogonial state. Similar development was observed previously in the related *Ramularia* species, i.e. *R. armoraciae* (Dring, 1961) and *R. deusta* (Baker *et al.,* 1950).

The phenomenon of light-induced sporulation in fungi has previously been reported during the 20$^{th}$ century. Stevens (1928a, 1928b) first observed that ultraviolet (UV) radiation stimulated both sexual and asexual reproduction of *Glomerella cingulata*. Mycologists subsequently recognised that reproduction in many fungi can be stimulated by light (Carlile, 1965; 1970). Hypothesis that near UV light could be an important factor necessary for the development of sexual reproduction-related structures in *R. collo-cygni* has been tested. Initial study using bright field (BF) and

DIC microscopy of inoculated fragments of barley straw in culture has confirmed the formation of stromatal knots embedded in stomata. Results showed that the exposure of crossing cultures to blue-black lamp caused an increase in numbers of observed multicellular bodies on straw fragments.

During the experiments with the straw inoculation assay, the development of another unreported multicellular body was observed. These sclerotium-like bodies consisted of undifferentiated pseudoparenchyma cells surrounded by heavily melanised peridium. It has been observed that these structures could sprout to produce conidiophores which led to the initial conclusion that they could be sclerotia, i.e. the vegetative 'organ' of aestivation. This was supported by previous studies of the life histories of related *Ramularia* species, specifically *R. vallisumbrosae* (Gregory, 1939), *R. onobrychidis* (Hughes, 1949), *R. deusta* (Baker *et al.,* 1950) and *R. armoraciae* (Dring, 1961). During the course of *R. collo-cygni* examination described here, several different temperature conditions have been tested in order to verify if sclerotia could serve their presumed function of overwintering. Interestingly, in 8 - 12 week old cultures exposed to the temperature of 4 ºC for a period of a week, a small number of the structures in which internal differentiation had taken place. Furthermore, some distinct hyphae in the interior of the structures were also observed which could be trichogynes, a specialised type of receptive hyphae. The initially spherical structures change appearance and became pear-shaped. This is reminiscent of sexual fruiting bodies in related ascomycetous species, such as *M. fijiensis* (Meredith and Lawrence, 1969). In fact, in some sclerotia of sister species, *R. vallisumbrosae* on narcissus, the hyaline hyphae within the body remained thin-walled and apparently discrete throughout the summer and winter

months (Gregory, 1939). The presence of hyphae in the centre and neck of the bodies also strongly resembled trichogynes. This suggested therefore that the structures might represent the fundaments of a yet undiscovered perithecial stage.

Subsequently, it has been observed that within some of the described structures a formation of cylindrical asci occured, which appeared to carry ascospores. However, this has only occurred for a few of several hundred sectioned bodies. Unfortunately, it was not possible to obtain viable ascospores to observe if they could produce typical *R. collo-cygni* colonies. Therefore, we cannot formally describe the sexual stage as required by the International Code of Botanical Nomenclature due to the lack of well-preserved ascospore material. Based on these observations, it would now be essential to continue studying these bodies in much greater detail to verify that they indeed represent the teleomorph of *R. collo-cygni.* As one possible approach, it is suggested here that subsequent studies should involve using samples that were exposed to natural environment as *in vitro* induction of sexual stage in *Mycosphaerella* species is generally thought to be difficult. Controlled environment experiments showed a very limited success in the banana pathogen *M. fijiensis* (Etebu *et al*., 2003), or failure in another barley pathogen, *Z. passerinii* (Ware *et al.* (2007).

In order to detect a potential recombination, two transgenic isolates expressing either GFP or DsRed were crossed, which proved successful in producing sclerotium-like bodies which carried spore-like structures that appeared to co-express both fluorescent protein markers. This proved that the recombination had occurred between these isolates. It is important however, to consider other potential

mechanisms that may have facilitated this recombination. For instance, parasexual recombination is thought to play an important role in increasing the diversity amongst fungal populations. The common feature of plant pathogenic fungi from all major groups is that they can adapt quickly to changing environments including overcoming plant disease resistance genes (Mehrabi *et al.,* 2011 and references therein). To achieve this, usually a mutation in a single effector gene of the pathogens is required. Thus, the host plant, i.e. resistance gene is unable to recognise the attack from the pathogen. Furthermore, it is also important to note that horizontal gene transfer (HGT) and horizontal chromosome transfer (HCT) phenomena allow for a broad pathogen host range.

It is not uncommon for filamentous fungi to lack sexual recombination in their life cycles (Roca *et al.*, 2005b). It has therefore been postulated that cell fusion not only improve the chances of colony establishment by distribution of nutrients or water within the environment, but in the apparent absence of sexual reproduction, it is nonself conidial anastomosis tubes (CAT) fusion- and vegetative hyphal fusion processes that may facilitate parasexual recombination instead. This may then be the cause of high levels of genetic variation found in filamentous fungi that lack sexual reproduction (Roca *et al.*, 2005a, b; Read & Roca, 2006; Ishikawa *et al.*, 2010). Roca *et al.* (2004) have suggested that CATs might act as biological bridges for genetic exchange between individuals of the same or different species and allow the introgression of genetic material (horizontal gene transfer), a mechanism for the acquisition of supernumerary chromosomes. The authors presented first evidence of the successful interspecific CAT fusion events between species that had presumably

led to the the exchange of genetic material between *Colletotrichum gossypii* and *C. lindemuthianum*.

Recently, several reports have appeared in the literature on HGT, HCT and hybridization between plant pathogenic fungi that affect their host range, including species of *Stagonospora / Pyrenophora* and *Fusarium* (Mehrabi *et al.*, 2011, and references therein). For instance, evidence exists that interspecific HGT of the ToxA gene from *Stagonospora nodorum* to *Pyrenophora tritici-repentis* enabled the latter fungus to cause a serious disease in wheat (Friesen *et al.*, 2006). The occurrence of nonpathogenic *Fusarium* species that has become pathogenic on tomato after HCT of a pathogenicity chromosome from *Fusarium oxysporum* f.sp *lycopersici*, has been reported (Ma *et al.,* 2010).

CAT fusion may occur in *R. collo-cygni* (M. Kaczmarek, SRUC; K.M. Lord, University of Edinburgh, unpublished). It would therefore be desirable to study this phenomenon further in order to verify if this process could also facilitate the increasing diversity of this important pathogen of barley. Together with the potential existence of sexual reproduction in this fungus, this could lead to the rapid development of fungicide resistant and more pathogenic strains. It is therefore suggested here that the potential mechanisms of recombination in *R. collo-cygni* should remain as one of the most intensely studied aspect of its biology in order to monitor the risk of future outbreaks by new virulent strains. Such new strains could therefore have a negative impact on barley production by the emergence of fungicide resistance development in general.

An important aspect of research on RLS has been the discovery and biochemical studies into polyketide toxins, produced by the fungus. These studies identified a number of closely related compounds, present in culture filtrates, called rubellins (Heiser *et al.,* 2003; 2004). These authors presented some preliminary evidence suggesting the role of these toxins in the necrotrophic phase of RLS development. Furthermore, Miethbauer *et al.* (2006) showed the presence of these coloured compounds within fungal hyphae. These findings were essential in order to develop a method of direct observation of rubellin *in planta*, described here. It is based on the properties of aromatic rings that are backbone of the biochemical structure of rubellins as predicted by Miethbauer *et al.* (2006). The putative rubellin autofluorescence spectra were determined by the application of lambda scan using CLSM that confirmed their physiochemical predictions (Miethbauer *et al.*, 2006). The putative rubellin accumulated in a vacuole-like vesicle, which confirms the results of Miethbauer *et al.* (2006). This mechanism may have evolved to reduce the potential self-toxicity of rubellin to the cells. Dothistromin production by red band needle blight pathogen of pine *D. septosporum*, has also been shown to be synthesised and stored by this fungus in vacuole-like vesicles (Bradshaw *et al.*, 2009). Both, dothistromin and rubellin produced by these closely related fungi share not only biochemical similarities but also aspects of cell biology.

Subsequently, this study also showed that discharge of the putative rubellin was correlated with symptom development. The presence of toxin in plant tissues, specifically in intercellular spaces that were colonised by a network of hyphae co-localised with the collapsed epidermis and mesophyll cells, and subsequent rapid symptom development. The findings demonstrated that rubellin production occurs late

in the infection cycle as was usually observed from 3 - 4 weeks after inoculation. The production of vacuole- like vesicles was a distinct feature of intercellular hyphae, which were initially observed to be unusually highly vacuolated.

In the related plant pathogen, *D. septosporum,* research on toxin called dothistromin has concentrated on the genetics behind its synthesis. Bradshaw *et al.* (2003) reported the existence of gene orthologs that were determined to be involved in aflatoxin production by *Aspergillus* spp. The authors demonstrated that the dothistromin biosynthesis involves genes arranged in a metabolic cluster. Following these findings, the hypothesis that rubellin biosynthesis could also be governed by a similar gene cluster to those found in *D. septosporum* and *Aspergillus* spp. was tested. Data confirmed the existence of gene orthologs within metabolic gene cluster in the recently sequenced *R. collo-cygni* genome (SRUC, unpublished) and suggests the putative molecular machinery that could be involved in rubellin synthesis. Future studies should therefore involve the analysis of gene expression to identify candidates for subsequent functional studies. For instance, gene knockout approach using transformation method developed by Thirugnanasambandam *et al.* (2011) could be used to generate mutants with impaired or deleted rubellin synthesis ability. Such mutants could then be used to determine their ability to infect plants which could ultimately confirm or reject the current hypothesis that rubellins are pathogenicity factors in *R. collo-cygni* (Heiser *et al.,* 2004). It suggests that rubellin production by the fungus results in oxidative stress, which in turn is involved in the induction of local necroses and formation of lesions (Walters *et al.,* 2008).

RLS has now become a plant disease of major importance for barley growers, despite being known for over a century (Cavara, 1893). The factors that contribute to

the increase in prevalence of RLS remain to be conclusively determined. It is therefore essential to employ all available tools and resources, such as the fluorescently tagged *R. collo-cygni* isolates (Thirugnanasambandam *et al.,* 2011) used extensively in this current biological study, to increase our understanding of *R. collo-cygni* infection of barley and to study other potentially important sources of the disease, such as alternate hosts. It is believed that it could lead to the development of new approaches and control measures to combat the disease. The transgenic isolates used in this study could now be used to support field trial experiments in order to find and characterise new resistance sources perhaps present in barley germplasm and to determine microscopically how any resistance may act against the pathogen. As the knowledge of the mode of action of the pathogen has now been significantly increased, it is suggested here that *R. collo-cygni* inoculation experiments could now be used for quantification of pathogen's development as an indicator of different susceptibility levels in a similar manner to that described for *Rhynchosporium commune* (Thirugnanasambandam *et al.,* 2010).

For determination of different stages of the lifecycle of this fungus, the transgenic *R. collo-cygni* isolates were also used to further investigate the spread of inoculum from seeds to plants and plants to seeds, and in addition, to address the question of whether *R. collo-cygni* is able to persist in barley as an endophyte. The nature of seed borne transmission has now been described in detail which could ultimately lead to the investigation and development of seed treatments that could control the asymptomatic growth and thus prevent symptom development and yield loss. Our study of infection biology highlights the necessity to reconsider what the parasite and the mutualist really mean. This study represents a new chapter in *R. collo-cygni*

genetics through the discovery of putative molecular rubellin biosynthesis machinery that could be involved in toxin production. This fundamental understanding could have major implications for the future development of breeding programmes that could employ the search for rubellin tolerant cultivars. Based on these intital findings the role of the metabolic cluster in rubellin production is now being investigated in a new PhD research project (Dussart F., SRUC and University of Edinburgh).

# Chapter 7

# References

## 7. References


Abe Y., Ono C., Hosobuchi M., and Yoshikawa H. (2002) Functional analysis of *mlcR*, a regulatory gene for ML-236B (compactin) biosynthesis in *Penicillium citrinum*. *Molecular Genetics and Genomics* **268:** 352–361.

Agrios G.N. (2005) Plant Pathology. Fifth Edition. Elsevier Academic Press.

Ahn J.H., Cheng Y.Q., and Walton J.D. (2002) An extended physical map of the *TOX2* locus of *Cochliobolus carbonum* required for biosynthesis of HC-toxin. *Fungal Genetics and Biology* **35:** 31–38.

Alexopoulos C.J., Mims C.W., Blackwell M. (1996) Introductory Mycology, 4th Edition. John Wiley & Sons, New York.

Allen E.A., Hazen B.E., Hoch H.C, Kwon Y., Leinhos G.M.E. *et al*. (1991) Appressorium formation in response to topographical signals by 27 rust species, *Phytopathology* 81 323-331.

Arie T., Christiansen S.K., Yoder O.C., Turgeon B.G. (1997) Efficient cloning of Ascomycete mating type genes by PCR amplification of the conserved *MAT* HMG Box. *Fungal Genetics and Biology* 21: 118-130.

Arie T., Kaneko I., Yoshida T., Noguchi M., Nomura Y., Yamaguchi I. (2000) Mating-type genes from asexual phytopathogenic ascomycetes *Fusarium oxysporum* and *Alternaria alternata*. *MPMI* 13: 1330–1339.

Armstrong A. (2013) BSc thesis, SRUC and University of Edinburgh.

Armstrong G.M. and Armstrong J.K. (1981) Formae speciales and races of *Fusarium oxysporum* causing wilt diseases. In: Nelson, P.E., Toussoun, T.A., Cook, R.J. (Eds.), *Fusarium*: Diseases, Biology and Taxonomy. The Pennsylvania State University Press, University Park, pp. 391–399.

Arnone A., Nasini G., Camarda L., Assante A. (1986) Secondary mould metabolites. Part 15. Structure elucidation of rubellins A and B, two novel anthraquinone metabolites from *Mycosphaerella rubella*. *Journal of the Chemical Society*, *Perkin Transactions* 1: 255–260.

Arnone A., Nasini G., Camarda L., Assante A. (1989) Secondary mould metabolites. XX. The structure of rubellins C and D, two novel anthraquinone metabolites from *Mycosphaerella rubella*. *Gazzetta Chimica Italiana* 119: 35–39.

Astell C.R., Ahlstrom-Jonasson L., Smith M., Tatchell K., Nasmyth K.A., Hall B.D. (1981) The sequence of the DNAs coding for the mating-type loci of *Saccharomyces cerevisiae*. *Cell* 27: 15–23.

Baayen R.P., O'Donnell K., Bonants P.J.M., Cigelnik E., Kroon L.P.N.M., Roebroeck E.J.A.,Waalwijk C. (2000) Gene geneologies and AFLP analyses in the *Fusarium oxysporum* complex identify monophyletic and nonmonophyletic formae speciales causing wilt and rot disease. *Phytopathology* 90: 891-900.

Baayen R.P., O'Donnell K., Bonants P.J.M., Cigelnik E., Kroon L.P.N.M., Roebroeck E.J.A., Waalwijk C. (2000) Gene genealogies and AFLP analyses in the *Fusarium oxysporum* complex identify monophyletic and nonmonophyletic formae speciales causing wilt and rot disease. *Phytopathology* 90, 891–900.

Babadoost M. (1997) Barley stripe. In: Marthe D.E. (ed.). Compendium of Barley Diseases: 124-125. APS Press, St. Paul, Mn, USA.

Baker K.F., Snyder W.C., Davis L.H. (1950) *Ramularia* leaf spots of *Lathyrus odoratus* and *L. Latifolius*. *Mycologia* 42: 403-422.

Balint-Kurti P.J. and Churchill A.C.L. (2004) Towards a molecular understanding of *Mycosphaerella*/banana interactions. In: *Banana Improvement: Cellular, Molecular Biology, and Induced Mutations* (Jain, S.M. and Swennen, R., eds), pp. 147–159. Plymouth: Science Publishers, Inc.

Balint-Kurti P.J., May G.D. and Churchill A.C.L. (2001) Development of a transformation system for *Mycosphaerella* pathogens of banana: a tool for the study of host/ pathogen interactions. *FEMS Microbiology Letters* 195; 9-15.

Bao J.R., Fravel D.R., O'Neill N.R., Lazarovits G., van Berkum P. (2002) Genetic analysis ofpathogenic and nonpathogenic *Fusarium oxysporum* from tomato plants. *Canadian Journal of Botany* 80: 271-279.

Barr M.E. (1956). Life history studies of *Mycosphaerella tassiana* and *M. typhae*. *Mycologia* 50: 501-513.

Bell A. and Mahoney D.P. (1996). Perithecium development in *Podospora tetraspora* and *P. vesticola. Mycologia* 88: 163-170.

Bhatnagar D., Ehrlich K.C., Cleveland T.E. (2003) Molecular genetic analysis and regulation of aflatoxin biosynthesis. *Applied Microbiology and Biotechnology* 61: 83-93

Blakeslee A.F. (1904). Sexual reproduction in the *Mucorineae*. *Proceeedings of The American Academy of Arts and Sciences* 40:205–319.

Bobrowicz P., Pawlak R., Correa A., Bel-Pedersen D., Ebbole D.J. (2002) The *Neurospora crassa* pheromone precursor genes are regulated by the mating type locus and the circadian clock. *Molecular Microbiology* 45: 795–804.

Bradshaw R.E. and Zhang S. (2006) Biosynthesis of dothistromin. *Mycopathologia* 162: 201–213.

Bradshaw R.E., Bhatnagar D., Ganley,R.J., Gillman,C.J.,Monahan,B.J. and Seconi,J.M.(2002).Dothistroma pini, a forest pathogen, contains homologs of aflatoxin biosynthetic pathway genes. *Applied and Environmental Microbiology* 68 (6), 2885-2892

Bradshaw, R.E.; Feng, Z.; Schwelm, A.; Yang, Y. & Zhang S. (2009) Functional Analysis of a Putative Dothistromin Toxin MFS Transporter Gene. *Toxins* 1:173-187. doi:10.3390/toxins1020173

Brakhaage A. (1998) Molecular regulation of b-lactam biosynthesis in filamentous fungi. *Microbiology and Molecular Biology Reviews* 62**:** 547–585.

Braun U. & Sutton B.C. (1991). Proposal to conserve *Ramularia* Unger (Fungi) against *Ramularia* Roussel (Algae). *Taxon* 40: 656-658.

Braun U. (1998). A monograph of *Cercosporella, Ramularia* and allied genera (*Phytopathogenic Hyphomycetes*. Vol.2).

Braun U. (2004). *Ramularia collo-cygni* (Ramularia Leaf Blight of barley): taxonomy and phylogeny. Meeting the Challenges of Barley Blights. *Proceedings of the Second International Workshop on Barley Leaf Blights* 7-11 April 2002, ICARDA, Aleppo, Syria: 370-375.

Brown D.W., Dyer R.B., McCormick S.P., Kendra D.F., and Plattner R.D. (2004) Functional demarcation of the *Fusarium* core trichothecene gene cluster. *Fungal Genetics* and *Biology* **41:** 454–462.

Brown D.W., Yu J.H., Keller H.S., Fernandes M., Nesbitt T.C., Keller N.P., *et al.* (1996) Twenty-five coregulated transcripts define a sterigmatocystin gene cluster in *Aspergillus nidulans*. *Proceedings of The National Academy of Sciences* **93:** 1418–1422.

Brown R.L., Cleveland T.E., Cotty P.J., Mellon J.E. (1992) Spread of *Aspergillus flavus* in cotton bolls, decay of intercarpellary membranes and production of fungal pectinases. *Phytopathology* 82: 462-467

Brunner P.C., Schürch S. and McDonald B.A. (2007) The origin and colonization history of the barley scald pathogen *Rhynchosporium secalis*. *Journal of Evolutionary Biology* 20: 1311–1321. doi: 10.1111/j.1420-9101.2007.01347.

Campbell R.E., Tour O., Palmer A.E., Steinbach P.A., Baird G.S, Zacharias, D.A, Tsien R.Y. (2002) A monomeric red fluorescent protein. *Proceedings of The National Academy of Sciences* 99: 7877–7882.

Carlier J., Fouré E., Gauhl F., Jones D.R., Lepoivre P., Mourichon X., Pasberg-Gauhl C. and Romero R.A. (2000a) Black leaf streak. In: *Diseases of Banana, Abacá and Enset* (Jones, D.R., ed.), pp. 37–79. New York: CABI Publishing.

Carlier J., Mourichon X. and Jones D.R. (2000b) Black leaf streak: the causal agent. In: *Diseases of Banana, Abacá and Enset* (Jones, D.R., ed.), pp. 48–56. New York: CABI Publishing.

Carlier, J., Mourichon, X. and Jones, D.R. (2000c) Sigatoka-like leaf spots: septoria leaf spot. In: *Diseases of Banana, Abacá and Enset* (Jones, D.R., ed.), pp. 93–96. New York: CABI Publishing.

Carlile M.J. (1965) Photobiology of fungi. *Annual Review of Plant Physiology* 16: 175- 202. .

Carlile M.J. (1965) Photobiology of fungi. Annual Review of Plant Physiology 16: 175-202.

Carlile M.J. (1970) The photoresponses of fungi. In P. Halldal [ed.] The photobiology of micro-organisms. John Wiley & Sons, Inc., New York. pp. 309-344.

Carlile, M.J. (1970) The photoresponses of fungi, p. 309-344. In P. Halldal [ed.] The photobiology of micro-organisms. John Wiley & Sons, Inc., New York.

Carmichael JW, Kendrick WB, Conners EL & Sigler L. (1980) Genera of Hyphomycetes. Edmonton: University of Alberta Press.

Cary J.W. and Bhatnagar D. (1995) Nucleotide sequence of an *Aspergillus parasiticus* gene strongly repressed by thiamine. *Biochimica et Biophysica Acta* 1261: 319–320.

Cary J.W., Bhatnagar D., Linz J.E. (2000b) Aflatoxins: Biological significance and regulation of biosynthesis. In: Cary J.W., *et al.,* eds. Microbial Foodborne Diseases. Lancaster, Pennsylvania: Technomic Publishing Co.; pp. 317–362.

Cary J.W., Enrlich K.C. (2006) Aflatoxigenicity in *Aspergillus*: Molecular genetics, phylogenetic relationships and evolutionary implications. *Mycopathologia* 162(3): pp 167-177.

Cary J.W., Montalbano B.G., and Ehrlich K.C. (2000a) Promoter elements involved in the expression of the Aspergillus parasiticus aflatoxin pathway gene avnA. *Biochimica et Biophysica Acta* 91377: 1-6.

Cavara F. (1893) Über einige parasitische Pilze auf dem Getreide. *Zeitschrift für Pflanzenkrankheiten* 3, 16-26.

Cavara F. (1894) Ulteriore contribuzione alla micologia Lombarda. *Aui l stituto Botanico della R . Unio ersita di Pavia* II ser. 3, 313-350.

Chang P.K., Cary J.W., Bhatnagar D., Cleveland T.E., Bennett J.W., Linz J.E., Woloshuk C.P., Payne G.A. (1993) Cloning of the *Aspergillus parasiticus apa-2* gene associated with the regulation of aflatoxin biosynthesis. *Applied and Environmental Microbiology* 59: 3273–3279.

Chang P.K., Skory C.D., Linz J.E. (1992) Cloning of a gene associated with aflatoxin $B_1$ biosynthesis in *Aspergillus parasiticus*. *Current Genetics* 21: 231–233

Chang, P.K. and Yu J. (2002) Characterization of a partial duplication of the aflatoxin gene cluster in Aspergillus parasiticus ATCC 56775. *Applied Microbiology and Biotechnology* 58: 632-636.

Chen H., Lee M.H., Daub M.E., Chung K.R (2007) Molecular analysis of the cercosporin biosynthetic gene cluster in *Cercospora nicotianae. Molecular Microbiology* 64(3): 755–770.

Chettri P. Calvo A.M., Cary J.W., Dhingra S., Guo Y., McDougal R.L., Bradshaw R.E.(2012) The veA gene of the pine needle pathogen *Dothistroma septosporum* regulates sporulation and secondary metabolism. *Fungal Genetics and Biology* 49: 141–151.

Choquer M., Dekkers K.A., Chen, H.Q., Cao L., Ueng P.P., Daub M.E., and Chung K.R. (2005) The *CTB1* gene encoding a fungal polyketide synthase is required for cercosporin biosynthesis and fungal virulence of *Cercospora nicotianae*. *MPMI* 18: 468–476.

Choquer M., Lee M.H., Bau H.J., and Chung K.R. (2007) Deletion of a MFS transporter-like gene in *Cercospora nicotianae* reduces cercosporin toxin accumulation and fungal virulence. *FEBS Letters* 581: 489–494.

Christensen M.J., Bennett R.J., Ansari H.A., Koga H., Johnson R.D., Bryan G.T., Simpson W.R., Koolaard J.P., Nickless E.M., Voisey C.R. (2008) *Epichloe* endophytes grow by intercalary hyphal extension in elongating grass leaves. *Fungal Genetics and Biology* 45: 84–93.

Christensen M.J., Bennett R.J., Schmid J. (2002) Growth of *Epichloe/ Neotyphodium* and p-endophytes in leaves of Lolium and Festuca grasses. *Mycological Research* 106: 93–106.

Chung, K.R., Daub, M.E., Kuchler, K., and Schüller, C. (2003) The *CRG1* gene required for resistance to the singlet oxygen-generating cercosporin toxin in *Cercospora nicotianae* encodes a putative fungal transcription factor. *Biochemical and Biophysical Research Communications* 302: 302–310.

Chung, K.R., Jenns, A.E., Ehrenshaft, M., and Daub, M.E. (1999) A novel gene required for cercosporin toxin resistance in the fungus, *Cercospora nicotianae*. *Molecular and General Genetics* 262: 382–389.

Claxton N. S., Fellers T. J. and Davidson M.W. (2005) Laser Scanning Confocal Microscopy. Department of Optical and Digital Imaging, National High Magnetic Field Laboratory, The Florida State University, Tallahassee, Florida 32310.

Coppin E., Debuchy R., Arnaise S., Picard M. (1997). Mating type and sexual development in filamentous Ascomycetes. *Microbiology and Molecular Biology Reviews* 61 (4): 411-428.

Corpet F. (1988) Multiple sequence alignment with hierarchical clustering. Nucleic Acids Research 16 (22): 10881-10890

Cromey, M.C.; Harvey, I.C.; Sheridan, J.E. & Grbavac, N. (2004) Occurrence, Importance and Control of Ramularia collo-cygni in New Zealand.

*Proceedings of the Second International Workshop on Barley Leaf Blights*. 7-11 April 2002, ICARDA, Aleppo, Syria: 337-342.

Crous P.W. (2009) Taxonomy and phylogeny of the genus *Mycosphaerella* and its related anamorphs. *Fungal Diversity* 38: 1-24.

Crous P.W. and Mourichon X. (2002) *Mycosphaerella eumusae* and its anamorph *Pseudocercospora eumusae* spp. nov.: causal agent of eumusae leaf spot disease of banana. *Sydowia*, 54: 35–43.

Crous P.W., Aptroot A., Kang J-C., Braun U., Wingfield M.J. (2000). The genus *Mycosphaerella* and its anamorphs. *Studies in Mycology* 45: 107-121.

Crous P.W., Groenewald J.Z., Aptroot A., Braun U., Mourichon X. and Carlier J. (2003) Integrating morphological and molecular data sets on *Mycosphaerella*, with specific reference to species occurring on *Musa*. In: *Mycosphaerella Leaf Spot Diseases of Bananas: Present Status and Outlook. Proceedings of the Workshop on Mycosphaerella Leaf Spot Diseases, San José, Costa Rica, 20–23 May 2002* (Jacome, L., Lepoivre, P., Marin, D., Oriz, R., Romero, R. and Escalant, J.V., eds), pp. 43–57. Montpellier: The International Network for the Improvement of Banana and Plantain.

Daub M.E. (1982b) Peroxidation of tobacco membrane lipids by the photosensitizing toxin, cercosporin. *Plant Physiology* 69: 1361–1364.

Daub M.E. and Ehrenshaft M. (2000) The photoactivated *Cercospora* toxin cercosporin: contributions to plant disease and fundamental biology. *Annual Review of Phytopathology* 38: 461–490.

Daub M.E. and Hangarter R.P. (1983) Production of singlet oxygen and superoxide by the fungal toxin, cercosporin. *Plant Physiology* 73: 855–857.

Daub M.E.(1982a) Cercosporin, a photosensitizing toxin from *Cercospora* species. *Phytopathology* 72: 370–374.

Daub M.E., and Briggs S.P. (1983) Changes in tobacco cell membrane composition and structure caused by the fungal toxin, cercosporin. *Plant Physiology* 71: 763–766.

Davis B.H. (1938). The cercospora leaf spot of rose caused by *Mycosphaerella rosicola. Mycologia* 30: 282-298.

Davis J.J. (1937). Notes on para sitic fungi in Wisconsin, xx. *Transactions of the Wisconsin Academy of Sciences, Arts and Letters* 30: 1-16.

de Wit P.J.G.M., van der Burgt A., Ökmen B., Stergiopoulos I., Abd-Elsalam K.A., *et al.* (2012) The Genomes of the Fungal Plant Pathogens *Cladosporium fulvum* and *Dothistroma septosporum* Reveal Adaptation to Different Hosts and Lifestyles But Also Signatures of Common Ancestry. *PLoS Genetics* 8(11): e1003088. doi:10.1371/journal.pgen.1003088

Deighton F.C. (1973) *Ramularia narkandensis* sp .nov. on *Fragaria* in India. *Transactions of The British Mycological Society* 60: 162-164.

Dekkers L.A., You B.J., Gowda V.S., Liao, H.L., Lee M.H., Bau H.J., *et al.* (2007) The *Cercospora nicotianae* gene encoding dual *O*-methyltransferase and FADdependent monooxygenase domains mediates cercosporin toxin biosynthesis. *Fungal Genetics and Biology* **44:** 444–454. doi:10.1016/j.fgb.2006.08.005.

Dodge B.O. (1920) The life history of *Ascobolus magnificus*. *Mycologia* 24:411–447.

Dring D.M. (1961) *Ramularia armoraciae* Fuckel. *Transactions of The British Mycological Society* 44: 333-336.

Du M., Schardl C. L., Nuckles E. M. and Vaillancourt L. J. (2005) Using mating-type gene sequences for improved phylogenetic resolution of *Colletotrichum* species complexes. *Mycologia* 97:641-658.

Eaton C.J., Cox M.P., Ambrose B., Becker M., Hesse U., Schardl C.L., Scott B. (2010) Disruption of signaling in a fungal-grass symbiosis leads to pathogenesis. *Plant Physiology* 153(4):1780-94. doi: 10.1104/pp.110.158451.

Ehrenshaft M., and Upchurch R.G. (1991) Isolation of lightenhanced cDNA clones of *Cercospora kikuchii*. *Applied and Environmental Microbiology* 57: 2671–2676.

Ehrlich K.C., Montalbano B.G., Cary J.W. (1999) Binding of the C6-zinc cluster protein, AFLR, to the promoters of aflatoxin pathway biosynthesis genes in *Aspergillus parasiticus*. *Gene* 230: 249–257.

Ehrlich K.C., Montalbano B.G., Cotty P.J. (2003) Sequence comparison of *aflR* from different *Aspergillus* species provides evidence for variability in regulation of aflatoxin production. *Fungal Genetics and Biology* 38: 63-74.

Ellis J.B. & Everhart B.J. (1885) North American species of *Ramularia* with descriptions of the species. *Journal of Mycology* 1: 73-83.

Etebu E., Pasberg-Gauhl C., Gauhl F. and Daniel-Kalio L.A. (2003) Preliminary studies of *in vitro* stimulation of sexual mating among isolates of *Mycosphaerella fijiensis*, causal agent of black Sigatoka disease in bananas and plantains. *Phytoparasitica*, 31, 69–75.

Faeth S.H. and Sullivan T.J. (2003) Mutualistic asexual endophytes in a native grass are usually parasitic. *The American Naturalist* 161(2): 310-325.

Faivre-Rampant, O., Geniès, L., Piffanelli, P. and Tharreau, D. (2013) Transmission of rice blast from seeds to adult plants in a non-systemic way. *Plant Pathology* 62: 879–887. doi: 10.1111/ppa.12003.

FAO (2007) Food and Agriculture Organization of the United Nations. http://faostat.fao.org/.

Flaherty J.E., Payne G.A. (1997) Overexpression of *aflR* leads to upregulation of pathway gene expression and increased aflatoxin production in *Aspergillus flavus*. *Applied and Environmental Microbiology* 63: 3995–4000.

Formayer H, Huss H. & Kromp-Kolb H. (2004) Influence of Climatic Factors on the Formation of Symptoms of *Ramularia collo-cygni. Proceedings of the Second International Workshop on Barley Leaf Blights. 7*-11 April 2002, ICARDA, Aleppo, Syria: 329-330.

Foster S.J. and Fitt B.D.L. (2003) Isolation and characterisation of the mating-type (MAT) locus from *Rhynchosporium secalis*. *Current Genetics* 44, 277–286.

Freeman E.M. (1904) The seed fungus of *Lolium temulentum* L., the darnel. *Philosophical Transactions of the Royal Society of London* Series B 196: 1–27.

Frei P. (2004) Ramularia collo-cygni: Cultivation, Storage, and Artificial Infection of Barley and Weed Grasses under Controlled Conditions. *Proceedings of the Second International Workshop on Barley Leaf Blights*. 7-11 April 2002, ICARDA, Aleppo, Syria: 351-354.

Frei P., Gindro K., Richter H. & Schürch S (2007) Direct-PCR detection and epidemiology of Ramularia collo-cygni associated with barley necrotic leaf spots. *Journal of Phytopathology* 155: 281–288.

Friesen T.L., Stukenbrock E.H., Liu Z.H. *et al.* (2006). Emergence of a new disease as a result of interspecific virulence gene transfer. *Nature Genetics* 38: 953–956.

Gardiner D.M., Jarvis R.S., and Howlett B.J. (2005) The ABC transporter gene in the sirodesmin biosynthetic gene cluster of *Leptosphaeria maculans* is not essential for sirodesmin production but facilitates self-protection. *Fungal Genetics and Biology* 42: 257–263.

Gardiner D.M., Waring P., and Howlett B.J. (2004) The epipolythiodioxopiperazine (ETP) class of fungal toxins: distribution, mode of action, functions and biosynthesis. *Microbiology* 151: 1021–1032.

Gilman J.C and Wadley B.N. (1952). The ascigerous stage of *Septoria querceti* Thuem. *Mycologia* 44: 216-220.

Glass N.L., Vollmer S.J., Staben C., Grotelueschen J., Metzenberg R.L., Yanofsky C. (1988) DNAs of the two mating-type alleles of *Neurospora crassa* are highly dissimilar. *Science* 241: 570–573.

Goodwin P.H., Hsiang T., Xue B.G. & Liu H.W. (1995) Differentiation of Gaeumannomyces graminis from other turfgrass fungi by amplification with primers from ribosomal internal transcribed spacers. *Plant Pathology* 44: 384–391.

Goodwin S.B. (2002) The barley scald pathogen *Rhynchosporium secalis* is closely related to the discomycetes *Tapesia* and *Pyrenopeziza*. *Mycological Research* 106: 645–654.

Goodwin S.B., Ben M'Barek S., Dhillon B., Wittenberg A.H.J., Crane C.F, *et al.* (2011) Finished Genome of the Fungal Wheat Pathogen *Mycosphaerella graminicola*Reveals Dispensome Structure, Chromosome Plasticity, and Stealth Pathogenesis. *PLoS Genetics* 7(6): e1002070, doi:10.1371/journal.pgen.1002070

Goodwin S.B., Waalwijk C., Kema G.H.J., Cavaletto J.R., Zhang G. (2003) Cloning and analysis of the mating-type idiomorphs from the barley pathogen *Septoria passerinii*. *Molecular and General Genetics* 269: 1–12.

Gregory P.H. (1939). The life history of *Ramularia vallisumbrosae* Cav. on Narcissus. *Transactions of The British Mycological Society* 23: 24-54.

Greif P. (2002). Importance of leaf spot Ramularia collo-cygni for barley growers and breeders. *Proceedings of the Second International Workshop on Barley Leaf Blights*, (ICARDA), Aleppo, Syria, April 2002: 7-11.

Groenewald M., Barnes I., Bradshaw R.E.,. Brown A.V., Dale A., Groenewald J.Z., Lewis K.J, Wingfield B.D., Wingfield M.J., and Crous P.W. (2007) Characterization and Distribution of Mating Type Genes in the Dothistroma Needle Blight Pathogens. *Phytopathology* 97(7): 825-834

Groenewald M., Groenewald J.Z., Harrington T.C., Abeln E.C.A. and Crous P.W. (2006) Mating type gene analysis in apparently asexual *Cercospora* species is suggestive of cryptic sex. *Fungal Genetics and Biology* 43:813-825.

Gross A., Holdenrieder, O., Pautasso, M., Queloz, V. and Sieber, T. N. (2014), *Hymenoscyphus pseudoalbidus*, the causal agent of European ash dieback. *Molecular Plant Pathology* 15: 5–21. doi: 10.1111/mpp.12073

Gwynne-Vaughan H.C.I., and Williamson H.S. (1932). The cytology and development of *Ascobolus magnificus*. *Annals of Botany* 46:653–670.

Haarmann T., Machado C., Lübbe Y., Correia T., Schardl C.L., Panaccione D.G., and Tudzynski P. (2005) The ergot alkaloid gene cluster in *Claviceps purpurea*: extension of the cluster sequence and intra species evolution. *Phytochemistry* **66:** 1312–1320.

Habermeyer J., Schieder A. & Briskina O. (2002) Strobis lindern Sonnenbrand. Strategien gegen nicht - parasitäre Blattverbräunungen an Gerste. - Die landwirtschaftliche Zeitschrift (dlz) - *Agrarmagazin* 2: 20-25.

Habgood R.M. Hayes J.D. (1971) Inheritance of Resistance to *Rhynchosporium secalis* in Barley. *Heredity* 27: 25-37.

Halliday C.L., Bui T., Krockenberger M., Malik R., Ellis D.H., Carter D.A. (1999) Presence of α and a mating types in environmental and clinical collections of

*Cryptococcus neoformans* var. *gattii* strains from Australia. *Journal of Clinical Microbiology* 37: 2920–2926.

Hamelin R.C., Bourassa M., Rail J., Dusabenyagasani M., Jacobi V., Laflamme G., (2000) PCR detection of *Gremmeniella abietina*, the causal agent of Scleroderris canker of pine. *Mycological Research* 104: 527-532.

Harvey I.C. (2002) Epidemiology and control of leaf and awn spot of barley caused by *Ramularia collo-cygni*. *New Zealand Plant Protection* 55: 331–335.

Hauptfleisch K. (1929) Studies of barley leaf blotch. *NachrBI. PFLSchutz DDR* 9, 27-8.

Havis N.D. & Oxley S.J.P. (2006) Investigating the life cycle of *Ramularia collo-cygni* using a PCR based diagnostics. *Ramularia collo-cygni*. A new disease and challenge in barley production. *Proceedings First European Ramularia Workshop*: 39-44.

Havis N.D., Gorniak, K., Carmona M.A., Formento A.N., Luque A.G., and Scandiani M.M. (2014) First Molecular Detection of Ramularia Leaf Spot (Ramularia collo-cygni) in Seeds and Leaves of Barley in Argentina. *Plant Disease* 98:2, 277-277.

Havis N.D., Nyman M. and Oxley S.J.P. (2014) Evidence for seed transmission and symptomless growth of *Ramularia collo-cygni* in barley (*Hordeum vulgare*). *Plant Pathology* 63: 929–936. doi: 10.1111/ppa.12162

Havis N.D., Oxley S.J.P., Piper S.R., Langrell S.R.H. (2006a) Rapid nested PCR-based detection of *Ramularia collo-cygni* direct from barley. *FEMS Microbiology Letters* 256: 217-223.

Havis N.D., Pastok M., Pyzalski S., Oxley S.J.P. (2006b) Investigating the life cycle of *Ramularia collo-cygni. Proceedings Crop Protection in Northern Britain* 2008: 219-224.

Heiser I., Hess M., Schmidtke K., Vogler U., Miethbauer S., Liebermann B. (2004) Fatty acid peroxidation by rubellin B, C and D, phytotoxins produced by *Ramularia collo-cygni* (Sutton et Waller). *Physiological and Molecular Plant Pathology* 64: 135-143.

Heiser I., Osswald W., Elstner E.F. (1998) The formation of reactive oxygen species by fungal and bacterial phytotoxins. *Plant Physiology and Biochemistry* 36, 703-713.

Heiser I., Sachs E., Liebermann B. (2003a). Photodynamic oxygen activation by rubellin D, a phytotoxin produced by Ramularia collo-cygni (Sutton et Waller). *Physiological and Molecular Plant Pathology* 62: 29-36.

Heiser I., Sachs E., Liebermann B., Elstner E.F. (2003b). Oxygen activation by the fungal phytotoxin rubellin D. *Free Radical Research* 37:12.

HGCA (2013) Ramularia leaf spot in barley. Information Sheet 21May 2013. http://www.hgca.com/media/175812/is21_ramularia_leaf_spot_in_barley.pdf

HGCA (2013).The HGCA barley disease management guide 2013. http://www.hgca.com/document.aspx?fn=load&media_id=6879&publicationId=5036.

Higgins B.B. (1920). Morphology and life history of some ascomycetes with special reference to the presence and function of spermatia I. *American Journal of Botany* VII: 435-444.

Higgins B.B. (1929). Morphology and life history of some ascomycetes with special reference to the presence and function of spermatia II. *American Journal of Botany* XVI: 287-296.

Higgins B.B. (1936). Morphology and life history of some ascomycetes with special reference to the presence and function of spermatia III. *American Journal of Botany* XXlIl: 598-602.

Hjortshøj R. L., Ravnshøj A. R., Nyman M., Orabi J., Backes G., Pinnschmidt H., & Havis N.D., Stougaard J., and Stukenbrock E.H. (2013) High levels of genetic and genotypic diversity in field populations of the barley pathogen *Ramularia collo-cygni*. *European Journal of Plant Pathology* 136: 51–60. doi: 10.1007/s10658-012-0137-8.

Hoch H.C., Staples R.C., Whitehead B., Comeau J., Wolf E.D. (1987) Signaling for growth orientation and cell differentiation by surface topography in *Uromyces*. *Science* 235: 1659-1662.

Hohn T.M., McCormick S.P., and Desjardins A.E. (1993) Evidence for a gene cluster involving trichothecene pathway biosynthetic genes in *Fusarium sporotrichioides*. *Current Genetics* **24:** 291–295.

Hughes S.J. (1949). Studies on some diseases of sainfoin (Onobrychis sativa) II. The life history *of Ramularia onobrychidis* Allescher. Trans. Brit. Mycol. Society 32: 34-59.

Huss H. (2004). The biology of *Ramularia collo-cygni*. Meeting the Challenges of Barley Blights.Proceedings of the Second International Workshop on Barley Leaf Blights, (ICARDA), Aleppo, Syria, April 2002: 321–328.

Huss H., Mayrhofer H., Wetschnig W. (1987) *Ophiocladium hordei* CAV. (Fungi imperfecti), ein für Österreich neuer parasitischer Pilz der Gerste. Der Pflanzenarzt 40: 167–169.

Ingham J. (1986) CMI Descriptions of Pathogenic Fungi and Bacteria: 861-870.

Ishikawa F.H., Souza E.A., Read N.D., Roca M.G. (2010). Live-cell imaging of conidial fusion in the bean pathogen, *Colletotrichum lindemuthianum*. *Fungal Biology* 114: 2-9.

Ito T. (1981) Dye binding and photodynamic action. *Photochemistry and Photobiology* **33:** 947–955.

Jenns A.E., Daub M.E. and Upchurch R.G. (1989) Regulation of cercosporin accumulation in culture by medium and temperature manipulation. *Phytopathology* **79:** 213–219.

Jones D.R. (2000) Sigatoka. In: *Diseases of Banana, Abacá and Enset* (Jones, D.R., ed.), pp. 79–92. New York: CABI Publishing.

Jones J.D.G. & Dangl J.L. (2006) The plant immune system. *Nature* 444: 323-329. doi:10.1038/nature05286

Jones W.T., Harvey D., Jones S.D., Sutherland P.W., Nicol M.J., Sergejew N., Debnam P.M., Cranshaw, N., Reynolds, P.H.S. (1995) Interaction between the phytotoxin dothistromin and *Pinus radiata* embryos. *Phytopathology* 85: 1099–1104.

Jones, D.R. (2000a) *Diseases of Banana, Abacá and Enset*. New York: CABI Publishing.

Kabir M. S., Ganley R. J. and Bradshaw R. E. (2014), Dothistromin toxin is a virulence factor in dothistroma needle blight of pines. *Plant Pathology* (in press) doi: 10.1111/ppa.12229

Kaiser WJ, Crous PW. 1998. *Mycosphaerella lupini* sp. nov., a serious leaf spot disease of perennial lupin in south-central Idaho, USA. *Mycologia* 53:726–731.

Kay J.G. Owen H. (1973) Transmission of *Rhynchosporium secalis* on Barley Grain. *Transactions of The British Mycological Society* 60, 405-411.

Keller N.P. and Hohn T.M. (1997) Metabolic pathway gene clusters in filamentous fungi. *Fungal Genetics and Biology* 21: 17-29.

Kema G.H.J., Yu D., Rijkenberg F.H.J., Shaw M.W., and Baayen R P. 1996. Histology of the pathogenesis of *Mycosphaerella graminicola* in wheat. *Phytopathology* 86:777-786.

Kim H., Ridenour J.B., Dunkle L.D., Bluhm B.H. (2011) Regulation of Stomatal Tropism and Infection by Light in *Cercospora zeae-maydis*: Evidence for Coordinated Host/Pathogen Responses to Photoperiod? *PLoS Pathogens* 7(7): e1002113. doi:10.1371/journal.ppat.1002113

Klich M.A., Yu J., Chang P.K., Mullaney E.J., Bhatnagar D., Cleveland T.E. (1995) Hybridization of genes involved in aflatoxin biosynthesis to DNA of aflatoxigenic and non-aflatoxigenic *Aspergilli. Applied Microbiology and Biotechnology* 44: 439-443

Kronstad J.W., Staben C. (1997) Mating type in filamentous fungi. *Annual Review of Genetics* 31: 245–276.

Lang W. (1910) Die Bluteninfektion von Weizenflugbranol. *Zentralbl. Bakteriol. Parasitenkd. Abt.* 2, 25: 86-101.

Lang W. (1917) Zur Ansteckung der Gerste durch *Ustilago nuda. Ber. Dtsch. Bot. Ges.* 35: 4-20.

Langrell S.R.H. (2002) Molecular detection of *Neonectria galligena* (syn. *Nectria galligena*). *Mycological Research* 106: 280–292.

Langrell S.R.H. (2005). Development of a nested PCR detection procedure for Nectria fuckeliana direct from Norway spruce bark extracts. *FEMS Microbiology Letters* 242: 185-193.

Leach C.M. (1972) An Action Spectrum for Light-Induced Sexual Reproduction in the Ascomycete Fungus *Leptosphaerulina trifolii*. *Mycologia* 64 (3): 475-490.

Lee H.K, Tewari J., Turkington T. (2001) Symptomless infection of barley seed by Rhynchosporium secalis. *Canadian Journal of Plant Pathology* 23: 315-317

Lee H.K., Tewari J.P., Turkington T.K. (2002) Quantification of seedborne infection by Rhynchosporium secalis in barley using competitive PCR. *Plant Pathology* 51, 217-224.

Liberato J.R., Peterson R.A., Gasparotto L., Ferrari J.T., Grice K., Porchun S.C. and Shivas R.G. (2009) Black sigatoka of banana (*Mycosphaerella fijiensis*). Available at Pest and Diseases Image Library, Species Content Page— http://www.padil.gov.au/viewPestDiagnosticImages.aspx?id=431; Plant Biosecurity Toolbox/Info Sheet— http://www.padil.gov.au/pbt/index.php?q=node/46&pbtID=166.

Liberato J.R., Peterson R.A., Gasparotto L., Ferrari J.T., Grice K., Groenewald M., Groenewald J. Z., Harrington T. C., Abeln E. C. A., and Crous P. W. (2006) Mating type gene analysis in apparently asexual *Cercospora* species is suggestive of cryptic sex. *Fungal Genetics and Biology* 43: 813-825.

Lindau G. (1907) Fungi Imperfecti, Hyphomycetes (1 Hfte). In Rabenhorsr's Kryptogamen Flora von Deutschland , Osterreich und der Schweiz, 2 Aft. 1 Bd, 8Abt, 1-852.

Linde C.C., Zala M., Ceccarelli S., McDonald B.A. (2003) Further evidence for sexual reproduction in *Rhynchosporium secalis* based on distribution and frequency of mating-type alleles. *Fungal Genetics and Biology* 40: 115–125.

Linde C.C., Zala M., Ceccarelli S., McDonald B.A. (2003) Further evidence for sexual reproduction in *Rhynchosporium secalis* based on distribution and frequency of mating-type alleles. *Fungal Genetics and Biology* 40: 115–125.

Linde C.C., Zhan J., McDonald B.A. (2002) Population structure of *Mycosphaerella graminicola* from lesions to continents. *Phytopathology* 92, 946–955.

Linsell K.J., Keiper F.J., Forgan A., Oldach K.H. (2011). New insight into the infection process of *Rhynchosporium secalis* in barley using GFP. Fungal Genet Biol. 48(2):124-131. doi: 10.1016/j.fgb.2010.10.001

Lorang J.M., Tuori R.P., Martinez J.P., Sawyer T.L., Redman R.S., Rollins J.A., Wolpert T.J., Johnson K.B., Rodriguez R.J., Dickman M.B., Ciuffetti L.M. (2001) Green Fluorescent Protein is Lighting Up Fungal Biology. *Applied and Environmental Microbiology* 67: 1987-1994.

Lord K.M. and Read N.D. (2011). Perithecium morphogenesis in *Sordaria macrospora*. *Fungal Genetics and Biology* 48: 388-399.

Ma L.J., van der Does H.C., Borkovich K.A. *et al.* (2010). Comparative genomics reveals mobile pathogenicity chromosomes in *Fusarium*. *Nature* 464: 367–373.

Makepeace J.C., Havis N.D., Burke J.I., Oxley S.J.P. and Brown J.K.M. (2008) A method of inoculating barley seedlings with *Ramularia collo-cygni. Plant Pathology* 57: 991-999.

Maor R., Puyesky M., Horwitz B.A., Sharon A. (1998). Use of green fluorescent protein (GFP) for studying development and fungal-plant interaction in *Cochliobolus heterostrophus*. *Mycological Research* 102 (4): 491-496.

Marcel S., Sawers R., Oakeley E., Angliker H., Paszkowski U. (2010) Tissue-adapted invasion strategies of the rice blast fungus *Magnaporthe oryzae*. *Plant Cell* 22: 3177–87.

Marchler-Bauer A. *et al.* (2009) CDD: specific functional annotation with the Conserved Domain Database. *Nucleic Acids Reserch* 37(D):205-10.

Marchler-Bauer A. *et al.* (2011) CDD: a Conserved Domain Database for the functional annotation of proteins. *Nucleic Acids Reserch* 39(D):225-9.

Marchler-Bauer A., Bryant S.H. (2004) CD-Search: protein domain annotations on the fly. *Nucleic Acids Reserch* 32(W):327-331.

Mathre D.E. (1997). Compendium of barley diseases. American Phytopathological Society Press

Matusinsky P., Leisova-Svoboda L., Gubis J., Hudcovicova M., Klcova L., Gubisova M., Marik P., Tvaruzek L., Minarikova V. (2011). Impact of seed-borne stage of *Ramularia collo-cygni* in barley seed. *Journal of Plant Pathology* 93, 679–89.

Matz M.V., Fradkov A.F., Labas Y.A., Savitsky A.P., Zaraisky A.G., Markelov M.L., Lukyanov S.A (1999) Fluorescent proteins from nonbioluminescent Anthozoa species. *Nature Biotechnology* 17, 969–973.

McGrann G.R.D, Stavrinides A, Russell J, Corbitt M.M, Booth A, Chartrain L, Thomas W.T.B, Brown J.K.M. (2014) A trade off between *mlo* resistance to powdery mildew and increased susceptibility of barley to a newly important disease, Ramularia leaf spot. *Journal of Experimental Botany* 65(4): 1025-1037.

Mehrabi R., Bahkali A.H., Abd-Elsalam A.K., Moslem M., M'Barek S.B., Gohari A.M., Jashni M.K., Stergiopoulos I., Kema G.H.J. and de Wit P.J.G.M. (2011). Horizontal gene and chromosome transfer in plant pathogenic fungi affecting host range. *FEMS Microbiology Reviews* 35: 542-554.

Meredith, D.S. and Lawrence, J.S. (1969) Black leaf streak disease of bananas (*Mycosphaerella fijiensis*): symptoms of disease in Hawaii, and notes on the conidial state of the causal fungus. *Transactions of The British Mycological Society* 52: 459–476.

Miethbauer S., Günther W., Schmidtke K.U., Heiser I., Gräfe S., Gitter B., Liebermann B. (2008) Uredinorubellins and caeruleoramularin, photodynamically active anthraquinone derivatives produced by two species of the genus *Ramularia. Journal of Natural Products* 71(8):1371-1375.

Miethbauer S., Haase S., Schmidtke K.U., Gunther W., Heiser I., Liebermann B. (2006) Biosynthesis of photodynamically active rubellins and structure elucidation of new anthraquinone derivatives produced by *Ramularia collo-cygni*. *Phytochemistry* 67, 1206-1213.

Miethbauer S., Heiser I., Liebermann B. (2003). The phytopathogenic fungus Ramularia collo-cygni produces biologically active rubellins on infected barley leaves. *Journal of Phytopathology* 151: 665-668.

Milgroom M.G. (1996) Recombination and the multilocus structure of fungal populations. *Annual Review of Phytopathology* 34, 457–477.

Minarikova V., Marik P. & Stemberkova L. (2004). Occurrence of a new fungal pathogen on barley, Ramularia collo-cygni, in the Czech Republic. Meeting the Challenges of Barley Blights. *Proceedings of the Second International Workshop on Barley Leaf Blights*, (ICARDA), Aleppo, Syria, April 2002: 360–364.

Minihofer T. (2003). Untersuchungen an *Ramularia collo-cygni* – einem parasitischen Pilz auf Gerste. Diplomarbeit, Institut für Pflanzenphysiologie der Universität Graz: 96.

Minto R.E. and Townsend C.A. (1997) Enzymology and molecular biology of aflatoxin biosynthesis. *Chemical Reviews* 97:m2537-2555.

Mourichon X. and Zapater M.F. (1990) Obtention *in vitro* du stade *Mycosphaerella fijiensis*, forme parfaite de *Cercospora fijiensis*. *Fruits* 45: 553–557.

Neergaard P. (1977). Seed pathology. Volume I and II. The Macmillan Press London and Basingstock.

Nevo E. (1992).Origin Evolution Population Genetics and Resources for Breeding of Wild Barley *Hordeum-Spontaneum* in the Fertile Crescent. In: Shewry P (ed) Barley: genetics, molecular biology and biotechnology. CAB International, Wallingford, Oxford, pp 19-43.

Newton A, Flavell A, George T, Leat P, Mullholland B, Ramsay L, Revoredo-Giha C, Russell J, Steffenson B, Swanston J, Thomas W, Waugh R, White P, Bingham I. (2011) Crops that feed the world 4. Barley: a resilient crop? Strengths and weaknesses in the context of food security. *Food Security* 3: 141-178.

Newton A.C., Searle J., Guy D.C., Hackett C.A., Cooke D.E.L. (2001) Variability in pathotype, aggressiveness, RAPD profile, and rDNA ITS1 sequences of UK isolates of Rhynchosporium secalis. *Zeitschrift fur Pflanzenkrankheiten und Pflanzenschutz-Journal of Plant Diseases and Protection* 108: 446-458.

Nguyen K.D., Au-Young S.H., Nodwell J.R. (2007). Monomeric red fluorescent protein as a reporter for macromolecular localisation in *Streptomyces coelicolor*. *Plasmid* 58: 167–173.

Niyo K.A., McNabb H.S.Jr., Tiffany L.H. (1986) Ultrastructure of the ascocarps, asci and ascospores of *Mycosphaerella populorum. Mycologia* 78: 202-212.

Nyman M., Havis N.D., Oxley S.J.P. (2009) Importance of seed-borne infection of *Ramularia collo*-cygni. Proceedings of the Second European Ramularia Workshop. *Aspects in Applied Biology* 92: 91-96.

O'Donnell K., Ward T.J., Geiser D.M., Kistler H.C., Aoki T. (2004) Genealogical concordance between the mating type locus and seven other nuclear genes supports formal recognition of nine phylogenetically distinct species within the *Fusarium graminearum* clade. *Fungal Genetics and Biology* 41: 600–623.

Obst A, and Baumer M, (1998) Nichtparasitär bedingte Blattverbräunungen an Gerste und anderen Getreidearten. Ursachen und Abwehrmaßnahmen. *Getreide* 4(2): 56-61.

Oerke E.C. Dehne H.W. (2004) Safeguarding production - losses in major crops and the role of crop protection. *Crop Protection* 23: 275-285.

Oxley S. (2007) Barley Disease Control, TN583, Scottish Agricultural College, Edinburgh, UK. www.sac.ac.uk/ consultancy/crops/publications/cropstechnotes

Oxley S., Havis N.D., Evans A., Waterhouse S. and Tongue L. (2010). A guide to the recognition and understanding of *Ramularia* and other leaf spots of barley. BASF 2010.

Oxley S.J.P., Havis N.D., Sutherland K.G. & Nuttall M. (2002). Development of a Rationale to Identify the Causal Agent of Necrotic Lesions in Spring Barley and to Identify Control Mechanisms. *HGCA Project Report No 282*. HGCA Publications, London, UK.

Paoletti M., Buck K.W., Brasier C.M. (2005) Cloning and sequence analysis of the *MAT-B* (*MAT-2*) genes from the tree Dutch elm disease pathogens, *Ophiostoma ulmi*, *O. novo-ulmi*, and *O. himal-ulmi*. *Mycological Research* 109: 983–991.

Payne G.A., Nystrom G.J., Bhatnagar D., Cleveland T.E., Woloshuk C.P. (1993) Cloning of the afl-2 gene involved in aflatoxin biosynthesis from *Aspergillus flavus*. *Applied and Environmental Microbiology* 59: 156–162.

Pedersen P.N. (1956) Infection of barley by loose smut, *Ustilago nuda* (Jens.) Rostr. *Friesia* 5: 341-348.

Peraldi A., Griffe L. L., Burt C., McGrann G. R. D. and Nicholson P. (2014) *Brachypodium distachyon* exhibits compatible interactions with *Oculimacula* spp. and *Ramularia collo-cygni*, providing the first pathosystem model to study eyespot and ramularia leaf spot diseases. *Plant Pathology* 63: 554–562. doi: 10.1111/ppa.12114

Pinnschmidt H.O. & Hovmøller M.S. (2004). Ramularia-bladplet pa byg. (Ramularia leaf spots of barley). Gron Viden, Markbrug 290, 6pp.

Pöggeler S. (2001) Mating-type genes for classical strain improvements of ascomycestes. Applied Microbiology and Biotechnology 56: 589–601.

Pons N. (1987) Notes on *Mycosphaerella fijiensis* var. *difformis*. *Transactions of The British Mycological Society* 89: 120–124.

Porchun S.C. and Shivas R.G. (2009) Black sigatoka of banana (*Mycosphaerella fijiensis*). Available at Pest and Diseases Image Library, Species Content Page—http://www.padil.gov.au/viewPestDiagnosticImages. aspx?id=431; Plant Biosecurity Toolbox/Info Sheet- http://www.padil.gov.au/pbt/index.php?q=node/46&pbtID=166.

Price M. S., Yu J., Nierman W. C., Kim H. S., Pritchard B., Jacobus C. A., Bhatnagar D., Cleveland T. E. and Payne G. A. (2006), The aflatoxin pathway regulator AflR induces gene transcription inside and outside of the aflatoxin biosynthetic cluster. *FEMS Microbiology Letters* 255: 275–279. doi: 10.1111/j.1574-6968.2005.00084.x

Prieto R., Woloshuk C.P. (1997) *ord1*, an oxidoreductase gene responsible for conversion of *O*-methylsterigmatocystin to aflatoxin in*Aspergillus flavus*. *Applied and Environmental Microbiology* 63:1661–1666.

Proctor R.H., Brown D.W., Plattner R.D., and Desjardins A.E. (2003) Co-expression of 15 contiguous genes delineates a fumonisin biosynthetic gene cluster in *Gibberella moniliformis*. *Fungal Genetics and Biology* **38:** 237–249.

Quaedvlieg W., Kema G.H., Groenewald J.Z., Verkley G.J., Seifbarghi S., Razavi M., Mirzadi-Gohari A., Mehrabi R., Crous P.W. (2011) *Zymoseptoria* gen. nov.: a new genus to accommodate *Septoria*-like species occurring on graminicolous hosts. Persoonia 26: 57-69. doi: 10.3767/003158511X571841.

Raju N.B. (2008) Six decades of *Neurospora* ascus biology at Stanford. *Fungal Biology Reviews* 22: 26–35.

Rathaiah Y. (1977) Stomatal tropism in C. beticola in sugarbeet. *Phytopathology* 67, 358-362

Read N.D. and Beckett A. (1996) Ascus and ascospore morphogenesis. *Mycological Research* 100: 1281–1314.

Roca M.G., Arlt J., Jeffree C.E., Read N.D. (2005b). Cell biology of conidial anastomosis tubes in *Neurospora crassa. Eukaryotic Cell* 4: 911-919.

Roca M.G., Davide L.C., Davide L.M.C., Mendes-Costa M.C., Schwan R.F., Wheals A.E. (2004). Conidial anastomosis fusion between *Colletotrichum* species. *Mycological Research* 108: 1320-1326.

Roca M.G., Read N.D., Wheals A.E. (2005a). Conidial anastomosis tubes in filamentous fungi. *FEMS Microbiology Letters* 249: 191-198.

Rohel, E.A., Payne, A.C., Fraaije, B.A. and HollomoD.W. (2001) Exploring Infection of Wheat and Carbohydrate Metabolism in *Mycosphaerella graminicola* Transformants with Differentially Regulated Green Fluorescent Protein Expression *MPMI* Vol. 14 (2): 156–163

Saccardo, P. A. (1895) *Sylloge fungorum* II, 1-753. Padua, Italy.

Sachs E. (2000). Das Auftreten der Ramularia-Blattfleckenkrankheit an Gerste in Bayern 1999, verursacht durch Ramularia collo-cygni Sutton &Waller. *Nachrichtenbl. Deut. Pflanzenschutzd* 52: 160–163.

Sachs E., Greil P., Amelung D. & Huss H. (1998). *Ramularia collo-cygni* – a re-discovered barley pathogen in Europe. *Mitt BBA* 357: 96–97.

Salamati S & Reitan L (2006). *Ramularia collo-cygni* on spring barley, an overview of its biology and epidemiology (von Tiedemann A, Schützendübel A, Koopman B, eds), *Book of Abstracts of the First European Ramularia Workshop, Georg-August University Göttingen, Germany, March 2006.* pp. 7-23. http://wwwuser.gwdg.de/~rcc/index.htm.

Schardl C.L., Leuchtmann A., Spiering M.J. (2004) Symbioses of grasses with seedborne fungal endophytes. *Annual Review of Plant Biology* 55: 315–340.

Schardl C.L., Young C.A., Hesse U., Amyotte S.G., Andreeva K. *et al.* (2013) Plant-symbiotic fungi as chemical engineers: multi-genome analysis of the *Clavicipitaceae* reveals dynamics of alkaloid loci. *PLoS Genetics* 9: e1003323. doi. 10.1371/journal.pgen.1003323.

Scheffer R.P. (1997). The nature of disease in plants. Cambridge University Press.

Scheuer C. (1999) Mycotheca Graecensis, Fasc. 11 (Nr. 201 - 220). *Fritschiana* (Graz) 20: 112.

Schutzendubel A, Stadler M, Wallner D, von Tiedemann A, 2008. A hypothesis on physiological alterations during plant ontogenesis governing susceptibility of winter barley to ramularia leaf spot. *Plant Pathology* 57: 518-526.

Schwelm A. and Bradshaw R.E. (2010) Genetics of dothistromin biosynthesis of Dothistroma septosporum: an update. *Toxins* 2, 2680–2698.

Schwelm A., Barron N.J., Baker J., Dick M., Long P.G., Zhang S. and Bradshaw R.E. (2009) Dothistromin toxin is not required for dothistroma needle blight in *Pinus radiata*. *Plant Pathology* 58: 293–304. doi: 10.1111/j.1365-3059.2008.01948.x

Seifert, K.A. (2009) Progress towards DNA barcoding of fungi. *Molecular Ecology Resources* 9: 83–89. doi: 10.1111/j.1755-0998.2009.02635.x

Sexton A.C. and Howlett B.J. (2001). Green fluorescent protein as a reporter in the *Brassica – Leptosphaeria maculans* interaction. *Physiological and Molecular Plant Pathology* 58: 13-21.

Shaner C., Campbell R.E., Steinbach P.A., Giepmans B.N.G., Palmer A.E., Tsien R.Y (2004) Improved monomeric red, orange and yellow fluorescent proteins derived from *Discosoma* sp. red fluorescent protein. *Nature Biotechnology* 22: 1567-1572.

Shear C.L., and Dodge B.O. (1927). Life histories and heterothallism of the red bread mould fungi of the *Monilia sitipholia* group. *Journal of Agricultural Research* 34: 1019–1042.

Sheridan J.E. (2000) Cereal Diseases 1999–2000 (Including Peas and Gooseberry Mildew). Disease Survey and Disease Control in the Waiarapa, New Zealand.Mycol. Plant Path. Rep. No. 37. Botany Department, Victoria University of Wellington, Wellington, New Zealand.

Skadsen R.W. and Hohn T.M. (2004) Use of *Fusarium graminearum* transformed with GFP to follow infection patterns in barley and *Arabidopsis*. *Physiological and Molecular Plant Pathology* 64: 45-53.

Skory C.D., Chang P.K., Cary J., Linz J.E. (1992) Isolation and characterization of a gene from *Aspergillus parasiticus* associated with the conversion of versicolorin A to sterigmatocystin in aflatoxin biosynthesis. *Applied and Environmental Microbiology* 58: 3527–3537.

Smith E.C. (1936) The effects of radiation on fungi. In B. M. Duggar [ed.] Biological effects of radiation, Vol. II. McGraw-Hill Book Co., New York, pp. 889-918.

Spellig T., Bottin A. and Kahmann R. (1996) Green fluorescent protein (GFP) as a new vital marker in the phytopathogenic fungus *Ustilago maydis*. *Molecular and General Genetics* 252: 503–509.

Spiering M.J., Moon C.D., Wilkinson H.H., and Schardl C.L. (2005) Gene cluster for insecticidal loline alkaloids in the grass-endophytic fungus *Neotyphodium uncinatum*. *Genetics* **169:** 1403–1414.

Sprague R. (1946) Additions to the fungi imperfecti on grasses in the United States. Mycologia 38, 52-64.

Sprague R. (1948) Some leafspot fungi on Western Gramineae. III . *Mycologia* 40, 295-313.

Sprague R. (1950) Diseases of Cereals and Grasses in North America . New York : Ronald Press.

Sprague R. (1955) Some leaf spot fungi on Western Gramineae. IX. *Mycologia* 47, 835-845.

Stabentheiner E., Minihofer T., Huss H. (2009) Infection of barley by *Ramularia collo-cygni*: Scanning electron microscopic investigations. *Mycopathologia* 168: 135-143. doi: 10.1007/s11046-009-9206-8.

Steenkamp E.T., WingWeld B.D., Coutinho T.A., Zeller K.A., Wingfield M.J., Marasa W.F.O., Leslie J.F. (2000) PCR-based identification of MAT-1 and MAT-2 in the *Gibberella fujikuroi* species complex. *Applied and Environmental Microbiology* 66: 4378–4382.

Stevens, F.L. (1928a) The sexual stage of fungi induced by ultra-violet rays. *Science* 67: 514-515.

Stevens, F.L. (1928b) Effects of ultra-violet radiation on various fungi. *Botanical Gazette* 86: 210-225.

Stoessl A., Abramowski Z., Lester H.H., Rock G.L., Towers G.H.N. (1990) Further toxic properties of the fungal metabolite dothistromin. *Mycopathologia* 112: 179–186.

Stukenbrock E.H., Banke S., Javan-Nikkhah M., McDonald B.A. (2007) Origin and domestication of the fungal wheat pathogen *Mycosphaerella graminicola* via sympatric speciation. *Molecular Biology and Evolution* 24:398–411, doi:10.1093/molbev/msl169

Stukenbrock E.H., Quaedvlieg W., Jahan Nikhan M., Crous P.W. and McDonald B.A. (2012*). Zymoseptoria ardabiliae* and *Z. pseudotritici*, two progenitor species of the septoria tritici leaf blotch fungus *Z. tritici* (synonym: Mycosphaerella graminicola). *Mycologia* 104(6): 1397–1407

Sutton B. & Waller J. (1988) Taxonomy of *Ophiocladium hordei* causing leaf lesions on Triticale and other Gramineae. *Transactions of The British Mycological Society* 90: 55–61.

Sutton B.C. and Pirozynski K.A. (1963) Notes on British microfungi. I. *Transactions of The British Mycological Society* 46: 505-522.

Tag A, Hicks J, Garifullina G, Ake C, Phillips TD, Beremand M, Keller N (2000) G-protein signalling mediates differential production of toxic secondary metabolites. *Molecular Microbiology* 38: 658–665.

Takemoto D., Tanaka A., Scott B. (2006) A p67(Phox)-like regulator is recruited to control hyphal branching in a fungal-grass mutualistic symbiosis. *Plant Cell* 18: 2807–2821

Tan Y.Y., Spiering M., Christensen M.J., Saunders K., Schmid J. (1997) In planta metabolic state of *Neotyphodium* endophyte mycelium assessed through use of the GUS reporter gene in combination with hyphal enumeration. In C.W. Bacon, N.S. Hill, eds., *Neotyphodium*/Grass Interactions. Plenum Press, New York, pp. 85–87.

Tanaka A., Christensen M.J., Takemoto D., Park P., Scott B. (2006) Reactive oxygen species play a role in regulating a fungus-perennial ryegrass mutualistic association. *Plant Cell* 18: 1052–1066

Tanaka A., Takemoto D., Hyon G.S., Park P., Scott B. (2008) NoxA activation by the small GTPase RacA is required to maintain a mutualistic symbiotic association between *Epichloe festucae* and perennial ryegrass. *Molecular Microbiology* 68: 1165–1178.

Taylor J.M.G., Paterson L.J. and Havis N.D. (2010) A quantitative real-time PCR assay for detection of *Ramularia collo-cygni* in barley (*Hordeum vulgare*). *Letters in Applied Microbiology* 50: 493-499.

Taylor J.W. (1995). Molecular phylogenetic classification of fungi. *Archives of Medical Research* 26:307–314.

The International Barley Genome Sequencing Consortium (2012) A physical, genetic and functional sequence assembly of the barley genome. *Nature* 491: 711–716. doi:10.1038/nature11543.

Thirugnanasambandam, A. (2011a) Role of seed-borne infection in *Rhynchosporium* and *Ramularia* epidemics in barley. *PhD Thesis, University of Dundee*.

Thirugnanasambandam, A., Wright, K. M., Atkins, S. D., Whisson, S. C. and Newton, A. C. (2011b) Infection of *Rrs1* barley by an incompatible race of the fungus *Rhynchosporium secalis* expressing the green fluorescent protein. *Plant Pathology*,60: 513–521. doi: 10.1111/j.1365-3059.2010.02393.x

Thirugnanasambandam, A., Wright, K. M., Havis, N., Whisson, S. C. and Newton, A. C. (2011a) *Agrobacterium*-mediated transformation of the barley pathogen *Ramularia collo-cygni* with fluorescent marker tags and live tissue imaging of infection development. *Plant Pathology* 60: 929–937. doi: 10.1111/j.1365-3059.2011.02440.x

Trail F., Chang P.K., Cary J, Linz J.E. (1994) Structural and functional analysis of the *nor*-1 gene involved in the biosynthesis of aflatoxins by *Aspergillus parasiticus*. *Applied and Environmental Microbiology* 60: 4078–4085.

Tucker S.L., Talbot, N.J. (2001) Surface attachment and pre-penetration stage development by plant pathogenic fungi. *Annual Review of Phytopathology* 39 385-417.

Tudzynski B. (2005) Gibberellin biosynthesis in fungi: genes, enzymes, evolution, and impact on biotechnology. *Applied Microbiology and Biotechnology* **66:** 597–611.

Turgeon B.G. (1998) Application of mating type gene technology to problems in fungal biology. *Annual Review of Phytopathology* 36: 115–137.

Turgeon B.G., Bohlmann H., CiuVetti L.M., Christiansen S.K., Yang G., Schafer W., Yoder O.C. (1993) Cloning and analysis of the mating type genes from *Cochliobolus heterostrophus*. *Molecular and General Genetics* 238: 270–284.

Turgeon B.G., Yoder O.C. (2000) Proposed nomenclature for mating type genes of filamentous ascomycetes. *Fungal Genetics and Biology* 31 1–5.

van West P., Reid B., Campbell T.A., Sandrock R.W., Fry W.E., Kamoun S., and Gow N.A.R.. (1999). Green fluorescent protein (GFP) as a reporter gene for the plant pathogenic oomycete *Phytophthora palmivora*. *FEMS Microbiology Letters* 178: 71–80.

Waalwijk C., Mendes O., Verstappen E.C.P., de Waard M.A. and Kema G.H.J. (2002) Isolation and characterization of the mating-type idiomorphs from the wheat Septoria Leaf Blotch fungus *Mycosphaerella graminicola*. *Fungal Genetics and Biology* 35: 277-286.

Walters D.R., Havis N.D, Oxley S.J.P. (2008) Ramularia collo-cygni: the biology of an emerging pathogen of barley. *FEMS Microbiology Letters* 279: 1-7.

Ware S.B, Verstappen E.C.P., Breeden J., Cavaletto. J.R., Goodwin S.B., Waalwijk C.,, Crous P.W., Kema G.H.J. (2007). Discovery of a functional *Mycosphaerella* teleomorph in the presumed asexual barley pathogen *Septoria passerinii*. *Fungal Genetics and Biology* 44: 389-397.

Watson AJ, Fuller LJ, Jeenes DJ, Archer DB (1999) Homologs of aflatoxin biosynthesis genes and sequence of aflR in *Aspergillus oryzae* and *Aspergillus sojae*. *Applied and Environmental Microbiology* 65: 307–310.

Weigel D. & Glazebrook J. (2008) Fixation, Embedding, and Sectioning of Plant Tissues *Cold Spring Harbour Protocols* 2008; doi: 10.1101/pdb.prot4941

White T.J., Bruns T., Lee S. & Taylor J. (1990) Amplification and Direct Sequencing of Fungal Ribosomal RNA genes for Phylogenetics. PCR Protocols: a Guide to Methods and Applications (Innis MA, Gelfand DH, Sninsky J.J. & White T.J., eds): 315–321. Academic Press, San Diego, CA

Whitehouse H.L.K. (1949) Heterothallism and sex in the fungi. *Biological Reviews* 12 :115–134.

Witthuhn R.C., Harrington T.C., Steimel J.P., WingWeld B.D., Wingfield M.J. (2000) Comparison of isozymes, rDNA spacer regions and *MAT-2* DNA sequences as phylogenetic characters in the analysis of the *Ceratocystis coerulescens* complex. *Mycologia* 92: 447–452.

Yabe K., Nakamura M., Hamasaki T. (1999) Enzymatic formation of G-group aflatoxins and biosynthetic relationship between G- and B-group aflatoxins. *Applied and Environmental Microbiology* 65: 3867–3872.

Yamazaki S., Okube A., Akiyama Y., and Fuwa K. (1975) Cercosporin, a novel photodynamic pigment isolated from *Cercospora kikuchii*. *Agricultural and Biological Chemistry* **39:** 287–288.

Young C.A., Felitti S., Shields K., Spangenberg G., Johnson R.D., Bryan G.T., *et al.* (2006) A complex gene cluster for indole-diterpene biosynthesis in the grass endophyte *Neotyphodium lolii*. *Fungal Genetics and Biology* 43: 679–693.

Young C.A., McMillan L., Telfer E., and Scott B. (2001) Molecular cloning and genetic analysis of an indolediterpene gene cluster from *Penicillium paxilli*. *Molecular Microbiology* 39: 754–764.

Yu J., Chang P.K., Ehrlich K.C., Cary J.W., Montalbano B., Dyer J.M., Bhatnagar D., Cleveland T.E. (1998) Characterization of the critical amino acids of an *Aspergillus parasiticus* cytochrome P-450 monooxygenase encoded by *ord*A that is involved in the biosynthesis of aflatoxins $B_1$, $G_1$, $B_2$, and $G_2$. *Applied and Environmental Microbiology* 64: 4834–4841.

Yu J.H, Chang P.K., Ehrlich K.C., Cary J.W., Bhatnagar D., Cleveland E., *et al.* (2004) Clustered pathway genes in aflatoxin biosynthesis. *Applied and Environmental Microbiology* 70: 1253–1262.

Yu J.H., Butcho R.A., Fernandes M., Keller N.P., Leonard T.J., Adams T.H. (1996) Conservation of structure and function of the aflatoxin regulatory gene aflR from *Aspergillus nidulans* and *A. flavus*. Current Genetics 29: 549–555.

Zhan J. and McDonald B.A. (2004) The interaction among evolutionary forces in the pathogenic fungus *Mycosphaerella graminicola*. *Fungal Genetics and Biology* 41: 590–599.

Zhan J., Kema G.H.J., Waalwijk C., McDonald B.A. (2002) Distribution of mating type alleles in the wheat pathogen *Mycosphaerella graminicola* over spatial scales from lesions to continents. *Fungal Genetics and Biology* 36: 128–136.

Zhan J., Pettway R.E. and McDonald B.A. (2003). The global genetic structure of the wheat pathogen *Mycosphaerella graminicola* is characterised by high nuclear diversity, low mitochondrial diversity, regular recombination, and gene flow. *Fungal Genetics and Biology* 38: 286–297.

Zhang S.G. Schwelm A., Jin H., Collins L.J., and Bradshaw R.E. (2007) A fragmented aflatoxin-like gene cluster in the forest pathogen *Dothistroma septosporum*. *Fungal Genetics and Biology* 44: 1342–1354.

# Appendix

## Protein sequence alignments of the components of the putative rubellin biosynthesis gene cluster

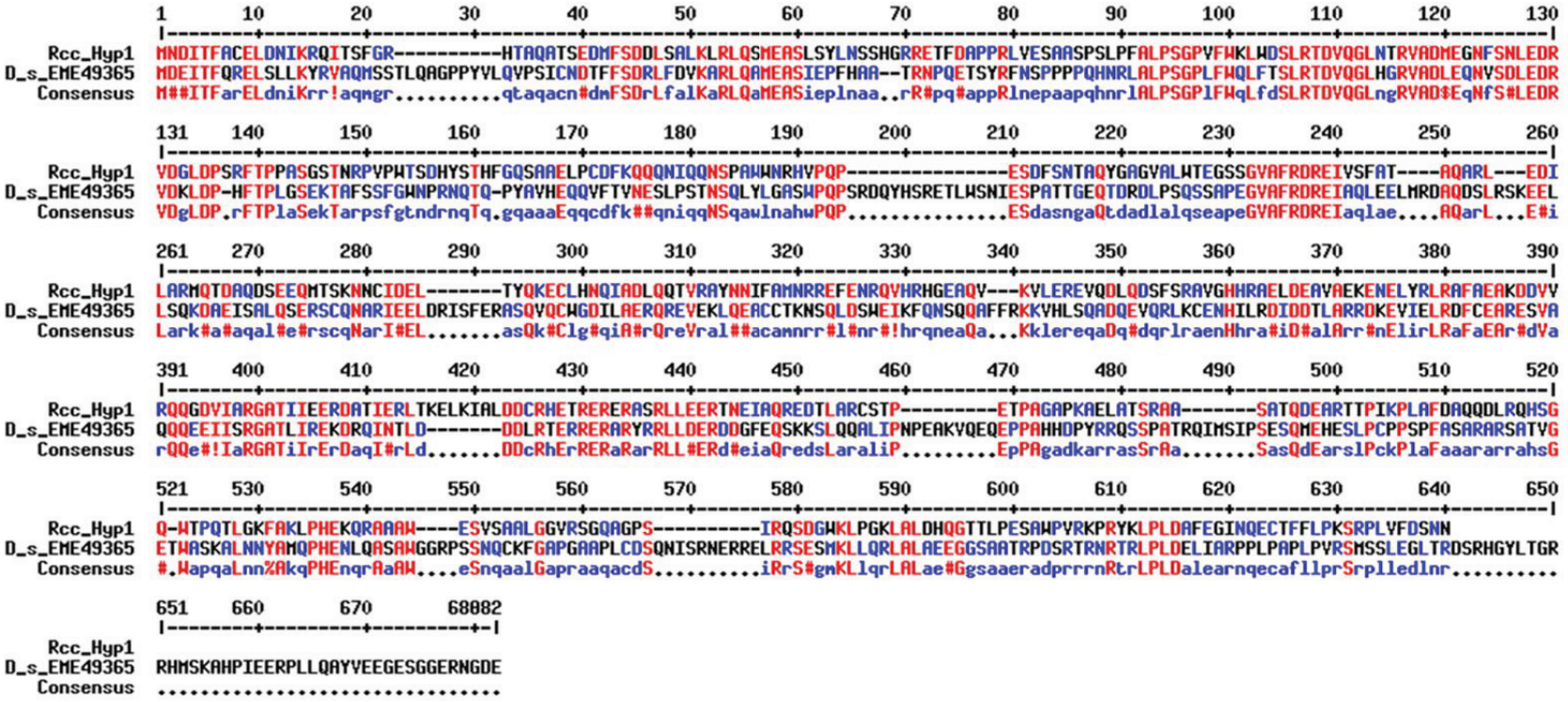


Appendix 1

Alignment of a Hyp1 ORFs and corresponding similar hypothetical proteins in *D. septosporum* EME49365.1

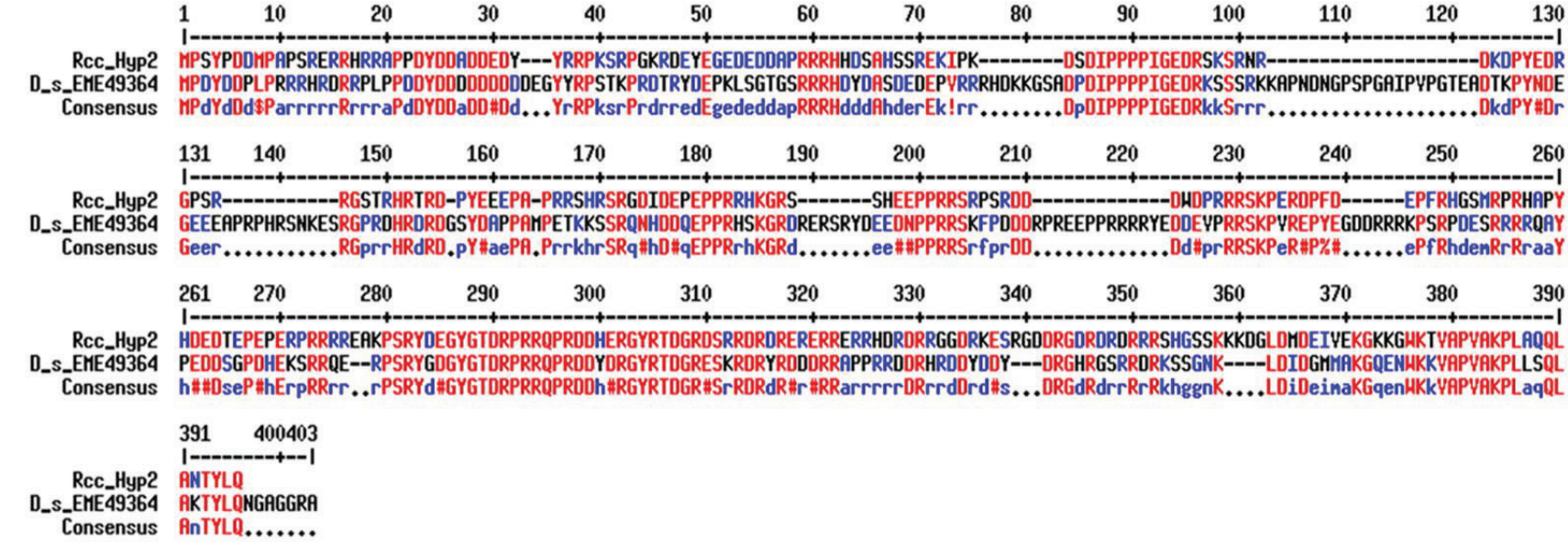




Appendix 2

Alignment of a Hyp2 ORFs and corresponding similar hypothetical proteins in *D. septosporum* EME49364.1

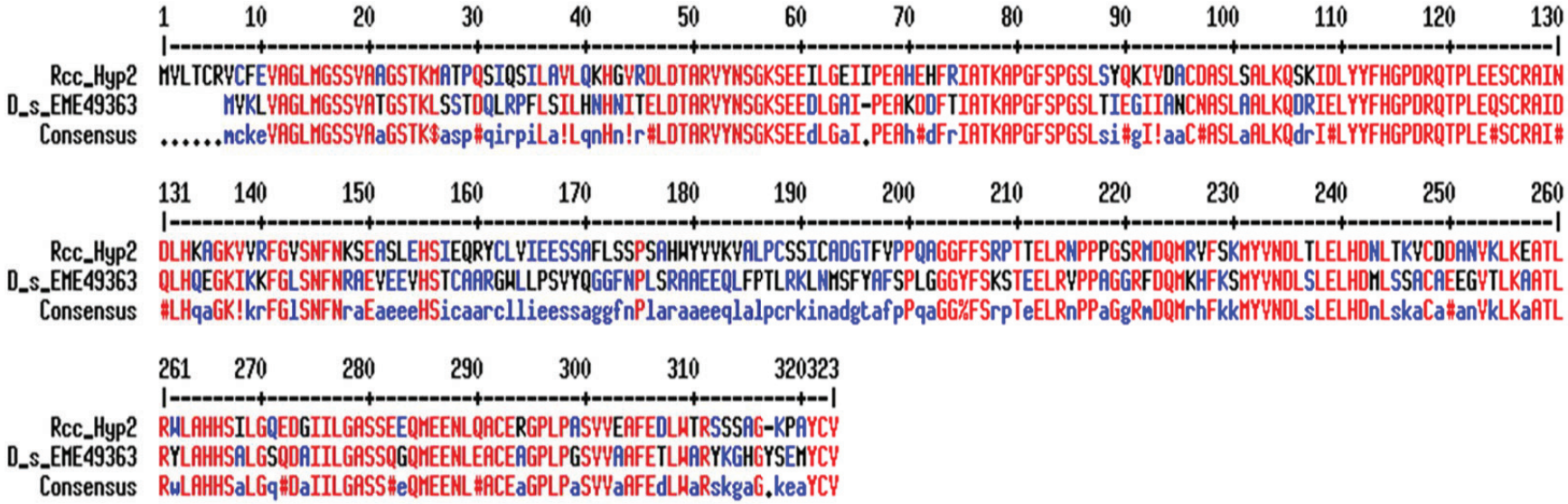




Appendix 3

Alignment of Hyp3/ aflB1 ORF and corresponding similar hypothetical protein in *D. septosporum* (EME49363.1)

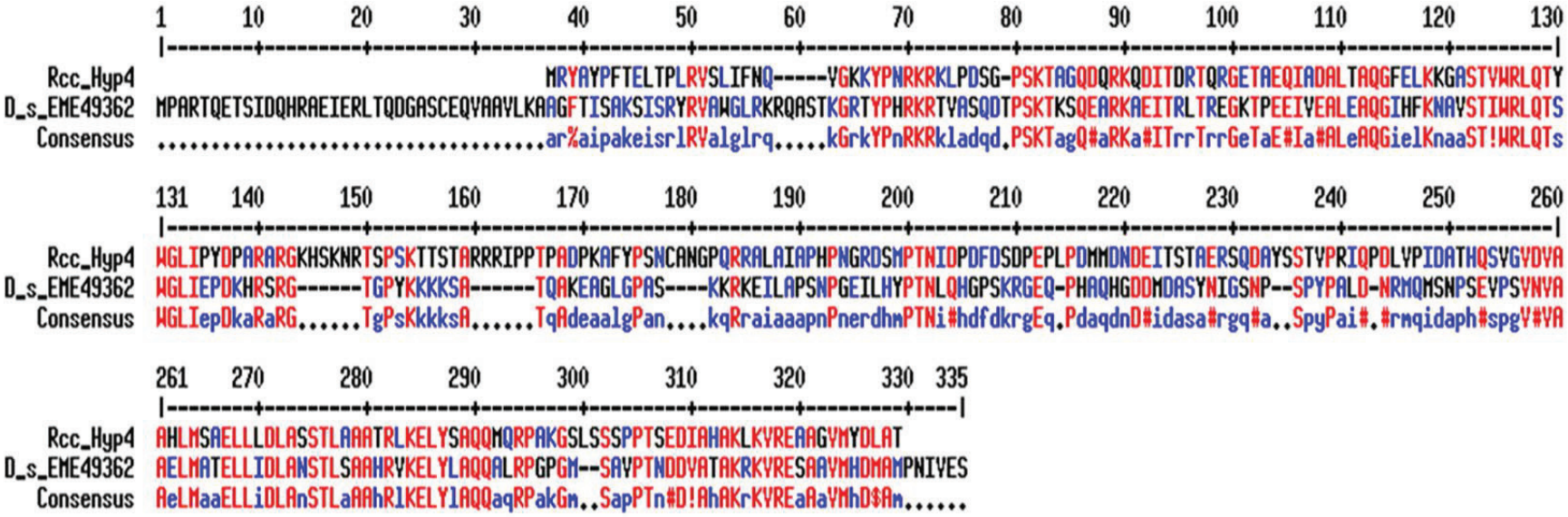


Appendix 4

Alignment of a Hyp4 ORF and corresponding similar hypothetical protein in *D. septosporum* EME49362.1.

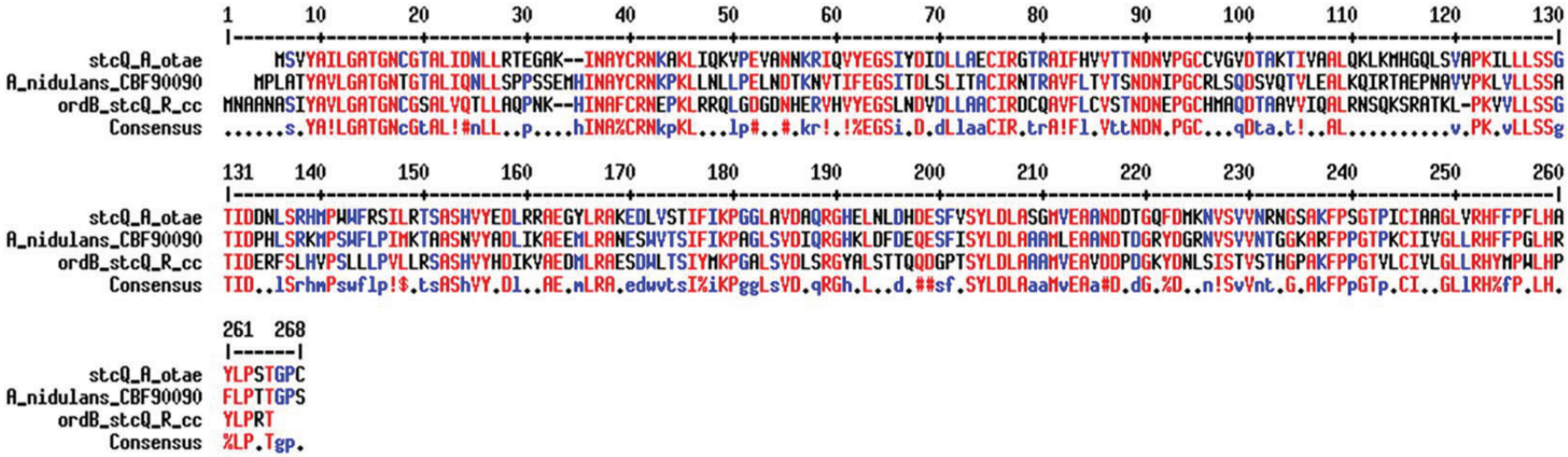




Appendix 5

Alignment of ordB/ stcQ ORF and corresponding similar stcQ protein in *A. otae* and *Aspergillus nidulans.*

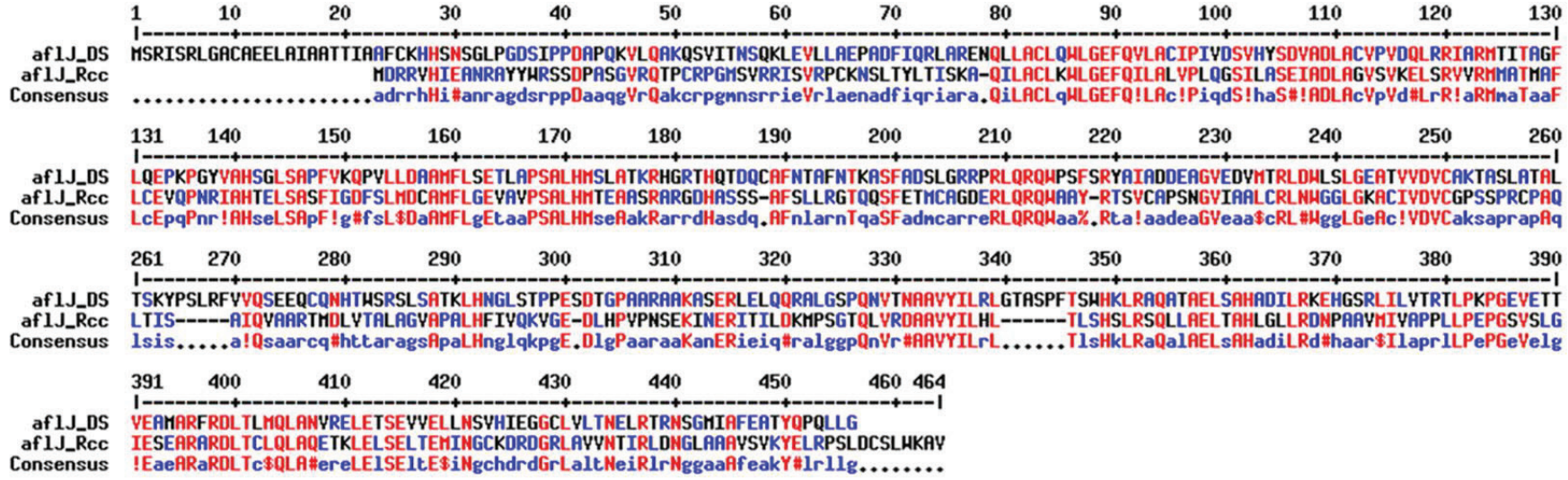




## Appendix 6

Alignment of aflJ/ aflS ORF and orthologous protein in *D. septosporum.*

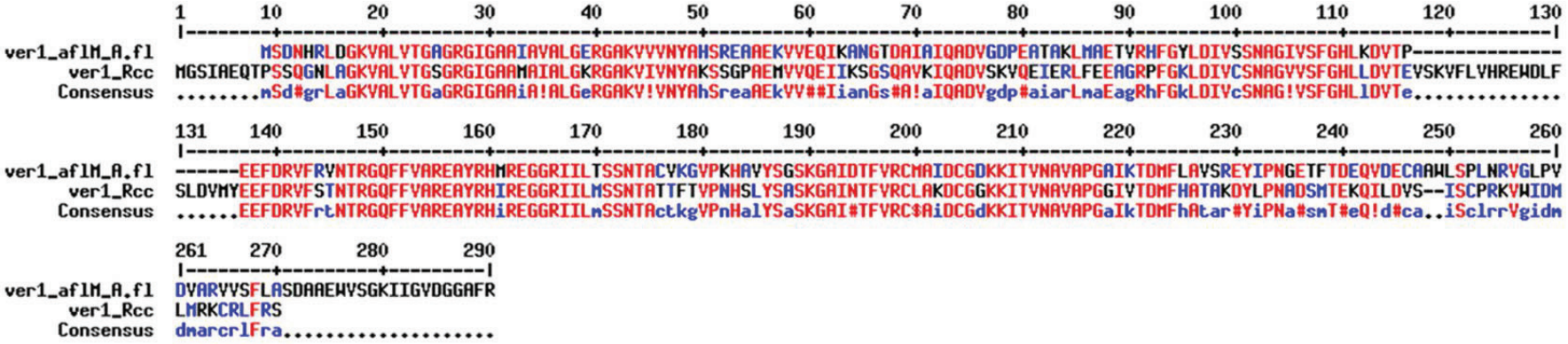


## Appendix 7

Alignment of ver-1/ aflM ORF and corresponding ver-1 protein in *A. flavus.*

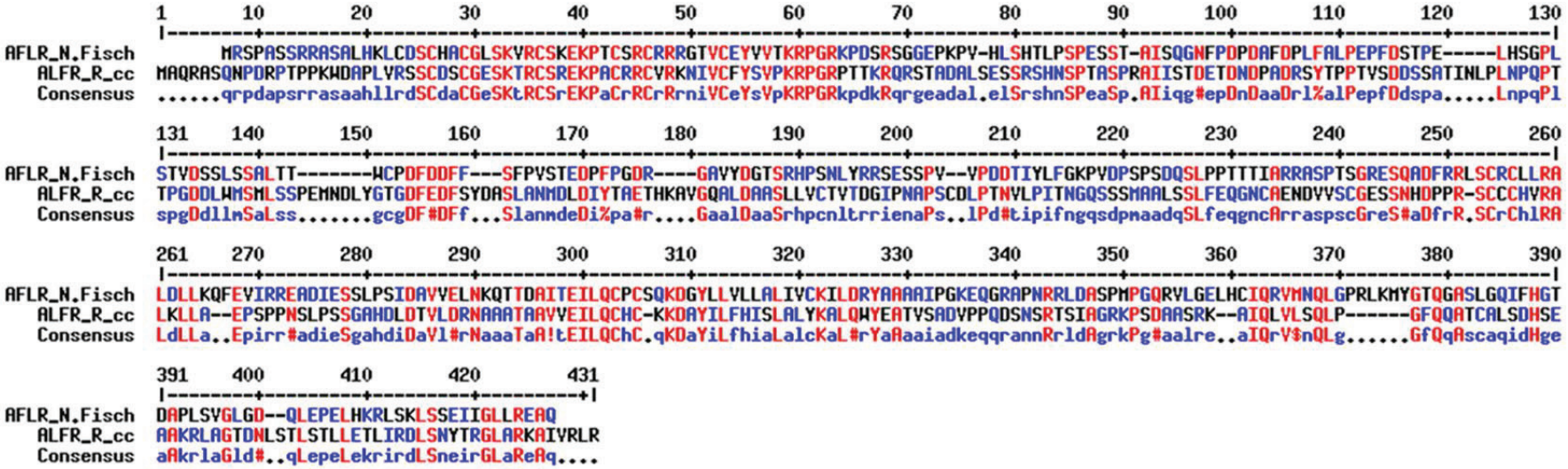




## Appendix 8

Alignment of aflR ORF and corresponding aflR protein in *N. fischeri.*

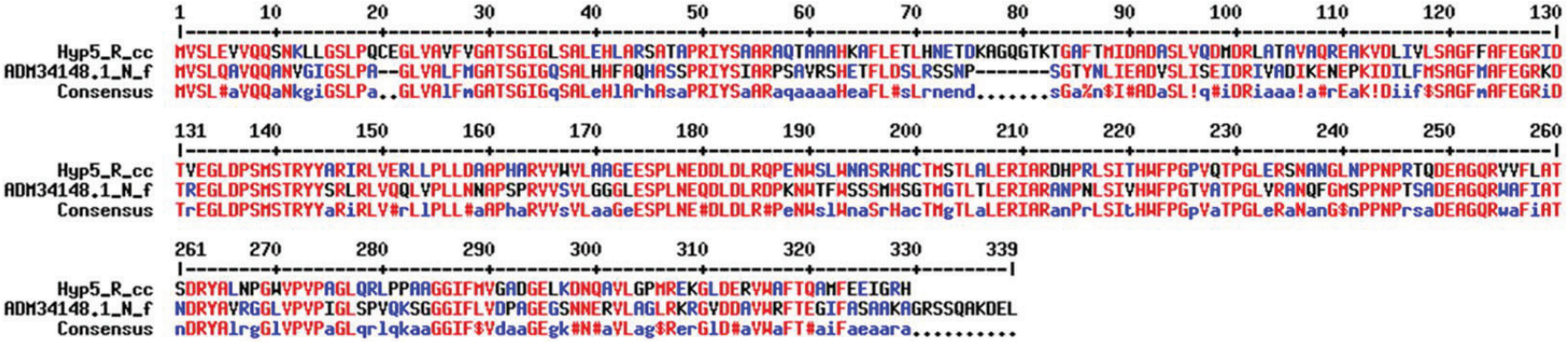


## Appendix 9

Alignment of Hyp5 ORF and corresponding highest blast hit in *Aspergillus* sp. MF297-2.


Appendix 10

Partial alignment of Hyp6 ORF and its ortholog in *N. fischeri.*

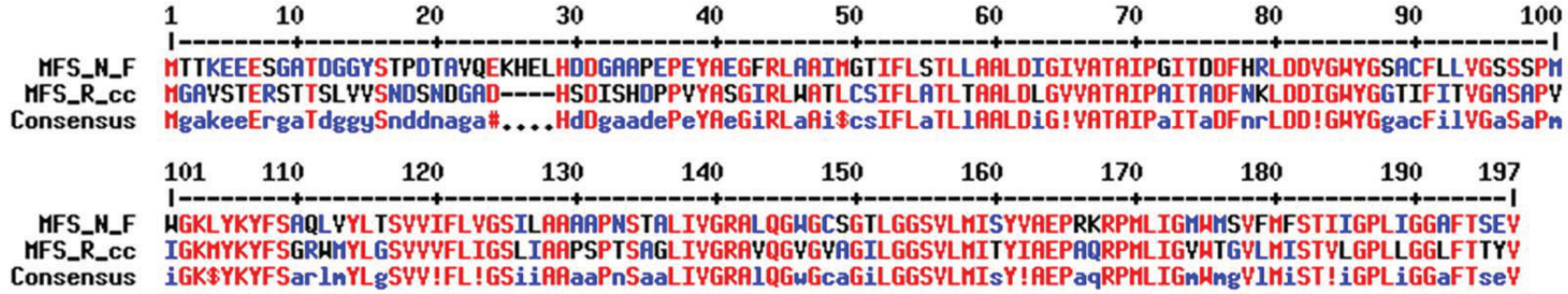


Appendix 11

Partial alignment of putative MFS transporter ORF and its ortholog in *N. fischeri.*

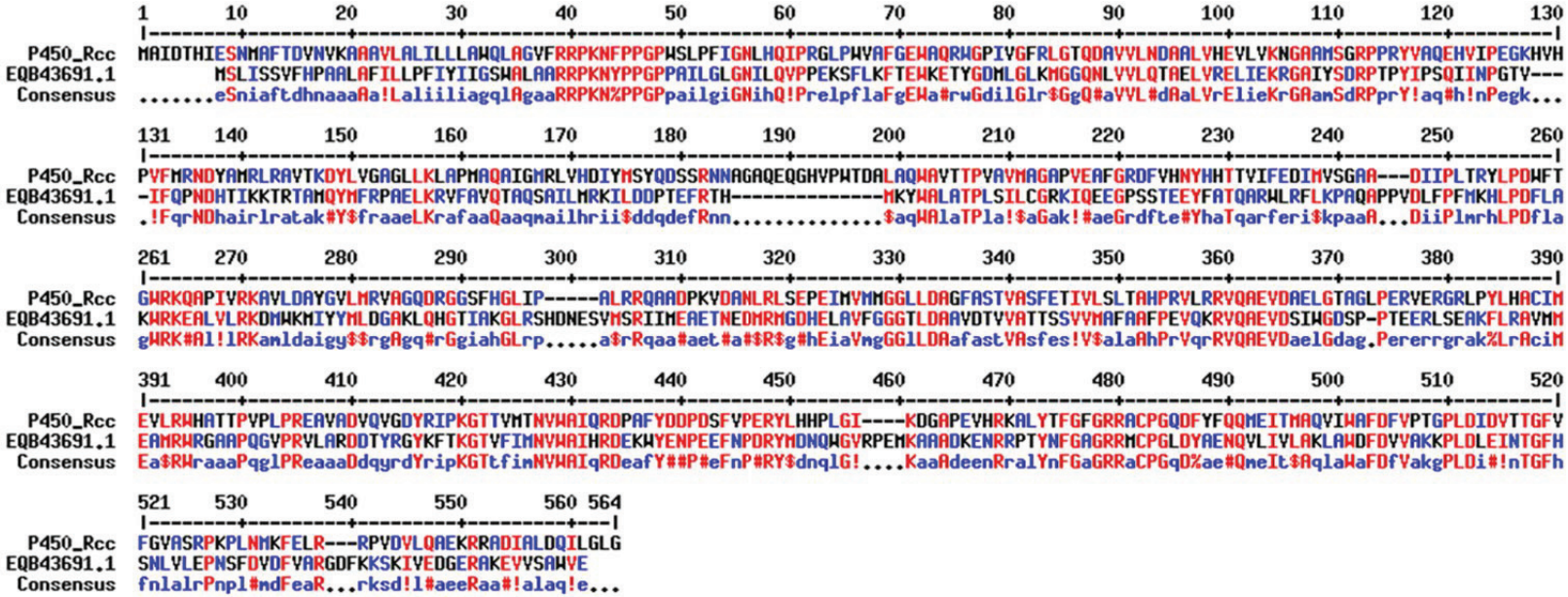




Appendix 12

Alignment of cytochrome P450 ORF and its ortholog in *C. gloeosporioides.*

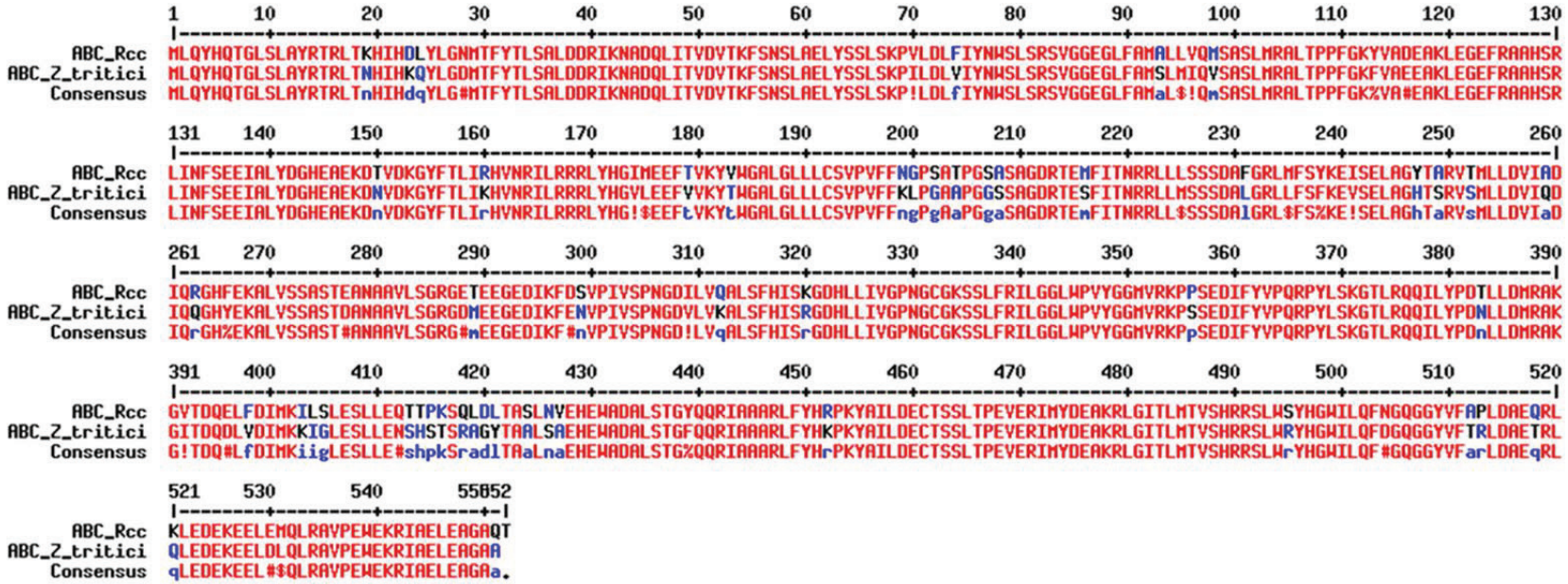




## Appendix 13

Partial alignment of putative ABC transporter ORF and its ortholog in *Z. tritici.*